

**The Development of New DNA Alkylating Antitumour Agents  
Modeled on the Natural Product CC-1065**

Author

Swan, Leesa Michelle

Published

2009

Thesis Type

Thesis (PhD Doctorate)

School

School of Biomolecular and Physical Sciences

DOI

[10.25904/1912/3327](https://doi.org/10.25904/1912/3327)

Rights statement

The author owns the copyright in this thesis, unless stated otherwise.

Downloaded from

<http://hdl.handle.net/10072/367931>

Griffith Research Online

<https://research-repository.griffith.edu.au>

**THE DEVELOPMENT OF NEW DNA ALKYLATING  
ANTITUMOR AGENTS MODELED ON THE  
NATURAL PRODUCT CC-1065.**

By

Leesa Michelle Swan

A thesis submitted to fulfill the requirements of the Doctor of  
Philosophy in the Faculty of Science at Griffith University, Brisbane,  
Queensland.

August, 2005.

Supervisor: Assoc. Professor David J. Young.

Faculty of Science,  
School of Science,  
Griffith University, Brisbane,  
Queensland, Australia.

The material presented in this thesis has not been previously submitted for a degree or diploma in any university, and to the best of my knowledge contains no material previously published or written by another person except where due acknowledgement is made in the thesis itself.

---

Leesa M. Swan

## ACKNOWLEDGMENTS

I would like to thank my supervisor, Associate Professor David Young for having enough faith in my abilities to take me on as a student, for providing support and encouragement and for not stifling my experimental endeavors. Thank you also for the time taken to review my thesis and the invaluable comments offered.

Many thanks also to the 'Young Ones' who guided me through all aspects of lab technique and the CC-1065 project.

Thanks must also go to Dr Peter Parsons at the Queensland Institute of Medical Research for his advice and enthusiasm regarding my project and the use of QIMR's world class facilities. Thanks also to the members of the Parsons group who took many hours to enlighten me on the various cellular assay techniques.

Thanks also to the funding body providing my APAWS scholarship. Although these people have no face, without this funding many people would never have the opportunity to realize their dreams.

Special thanks to my Mother and Father who made me believe that I could achieve anything I put my heart and mind to.

Last but not least, the person I would most like to thank is Gabrielle Pavia, who held my hand from the very start of my PhD to the completion of my thesis. Without her support, encouragement, patience and friendship this thesis would not exist. As such, I dedicate this thesis to Gabby.

## TABLE OF CONTENTS

### 1 INTRODUCTION

#### 1.1 CC-1065

##### 1.1.1 The Origin of CC-1065

##### 1.1.2 Structure

#### 1.2 Alkylating Mechanism

##### 1.2.1 Alkylating Mechanism and Sequence Selectivity of CC-1065

##### 1.2.2 N-3 Adenine Versus N-3 Guanine Alkylation

##### 1.2.3 Sequence Selectivity of (-)-CC-1065

##### 1.2.4 Ring Cyclisation of *Seco* Prodrug Analogues

##### 1.2.5 Reductively activated CC-1065 Prodrugs

##### 1.2.6 Selective Metal Cation Activation of the CPyI Alkylating Subunit

##### 1.2.7 Catalysis of the Alkylating Mechanism

#### 1.3 Covalent and Noncovalent Binding Stability and Sequence Specificity

##### 1.3.1 A Minor Role for Covalent Binding in Sequence Selectivity

##### 1.3.2 Noncovalent Binding Dominates the Control of Sequence Selectivity and Facilitates Stability

- 1.4 **Structural Analogues of CC-1065**
  - 1.4.1 **Variation of the Alkylating Subunit**
  - 1.4.2 **Variation in the Noncovalent Binding Subunit**
  - 1.4.3 **Variation in Linker and Terminal Amides**
  - 1.4.4 **Water Solubilised CPI Analogues Containing Polypyrole  
Minor Groove Binders**
  - 1.4.5 **Summary**
  
- 1.5 **Recent Advances in CC-1065 Development**
  - 1.5.1 **Glucoronide Derivatives of CC-1065 for use in ADEPT**
  - 1.5.2 **The Relationship between Reactivity and Cytotoxic  
Potency**
  - 1.5.3 **Achiral Compounds**
  - 1.5.4 **The Synthesis of New CC-1065 Analogues Bearing  
Different DNA-Binding Subunits**
  
- 1.6 **Synthetic Analogues of CC-1065 in Clinical Trials**
  - 1.6.1 **Adozelesin**
  - 1.6.2 **Carzelesin**
  - 1.6.3 **U-71,184**
  - 1.6.4 **Bizelesin**
  
- 1.7 **Mechanisms of Cytotoxic Action by CC-1065 and Related  
Structural Analogues**
  - 1.7.1 **Overview**
  - 1.7.2 **The Inhibition of DNA Processing Enzymes**
  - 1.7.3 **CC-1065 Cell Cycle Effects**
  - 1.7.4 **Activation of Apoptosis**
  - 1.7.5 **CC-1065 DNA Adduct Recognizing Protein**

- 1.8 Recent Prodrug Studies
  - 1.8.1 Background
  - 1.8.2 Overcoming Poor Water solubility
  - 1.8.3 Albumin Binding Prodrugs of CC-1065

1.9 Project Objectives

- 1.9.1 Preliminary Studies
- 1.9.2 Objectives

1.10 References

**2 RESULTS AND DISCUSSION: ORGANIC SYNTHESIS**

2.1 Scheme 1: Synthesis of 4-Aminophenethyl Halide Derivatives

2.2 Scheme 2: Synthesis of 4-Aminophenethyl Fluoride Hydrochloride

2.3 Scheme 3: 1<sup>st</sup> Attempted Synthesis of 4-Aminophenethyl Iodide Hydrochloride

2.4 Scheme 4: 2<sup>nd</sup> Attempted Synthesis of 4-Aminophenethyl Iodide Hydrochloride

- 2.5 Scheme 5: Synthesis of 2-{4-[2,2,2-trifluoroacetyl)amino]phenyl}-ethyl trifluoroacetate
- 2.6 Scheme 6: Synthesis of 4-Aminophen-2(d<sub>2</sub>)-ethyl Bromide Hydrochloride
- 2.7 Scheme 7: Synthesis of 4-Hydroxyphenethyl Halides
- 2.8 Scheme 8: First Attempted Synthesis of 4-(2-Chloroethyl-*N*-(3-pyridinylmethyl)aniline Dihydrochloride
- 2.9 Scheme 9: Second Attempted Synthesis of 4-(2-Chloroethyl-*N*-(3-pyridinylmethyl)aniline Dihydrochloride
- 2.10 Scheme 10: Third Attempted Synthesis of 4-(2-Chloroethyl-*N*-(3-pyridinylmethyl)aniline Dihydrochloride
- 2.11 Scheme 11: Synthesis of 4-(2-chloroethyl)-*N*-(3-pyridinylmethyl)aniline Dihydrochloride
- 2.12 Scheme 12: Synthesis of 4-(2-chloroethyl)-*N*-(2-pyridinylmethyl)aniline Dihydrochloride
- 2.13 Scheme 13: Synthesis of *N,N'*-bis[4-(2-chloroethyl)phenyl]-2,6-pyridinedimethylamine Trihydrochloride
- 2.14 Scheme 14: Synthesis of 4-(2-chloroethyl)-*N*-[3-(2-pyridinyl)propyl]aniline Dihydrochloride

- 2.15 Scheme 15: Synthesis of N-benzyl-4-(2-chloroethyl)aniline Hydrochloride
- 2.16 Mechanistic Studies of 4-Aminophenethyl-2d<sub>2</sub>-Bromide Hydrochloride
  - 2.16.1 Pathway A: Alkylation via Direct S<sub>N</sub>2 Attack onto the C1 Methyl Halide Carbon
  - 2.16.2 Pathway B: Ar<sub>1,3</sub> Cyclisation followed by S<sub>N</sub>2 Attack onto the C1 or C2 Centre
  - 2.16.3 Nuclear Magnetic Resonance Studies
- 2.17 References

### 3 ORGANIC SYNTHESIS: EXPERIMENTAL

- 3.1 General Preparation
  - 3.1.1 Experimental Setup for Moisture/Oxygen Sensitive Reactions
  - 3.1.2 Solvents
  - 3.1.3 Reagents
- 3.2 Instrumentation
  - 3.2.1 NMR Spectroscopy
  - 3.2.2 Microanalysis
  - 3.2.3 Melting Points
  - 3.2.4 Mass Analysis
  - 3.2.5 UV Absorption
- 3.3 Chromatography Techniques

- 3.4 The Synthesis of Simple DNA Alkylating CPI Analogues
  - 3.4.1 Synthesis of 4-Aminophenethyl Bromide.HCl
  - 3.4.2 Synthesis of 4-Aminophenethyl Chloride.HCl
  - 3.4.3 Synthesis of 4-Aminophenethyl Fluoride.HCl
  - 3.4.4 First Attempted Synthesis of 4-Aminophenethyl Iodide.HCl
  - 3.4.5 Second Attempted Synthesis of 4-Aminophenethyl Iodide.HCl
  - 3.4.6 Synthesis of 4-Aminophenethyl Mesylate.HCl
  - 3.4.7 Synthesis of 4-Acetamidophenethyl Bromide
  - 3.4.8 Synthesis of 4-Acetamidophenethyl Chloride
  - 3.4.9 Synthesis of 2-{4-[2,2,2-Trifluoroacetyl)amino]phenyl}ethyl Trifluoroacetate
  
- 3.5 Mechanistic Studies Involving 4-Aminophenethyl-2d<sub>2</sub> Bromide
  - 3.5.1 Synthesis of 4-Aminophenethyl-2d<sub>2</sub>-Bromide
  - 3.5.2 Synthesis of 4-Hydroxyphenethyl Bromide
  - 3.5.3 Synthesis of 4-Hydroxyphenethyl Chloride
  
- 3.6 Synthesis of Mono- and Bisalkylators Incorporating Pyridyl/Benzyl Noncovalent Binding Subunits
  - 3.6.1 First Attempted Synthesis of 4-(2-Chloroethyl)-*N*-(3-pyridinylmethyl)aniline Dihydrochloride
  - 3.6.2 Second Attempted Synthesis of 4-(2-Chloroethyl)-*N*-(3-pyridinylmethyl)aniline Dihydrochloride
  - 3.6.3 Third Attempted Synthesis of 4-(2-Chloroethyl)-*N*-(3-pyridinylmethyl)aniline Dihydrochloride
  - 3.6.4 Synthesis of 4-(2-Chloroethyl)-*N*-(3-pyridinylmethyl)aniline Dihydrochloride
  - 3.6.5 Synthesis of 4-(2-Chloroethyl)-*N*-(2-pyridinylmethyl)aniline Dihydrochloride
  - 3.6.6 Synthesis of *N,N'*-[Pyridine-2,6-diyl(methylene)]bis[4-chloroethyl)aniline] Trihydrochloride

- 3.6.7 Synthesis of 4-(2-Chloroethyl)-*N*-[3-(2-pyridinyl)propyl]aniline Dihydrochloride
- 3.6.8 Synthesis of *N*-benzyl-4-(2-chloroethyl)aniline Hydrochloride

### 3.7 References

## 4 CYTOTOXICITY STUDIES – RESULTS AND DISCUSSION

### 4.1 Introduction

### 4.2 Treatment

- 4.2.1 Cytotoxic Agents
- 4.2.2 Cell Abrogating Compounds
- 4.2.3 Hormone Manipulation

### 4.3 Cell Types

- 4.3.1 HeLa
- 4.3.2 MM96L
- 4.3.3 MM418c5
- 4.3.4 DU146 and Pc-5
- 4.3.5 NFF
- 4.3.6 HaCat

### 4.4 Cell Survival Studies

- 4.4.1 Necrosis and Programmed Cell Death

- 4.4.2 The Effect of Varying Concentrations of Synthesized Alkylating Compound on a Range of Cell Lines
- 4.4.3 The Cytotoxicity of Mono- and Bisalkylators Incorporating Pyridyl/Benzyl Noncovalent Binding Subunits Against Various Cell Lines
- 4.4.4 Summary of Results

#### 4.5 References

## 5 FURTHER PRELIMINARY BIOLOGICAL STUDIES – RESULTS AND DISCUSSION

### 5.1 Reporter Assays

#### 5.1.1 Probing for AT Sequence Selectivity

#### 5.1.2 Probing for CG Sequence Selectivity

### 5.2 Drug Stability

#### 5.2.1 Compound Solubility

#### 5.2.2 Compound Stability

#### 5.2.3 Assessment of Drug Stability Following Incubation with Various Nucleophiles

### 5.3 Cell Cycle Studies

#### 5.3.1 The Eukaryotic Cell Cycle

#### 5.3.2 Protein Kinases and Regulation of the Cell Cycle

#### 5.3.3 Specific Cyclin-CDK Complexes

#### 5.3.4 Cell cycle Inhibitors

- 5.3.5 Checkpoints
- 5.3.6 Role of the Cell Cycle in Tumour Formation
- 5.3.7 The Application of CDK Inhibition in Cancer Therapeutics
- 5.3.8 Determination of Cell Cycle Phase
- 5.3.9 The Effect of Various DNA Alkylating Compounds on the MM96L Cell Cycle
- 5.3.10 The Effect of Compound 4 on Other Cell Lines
- 5.3.11 The Effect on the MM96L Cell Cycle Following Treatment of MM96L Cells with Compound 4 in Combination with either Hydroxyurea (HU) or Albendazole (AB)
- 5.3.12 Cell Cycle Summary

#### 5.4 Adenoviral Assays

- 5.4.1 Host Cell Reactivation (HCR) Assays
- 5.4.2 Viral Capacity
- 5.4.3 Adenoviral Assay Summary

#### 5.5 *in-vivo* Studies

#### 5.6 Future Work

- 5.6.1 Reporter Assays
- 5.6.2 Drug Stability Studies
- 5.6.3 Cell Cycle Studies
- 5.6.4 Adenoviral Assays
- 5.6.5 *in-vivo* Studies

#### 5.7 References

## **6 BIOLOGICAL EXPERIMENTAL**

### **6.1 General Preparation**

### **6.2 Experimental Procedure**

#### **6.2.1 Cell Survival Assays**

#### **6.2.2 CPR- $\beta$ -Galctosidase Assays**

#### **6.2.3 Luciferase Assays**

#### **6.2.4 Drug Stability**

#### **6.2.5 Cell Cycle Studies**

#### **6.2.6 Adenoviral Assays**

## **APPENDIX 1 – COMMON REAGENTS USED IN BIOLOGICAL ASSAYS**

### **References**

## ABBREVIATIONS

<b>ACDPI</b>	5-amino-3-carbamoyl-1,2-dihydro-3 <i>H</i> -pyrrolo-[3,2- <i>e</i> ]indole-7-carboxylate
<b>APB</b>	4-aminophenethyl bromide hydrochloride
<b>ADEPT</b>	Antibody-directed enzyme prodrug therapy
<b>BOC</b>	<i>N-tert</i> butyloxy carbonyl
<b>CBI</b>	1,2,9,9a-tetrahydrocyclopropa[ <i>d</i> ]benz[ <i>e</i> ]indol-4-one
<b>CBI<sub>n</sub></b>	1,2,9,9a-tetrahydro-1 <i>H</i> -cyclopropa[ <i>d</i> ]benz[ <i>e</i> ]inden-4-one
<b>CBQ</b>	2,3,10,10a-tetrahydro-1 <i>H</i> -cyclopropa[ <i>d</i> ]benz[ <i>f</i> ]quinol-5-one
<b>CCBI</b>	1,2,9,9a-tetrahydro-7-methoxycyclopropa[ <i>d</i> ]benz[ <i>e</i> ]indol-4-one
<b>CDPI</b>	3-carbamoyl-1,2dihydro-3 <i>H</i> -pyrrolo[3,2- <i>e</i> ]indole-7-carboxylate
<b>CI</b>	1,2,7,7a-tetrahydrocyclopropa[1,2- <i>d</i> ]indol-4-one
<b>CPI</b>	1,2,8,8a-tetrahydro-7-methyl-cyclopropa[ <i>d</i> ]pyrrolo[3,2- <i>e</i> ]indol-4-one
<b>CPyI</b>	1,2,9,9a-Tetrahydrocyclopropa[ <i>c</i> ]pyrido[3,2- <i>e</i> ]indol-4-one-7-carboxylate
<b>CPzI</b>	1,2,9,9a-Tetrahydrocyclopropa[ <i>c</i> ]pyrazolo[3,2- <i>e</i> ]indol-4-one
<b>CNA</b>	1,2,3,4,11,11a-hexahydrocyclopropa[ <i>c</i> ]naphthol[2,1- <i>b</i> ]azepin-6-one

<b>D<sub>37</sub></b>	The dose required to reduce cell survival to 37%.
<b>D<sub>50</sub></b>	The dose required to reduce cell survival to 50%.
<b>DA</b>	Duocarmycin A
<b>DARP</b>	DNA adduct recognizing protein
<b>DCM</b>	Dichloromethane
<b>DMSO</b>	Dimethylsulphoxide
<b>DNA</b>	Deoxyribonucleic acid
<b>DSA</b>	Duocarmycin SA
<b>HPC</b>	4-hydroxyphenethyl bromide
<b>HPLC</b>	High pressure liquid chromatography
<b>IC<sub>50</sub></b>	The concentration of agent required to inhibit the growth of the indicated cell line by 50% in a 72 hour assay.
<b>ISC</b>	Interstrand Crosslinks
<b>MCBI</b>	1,2,9,9a-tetrahydro-7-methoxycyclopropa[c]benz[e]indol-4-one
<b>MTT</b>	3-[4,5-Dimethylthiazol-2-yl]-2,5-diphenyltetrazolium bromide
<b>NADH</b>	Nicotinamide adenine dinucleotide hydride
<b>NADPH</b>	Nicotinamide adenine dinucleotide phosphate
<b>NMR</b>	Nuclear Magnetic Resonance
<b>ppm</b>	Parts per million

<b>RBF</b>	Round bottom flask
<b>RPA</b>	Replication protein A
<b>TACDPI</b>	5-trimethylammonio-3-carbamoyl-1,2-dihydro-3 <i>H</i> -pyrrolo[3,2- <i>e</i> ]indole-7-carboxylate
<b>TEA</b>	Triethylamine
<b>THF</b>	Tetrahydrofuran
<b>TMI</b>	5,6,7-trimethoxyindole-2-carboxylate

## **ABSTRACT**

Preliminary studies have revealed that the 4-hydroxyphenethyl halides possess the minimal structural requirements needed to mimic the DNA alkylation profile characteristic to *seco*-CPI subunits. Subsequent assessment of the 4-aminophenethyl halides showed that these adducts exhibit approximately four times the *in vitro* cytotoxicity demonstrated by their phenolic counterparts. The incorporation of these simpler compounds into more complex molecules containing non-covalent binding subunits was expected to increase both cytotoxicity and sequence selectivity.

Biological assessment of the synthesized compounds established that the simplest compound, 4-aminophenethyl bromide, was a potent antitumor drug which exhibited selectivity for tumor cells over normal fibroblastic cells. This makes 4-aminophenethyl bromide an interesting candidate for further *in vivo* assessment.

## **CHAPTER 1 – INTRODUCTION**

### **1.1 CC-1065:**

#### **1.1.1 The Origin of CC-1065 -**

CC-1065 is an exceptionally potent DNA interactive antitumor antibiotic belonging to the alkylating class of anticancer agents. First isolated from the bacterium *Streptomyces zelenis* in 1978, CC-1065 was found to display remarkably efficient *in vitro* and *in vivo* potency against L1210 and P388 leukaemic cell lines and B16 melanoma,<sup>1,2,3</sup> with an *in vivo* cytotoxic activity 50 – 1000 times greater than other drugs in clinical use.<sup>4</sup> The induction of delayed hepatotoxicity by CC-1065 at therapeutic antineoplastic doses in nontumored mice<sup>2,5,6</sup>, accompanied by dramatic changes in hepatic mitochondrial morphology<sup>7</sup>, precluded clinical application. This discovery led to the pursuit of modified agents, the most recent being Adozelesin (section 1.6.1), Carzelesin (section 1.6.2) and Bizelesin (section 1.6.4), all of which exhibit antitumor activity without displaying such delayed toxic effects.<sup>8,9</sup>

#### **1.1.2 Structure –**

Intensive NMR and IR investigations as well as chemical degradation studies allowed the elucidation of the structure of CC-1065 in 1980<sup>1</sup> with confirmation arising from X-ray crystallography in 1981.<sup>10</sup> The CC-1065 molecule consists of three amide linked benzodipyrrole moieties (Figure 1). The left hand cyclopropylpyrroloindole (CPI) subunit is responsible for covalent DNA alkylation. The middle and right hand subunits, which resemble the closely related phosphodiesterase inhibitors PDE-I and PDE-II,<sup>11</sup> are responsible for noncovalent DNA interactions.<sup>1</sup>

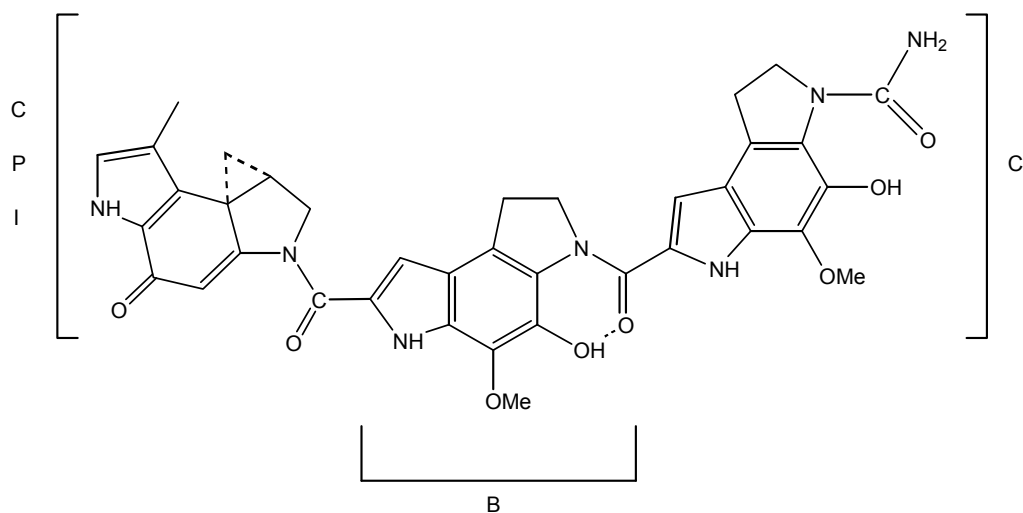


**Figure 1 - The Structure of CC-1065.**

Each of the moieties in the molecule are approximately planer. CC-1065, however, has a partially twisted conformation resulting from an angle of approximately  $16^\circ$  between moieties B and C and a larger angle of  $55^\circ$  between the CPI subunit and B.<sup>10</sup> An intramolecular hydrogen bond between the hydroxyl group of B and the amide carbonyl of C constrains the twist, producing within the molecule a contorted arrangement which mimics the pitch of B-form DNA making the molecule well suited for positioning within the minor groove.<sup>2,5,12,13</sup> Further promotion of CC-1065 association with the minor groove of duplex DNA occurs through the enhancement of noncovalent contacts by hydrogen bond donors and acceptors which are found on the outer periphery of the curved molecule.<sup>10</sup>

## 1.2 ALKYLATING MECHANISM:

### 1.2.1 Alkylating Mechanism and Sequence Selectivity of CC-1065 –

CC-1065 and its analogs exhibit their antitumor activity via irreversible alkylation of N-3 of adenine in the minor groove of DNA (Figure 2).<sup>2,5,14</sup> This alkylation proceeds in a sequence selective manner within AT rich regions<sup>14</sup> and is determined by both covalent and noncovalent drug-DNA interactions which subsequently result in cell death via several mechanisms (Section 1.6).<sup>11</sup> The molecule overlaps with five base pairs with high sequence specificity existing for the sequences 5'-PuNTTA\* (Pu = purine, N = any base) and 5'-AAAAA\* where A\* is the site at which alkylation occurs. The mechanism involves protonation of the quinone carbonyl followed by S<sub>N</sub>2 attack by the N-3 nitrogen of adenine at the methylene group of the cyclopropane ring. More recent studies have indicated that CC-1065 may crosslink DNA in tumor cells (10-15% of all DNA lesions) and is proposed to occur through enzymatic demethylation of *o*-methoxy-phenol moiety to *o*-quinone.<sup>15</sup>

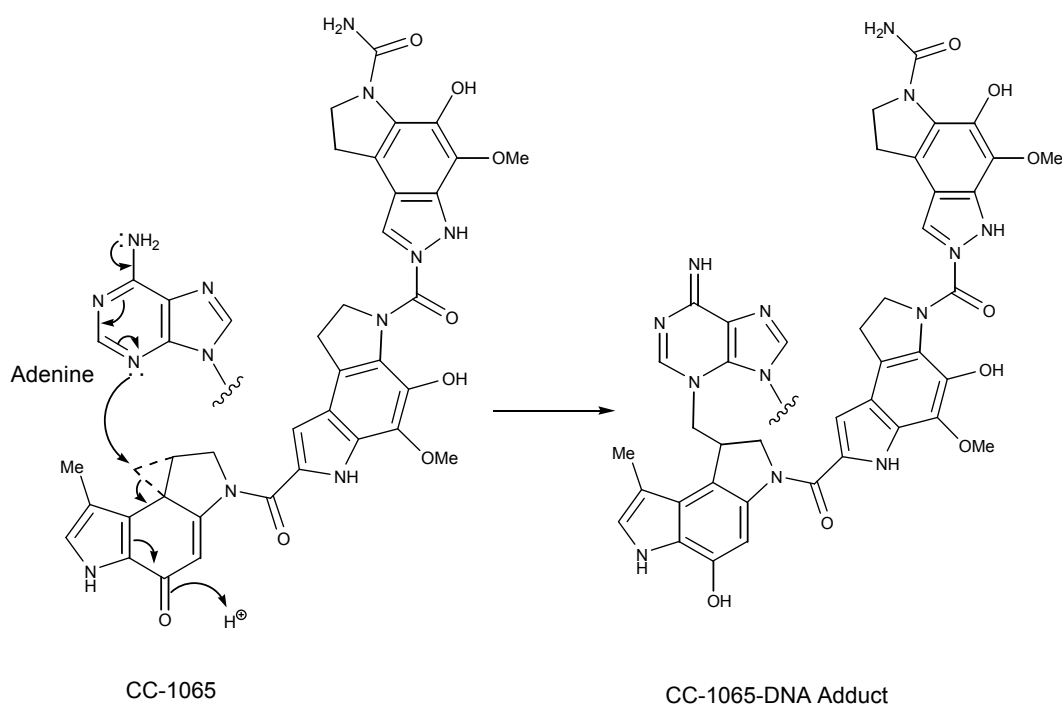


*Figure 2 – Alkylation of DNA by CC-1065.*

Strong reversible binding first occurs in the minor groove of double stranded DNA, followed by covalent bonding at the appropriate adenine and concomitant cyclopropyl ring opening.<sup>16</sup> This covalent adduct formation results in bending of DNA into the minor groove by 17-22°.<sup>14,17</sup>

CC-1065 shows an obvious three base sequence preference of the order: 5'-AAA\*=5'-TTA\*>5'-TAA\*>5'-ATA\*. Furthermore, the drug exhibits a strong preference for the fourth 5' base to be an A or a T and a weak preference for the fifth 5' base to be an A or a T.<sup>14</sup> The requirement for the first three base pairs to be either an A or a T results from the need for an adenine for covalent drug alkylation as well as the facilitation of central and right-hand subunit binding in the minor groove.

### 1.2.2 N-3 Adenine Versus N-3 Guanine Alkylation –

Alkylation by CC-1065 occurs primarily at N-3 of adenine, forming 86%-92% of the alkylated sites, however trace N-3 guanine alkylation has been observed under certain conditions. These conditions include the absence of high affinity sites, the use of excess agent or the protection of high affinity sites by compounds such as distamycin.<sup>14</sup>

### 1.2.3 Sequence Selectivity of (-)-CC-1065 –

The unnatural enantiomer, (-)-CC-1065, shows a markedly different sequence selectivity with a preferential three base sequence of the following order: 5'-AA\*A>5'-TA\*A>5'-AA\*T>5'-TA\*T.<sup>14</sup> However, while the consensus sequences (i.e. recognition sites) are not identical, nearly half of the adenines which are alkylated by each enantiomer are essentially the same.<sup>18</sup> This allows the same space in the minor groove to be accessible to either enantiomer. One such group of sequences contains a (-)-CC-1065 alkylated adenine 1-2 basepairs to the 5' side of the adenine that is targeted by (+)-CC-1065, therefore generating overlapping sequences.<sup>18</sup> However, regardless of this similarity in adenine alkylation sites there are some exceptions:

- (1) The very high affinity (-)-CC-1065 alkylation site, 5'-AATT reacts poorly with (+)-CC-1065.
- (2) The highly (+)-CC-1065 accommodating sites incorporating 5'-A/TA\*A/T are poorly reactive towards (-)-CC-1065.

- (3) Sequences in which the target adenine is within or directly 5' to a 5'AAG sequence are highly reactive toward (+)-CC-1065 but not (-)-CC-1065.<sup>17</sup>

Molecular modeling has shown that (-)-CC-1065 is orientated oppositely in the minor groove to the natural enantiomer and lies to the 3' side of the covalent adduct.<sup>16</sup> However, despite the differences in orientation, alkylation with either the natural or unnatural enantiomer leads to occupation of corresponding or overlapping sequences in the minor groove.<sup>18</sup>

Although the unnatural enantiomer of CC-1065 is similar to (+)-CC-1065 in that it demonstrates the same preference for minor groove AT sites, exhibits similar DNA alkylation efficiency and shows similar rates of DNA alkylation as well as indistinguishable *in vitro* and comparable *in vivo* activity,<sup>14</sup> the simpler analogues of (-)-CC-1065 fail to alkylate under the same conditions and are therefore considered to be biologically nonpotent.<sup>18</sup>

#### 1.2.4 Ring Cyclisation of *Seco* Prodrug Analogues –

Uncyclised (*seco*) CPI containing prodrugs of CC-1065 also exhibit remarkable DNA binding and antitumor activity comparable to the cyclised analogues indicating that the cyclopropane ring is not obligatory for the observation of DNA alkylation.<sup>19-21</sup> This observation gave rise to the proposal that ring closure must precede covalent bond formation (Figure 3) via the following mechanism (where X = a leaving group):

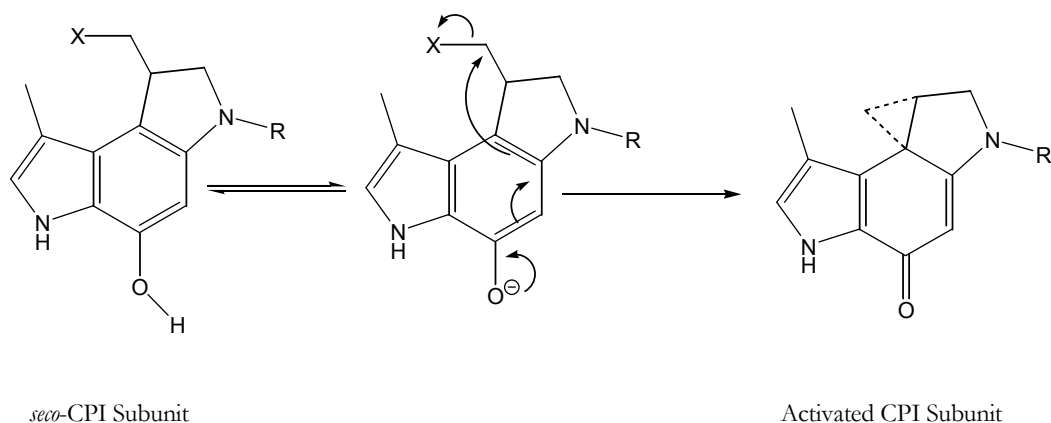


**Figure 3 - Ring Cyclisation of *seco*-CPI analogues.**<sup>13,14</sup>

The relative cytotoxicities of the *seco* agents is dependent on the relative leaving ability of the group on the C3 methylene carbon where agents containing halide leaving groups have been found to be more reactive than alcohols. Compounds bearing a methylsulfonyl leaving group are even more potent than those bearing a chlorine, reflecting the relative leaving group abilities of these two anions. A better leaving group increases the electrophilicity of the C3 methylene carbon, increasing the rate of cyclisation via Ar<sub>1-3</sub> participation.<sup>22</sup> Furthermore, the electron density of the benzene ring further influences the rate of cyclisation. Electron-donating groups on the benzene ring promote cyclisation via an increase in the nucleophilicity of C9 whereas electron-withdrawing groups (such as NO<sub>2</sub> or Br) impede cyclisation by the opposite effect.<sup>23</sup>

**Note:** Studies with reactive agents that are not able to undergo ring closure due to the absence of the hydroxyl group indicate that, in some molecules, the closure of the cyclopropane is not essential for alkylation to proceed.<sup>24</sup>

### 1.2.5 Reductively Activated CC-1065 Prodrugs –

Two classes of reductively activated CC-1065 prodrugs have recently been reported which exhibit AT-selective CC-1065 like alkylation and enhanced selectivity toward tumor cells. The first group uses antibody-directed enzyme prodrug therapy (ADEPT). In this approach an enzyme is conjugated to an antibody which targets a tumor-specific cell surface antigen. Subsequent administration of the prodrug substrate results in the enzyme catalyzed release of the free drug at the tumor site.<sup>25</sup> Importantly, a single enzyme is able to catalyze the release of the active compound and as such only small amounts of antibody are required.

One such prodrug system under evaluation is the nitro substituted *seco*-CI class of compounds (Figure 4) which are enzymatically reduced to the corresponding hydroxylamine by aerobic nitroreductases.<sup>25</sup> Known substrates for this *Escherichia coli* B nitroreductase are actinomycin D and mitomycin C which are activated by reductive fragmentation of the nitrobenzyloxycarbonyl group, as well as dinitrobenzamide mustards and a 4-nitrobenzyloxycarbonyl enediyne derivative.<sup>25</sup> Importantly, the presence of a cofactor (i.e. NADH or NADPH) is required for enzymatic activation (Table 1).

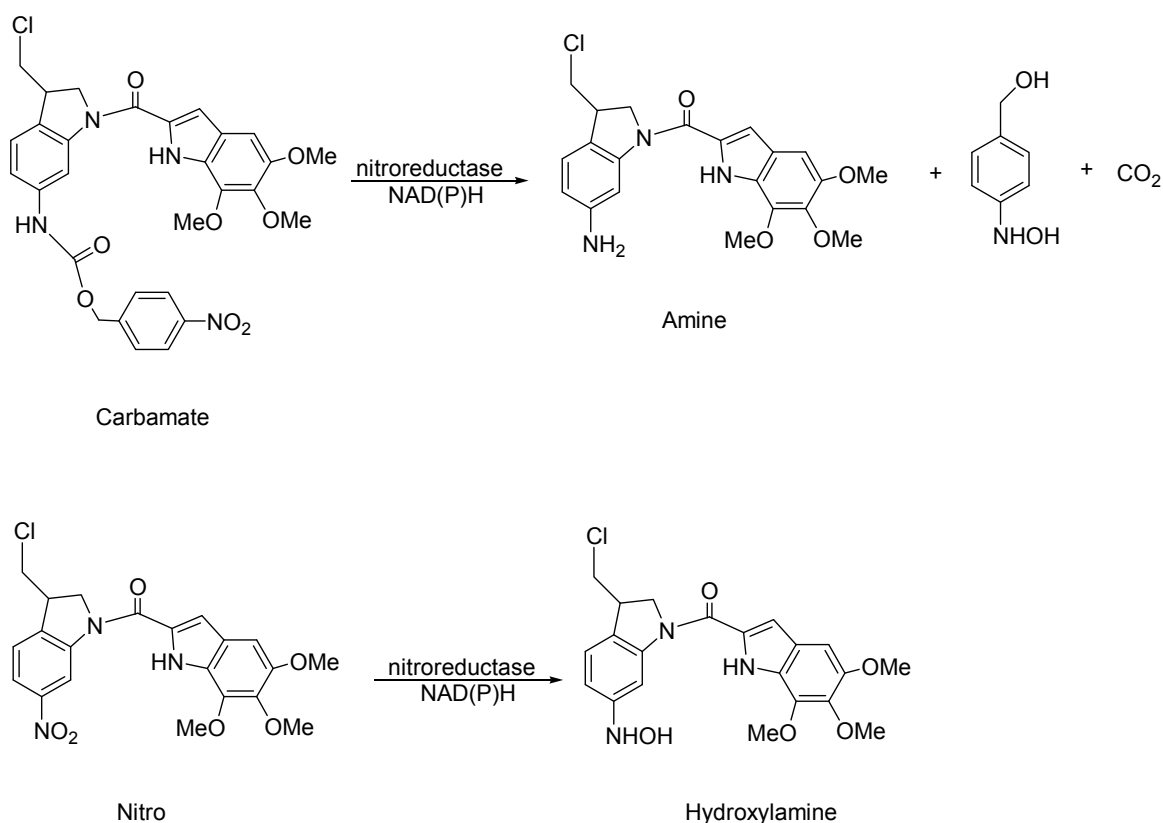


**Figure 4 - Nitro Substituted *seco*-Cl Analogues**

Prodrug	IC <sub>50</sub> (nM)			Ratio <sup>a</sup>
	Prodrug Alone	Prodrug + NADH	Prodrug + NADH + Enzyme	
Carbamate	15000 ± 3200	11300 ± 4500	598 ± 140	23.2 ± 2.6
Amine	23.6 ± 3.4	26.6 ± 0.2	27.8 ± 8.8	0.9 ± 0.2
Nitro	2310 ± 300	237 ± 45	6.4 ± 0.7	402 ± 41

**Table 1:** IC<sub>50</sub> Values Measured for the Prodrug Alone, Prodrug with NADH and Prodrug with NADH and the Enzyme *E.coli* B Nitroreductase and Cofactor. (a) IC<sub>50</sub> (prodrug) / IC<sub>50</sub> (Prodrug + NADH + Enzyme).

A second class of drugs also requiring reductive activation for DNA alkylation are the quinone containing mitomycin related compounds (Figure 5).<sup>26,27</sup> The mechanism of alkylation is believed to involve bioreduction, followed by spirocyclisation and DNA alkylation.

These agents have been found to exhibit preferential selectivity for DT-Diaphorase (NQO1) containing tumors (i.e. renal and melanoma cell lines) due to the reductive ability of this enzyme, as compared to DT-Diaphorase deficient cell lines such as leukemia, nonsmall cell lung cancer, colon, CNS, ovarian, prostate and breast cancer.<sup>27</sup>

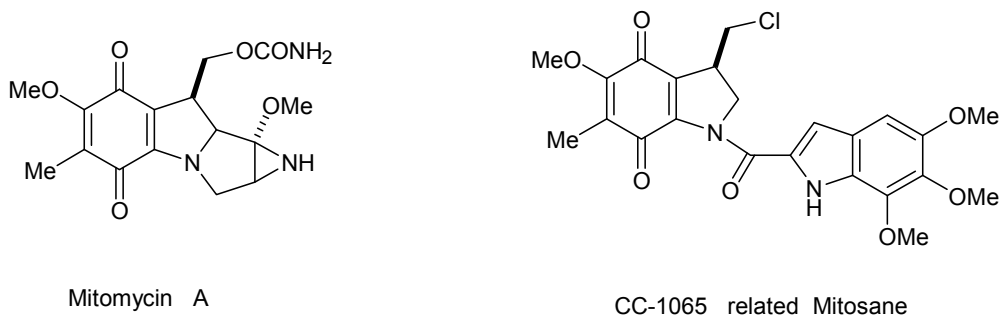


**Figure 5 - Quinone Containing Mitomycin Related Compounds**

### 1.2.6 Selective Metal Cation Activation of the CPyI Alkylating Subunit –

The synthesis and evaluation of the CPyI alkylating subunit (i.e. 1,2,9,9a-Tetrahydrocyclopropa[*c*]pyrido[3,2-*e*]indol-4-one-7-carboxylate) containing an 8-ketoquinoline structure has revealed a unique selective activation of this compound via metal cation complexation.<sup>28,29</sup> Studies involving the complexation of CPyI with 1, 10, 100 and 1000 equivalents of various metal cations has revealed that the reaction rate corresponds to the relative stability of the resulting metal complexes (i.e.  $\text{Cu}^{2+} > \text{Ni}^{2+} > \text{Zn}^{2+} > \text{Cr}^{2+} > \text{Fe}^{2+} > \text{Mn}^{2+} > \text{Mg}^{2+}$ )<sup>28,29,30</sup> with significant enhancement seen at 1 and 10 equivalents and marked effects seen at 100 and 1000 equivalents (Figure 6).

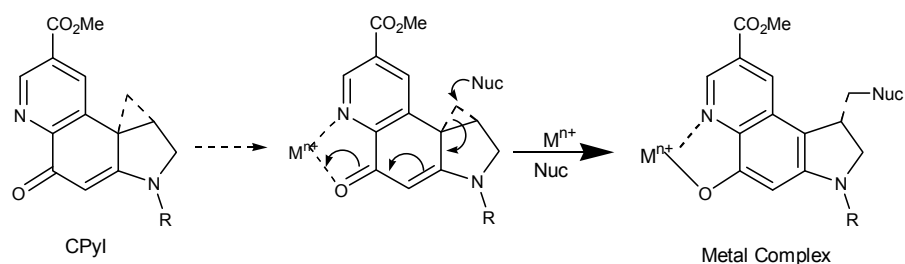


**Figure 6 – Metal Catalyzed Addition to N-Boc-CPyI**

This enhancement in rate and efficiency however, was not observed with similar treatment of the related N-Boc-DSA or N-Boc-CBI and is believed to be directly related to the absence of the 8-ketoquinoline structure which is essential for metal cation complexation (Figure 7). Furthermore, the natural (+)-enantiomer of CPyI proved more potent (3-30x)<sup>29</sup> than the unnatural (-)-enantiomer.

The DNA alkylation efficiency of CPyI which normally occurs at concentrations of  $10^{-2}$ M (as for N-Boc-DSA and N-Boc-CBI) was markedly increased with the addition of  $\text{Cu}(\text{acac})_2$  (100 x),  $\text{Ni}(\text{acac})_2$  (100-1000 x) and  $\text{Zn}(\text{acac})_2$  (1000 x) with no change in alkylation selectivity. In particular DNA alkylation enhancement at CPyI concentrations as low as  $10^{-5}$  M with the addition of  $\text{Zn}(\text{acac})_2$  (1000 equivalents) was exceptional (1000 x) and has previously not been observed for simple alkylation subunits. The observation that the DNA alkylation selectivity is unaffected by metal cation catalysis provides further evidence that the source of selectivity is not necessarily related to acid catalysis but instead derived from the noncovalent binding selectivity.

This increased enhancement with metal cation catalysis provides an exploitable mechanism for tumor selectivity due to the significant differences in metal concentrations in cancerous and non-cancerous tissues. For example, Zn is found in breast carcinoma at levels 700% higher than normal breast cells while lung cancer showed a 10x difference. Ongoing studies will reveal whether these Zn activated agents may be effective agents against both breast and lung cancer.<sup>28,29</sup>

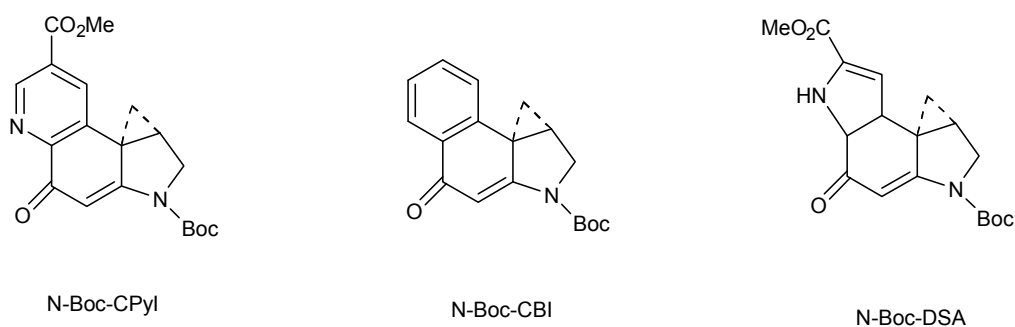


**Figure 7 – N-Boc Analogues of CC-1065 and Duocarmycin**

### 1.2.7 Catalysis of the Alkylation Mechanism –

Activation of the alkylating subunit via carbonyl protonation was initially thought to be exclusively pH dependent. This theory was based on studies which disclosed that the CPI group is remarkably stable within the pH range 5 – 7, but has been seen to promptly solvolyse at pH 3 to give ring opened products which are equivalent to the ring opened adducts formed during DNA alkylation.<sup>14,24</sup> Furthermore, it was believed that the activation of the carbonyl occurred at a strategically placed phosphate in the DNA backbone two base pairs removed from the alkylation site in the 5'-direction.<sup>13,23,31</sup> More recent studies, however, have indicated that certain analogs maintain activity even at pHs where the DNA phosphate backbone is fully ionized (i.e. > 7.4).

This activity has been ascribed to a DNA binding-induced conformational change in the agent which disrupts the stability brought about by vinylogous amide conjugation, thereby promoting nucleophilic attack.<sup>32</sup> Evidence to support this originates from comparative studies involving the simple amine and amide derivatives of CPI, CBI and CBQ (Sect. 1.3.1). While the amine derivatives are stable at pH 7 and do not exhibit solvolysis, their amide counterparts react rapidly with DNA. This is thought to be a consequence of “shape dependent catalysis” involving the disruption of vinylogous amide stabilization with the spirocyclopropylcyclohexadienone upon binding to AT rich sequences of DNA.<sup>32</sup> The removal of the linking amide diminishes the capacity for DNA alkylation even in acidic media providing further evidence for the shape dependent catalysis theory.<sup>33</sup>

The evaluation of CBI<sub>n</sub> (Figure 8), a carbocyclic analogue of CC-1065 not containing the amide has provided further evidence for this mechanism of catalysis. Removal of the nitrogen and therefore the amide stabilization was found to increase the reactivity 3200 times (pH 3) but did not alter the S<sub>N</sub>2 reaction mechanism.<sup>34</sup> As a result it is believed that the amide is responsible for the stabilization and solvolysis reactivity, independent of pH providing further evidence for the DNA binding-induced conformational change mechanism of catalysis.<sup>35</sup>

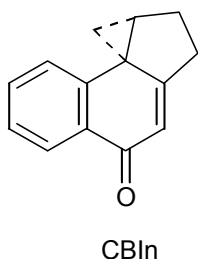


*Figure 8 - CBI<sub>n</sub>*

### **1.3 COVALENT AND NONCOVALENT BINDING STABILITY AND SEQUENCE SPECIFICITY:**

#### **1.3.1 A Minor Role for Covalent Binding in Sequence Selectivity –**

The alkylating subunit has been advocated by earlier investigations as playing a role in defining the sequence specificity of the molecule.<sup>18,36</sup> There are three steps via which covalent binding occurs, beginning with noncovalent binding through the formation of van der Waals contacts, hydrogen bonding and the displacement of water molecules from the minor groove. The noncovalently bound molecules then facilitate a conformational change locally in the DNA which facilitates bond formation by optimizing the distance and geometry between N-3 of adenine and the methylene carbon of the cyclopropane. This conformational change is followed by covalent binding between the alkylation subunit and N-3 of adenine.<sup>37</sup>

For the conformational change in the local DNA structure to occur a distortion energy is necessary. This is the underlying mechanism by which covalent binding is thought to enable

sequence specificity. Those sequences having a lower deformation energy barrier, and therefore an increased propensity to undergo the local conformational changes required for bonding, are thought to be favored in the covalent reaction of adenine with the drug.<sup>37,38</sup>

This premise is a result of studies involving analogues of the CC-1065 alkylating subunit linked to zero, one or two indole subunits, designated CPI, CPI-I<sub>1</sub> and CPI-I<sub>2</sub> (Figure 9). The specificity of CPI and CPI-I<sub>1</sub> was similar to that of CPI-I<sub>2</sub> indicating that the alkylating subunit may play a role in mediating sequence selectivity.<sup>18</sup>

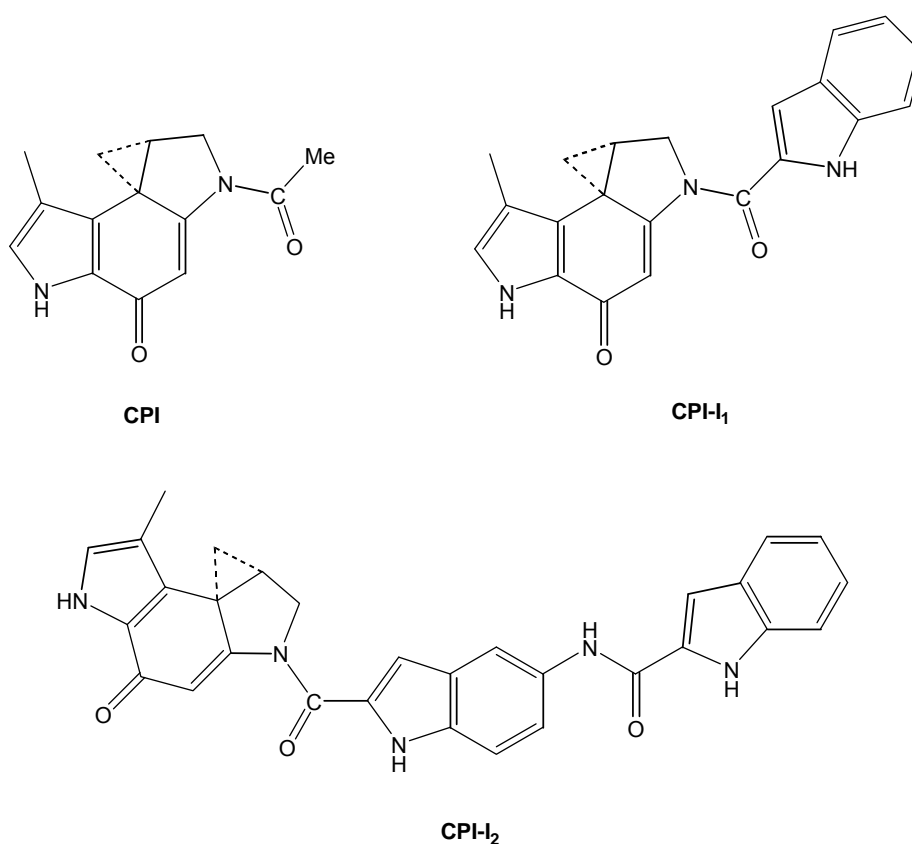


*Figure 9 – Synthetic Analogues Used in the Determination of Covalent Binding Specificity.*

However, while this proposal was favored in earlier investigations, recent studies have indicated that noncovalent binding plays the predominant role in the determination of sequence selectivity.

### **1.3.2 Noncovalent Binding Dominates the Control of Sequence Selectivity and Facilitates Stability -**

The steric accessibility of noncovalent binding subunits to the alkylation site has recently been proposed to dominate the control of sequence selectivity. Because alkylation requires that the agents are allowed to deeply penetrate into the minor groove, larger agents containing noncovalent subunits are unable to penetrate certain sites that are sterically hindered thereby resulting in further sequence selectivity. This is the reason that alkylation selectivity occurs primarily at A/T rather than G/C rich sites. The distended 2-amino group of guanine interrupts the minor groove cleft preventing deep penetration as well as destabilizing noncovalent binding.<sup>18,39</sup>

Furthermore, although the analogues CPI, CPI-I<sub>1</sub> and CPI-I<sub>2</sub> show similar sequence specificity, more complex pyrroloindole subunits of CC-1065 have been seen to have a detectable influence on the specificity for certain sites. Therefore, it seems evident that the hydrogen bonding and van der Waals contacts of subunits B and C, also serve to fine-tune the sequence specificity.<sup>37</sup>

While covalent binding was believed (particularly by earlier groups) to play a minor role in sequence specific recognition, it is unable to provide adequate biological activity due to the low intensity of DNA alkylation facilitated by the alkylating subunit alone. Therefore, the noncovalent interactions by the B and C subunits, as well as dominating sequence specificity control, serve to appreciably increase the rate of alkylation of susceptible adenines.

The strong noncovalent binding forces which have been attributed to the central and right-hand subunits have also been observed to stabilize the DNA-drug adduct and therefore counter the reversibility of the alkylation reaction.<sup>16,40-42</sup>

Although DNA-drug adduct formation is generally irreversible in aqueous solution due to the extreme water insolubility of the drug, reversibility can occur via a retrohomologous Michael reaction. This occurs in aqueous/organic solvent mixtures at high temperatures.<sup>42</sup>

## **1.4 STRUCTURAL ANALOGUES OF CC-1065:**

### **1.4.1 Variation of the Alkylating Subunit –**

#### **1.4.1a CBI:**

The discovery of CC-1065 and the subsequent disclosure that it induced delayed death in mice illustrated the need for the synthetic development of analogues which had equivalent cytotoxicity, without the undesirable characteristic of delayed toxicity. Because of the importance of the left-hand subunit in controlling the antitumor potential of the molecule,<sup>41</sup> initial synthetic studies dealt with replacement of the left-hand CPI with the more stable CBI analogues (Figure 10).<sup>43</sup> Both the *in vivo* and *in vitro* potencies of the CBI compounds correlated very closely to those of CC-1065,<sup>43,44</sup> however they still retained the delayed effect of toxicity exhibited by CC-1065. This delayed toxicity has been proposed to result from the duplex winding effect that is associated with the noncovalently binding subunits of (+)-CC-1065. Simplified CPI and CBI analogues lacking the noncovalent binding skeleton are free of this delayed toxicity.

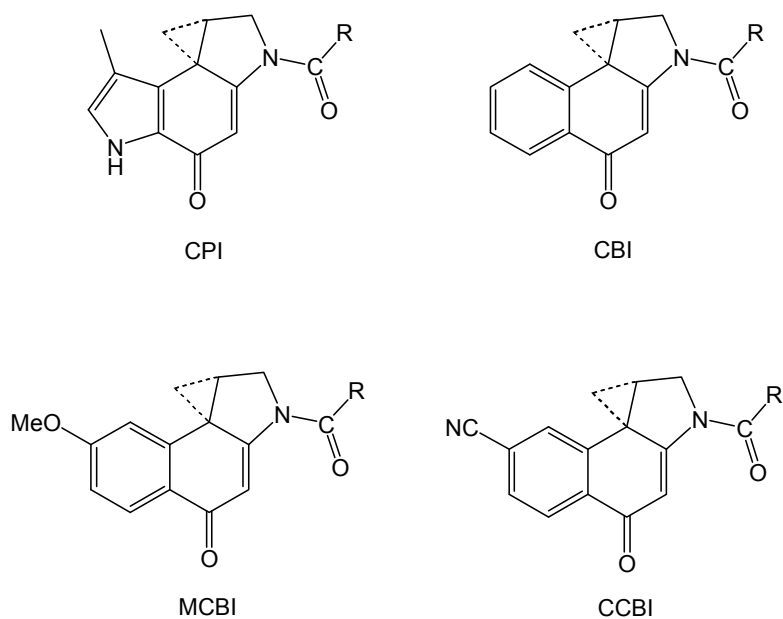


**Figure 10– CC-1065 Analogues CBI, MCBI, CCBI and CPI**

Like the CPI agents, the CBI-CDPI<sub>n</sub> analogues are stable in aqueous solution at neutral pH. However, under more acidic conditions CBI analogues exhibit greater stability. Furthermore the natural enantiomers proved to be approximately eight times more potent than the unnatural enantiomers.<sup>45</sup> The *seco*-1-chloro-methyl CBI containing agents possess an indistinguishable activity to that of the CBI based agents. The relative cytotoxic potentials of the CBI analogues compared to (+)-CC-1065 is as follows: (+)-CBI-CDPI<sub>2</sub> ~ (+)-CBI-CDPI<sub>1</sub> >> (-)-CBI-CDPI<sub>2</sub> >> (-)-CBI-CDPI<sub>1</sub> >> (+)-CC-1065.<sup>45</sup>

The enhanced activity of analogues containing the CBI alkylating subunit, over the CPI analogues is assumed to be associated with the decreased strain of six membered compared to five membered aromatic rings.<sup>46</sup> This expansion results in a fourfold decrease in reactivity, as well as a fourfold enhancement of stability and cytotoxic potency without altering sequence selectivity.<sup>14,46</sup> Furthermore the increased rate of CBI DNA alkylation has been attributed to the decrease in steric bulk surrounding the C7 centre of CPI due to the absence of the C7 methyl group. Interestingly, it has been found that a C7 methoxy (MCBI) or C7 cyano substituent (CCBI) (Figure 10) have only a small effect on the reactivity of the agents.<sup>14</sup>

As a result of these observations, it was proposed that a direct relationship between functional stability and cytotoxicity and an inverse relationship between solvolytic reactivity and cytotoxicity existed.<sup>43,47</sup> This supports the proposal that the observed enhancement of CBI cytotoxicity over CPI containing analogues is due to the increased stability and therefore enhanced delivery to the intracellular target.<sup>14,47</sup>

#### 1.4.1b MCTFCPI:

The recent development of MCTFCPI derivatives (Figure 11), bearing methoxycarbonyl and trifluoromethyl groups, has revealed more potent CPI analogues with increased antitumor activity and decreased toxicity against murine leukemia than the known CPI derivatives, including the clinical candidate Adozelesin (section 1.6.1).<sup>48</sup>

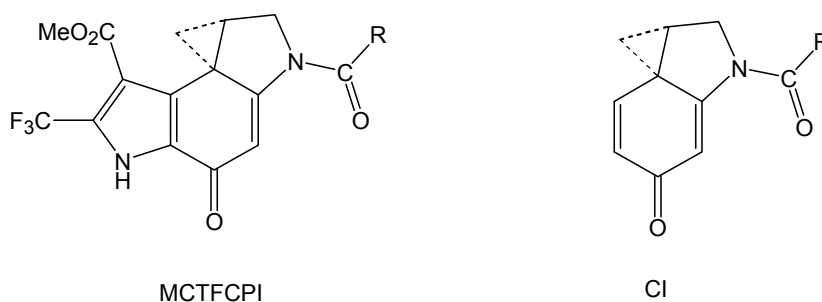


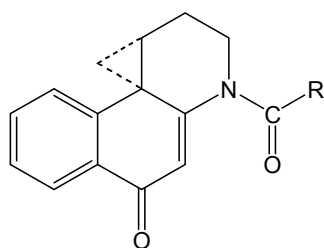
*Figure 11 – CPI Analogues, MCTFCPI and CI*

#### 1.4.1c CI:

CI (Figure 11) has been found to constitute the minimum, potent pharmacophore of CC-1065 and the duocarmycins.<sup>21,33,49</sup> The CI-based agents are extremely reactive electrophiles and show similar alkylation selectivities to CC-1065 and the duocarmycins. However, they alkylate DNA less efficiently and less selectively and exhibit decreased cytotoxic potency. This decrease in selectivity was thought to result from the removal of the CPI C7 methyl group leading to the speculation that the pyrrole segment (in particular the C7 methyl group) played an important function in alkylation selectivity. The CI alkylating subunits follow a similar alkylation intensity trend to CBI analogues, i.e. CI-CDPI<sub>2</sub>>CI-CDPI<sub>1</sub>>>N-Boc-CI, with the natural enantiomers possessing more potent alkylating activity.<sup>38</sup>

#### 1.4.1d CBQ:

The CBQ based agents (Figure 12) have been found to alkylate DNA at the same sites as the corresponding enantiomers of agents incorporating CPI, CBI and CI. However, consistent with their reactivity, they exhibit less selectivity and alkylate with lower efficiency.



CBQ

*Figure 12 – CBQ*

As previously discussed, agents showing greater solvolytic stability exhibit enhanced cytotoxic potential,<sup>50-52</sup> probably due to their more effective delivery to the target DNA.<sup>14,36,43</sup> Solvolysis reactivity has been shown to be influenced by the N2 substituent which determines the ease of C4 carbonyl protonation required for solvolysis, where stronger electron withdrawing substituents exhibit slower solvolysis rates and therefore greater stability and cytotoxic activity.<sup>14,45</sup> The correlation between the solvolytic reactivity ( $k_{\text{solv}}$ , pH 3) and the cytotoxic potential ( $IC_{50}$ ) of CBQ analogues is shown (Table 2).

R	$k_{\text{solv}}$ ( $\text{s}^{-1}$ , pH 3)	IC <sub>50</sub>	
SO <sub>2</sub> Et	$0.5 \times 10^{-6}$	24 nM	
COEt	$2.0 \times 10^{-6}$	110 nM	
CO <sub>2</sub> CH <sub>3</sub>	$3.4 \times 10^{-6}$	140 nM	
CONHMe	$5.4 \times 10^{-6}$	200 nM	

**Table 2:** Correlation Between Solvolytic Reactivity, Biological Potency and Electron-Withdrawing Properties of the N<sup>2</sup> Substituent of CBQ.<sup>48</sup>

X-ray crystallographic comparisons of CBI and CBQ agents have provided an additional explanation for the observed variance in solvolytic stability, and, therefore cytotoxic potency. The explanation stems from an elemental difference in the geometry and alignment of the cyclopropane relative to the cyclohexadienone  $\pi$ -system (Figure 13). The orbital of the cyclopropane bond bound to C9a in the CPI and CBI subunits is almost perpendicular to the plane of the cyclohexadienone. As such, it overlaps with the  $\pi$ -system of the developing solvolysis (phenol) product. However, the cyclopropane bond to the tertiary carbon is almost in the plane of the cyclohexadienone and has an orbital orthogonal to the  $\pi$ -system of the solvolysis product. Consequently, nucleophilic addition occurs almost exclusively at the least substituted carbon, overriding any preference for ring expansion.<sup>47</sup>

In contrast, the cyclohexadienone  $\pi$ -system of the CBQ agents bisects the cyclopropane. As a result of this bisection, the bonds extending to the secondary and tertiary carbons are equally aligned with the  $\pi$ -system allowing both cyclopropane bonds to be equivalently aligned for cleavage and addition.<sup>47</sup> In summary, the increased reactivity and therefore decreased cytotoxic activity of CBQ based agents in comparison to the CBI and CPI based agents is related to their heightened solvolytic reactivity, which results from nucleophilic addition occurring at both cyclopropane bonds. Nucleophilic addition in the CPI and CBI agents occurs almost solely at the least substituted carbon within the cyclopropane ring and as such, enhancement of solvolytic stability results.<sup>14</sup>

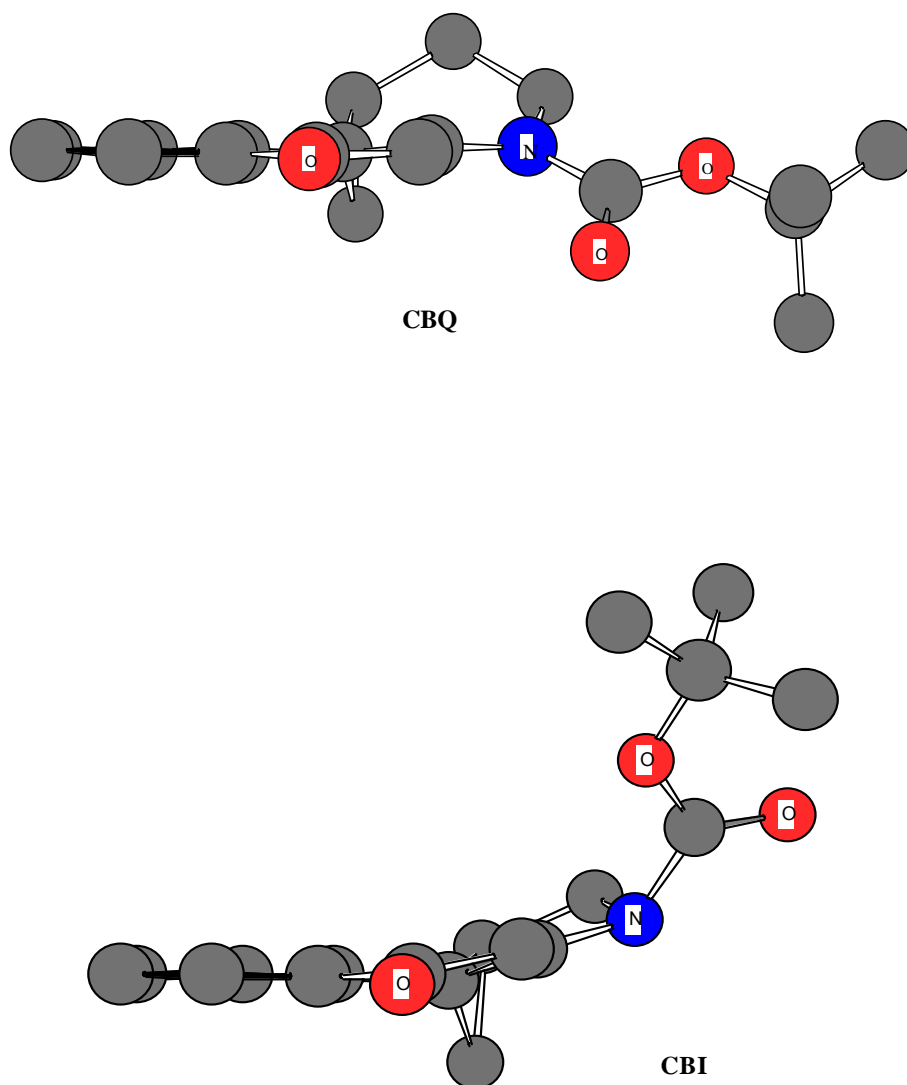


*Figure 13 – Comparison of the Alignment of the Cyclopropane with the Cyclohexadienone in CBQ and CBI.*

The CBQ cyclopropane bond lengths (1.528 and 1.543 Å relative to the lengths 1.508 and 1.532 Å of the CBI subunits) and weaker bond strengths also reflect this enhanced solvolysis reactivity. It is thought the lengthening of these bonds may result from delocalisation of both cyclopropane bonds with the cyclohexadienone  $\pi$ -system.<sup>47</sup>

#### 1.4.1e CNA:

CNA is a seven membered analogue of the CC-1065 alkylating subunit exhibiting a reactivity that is 4750x and 75x that of the corresponding CBI and CBQ subunits respectively. This increased reactivity is related to a decrease in vinylogous amide stabilization upon N-acylation (Figure 14) that results from an increase in the C-N bond length from 1.390 Å (CBI) and 1.415 Å (CBQ) to 1.428 Å.

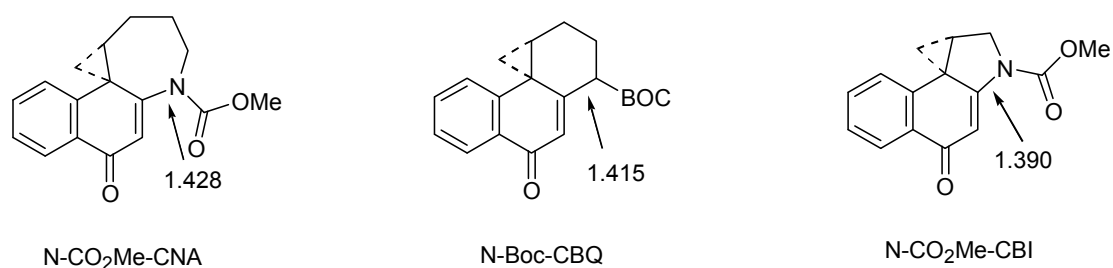


*Figure 14 – Bond Lengths of CNA, CBQ and CBI*

The decrease in vinylogous amide conjugation resulting from N-acylation is also accompanied by an increase in length and therefore realignment of the reactive cyclopropane bonds, allowing their favorable conjugation with the cyclohexadienone  $\pi$  system. Another factor resulting in decreased vinylogous amide stabilization and therefore increased reactivity is the increase in the  $\chi_1$  dihedral angle of the N<sup>2</sup> amide (Figure 15). This angle is so large in N-CO<sub>2</sub>Me-CNA that the acyl group is nearly perpendicular to the plane of the cyclohexadienone  $\pi$  system and vinylogous amide conjugation is virtually absent<sup>53</sup>. As a result of these three factors, CNA-based agents exhibit a cytotoxicity that is more potent than the corresponding CBQ, CBI and CI-based alkylating agents.

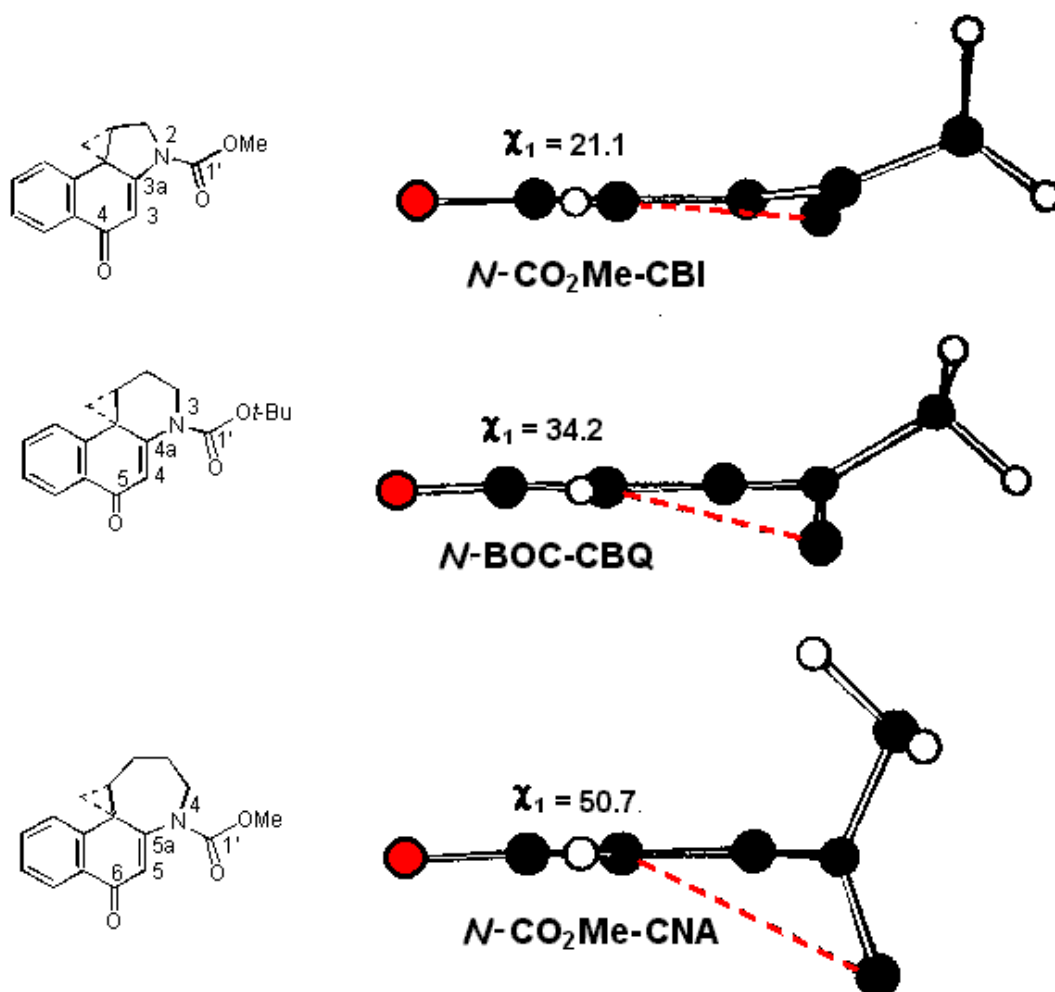


*Figure 15 – Stick Models Showing the  $\chi_1$  Twist Angle of the Vinylogous Amide (Taken from Reference 53)*

#### 1.4.1f C-4 Carbonyl Relocation:

Studies conducted by Boger *et al.*<sup>54</sup> looked at the effects of isomerically repositioning the C-4 carbonyl of CI and CBI adducts to the C-6 and C-8 positions respectively (figure 16). Structural studies have indicated that the C-4 carbonyl of the natural DNA-agent adduct projects out of the minor groove hence encouraging backbone phosphate protonation. This is thought to activate the agent for DNA alkylation thereby influencing sequence selectivity.<sup>54</sup>

In contrast, relocation of the carbonyl group to the C-6 and C-8 position would require that it project into the minor groove placing it out of proximity to the phosphate backbone. However, these studies indicate that these analogues retain sequence selectivity specific to their C-4 carbonyl counterparts thereby suggesting that protonation of the C-4 carbonyl is not mandatory in determining sequence selectivity.<sup>54</sup>

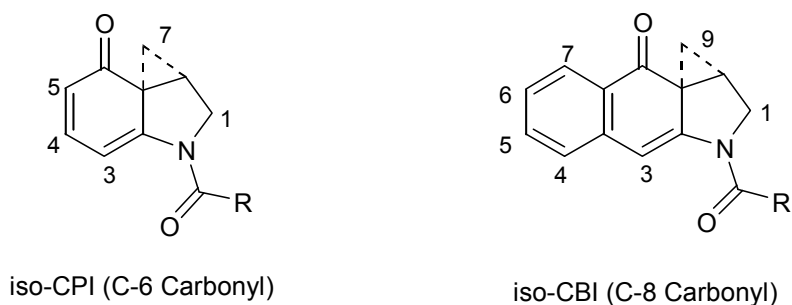


*Figure 16 – iso-CPI and CBI Analogues*

#### 1.4.1g Comparison of Alkylating Subunit Analogs.

The order of stability of the common alkylating subunits is CNA>CBQ>DSA=CBI=MCBI=CCBI >C7-MeCPI>DA>CI. This order can be ascribed to the gain in delocalisation energy that accompanies aromatisation in systems that bear a fused aromatic ring. The increased stability of DSA (Figure 17) over CPI, and DA (Figure 17) over CI can be attributed to the conjugated electron-withdrawing group that diminishes C4 carbonyl protonation which is required for solvolysis.<sup>56</sup> Furthermore, the increased stability of CBI over CPI results from the decrease in strain that results with the substitution of a five membered ring for a six membered ring.<sup>45</sup>

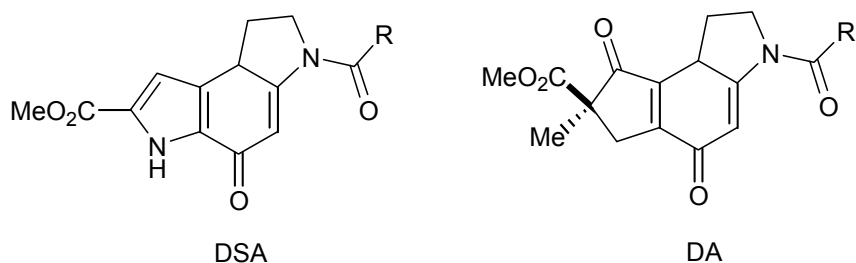


*Figure 17 – DSA and DA.*

The development of a pyrazole analogue, CpzI, (Figure 18) of the CPI alkylating class of agents has recently been reported.<sup>51</sup> The rationale for this investigation was based on the proposal that the electron withdrawing nitrogen on the pyrazole functionality may play a similar role to that of the carbomethoxy group of DSA. The presence of this electron withdrawing group has been shown to effectively slow down C4 carbonyl protonation which is required for solvolysis and cyclopropyl ring opening. As a result of this enhanced stability a two-fold increase in cytotoxic potential over CPI was observed.<sup>51</sup>

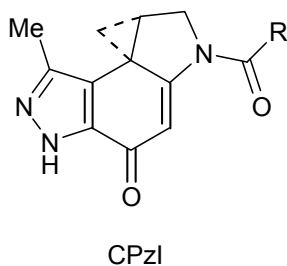


*Figure 18 – CPzI.*

#### 1.4.2 Variation in the Noncovalent Binding Subunit –

##### 1.4.2a CDPI<sub>n</sub>:

An important role of the noncovalent binding subunits of the natural enantiomers is stabilization of the potentially reversible covalent alkylation.<sup>16</sup> An additional role includes the restriction of the number of accessible adenine alkylation sites through bonding in the sterically more accessible A-T rich minor groove.<sup>57</sup>

In order to examine this important contribution of the central and right hand units on sequence selectivity, the CDPI analogue (Figure 19) which lacks the 4-hydroxy and 5-methoxy groups was developed. Like its predecessor PDE-I, this agent was found to exhibit a preference for A-T rich regions of DNA due to its stabilization within the narrow and more readily accessible A-T rich minor groove.<sup>58</sup>

CPI analogues bearing the CDPI noncovalent binding subunits were found to exhibit indistinguishable properties to the CC-1065 precursor indicating that the 4-hydroxy and 5-methoxy groups made no contribution to the alkylation efficiency or selectivity.<sup>41,59</sup>

In fact, the CDPI<sub>n</sub> based agents were found to follow the pitch of the minor groove more accurately than CC-1065. The absence of the C4 phenol in CDPI accounts for this phenomenon, as the hydrogen bonding which occurs in CC-1065 between the phenol and nearby carbonyl is thought to introduce an exaggerated pitch and prevent close association with the minor groove of DNA.<sup>14,59</sup>

The binding constant order for the CDPI<sub>n</sub> series, CDPI<sub>3</sub>>CDPI<sub>4</sub>>CDPI<sub>2</sub>>CDPI<sub>1</sub>, showed the CDPI<sub>3</sub> trimer to possess optimum binding due to its ability to span the largest site accessible, with synchronous binding of both ends of the agent.<sup>40,59</sup> Because of the absence of functional groups which could provide hydrogen bonding to DNA, most of the CDPI interactions occur through van der Waals contacts.<sup>14,59</sup>

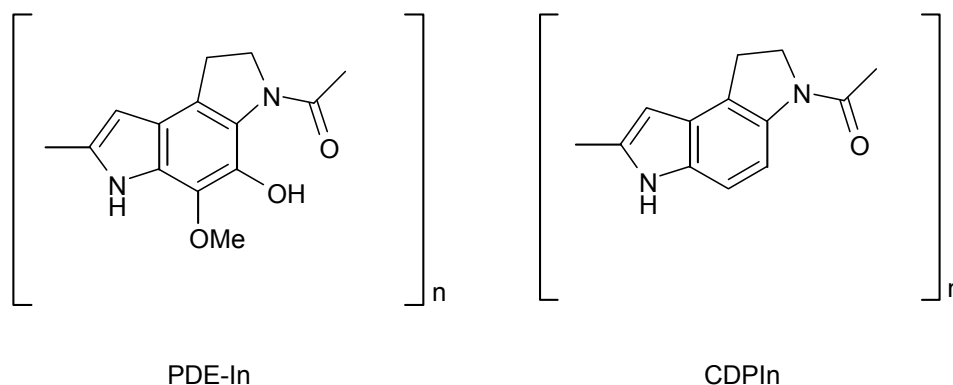
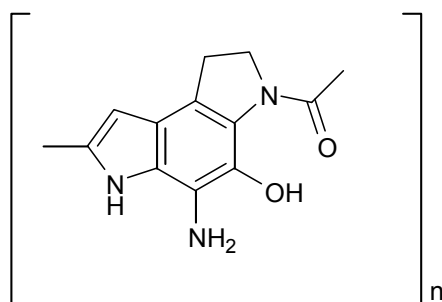


**Figure 19 – PDE-I<sub>n</sub> and CDPI<sub>n</sub>**

#### 1.4.2b ACDPI<sub>n</sub>:

ACDPI (Figure 20) differs from CDPI only in that it possesses a C5 amino substituent. However, this additional functionality proved detrimental to the molecules binding affinity through the introduction of unfavorable electrostatic interaction with the negatively charged phosphate backbone.<sup>41,58</sup> The C5 amino group introduction however, did not alter the selectivity for AT rich regions of DNA.<sup>58</sup>

In spite of the reduction in binding affinity, the ACDPI series was found to possess a corresponding binding constant order with the ACDPI<sub>3</sub> trimer possessing the most favorable binding. Full structure binding was not possible as the size of the agent was increased beyond three subunits, as the binding termini lie on opposite faces of the helix.<sup>58</sup>



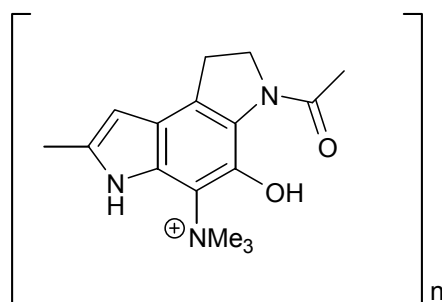
ACDPI<sub>n</sub>

*Figure 20 - ACDPI<sub>n</sub>*

#### 1.4.2c TACDPI<sub>n</sub>:

Following the discovery that electronegative substituents (such as the C5 amino group in ACDPI) resulted in a decrease in binding affinity, analogues possessing an electropositive C5 substituent were developed. The TACDPI series (Figure 21) possesses an electropositive trimethylammonium substituent which increases the DNA binding affinity via the stabilization of electrostatic interactions.<sup>58</sup> Consistent with expectations, the binding affinity of the agents in this series increased as the size of the agent increased (TACDPI<sub>3</sub>>TACDPI<sub>2</sub>>TACDPI<sub>1</sub>).

The binding affinity of the TACDPI series significantly exceeds that of the ACDPI series and surpasses that of the CDPI series. This observation was related to the favorable electrostatic interactions between the electropositive trimethylammonium substituent and the negatively charged phosphates in the DNA backbone.



TACDPI<sub>n</sub>

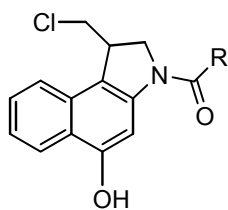
*Figure 21 - TACDPI<sub>n</sub>*

### 1.4.3 Variation in Linker and Terminal Amides –

Studies conducted by Wang *et al.*<sup>60</sup> further support for the theory that hydrophobic interactions and van der Waals contracts between the drug and DNA are vital in determining the potency of CC-1065 class compounds.

This study reported the biological activity of CBI analogues possessing altered linkers and terminal amides. Here it was shown that analogues comprising two indoles (B), or an indole and benzofuran moiety (C), are more potent than analogues comprising a single indole (A) (Figure 22).<sup>60</sup>

Further comparisons between terminal amides supported this trend by showing a 50-fold increase in potency for analogues bearing the more hydrophobic butyramino group (D) compared to their acetamino counterparts (C).<sup>60</sup>



R =

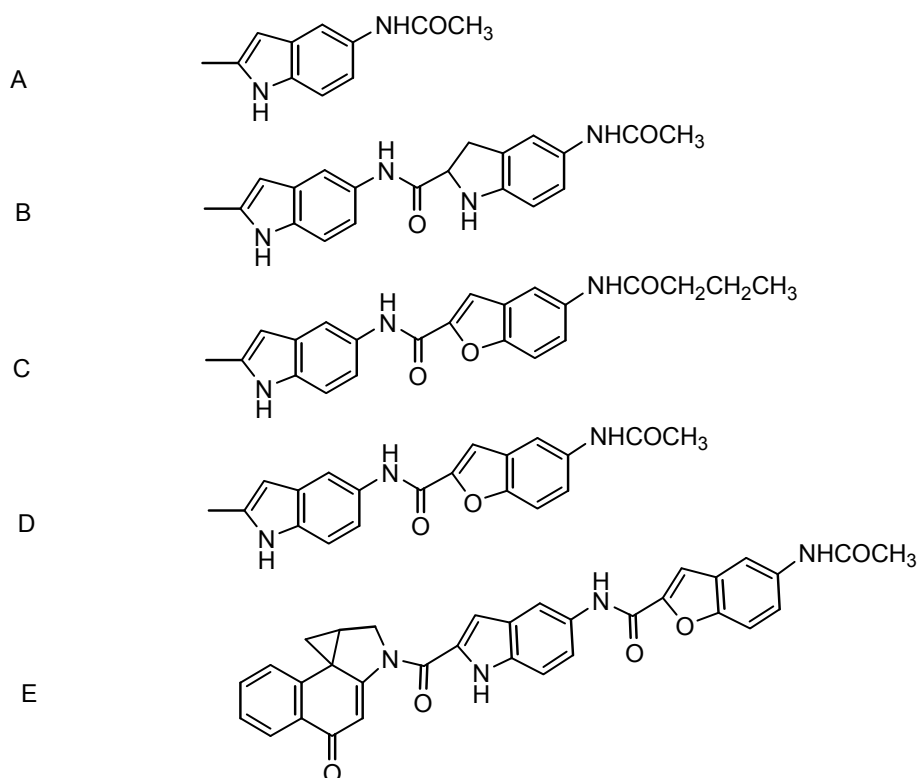


*Figure 22 – Terminal Amide and Linker Variation*

#### 1.4.4 Water Solubilised CPI Analogues Containing Polypyrrole Minor Groove Binders -

In order to overcome the poor water solubility and limited sequence specificity of individual alkylating subunits, Baraldi et al<sup>61</sup> has recently synthesized and evaluated a series of hybrids which combine the simple CPI alkylating subunit with polypyrrole minor groove binders.

These lexitropin groove binders (consisting of either one or two N-methyl pyrroles) serve as DNA binding vectors which can permeate cell membranes and have the potential to control

specific gene expression, therefore enhancing delivery and sequence specificity of the reactive group.<sup>61</sup> Furthermore, the water solubility of the hybrid compounds overcame the administration problems of previous CC-1065 derivatives.

The hybrids (Figure 23) were found to be between 8 and 70 fold more potent than the alkylating subunit alone. Compound (n=3) was the most active ( $IC_{50} = 7.4$  nM) and displayed preferential sequence specific DNA alkylation at the third adenine in the sequence 5'-ACAAAAATCG-3'. Compounds (n=1) and (n=2) displayed slightly lower cytotoxicity at  $IC_{50}$  values of 58 and 19 nM respectively.<sup>61</sup>

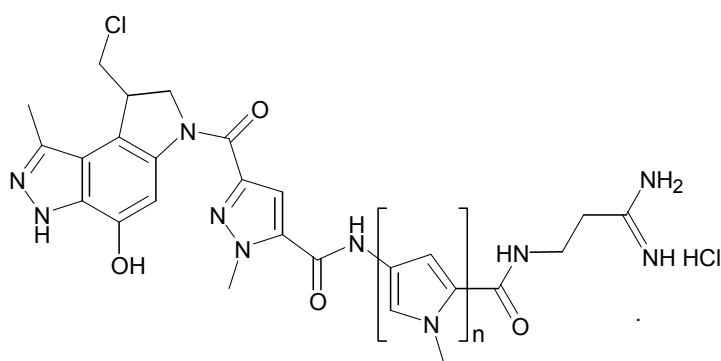


**Figure 23 - CPI-Lexitropin Hybrids**

#### 1.4.5 Summary –

While the substitution of either the alkylating or nonalkylating binding subunits has a broad range of effects with respect to solvolytic stability, reactivity, sequence selectivity, rate and efficiency of alkylation and cytotoxicity, all agents consisting of these subunits alkylate within A-T rich minor groove regions of DNA.

This concurrence results from the steric accessibility of A-T rich regions which permit the deeper penetration that is required for stabilizing van der Waals contacts, hydrogen bonding and hydrophobic binding to occur. Furthermore, X-ray crystallographic studies have shown the A-T rich minor groove is constricted thereby enhancing the stabilizing van der Waals contacts.

Several trends can be observed within the DNA alkylating and non-alkylating subunit analogues. As the alkylation subunit reactivity increases the efficiency of DNA alkylation decreases due to the detrimental expenditure of the more reactive subunits.<sup>62</sup> Furthermore, as the number of noncovalently binding subunits increases up to three, there is a corresponding increase in the DNA binding affinity. More recently, this same trend has been demonstrated by CBI analogues containing dimeric monocyclic, bicyclic and tricyclic heteroaromatic replacements.<sup>63</sup> As a result, the rate and efficiency of DNA alkylation is enhanced<sup>13</sup> with a concomitant increase in cytotoxicity. Finally, the more electropositive the pendant substituent on these subunits, the greater the interaction with the phosphate anions on the DNA backbone and the tighter the binding.<sup>56</sup>

## **1.5 RECENT ADVANCES IN CC-1065 DEVELOPMENT:**

### **1.5.1 Glucoronide derivatives of CC-1065 for use in ADEPT**

As previously discussed in Section 1.2.5, the use of ADEPT is advantageous in that it enhances the tumor versus non-tumor cell drug specificity. Recently, Wang *et al.*<sup>64</sup> reported the synthesis of several glucoronide derivatives of CC-1065 that are less toxic than their hydroxyl counterparts (Figure 24).

The enzyme,  $\beta$ -glucuronidase is responsible for the cleavage of the glucoronide group from the prodrug and is abundant in breast tumors. As such, it was envisaged that this therapy would be useful in the treatment of such cancers. Give that  $\beta$ -glucuronidase levels in human serum are relatively low, glucoronide derivatives are more likely to remain stable in blood following i.v. administration.

When tested against U937 monocytic leukemia cells, the glucoronide analogues (Figure 24, n=1 and n=2) were approximately 2- and 6-fold less toxic than their hydroxyl counterparts. The IC<sub>50</sub> values reported for these agents were however diminished (IC<sub>50</sub> 1.4nM and IC<sub>50</sub> 0.6nM *c.f.* hydroxyl counterparts i.e. IC<sub>50</sub> 0.6nM and IC<sub>50</sub> 0.1nM).

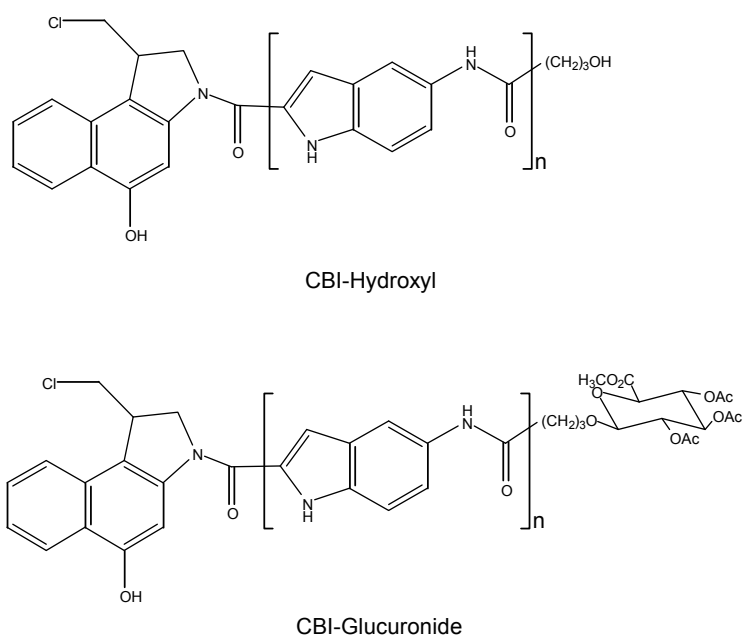


**Figure 24 – Derivatives of CC-1065**

### 1.5.2 The Relationship between Reactivity and Cytotoxic Potency –

Recent studies by Boger *et al.*<sup>69,70</sup> upon N-aryl and N-alkenyl CBI derivatives (Figure 25) indicate that a parabolic relationship exists between reactivity and cytotoxic potency. This was determined by plotting the data from solvolytic and cytotoxicity studies ( $-\log k$ , pH3 versus  $IC_{50}$ ) on both natural and unnatural enantiomers of the aforementioned derivatives. As expected, the unnatural enantiomers were 5- to 10-fold less potent than the natural enantiomers.

As hypothesized, the parabolic relationship establishes that while alkylating compounds need to possess sufficient stability to reach their target they also need to possess sufficient reactivity toward DNA upon reaching their target to maintain their cytotoxicity.<sup>69,70</sup>

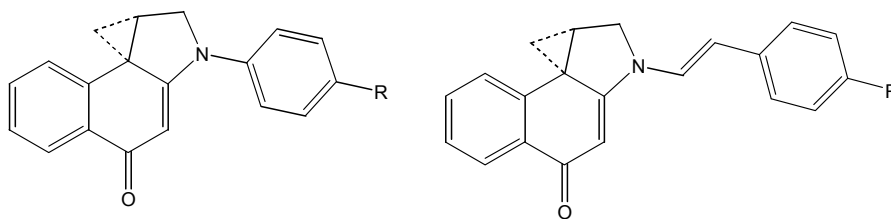


**Figure 25 - N-aryl and N-alkenyl CBI Derivatives**

### 1.5.3 Achiral Compounds –

Seven achiral *seco*-amino-CBI analogues of CC-1065 were recently synthesized by Sato *et al.* and evaluated for their anticancer and DNA binding properties (Figure 26).<sup>71</sup> Each of these compounds contained a substituted 2-chloroethylnaphthalene moiety and lacked a stereocenter. The exposure of these drugs to several cell lines indicated that each compound demonstrate significant cytotoxicity, with IC<sub>50</sub> values in the sub-micromolar range.

Like their *seco*-CC-1065 analogues, the achiral analogues exert their cytotoxicity through the induction of apoptosis.<sup>71</sup> Furthermore, several of these compounds lack the delayed *in vivo* toxicity previously shown by their racemic counterparts, and as such may form a novel class of antitumor CC-1065 analogues.

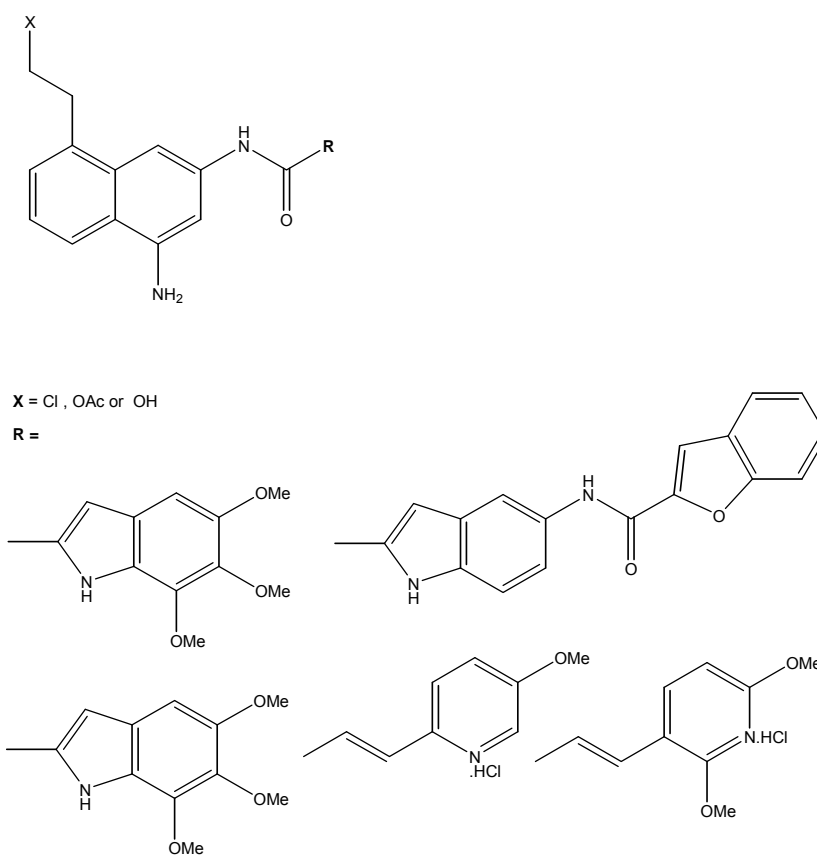


**Figure 26 – Achiral seco-Amino-CBI Analogues of CC-1065**

#### 1.5.4 The Synthesis of New CC-1065 Analogues Bearing Different DNA-Binding Subunits

Substituents on the DNA-binding subunits of CC-1065 have been found to have profound effects on the compound's antitumor potency and efficacy. A C5-acyl group was found to increase the agent's potency by more than 1000-fold *in vitro*.<sup>72,73</sup> Recent studies have shown that CC-1065 analogues bearing terminal C5-NO<sub>2</sub> and -F moieties on the DNA-binding subunit demonstrate increased drug potency and antitumor efficacy. In contrast, the substitution of C5-OCH<sub>3</sub> at this same site resulted in reduced potency and caused delayed death in mice (Figure 27).<sup>74</sup>

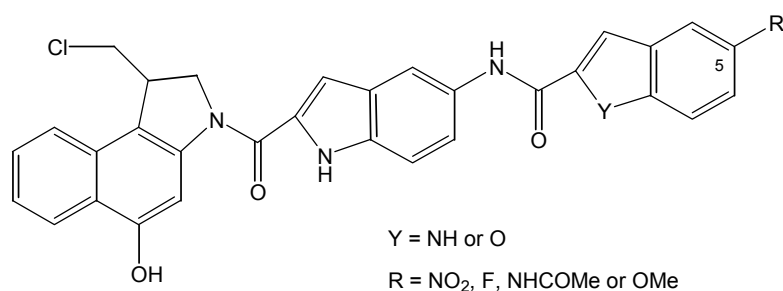


**Figure 27 – New CC-1065 Analogues**

The results from these studies demonstrate that an electron-withdrawing moiety at C5 leads to increased cytotoxicity. As such, compounds bearing -NO<sub>2</sub> and -F at C5 on the DNA-binding subunit are more potent than those bearing amido and -OMe groups at the same substitution site.<sup>74</sup>

## **1.6 SYNTHETIC ANALOGUES OF CC-1065 IN CLINICAL TRIALS:**

### **1.6.1 Adozelesin –**

The first clinical candidate developed within the CC-1065 class of DNA alkylators was Adozelesin (U-73,975) (Figure 28). This agent exhibits comparable potency and antitumor activity to CC-1065.<sup>14</sup> The use of Adozelesin is preferable because it does not exhibit the delayed toxicity characteristic of CC-1065 and its analogues.<sup>57-59</sup> It has been proposed that this absence of delayed toxicity is related to the reversibility of the Adozelesin-DNA binding. Furthermore, oxidation of the methoxy groups of the central and right-hand subunits to an extended *para*-quinone imine is thought to contribute to the delayed toxicity of (+)-CC-1065.<sup>14</sup> The absence of these groups in Adozelesin and the following clinical candidates may be a further reason for the absence of this delayed toxicity.

Adozelesin's mechanism of cytotoxicity has been attributed to the inhibitory effect upon the initiation<sup>75</sup> and more recently elongation phases of DNA replication without affecting RNA or protein metabolism.<sup>76</sup> This mechanism has been exhibited by both UV radiation and the widely studied methyl methane sulfonate and is believed to be a direct result of the activation of an intra-S-phase DNA damage checkpoint upon Adozelesin binding.<sup>76</sup> Studies involving

SV40 DNA indicate that this activation results in an increase in p53 protein levels, inactivation of replication protein A (RPA) and therefore disruption of the p53-RPA complex that is required for DNA replication.<sup>78</sup>

Although Adozelesin exhibits an unfavorably short half life of less than 1 hour<sup>79</sup> it exhibits exceptional broad spectrum *in vivo* activity, exhibiting a curative response to P338 and L1210 leukemia as well as Lewis lung carcinoma with single administration. Phase I trials indicated that Adozelesin was well tolerated at doses as high as 188mg/m<sup>2</sup> and has been recommended for phase II trials.<sup>79</sup>

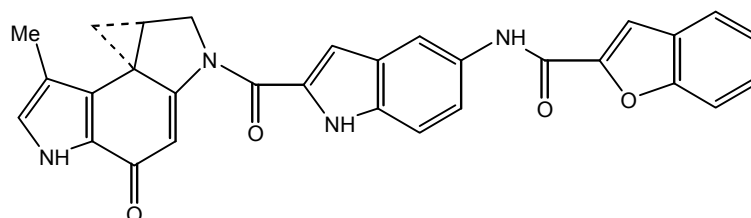


**Figure 28 – Adozelesin**

### 1.6.2 Carzelesin –

Carzelesin (Figure 29) is a CPI derived prodrug which requires either chemical and/or enzymatic activation for conversion to the active DNA alkylating product. Although similar in structure to Adozelesin, differences include the presence of a chloromethyl substituent in place of the cyclopropane and a diethylamino substituent on the right hand benzofuran moiety which has been found to improve the efficiency of the agent against L1210 leukemia *in vivo*.<sup>80</sup>

The final and most significant alteration which is central to the longer half life of Carzelesin is the presence of a phenylurethane moiety which is bonded to the phenolic oxygen. While the principal purpose of the phenylurethane moiety is to modulate the rate of formation of the cyclopropane containing drug, increased stability also occurs as a result of this modification.<sup>80</sup>

Two steps are required for the conversion of Carzelesin to its active alkylating form. The first step involves hydrolysis of the phenylurethane moiety either in the liver or in serum to form the intermediate U-76,073. This is followed by ring closure of the chloromethyl substituent to form the cyclopropane containing U-76,074.

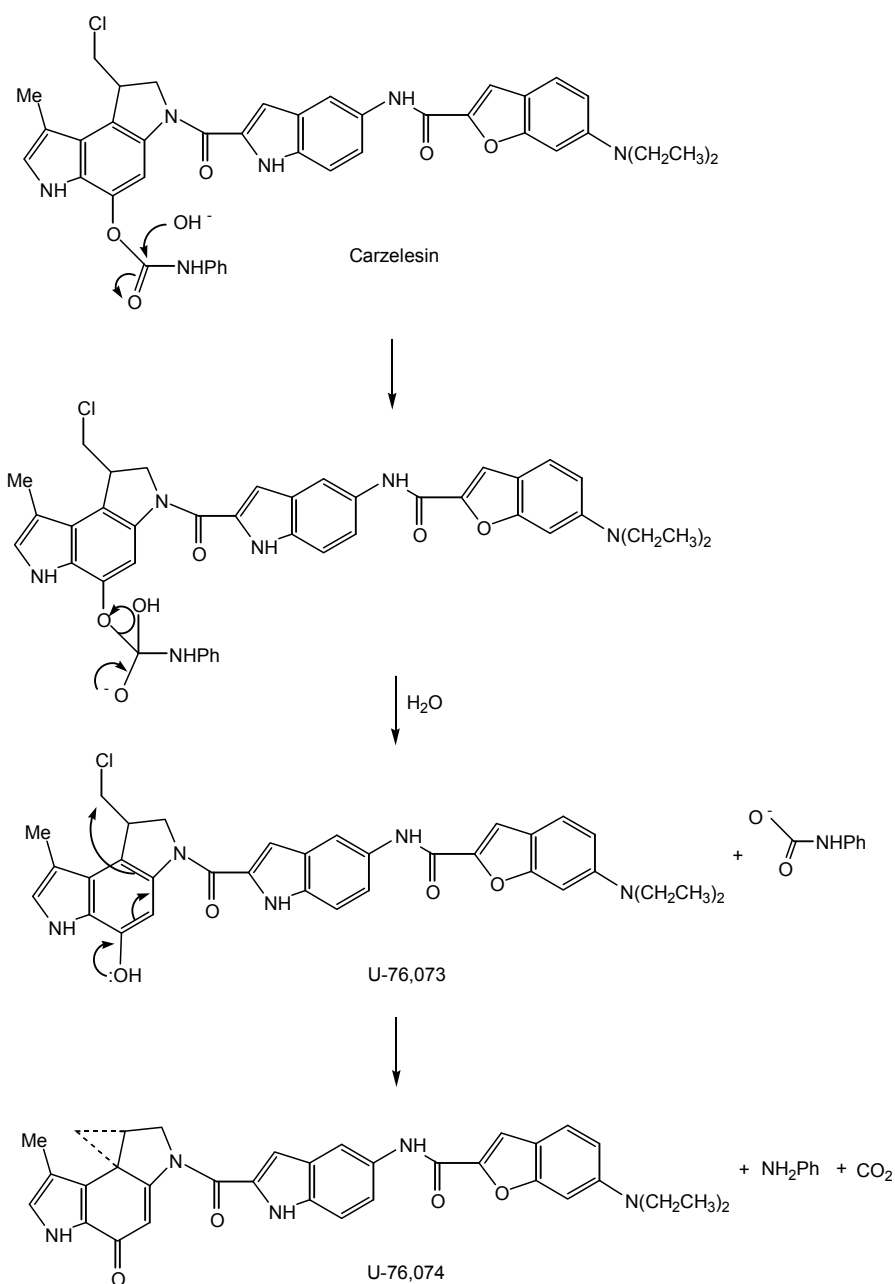


**Figure 29 – Carzelesin and Major Degradation Products, U-76,073 and U-76,074**

Carzelesin possesses an advantage in that it is more efficacious than Adozelesin against L1210 leukemia and pancreatic ductal adenocarcinoma which have been reported to be resistant to all other agents tested.<sup>81</sup> Carzelesin also proved to be effective against Lewis lung carcinoma, colon CX-1 adenocarcinoma, lung LX-1 tumors and prostatic DU-145 independent of the route of administration.<sup>81</sup>

Even more promising was the ability of Carzelesin to induce 100% complete remissions in studies of mice bearing early stage human ovarian 2780 carcinoma, with no tumor regrowth even after treatment termination. This exceeds the results obtained in studies with Adozelesin where tumor regrowth became evident shortly after termination of the agents administration.<sup>81</sup>

The increased therapeutic efficacy of Carzelesin is thought to be related to its slower rate of clearance and therefore better cellular distribution, which is conferred by increased stability of the prodrug mode of delivery.<sup>81</sup>

### 1.6.3 U-71,184 –

U-71,184 (Figure 30) is a potent antitumor agent, which demonstrates greater potency than CC-1065 and does not exhibit delayed death in mice. Essentially, U-71,184 (which is very similar in structure to Adozelesin) possesses similar dimensions and electronic features to CC-1065, however it is a simplified model which confers the added advantage of being more synthetically accessible.<sup>82</sup>

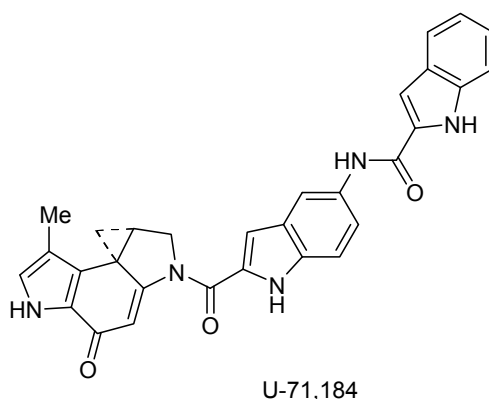


*Figure 30 – U-71,184*

### 1.6.4 Bizelesin –

Bizelesin (U-77,779) is an extremely cytotoxic CPI containing bisalkylator which has been investigated in preclinical trials and shown to have high specificity, relative to Carzelesin, toward all types of colorectal cancer. This compound differs from the preceding analogues in

its ability to cross-link DNA (Figure 31). This cross-linking activity is enabled by the two chloromethyl moieties that are connected by an indole-ureido-indole spacer.<sup>83</sup>

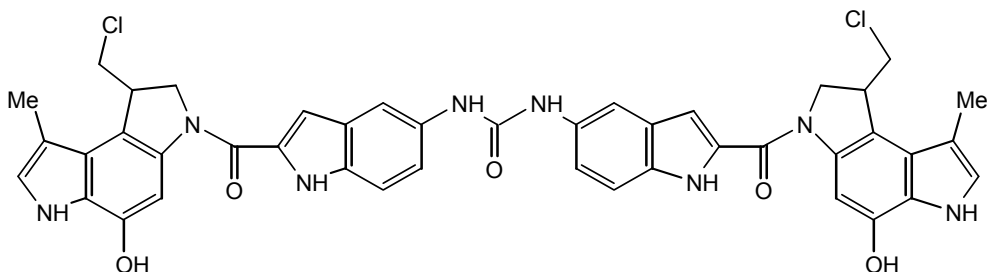


**Figure 31 - Bizelesin**

CC-1065 and its later analogues, Bizelesin shows a preference for A-T rich regions of the minor groove and both chloromethyl moieties interact covalently with adenine at N-3.<sup>12</sup> U-77,779 was found to induce ISC at two major sequences. The first spans 6 nucleotides with preference for two 5'-TTA-3' sequences within the 5'TAATTA-3' sequence.<sup>84</sup> The second prefers bent DNA tracts and spans 7 nucleotides.<sup>84</sup> The advantage of Bizelesin is that it lacks the delayed toxicity of many of the preceding CC-1065 analogues and induces fewer lesions than Adozelesin.<sup>83-87</sup> Also favorable is the enhanced stability, sequence selectivity, antitumor efficacy and cytotoxicity<sup>80</sup> of the interstrand cross-links (ISC) (Figure 32) formed by Bizelesin over its monoalkylating counterparts.<sup>80</sup> Conversion of the chloromethyl moieties to cyclopropyl intermediates is assumed to occur prior to covalent interaction with DNA.<sup>83</sup>

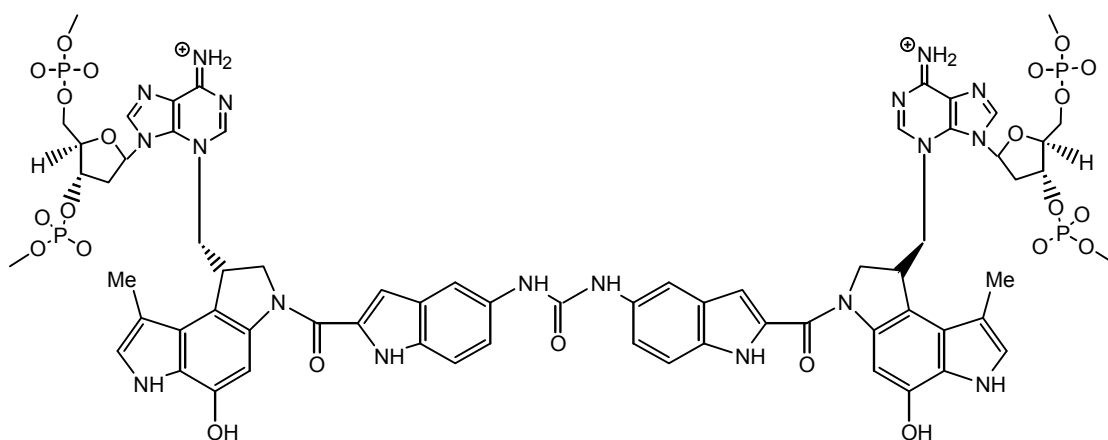


**Figure 32 – Bizelesin and ISC Formation By Bizelesin**

Bizelesin shows a high propensity for alkylation at the site 5'-TAATTA\*<sup>81</sup> with initial monoalkylation preference for sites which are found six basepairs to the 3' side of thymidine.<sup>88</sup> Alkylation at non-adenine bases (particularly at G) also occurs in a number of cases and is thought to be due to the immobilization of the second alkylation arm by the first, at a normally non-reactive base.<sup>85</sup> This non-adenine alkylation has been shown to be the second step in the formation of cross-links and occurs much slower than the first.

Unlike the corresponding monoalkylators, the binding of Bizelesin to duplex DNA does not result in any net bending of DNA and has even been observed to eliminate the bending usually found in A-tract containing DNA.<sup>16,82</sup> The absence of any obvious conformational change in Bizelesin cross-linked DNA is a consequence of drug induced bending into the minor groove on opposite sites of the helix, effectively canceling out any net bending around the cross-linked region.<sup>63,7</sup>

In nearly all cases, cross-links were found to form between one adenine and another six basepairs away on the opposite strand.<sup>7,79,89</sup> Because interstrand cross links have been proposed to form at sites at which minimal distortion energy is required,<sup>85</sup> it is thought that ISC formation between one adenine and another (or a non-adenine base) six base pairs apart is preferred due to the lower distortion energy provided by the more favorable cross link conformation.<sup>83</sup> Of all the clinical candidates currently in trial Bizelesin exhibits the most promising attributes.

## **1.7 MECHANISMS OF CYTOTOXIC ACTION BY CC-1065 AND RELATED STRUCTURAL ANALOGUES.**

### **1.7.1 Overview –**

CC-1065 is an exceptionally potent antitumor agent that is capable of inducing a growth inhibition of up to 90 percent in certain cancer cell lines, at concentrations as low as 40 picograms/millilitre.<sup>90</sup> The mechanisms by which CC-1065 and its structurally related analogues exert these biological effects are believed to include: inhibition of DNA processing enzymes, activation of apoptosis and cell cycle intervention.

### **1.7.2 The Inhibition of DNA Processing Enzymes –**

CC-1065 and analogues of this agent have been found to exert an inhibitory effect upon several DNA processing enzymes, including DNA polymerase, helicase, T4 ligase and S1 nuclease. Because of the importance of these enzymes in essential cellular activities, any termination of their activity results in cell death.

#### **1.7.2a Polymerase Inhibition:**

CC-1065 and particular synthetic analogues of varying cytotoxicity are able to inhibit the progression of *E. Coli* DNA polymerase, Klenow fragment and T4 DNA polymerase, resulting in the termination of replication and subsequent cell death.<sup>4,14,91</sup> This inhibition is thought to result from the hindrance of base pairing around the lesion site (due to blockage of polymerase progression by the drug-DNA adduct) rather than the repression of polymerase binding.

The pause site of the polymerase is one base before the modified adenine within the sequence 5'-GATTA\* and two bases before the modified adenine in the sequence 5'-AGTTA suggesting an inherent difference in the conformation of these two sequences.<sup>4</sup> As a result it can be seen that the termination of polymerase progression is dependent on the conformational distortion which occurs as a consequence of drug-DNA adduct formation.

CC-1065 is a powerful mutagen and is capable of inducing base pair misincorporation prior to the modified adenine, particularly when alkylation occurs within the sequence 5'-GATTA\*.<sup>4</sup> Usually this mutation involved the misincorporation of dA for dG before the modified adenine.

#### **1.7.2b Helicase Inhibition:**

Helicase II plays an important role in replication, transcription, recombination and repair<sup>92</sup> and, as such, any inhibition of its unwinding ability results in subsequent cell mortality.

In addition to the bending and stiffening of the helix caused by CC-1065 and various related analogues, a significant DNA winding effect of 1 base pair per adduct site has been observed and is implicated in the delayed lethality of these drugs.<sup>4,14,93</sup> This inhibition of unwinding by select analogues has been found to result in inhibition of unwinding by helicase II and T4 dda

helicases, due to entrapment of the enzyme and stabilization of the duplex, particularly when the covalent modification takes place on the displaced strand.<sup>91</sup> Even more significant is the unwinding inhibition with transmission of winding effects in a direction opposite to that of the unwinding by helicase.

### 1.7.3 CC-1065 Cell Cycle Effects –

CC-1065 induces cellular death via inhibition at specific points of the cell cycle. The cell cycle is divided into interphase (consisting of cellular division) and mitosis (M) incorporating G1 (the gap between M and S), S (the period of DNA synthesis) and G2 (the gap between replication and M).<sup>77</sup> CC-1065 blocks the progression of cells at G2 and M, with least cell lethality within the S phase, although progression is slower.<sup>5,14,91</sup> In studies with CHO cell lines 1% survival was observed at mitosis and as the cells progressed through G1 (10-40% survival) to S a significant survival rate of 80 – 100% was detected.<sup>91</sup>

While these observations correlate with those obtained in studies using other analogues of CC-1065, an exception was noted with U-71,184 and U-66,694 (Figure 33). The lethality of CC-1065 does not increase with the duration of exposure, but the lethality of U-71,184 and U-66,694 does. Furthermore, in contrast to CC-1065, these distinct analogues are most lethal to cells within the late G1 or early S cells.

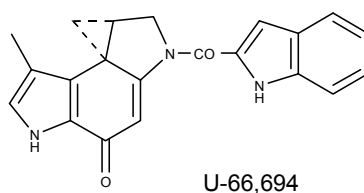


**Figure 33 – U-66,694**

### 1.7.4 Activation of Apoptosis –

Studies involving the cytotoxic effects of CC-1065 on L1210 and Molt-4 cells have indicated that apoptotic death is initiated at concentrations below that observed for cell death by necrosis in nonsensitive cell lines.<sup>14</sup> Apoptosis characteristically results in condensation of nuclear chromatin, fragmentation of genomic DNA, cell shrinkage and blebbing, compaction

of cytoplasmic organelles, loss of surface features such as microvilli and desmosomes<sup>94</sup> and fragmentation into apoptotic bodies.<sup>95</sup> Elevation in  $\text{Ca}^{2+}$  levels in lysosomes is also seen during apoptosis. Furthermore, lysosomal fragility or damage due to DNA damaging agents causes the release of acid hydrolases into the surrounding cytoplasm, resulting in the destruction of cells. Although the mechanism via which CC-1065 initiates apoptosis is not yet thoroughly understood, studies of other classes of antitumor active drugs indicate that the conformational change induced by these drugs allows an endonuclease to access the DNA, causing DNA fragmentation which subsequently triggers apoptosis.<sup>96</sup>

### **1.7.5 CC-1065 DNA adduct recognizing proteins –**

#### **1.7.5a *uvrABC*:**

The *uvr* proteins A, B and C are involved in initiating nucleotide excision repair by the recognition of DNA damage that is caused by alkylating agents such as CC-1065.<sup>95</sup> The mechanism via which this occurs entails the initial binding of the  $(UvrA)_2UvrB$  complex to the damaged DNA. The subsequent binding of *uvrC* changes the tertiary structure of the DNA resulting in activation of the phosphodiesterase excision function of *uvrB* at the 3' end of the DNA damage. This further alters the DNA structure causing initiation of the *uvrC* 5' phosphodiesterase and consequential excision of the DNA adduct.<sup>97</sup>

#### **1.7.5b *DARP*:**

A final mechanism by which CC-1065 is thought to induce cytotoxicity is via the activation of *DARP* (DNA adduct recognizing protein). *DARP* is thought to recognize the structural alteration in DNA which is induced upon CC-1065 binding. This protein is thought to act by either inhibiting the binding of repair enzymes or shielding the excision repair of CC-1065/DNA adducts, leading to cellular death.<sup>98</sup>

## **1.8 RECENT PRODRUG STUDIES**

### **1.8.1 Background –**

A prodrug is an active drug that has been chemically transformed into an inactive derivative (referred to as drug latention) that is converted to the parent drug within the body before or after reaching the site of action by virtue of chemical or enzymatic attack. Prodrugs are prepared to alter drug pharmacokinetics, improve stability and solubility, decrease toxicity, increase specificity and increase the duration of the pharmacological affect of the drug. By altering the pharmacokinetics, the drug bioavailability is increased by enhancing absorption, distribution, biotransformation and excretion of the drug.

In designing prodrugs it is important to consider the following factors:

- (a) The linkage between the carrier and the drug should usually be a covalent bond<sup>99</sup>
- (b) The prodrug should be inactive or less active than the active parent compound. Tietze *et al.*<sup>100,101</sup> have devised a model to evaluate the activity of prodrugs versus the active parent whereby the drug should have a high cytotoxicity with an IC<sub>50</sub> value of less than 10 nM and a QIC<sub>50</sub> above 1000 ( $QIC_{50} = IC_{50} \text{ prodrug} / IC_{50}(\text{prodrug} + \text{corresponding enzyme})$ );
- (c) The prodrug has to be a reversible or bioreversible derivative of the drug<sup>101</sup>; and
- (d) The carrier moiety must be non-toxic and inactive when released<sup>102</sup>.

More recent studies (i.e. 2006 – current) involving CC-1065 and its analogues have focused on antibody directed enzyme prodrug therapy (ADEPT) (Figure 34). As previously discussed in Section 1.2.5, ADEPT is used for the selective treatment of cancer, whereby a prodrug is enzymatically converted into a cytotoxic compound at the surface of malignant cells by employing an antibody-enzyme conjugate.<sup>101</sup>

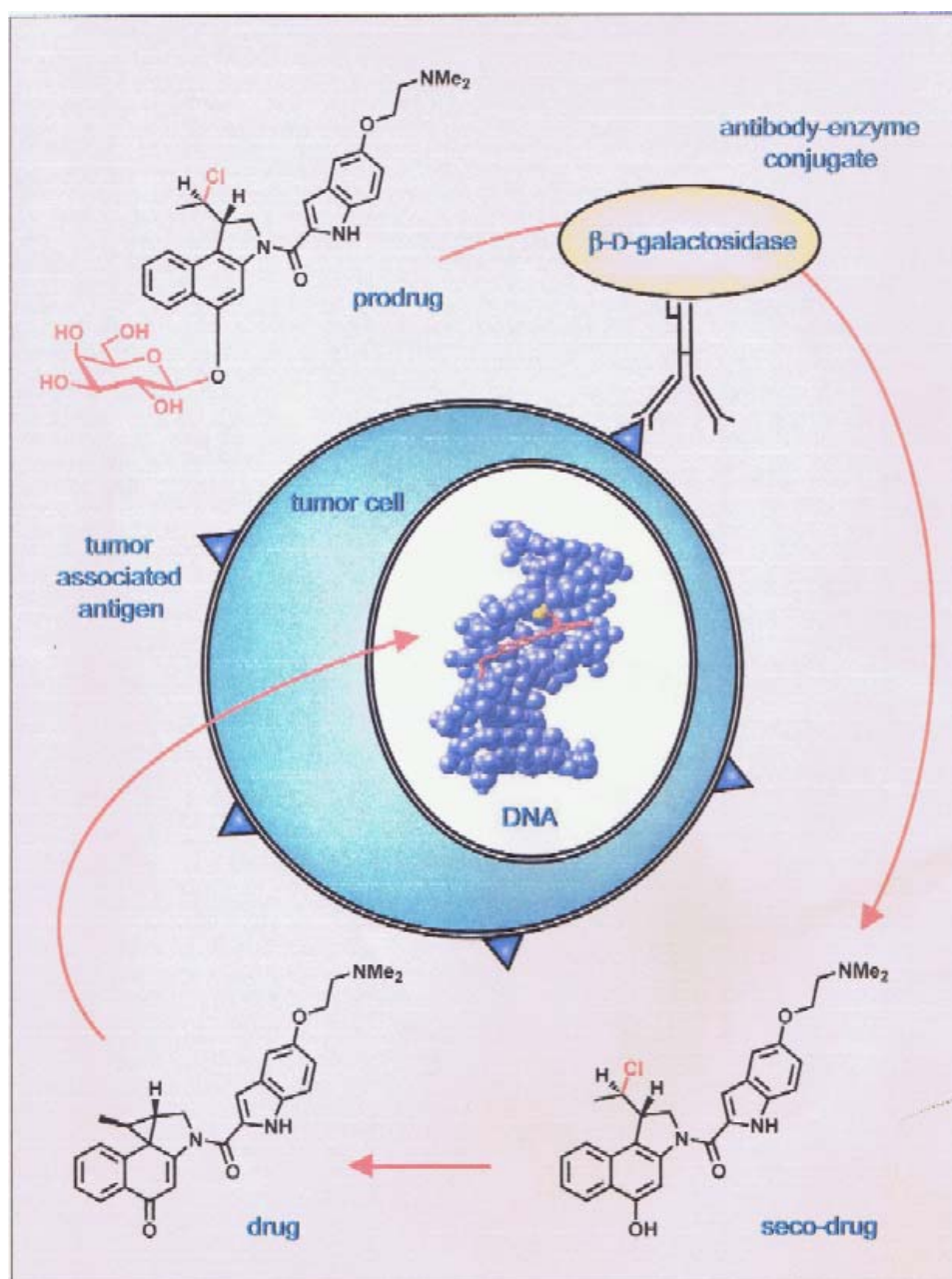


Figure 34 – ADEPT Therapy (Taken from Reference 100)

The use of monoclonal antibodies in prodrug therapy (ADEPT) overcomes the lack of tumor specificity displayed by CC-1065 and its analogues by targeting specific markers on the surface of tumor cells.<sup>102</sup> While specific, monoclonal antibodies exhibit little or no cytotoxicity toward tumor cells on their own, but may be efficacious when combined with anticancer agents.

These monoclonal antibody-enzyme conjugates are stable in circulation and are virtually non-toxic until they bind, via the antibody component, to the tumor cell.<sup>103</sup> Because many tumor cells exhibit unique surface antigens, drug specificity is afforded as only cells displaying the target antigen will be bound by the antibody-enzyme conjugate.

While earlier ADEPT studies demonstrated exceptional target-specific antitumor activity, such analogues used in these studies are extremely water insoluble.<sup>104</sup> Recent studies have endeavoured to overcome such problems.

### 1.8.2 Overcoming Poor Water Solubility

Previous studies by Tietz *et al.*<sup>101</sup> utilized glycosidic *seco* CC-1065 antibody conjugates (Figure 35) bearing a bisindoyl carboxylic acid moiety that can be hydrolysed enzymatically with a glycohydrolase, liberating the drug. These compounds were shown to have marked tumor specificity but poor water solubility.

In order to overcome these insolubility problems, Tietze *et al.*<sup>101,102</sup> recently designed a group of indole-2-carboxylic acid derivatives with enhanced water solubility, that could be used as DNA-binding units in CC-1065 analogues and their corresponding prodrugs<sup>101</sup> (Figure 35, Table 3, Compounds a-e). Importantly, these compounds retained the C-5 alkoxy group as shown to be required for high potency by Boger *et al.*<sup>72</sup> Furthermore, their design was based upon work by Denny *et al.*<sup>65</sup> which showed that minor-groove binding side chains of the TMI-type possessing a 5-alkoxy group and a solubilising dimethylaminoethyl group (as part of the 5-alkoxy substituent or at another position), retain or enhance the cytotoxicity of the parent drug and increase water solubility.<sup>101</sup>

As predicted, these compounds were shown to have increased water solubility and as such were subsequently used for the synthesis of prodrug analogues of CC-1065 in order to overcome the problem of poor water solubility during biological testing within the ADEPT approach (Figure 34).<sup>103</sup> The results of biological testing involving compounds 1a-e and 2a-e are shown in Table 3.

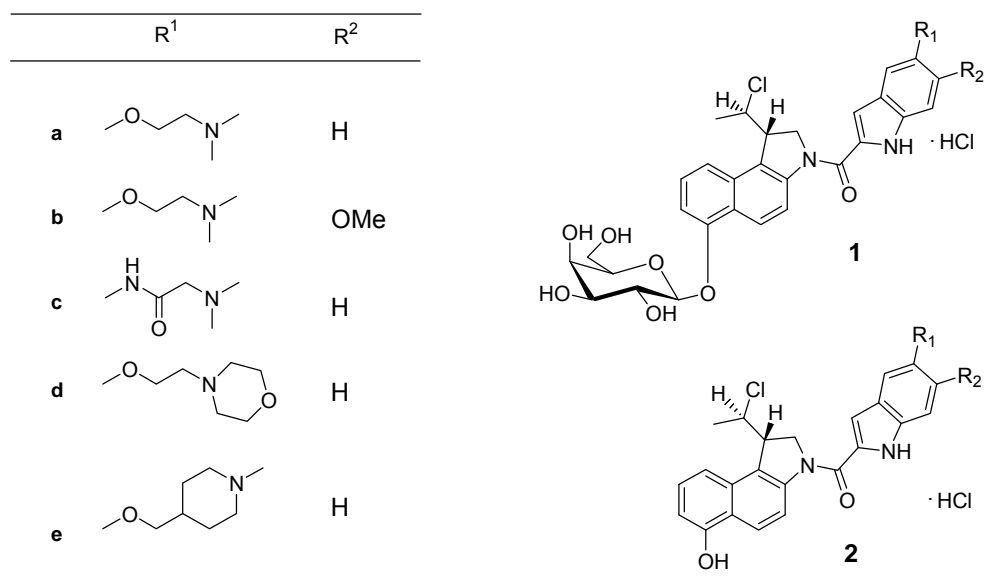


**Figure 35 – Recently Synthesized Galactosidic Prodrugs with Solubilising Sidechains**

Compound	Addition of $\beta$ -D-galactosidase	IC <sub>50</sub> (nM)	QIC <sub>50</sub>
1a	-	$3.6 \times 10^3$	4800
1a	+	0.75	
2a	-	0.75	
1b	-	$9.4 \times 10^2$	4300
1b	+	0.22	
2b	-	0.20	
1c	-	$7.7 \times 10^3$	1300
1c	+	5.9	
2c	-	3.8	
1d	-	$1.5 \times 10^3$	600
1d	+	2.5	
2d	-	3.7	
1e	-	$8.3 \times 10^2$	1100
1e	+	0.75	
2e	-	0.80	

**Table 3:** In vitro cytotoxicity of  $\beta$ -D-galactosidic prodrugs ((+)-1a-e) in the presence or absence of  $\beta$ -D-galactosidase and the seco-drug hydrochlorides ((+)-2a-e) against human bronchial carcinoma cells (A549).<sup>100</sup>

The results in Table 3 indicate that all prodrugs (excluding (+)-1d) meet the requirements for use in ADEPT therapy (ie.  $IC_{50}$  value of less than 10 nM and a  $QIC_{50}$  above 1000). In fact, compounds (+)-1a and (+)-1b are far superior to any of the compounds utilized to date in ADEPT and as such are marked as clinical candidates. As well as the presence of the glycoside protecting group, this superiority in activity can be attributed to the increase in water solubility afforded by the addition of the indole-2-carboxylic acid derivatives to the molecule. Both of these factors can be utilized in future work.

### 1.8.2 Albumin Binding Prodrugs of CC-1065

A recently developed albumin binding prodrug of CC-1065 known as (+)-FDI-CBI ( $IC_{50}$  (L1210 cell line) =  $0.17 \mu\text{M} \pm 0.06$ ) has shown significantly improved antitumor efficacy in animal models without causing delayed toxicity.<sup>104</sup> This compound readily binds serum albumin in animal models increasing its delivery to the tumor site. Given that human serum albumin (HSA) is known to accumulate in solid tumors, the albumin bound drug (+)-FDI-CBIM readily accumulates in solid masses ( $IC_{50}$  (L1210 cell line) =  $25 \mu\text{M} \pm 8$ ) where it is converted by an esterase to the free drug, (+)-FDI-CBI (Figure 36).<sup>104</sup>

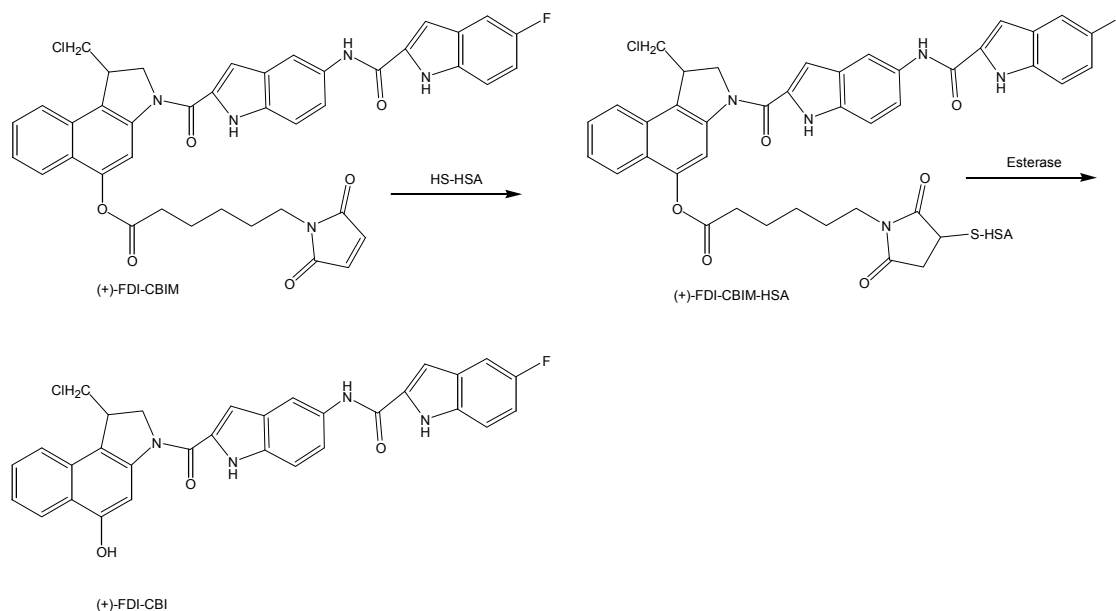


**Figure 36 – Formation of the HSA conjugate and subsequent production of (+)-FDI-CBI within a solid tumor mass.**

## **1.9 PROJECT OBJECTIVES**

### **1.9.1 Preliminary Studies –**

Preliminary studies have revealed that the 4-hydroxyphenethyl halides possess the minimal structural requirements needed to mimic the DNA alkylation profile characteristic to *seco* precursors.<sup>19</sup> Subsequent examination of the 4-aminophenethyl halides showed that these adducts exhibit approximately four times the *in vitro* cytotoxicity demonstrated by their phenolic counterparts.<sup>105-107</sup> The following project aims to extend this research, investigating the DNA alkylation profile of 4-aminophenethyl halide derivatives following their exposure to an extensive series of biological assays. The subsequent incorporation of these simpler compounds into more complex molecules containing non-covalent binding subunits was envisaged to increase both cytotoxicity and sequence selectivity.

### **1.9.2 Objectives –**

On the basis of the preceding information the aims of my project were as follows:

- (a) To determine the alkylation profile of 4-aminophenethyl halides and close derivatives against a broad spectrum of biological assays including tumor and non-tumor cell lines. These assays were conducted in conjunction with the Queensland Institute of Medical Research and involved kinetic and drug stability studies together with reporter assays, cell cycle studies, adenoviral assays and mouse model studies. Based on this information, structural changes were incorporated in order to optimize the inverse relationship between solvolytic stability and toxicity (Figure 37).
- (b) Preliminary molecular modeling was employed to assess the size and configuration of various heterocyclic systems intended to serve as minor groove binding ligands once linked to simplified alkylating subunits i.e. *seco-para*-aminophenethyl halides.
- (c) Based on this information, several monoalkylating and bisalkylating compounds were designed to incorporate minor groove binding ligands including benzyl and pyridyl subunits (Figure 36).

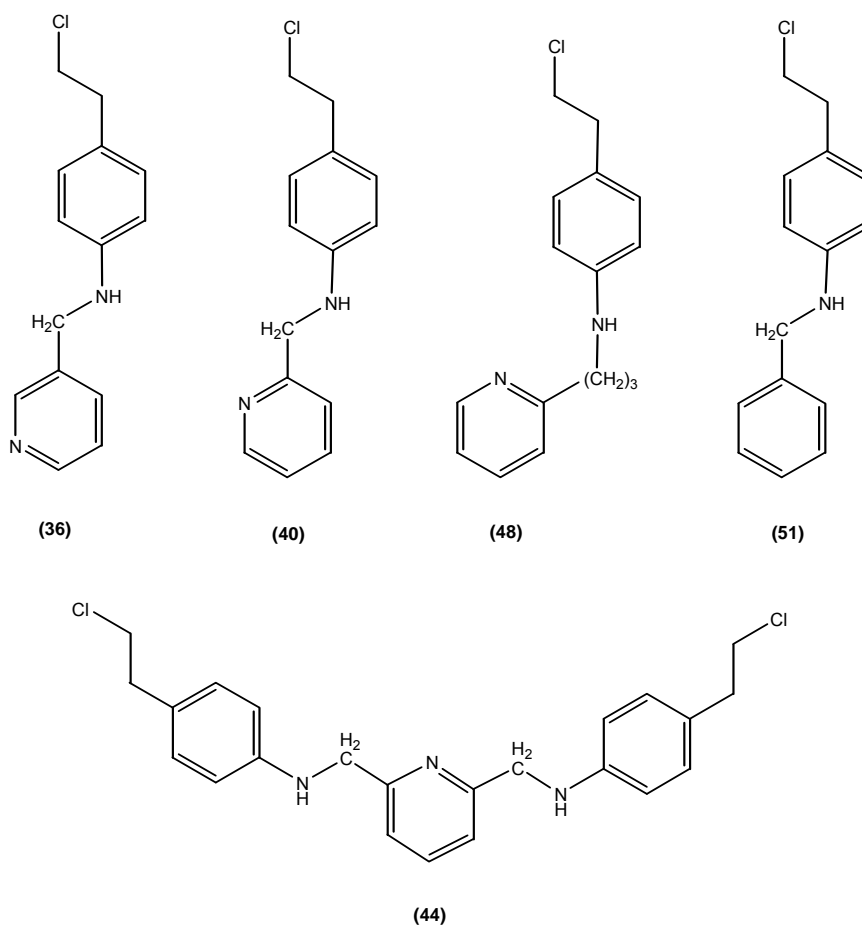


**Figure 37 – Mono- and Bisalkylating Compounds Incorporating Benzyl and Pyridyl Subunits**

The simple bisalkylating compound consisted of two 4-aminophenethyl halides joined with a heterocyclic (2,6-pyridinedimethyl) linker. The low energy conformations of the ring closed *seco* agent have been shown to have an approximate distance between the reactive cyclopropane units of 10 – 16 Å which is sufficient to span two adenines separated by two or three bases in the same strand (i.e. ANNA 11.50 Å; ANNNA 14.88 Å) or to bridge the gap between two adenines on opposite strands (>7.9 Å). It was envisaged that this compound would exhibit enhanced DNA sequence selectivity and cytotoxicity relative to the corresponding monoalkylating analogues as demonstrated by the bisalkylator Bizelesin<sup>7</sup>.

## **1.10 REFERENCES**

1. Martin, D. G., Chidester, C. G., Duchamp, D. J., Mizzark, S. A. *J. Antibiotics*, **1980**, 33(8), 902-903.
2. McHugh, M. M., Woynarowski, J. M., Mitchell, M. A., Gawron, L. S., Weiland, K. L., Beerman, T. A. *Biochemistry*, **1994**, 33, 9158-9168.
3. Wieranga, W. *J. Am. Chem. Soc.*, **1981**, 103, 5621-5623.
4. Sun, D. and Hurley, L. H. *Biochemistry*, **1992**, 31, 2822-2829.
5. Reynolds, V. L., McGovern, J. P., Hurley, L. H. *J. Antibiotics*, **1986**, 34(3), 319-334.
6. McGovern, J. P., Clarke, G. L., Pratt, E. A., Dekoning, T. F. *J. Antibiotics*, **1984**, 37, 63-70.
7. Baraldi, P. G., Cacciari, B., Guiotto, A., Romagnoli, R., Zaid, A. N., Spalluto, G. *Il Farmaco*, **1999**, 54, 15-25.
8. Volpe, D. A., Tomaszewski, J. E., Parchment, R. E., Garg, A., Flora, K. P., Murphy, M. J., Grieshaber, C. K. *Cancer Chemother. Pharmacol.*, **1996**, 39, 143-149.
9. Cobuzzi, R. J., Burhans, W. C., Beerman, T. A. *J. Biol. Chem.*, **1996**, 271(33), 19852-19859.
10. Chidester, C. G., Krueger, W. C., Mizzark, S. A., Duchamp, D. U., Martin, D. G. *J. Am. Chem. Soc.*, **1981**, 103, 7629-7635.
11. Moody, C. J., Pass, M., Rees, C. W., Tojo, G. *J. Chem. Soc., Chem. Commun.*, **1986**, 1062-1063.
12. Hurley, L. H., Reynolds, V. L. *Science*, **1984**, 226, 843-844.
13. Martin, D. G., Biles, C., Gerpheide, S. A., Hanka, L. J., Krueger, W. C., McGovern, J. P., Mizzak, S. A., Neil, G. L., Stewart, J. C., Visser, J. *J. Antibiotics*, **1981**, 34(9), 1119-1123.
14. Boger, D. L. and Johnson, D. S. *Agnew. Chem. Int. Ed. Engl.*, **1996**, 35, 1438-1474.
15. Skladanowski, A., Koba, M., Konopa, J. *Biochemical Pharmacology*, 61 (2001), 67-72.
16. Boger, D. L., Coleman, R. S., Invergo, B. J., Sakya, S. M., Ishizaki, T., Munk, S. A., Zarrinmayeh, H., Kitos, P. A., Thompson, S. *J. Am. Chem. Soc.*, **1990**, 112, 4623-4632.
17. Sun, D., Lin, C. H., Hurley, L. H. *Biochemistry*, **1993**, 32, 4487-4495.
18. Hurley, L. H., Warpehoski, M. A., Lee, C. S., McGovern, J. P., Scahill, T. A., Kelly, R. C., Mitchell, M. A., Wicnienski, N. A., Gebhard, I., Johnson, P. D., Bradford, V. S. *J. Am. Chem. Soc.*, **1990**, 112, 4633-4649.
19. White, R. H., Parsons, P. G., Prakash, A. S., Young, D. J. *Bioorganic and Medicinal Chem. Lett.*, **1995**, 5(16), 1869-1874.

20. Boger, D. L., Nishi, T., Teegarden, B. R. *J. Org. Chem.*, **1994**, 59, 4943-4949.
21. Boger, D. L., Ishizaki, T., Zarrinmayeh, H., Munk, S. A., Kitos, P. A., Suntornwat, O. *J. Am. Chem. Soc.*, **1990**, 112, 8961-8971.
22. Baird, R., Winstein, S. *J. Am. Chem. Soc.*, **1963**, 85, 567-575.
23. Wang, Y., Gupta, R., Huang, L., Lown, J. W. *J. Med. Chem.*, **1993**, 36, 4172-4182.
24. Boger, D. L., Munk, S. A., Zarrinmayeh, H. *J. Am. Chem. Soc.*, **1991**, 113, 3980-3983.
25. Tercel, M., Denny, W. A., Wilson, W. R. *Bioorganic and Medicinal Chemistry Letters*, **1996**, 6(22), 2741-2744.
26. Boger, D. L. and Garbaccio, R. M. *J. Org. Chem.*, **1999**, 64, 8350-8362.
27. Ouyang, A and Skibo, E. B. *J. Org. Chem.*, **1998**, 63, 1893-1900.
28. Boger, D. L., Wolkenberg, S. E., Boyce, C. W. *J. Am. Chem. Soc.*, **2000**, 122, 6325-6326.
29. Boger, D. L. and Boyce, C. W. *J. Org. Chem.*, **2000**, 65, 4088-4100.
30. Ellis, D. A., Wolkenberg, S. E., Boger, D. L. *J. Am. Chem. Soc.*, **2001**, 123, 9299-9306.
31. Boger, D. L. and Garbaccio, R. M. *J. Org. Chem.*, **1999**, 64, 5666-5669.
32. Boger, D. L. and Garbaccio, R. M. *Acc. Chem. Res.* **1999**, 32, 1043-1052.
33. Boger, D. L., Santillan, A., Searcey, M., Jin, Q. *J. Am. Chem. Soc.*, **1998**, 120, 11554-11557.
34. Boger, D. L. and Turnbull, P. *J. Org. Chem.*, **1998**, 63, 8004-8011.
35. Warpehoski, M. A. and Harper, D. E. *J. Am. Chem. Soc.*, **1994**, 116, 7573-7580.
36. Boger, D. L. and Johnson, D. S. *J. Am. Chem. Soc.*, **1995**, 117, 1443-1444.
37. Hurley, L. H., Lee, C. S., McGovern, J. P., Warpehoski, M. A., Mitchell, M. A., Kelly, R. C., Aristoff, P. A. *Biochemistry*, **1988**, 27, 3886-3892.
38. Hurley, L. H., Needham-VanDevanter, D. R., Lee, C., S. *Proc. Natl. Acad. Sci.*, **1987**, 84, 6412-6416.
39. Boger, D. L., Zarrinmayeh, H., Munk, S. A., Kitos, P. A., Suntornwat, O. *Proc. Natl. Acad. Sci. USA.*, **1991**, 88, 1431-1435.
40. Warpehoski, M. A., Harper, D. E., Mitchell, M. A., Monroe, T. J. *Biochemistry*, **1992**, 31, 2502-2508.
41. Boger, D. L. and Ishizaki, T. *Tetrahedron Letters*, **1990**, 31(6), 793-796.
42. Boger, D. L. and Yun, W. *J. Am. Chem. Soc.*, **1993**, 115, 9872-9873.
43. Boger, D. L., Boyce, C. W., Garbaccio, R. M., Goldberg, J. A. *Chem. Rev.*, **1997**, 97, 787-828.

44. Aristoff, P. A., Johnson, P. D., Daekyu, S., Hurley, L. H. *J. Med. Chem.*, **1993**, 36, 1956-1963.
45. Boger, D. L. and Ishizaki, T. *J. Org. Chem.*, **1990**, 55, 5823-5832.
46. Boger, D. L., Mesini, P., Tarby, C. M. *J. Am. Chem. Soc.*, **1994**, 116, 6461-6462.
47. Boger, D. L. and Yun, W. *J. Am. Chem. Soc.*, **1994**, 116, 5523-5524.
48. Fukuda, Y., Furuta, H., Shiga, F., Oomori, Y., Kusama, Y., Ebisu, H. *Bioorg. and Med. Chem. Lett.*, **1997**, 7(13), 1683-1688.
49. Boger, D. L., Ishizaki, T., Zarrinmayeh, H. *J. Org. Chem.*, **1990**, 55, 4499-4502.
50. Boger, D. L., Munk, S. A., Ishizaki, T. *J. Am. Chem. Soc.*, **1991**, 113, 2779-2780.
51. Baraldi, P. G., Cacciari, B., Pineda de las Infantas, M. J., Romagnoli R., Spalluto, G., Cozzi, P., Mongelli, N. *Anticancer Drug Design*, **1997**, 12, 67-74.
52. Boger, D. L. and Yun, W. *J. Am. Chem. Soc.*, **1994**, 116, 7996-8006.
53. Boger, D. L. and Turnbull, P. *J. Org. Chem.*, **1997**, 62, 5849-5863.
54. Boger, D. L., Garbaccio, R. M., Qing, J. *J. Org. Chem.* **1997**, 62, 8875-8891.
55. Boger, D. L. Wysocki, R. J., Ishizaki, T. *J. Am. Chem. Soc.*, **1990**, 112, 5230-5240.
56. Boger, D. L., McKie, J. A., Cai, H., Cacciari, B., Baraldi, P. G. *J. Org. Chem.*, **1996**, 61, 1710-1729.
57. Boger, D. L., Invergo, B. J., Coleman, R. S., Zarrinmayeh, H., Kitos, P. A., Thompson, S. C., Leong, T., McLaughlin, L. W. *Chem. Biol. Interact.*, **1990**, 73, 29-32.
58. Boger, D. L. and Sakya, S. M. *J. Org. Chem.*, **1992**, 57, 1277-1284.
59. Boger, D. L. and Coleman, R. S. *J. Am. Chem. Soc.*, **1988**, 110, 4796-4807.
60. Wang, Y., Yuan, H., Ye, W., Wright, S. C., Wang, W., Larrick, J. W. *J. Med. Chem.*, **2000**, 43, 1541-1549.
61. Baraldi, P. G., Balboni, G., Pavani, M. G., Spalluto, G., Tabrizi, M. A., De Clercq, E., Balzarini, J., Bando, T., Sugiyama, H., Romagnoli, R. *J. Med. Chem.*, **2001**, 44, 2536-2543.
62. Boger, D. L. and Mesini, P. *J. Am. Chem. Soc.*, **1995**, 117, 11647-11655.
63. Boger, D. L., Schmitt, H. W., Fink, B. E., Hedrick, M. P. *J. Org. Chem.*, **2001**, 66, 6654-6661.
64. Wang, Y., Yuan, H., Wright, S., Wang, H., Larrick, J. *Bioorg. Med. Chem.*, **2003**, 11(7), 1569-1575.
65. Y. Wang, H. Yuan, W. Ye, S.C. Wright, H. Wang and J.W. Larrick. *J. Med. Chem.* **43** (2000), 1541.

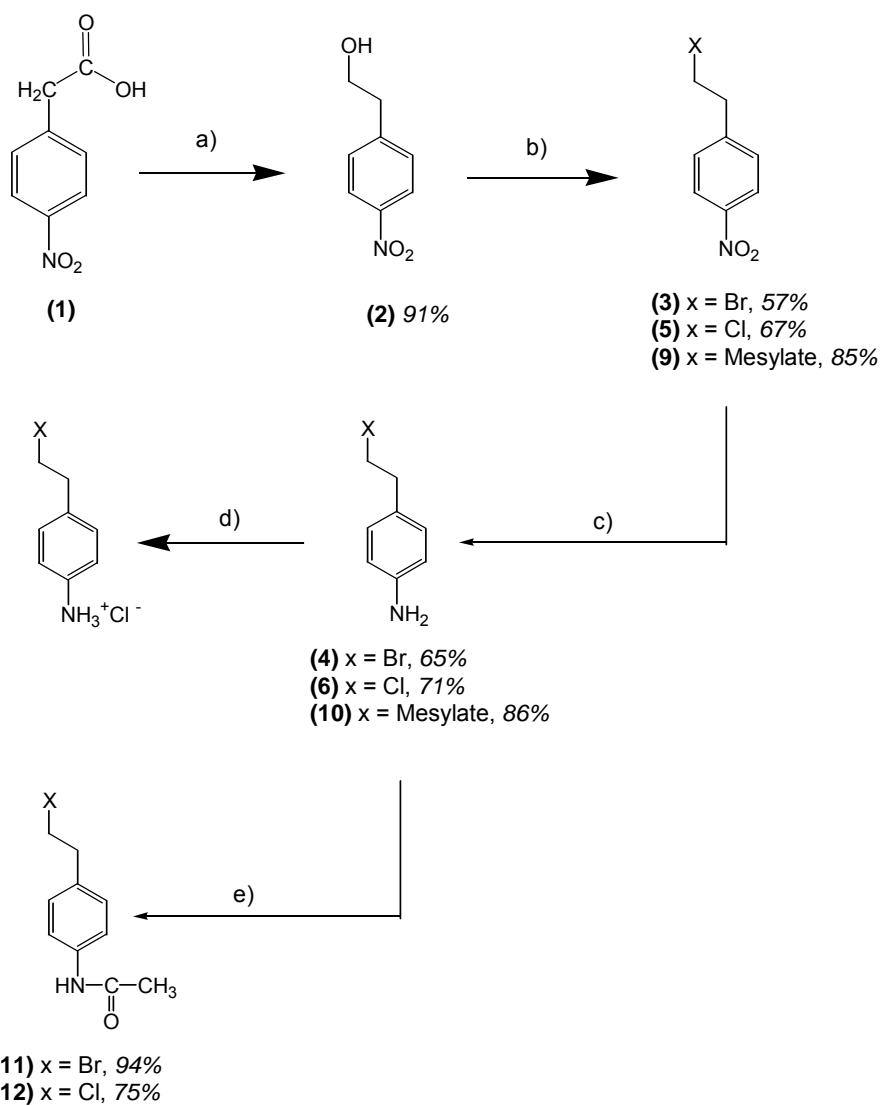
66. L.F. Tietze, M. Lieb, T. Herzig, F. Hauernt and I. Schuberth. *Bioorg. Med. Chem.* **9** (2001), 1929.
67. P.G. Baraldi, G. Balboni, M.G. Pavani, G. Spalluto, M.A. Tabrizi, E.D. Clercq, J. Balzarini, T. Bando, H. Sugiyama and R. Romagnoli. *J. Med. Chem.* **2001**, 44, 2536.
68. D.L. Boger, T.V. Hughes and M.P. Hedrick. *J. Org. Chem.* **2001**, 66, 2207.
69. Parrish, J., Trzuppek, J., Hughes, T., Hwang, I., Boger, D. *Bioorg. Med Chem*, **2004**, 12(22), 5845-5856.
70. Parrish, J., Hughes, T., Hwang, I., Boger, D. *J. Am. Chem. Soc.*, **2003**, 126(1), 80-81.
71. Sato, A., McNulty, L., Cox, K., Kim, S., Scott, A., Daniell, K., Summerville, K., Price, C., Hudson, S., Kiakos, K., Hartley, J., Asao, T., Lee, M. *J. Med Chem*, **2005**, 48(11), 3903-3918.
72. Boger, D. L.; Stauffer, F.; Hedrick, M. P. *Bioorg. Med. Chem. Lett.* **2001**, 11, 2021-2024.
73. Amishiro, N.; Nagamura, S.; Kobayashi, E.; Okamoto, A.; Gomi, K.; et al. *Bioorg. Med. Chem.* **2000**, 8, 1637-1643.
74. Wang, Y., Li, L., Ye, W., Zhiming, T., Jiang, W., Wang, H., Wright, S., Larrick, J. *J. Med. Chem.*, **2003**, 46(4), 634-637.
75. Weinberger, M., Trabold, P. A., Lu, M., Sharma, K., Huberman, J. A., Burhans, W. C. *J. Biol. Chem.*, **1999**, 274, 50, 35975-35984.
76. Liu, J-S., Kuo S-R.,McHugh, M. M., Beerman, T. A., Melendy, T. *J. Biol. Chem.*, 2000, 275, 2, 1391-1397.
77. Weinberger, M., Trabold, P. A., Lu, M., Sharma, K., Huberman, J. A., Burhans, W. C. *The Journal of Biological Chemistry*, **1999**, 274, 50, 35975-35984.
78. Wierenga, W. *Drugs of the Future*, **1991**, 16(8), 741-750.
79. Weiland, K. L. and Dooley, T. P. *Biochemistry*, **1991**, 30, 7559-7565.
80. Li, L. H., DeKoning T. F., Kelly, R. C., Krueger W. C., McGovern, J. P., Padbury, G. E., Petzold, G. L., Wallace, T. L., Ouding, R. J., Prairie, M. D., Gebhard, I. *Cancer Res.* **1992**, 52, 4904-4913.
81. Shamdas, G. J., Alberts, D. S., Modiano, M., Wiggins, C., Power, J., Kasunic, D. A., Elfrinng, G. L., Earhart, R. H. *Anticancer Drugs*, **1994**, 5(1), 10-14.
82. Warpehoski, M. A. *Tetrahedron Lett.*, **1986**, 27(35), 4103-4106.
83. Walker, D. L., Reid, J. M., Ames, M. M. *Cancer Chemother. Pharmacol.*, **1994**, 34, 317-322.
84. Gibson, N. J. *Pharm. Pharmacol.*, **1993**, 45(Suppl. 1), 331-342.

85. Sun, D. and Hurley, L. H. *J. Am. Chem. Soc.*, **1993**, 115, 5925-5933.
86. Ding, Z. M., and Hurley, L. H. *Anti-Cancer Drug Design*, **1991**, 6, 427-452.
87. McHugh, M. M., Kuo, S., Walsh-O'Beirne, M. H., Liu, J., Melendy, T., Beerman, T. S. *Biochemistry*, **1999**, 38, 11508-11515.
88. Gibson, N. W. *J. Pharm. Pharmacol.* **1993**, 45(Suppl. 1), 331-342.
89. Soon-Lee, C., Gibson, N. W. *Biochemistry*, **1993**, 32, 2592-2600.
90. Hanka, L. J., Dietz, A., Gerrpheide, S. A., Kuentzel, S. L., Martin, D. G. *J. Antibiotics*, **1978**, 31(12), 1211-1217.
91. Wieranga, W., Bhuyan, B. K., Kelly, R. C., Krueger, W. C., Li, L. H., McGovern, J. P., Swenson, D. H., Warpehoski, M. A. *Adv. Enzyme Reg.*, **1986**, 25, 141-155.
92. Alberts, B., Bray, D., Lewis, J., Raff, M., Roberts, K., Watson, J. D. *Molecular Biology of the Cell*. Garland Publishing, Inc. New York. **1994**, 864-870.
93. Sun, D. and Hurley, L. H. *J. Med. Chem.*, **1992**, 35, 1773-1782.
94. Bowen, I. D., Bowen, S. M. *Programmed Cell Death in Tumors and Tissues*, **1988**, Chapman and Hall, London, 189-203.
95. Evan, G. *Chem. and Biol.*, **1994**, 1, 137-141.
96. Ormerod, M. G., Neill, C. F., Robertson, D. and Harrap, K. R. *Expt. Cell Res*, **1994**, 211, 271-237.
97. Nazimiec, M., Lee, C., Tang, Y., Ye, X., Case, R., Tang, M. *Biochemistry*, **2001**, 40, 11073-11081.
98. Asai, A., Yano, K., Mizukami, T., Nakano, H. *Cancer Res.*, **1999**, 59, 5417-5420.
99. Boyd, S. E., Chen, L., Ganwar, S., Guerlavais, V., Horgan, K., Sufi, B. *PCT Int. Appl.* **2007**.
100. Tietz, L. F., Major, F., Schuberth, I., Spiegel, D. A., Krewer, B., Maksimenka, K., Bringmann, G., Magull, J. *Chem. Eur. J.*, **2007**, 13, 4396-4409.
101. Tietz, L. F. and Major, F. *Eur. J. Org. Chem.*, **2006**, 2314-2321.
102. Tietz, L. F. and Krewer, Birgit. *Anti-Cancer Agents in Med. Chem.*, **2009**, 9(3), 304-325.
103. Hamann, P., R. *Expert Opinion on Therapeutic Patents*, **2005**, 15(9), 1087-1103.
104. Wang, Y., Jiang, J., Jiang, X., Cai, S., Han, H., Li, L., Tian, Z., Jiang, W., Zhang, Z., Xiao, Y., Wright, S., Larrick, J. W. *Bioorg. Med. Chem.*, **2008**, 16, 6552-6559.
105. Chari, R. V. J., Abstracts of Papers, 233<sup>rd</sup> ACS National Meeting, Chicago, IL, United States, March 25-29, **2007**.

106. Zhao, R. Y., Sun, D., Cavanagh, E., Miller, M., Leece, B., Erickson, H., Singh, R., Kovtun, Y., Goldmacher, V., Chari, R. Abstracts of Papers, 234<sup>th</sup> ACS National Meeting, Boston, MA, United States, August 19-23, **2007**.
107. Shalders, R. L., Blanch, G., Brown, C. L., Prakash, A. S., Young, D. J. *Chem. Biol. Interact.*, **1999**, 117(1), 83-94.

**CHAPTER 2 – RESULTS AND DISCUSSION:**  
**ORGANIC SYNTHESIS**

**2.1 SCHEME 1: SYNTHESIS OF 4-AMINOPHENETHYL HALIDE DERIVATIVES**



Reagents: a)  $\text{BH}_3 \cdot \text{SMe}_2$  b)  $\text{PBr}_3$  (X=Br),  $\text{SOCl}_2$  (X=Cl),  $\text{MeSO}_2\text{Cl}$  (X= mesylate) c) Tin/HCl d) Ether/HCl e) Acetic Anhydride

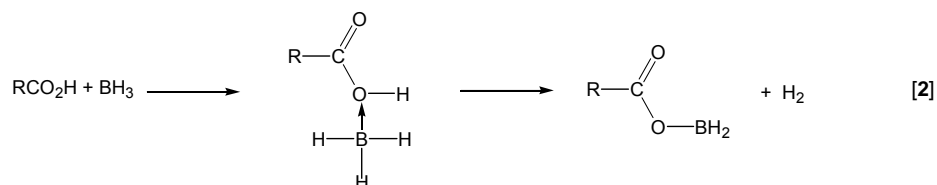
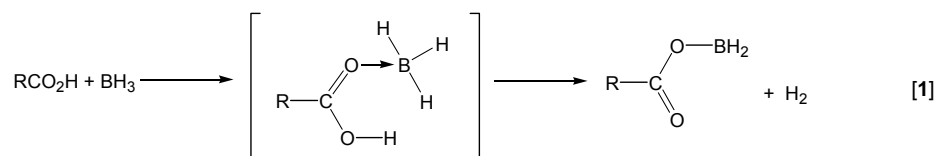
Scheme 1

Scheme 1 details the synthesis of the 4-aminophenethyl halide hydrochlorides **(4)** and **(6)**, and their respective acetamides **(11)** and **(12)**, together with 4-aminophenethyl mesylate hydrochloride **(10)**. It was envisaged that compounds **(4)** and **(6)** would possess antitumor activity through their ability to alkylate DNA and impede DNA synthesis, thereby resulting in cellular death.

Borane dimethyl sulfide in THF was employed in the selective reduction of the carboxylic acid **(1)**. Literature evidence revealed that this reagent demonstrates exceptional selectivity for carboxylic acids in the presence of additional reducible groups, such as NO<sub>2</sub>.<sup>1</sup> The absence of any amine product following reduction of **(1)** with 2.0 M borane dimethyl sulfide (BMS) demonstrated this fact.

The initial reaction conditions employed 2 equivalents of BMS at room temperature for 12 hours.<sup>2,3</sup> The compound proved easy to isolate from residual borane dimethyl sulfide via the addition of water and hence conversion of the latter to water soluble borane salts. Recrystallization from ethanol provided the pure product **(2)** as yellow crystals. Relatively low yields (30%) were obtained from this reduction method (Section 4.4.1(i)) and as such, experimental variation was required.

While the initial reaction of BMS with **(1)** was slow, and yields were low, evidence from literature suggested that carboxylic acids were rapidly and quantitatively reduced to their corresponding primary alcohols when dimethyl sulfide was distilled out of the reaction mixture as the reaction proceeded (Section 3.4.1(i)). Brown and coworkers<sup>4,5</sup> have previously demonstrated that the reduction mechanism proceeds through a transfer of borane from its complexes to the oxygens of the carboxylic acid group as illustrated in equations **[1]** and **[2]**. As such, a decrease in the rate of BMS reduction could be attributed to the accumulation of dimethyl sulfide (b.p. 38°C) as the reaction proceeded, which would not only serve to repress the transfer of borane to the carboxylic acid, but also result in a reduction in the temperature of the refluxing mixture. As such, the advantages associated with the removal of dimethyl sulfide from the reaction mixture were obvious.

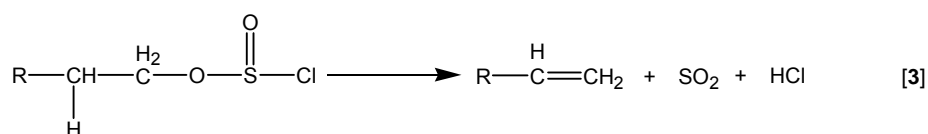


The modified method for the reduction of **(1)** utilized a flask equipped with a Vigreux column maintained under an inert atmosphere of nitrogen. A Vigreux column was employed because of its ability to separate compounds with similar boiling points at reduced pressures (i.e. dimethyl sulfide (38°C) and THF (67°C)).<sup>6</sup> A solution of **(1)** in THF (100 mL) and BMS (1 eq) was stirred at reflux until the distillation of dimethyl sulphide was complete (4 hours). The reaction was quenched with water and extracted into chloroform to remove the borane salts. The crude product was recrystallized from 10% water/ethanol and dried under high vacuum to give **(2)** as yellow crystals. As expected, a much higher yield of product (91% c.f. 30%) was obtained.

The bromination of **(2)** was carried out with phosphorous tribromide (1 eq, reflux, 4 hrs) under an inert atmosphere of nitrogen.<sup>7,8</sup> While HBr was recognized as a potential reagent for this purpose, extensive studies previously conducted by Bennett *et al.* indicate that **(2)** shows a very slow rate of reactivity with HBr ( $k=1.65 \times 10^4$ ).<sup>9</sup> As such, PBr<sub>3</sub> was chosen for its ability to readily brominate primary alcohols under mild conditions (c.f. hydrobromic acid). Initial attempts produced poor yields of **(3)** contaminated with starting material. In subsequent attempts the reaction time was increased from 4 hours to 12 hours, providing satisfactory yields of up to 57%. Purification by flash chromatography (10% MeOH/DCM) provided an easy method for the separation of **(3)** as orange crystals from its starting material.

Thionyl chloride was utilized in the chlorination of phenethyl alcohol **(2)** to give **(5)** (67% yield). Like the bromination of **(2)** with PBr<sub>3</sub>, this reagent employs mild conditions and is less

acidic than HCl. Initial attempts involved the use of neat reagent at reflux for 2 hours.<sup>10</sup> This procedure resulted in elimination of the alcohol and/or chloride group to give 4-nitrostyrene as determined by <sup>1</sup>H nmr spectroscopy. This presumably resulted from elimination of the chlorosulphite as shown in equation [3]. In order to discourage elimination, the reaction mixture was diluted with chloroform and performed over a longer period of time (i.e. 24 hours). Purification was readily achieved by flash chromatography (10% MeOH/DCM).

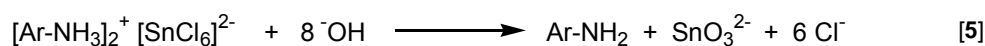


The mesylation of 4-nitrophenethyl alcohol required two equivalents of methanesulphonyl chloride in chloroform under nitrogen for 6 hours.<sup>11</sup> Purification by flash chromatography (10% MeOH in CHCl<sub>3</sub>) yielded pure product (**9**) in 85% yield as an orange oil.

Reduction of the nitro groups of (**3**) and (**5**) was achieved using Sn/HCl in anhydrous diethyl ether (reflux, 48 hrs).<sup>12</sup> Initial low yields (<10%) were attributed to low concentrations of HCl and/or the presence of H<sub>2</sub>O in the reaction. Studies conducted by Xing *et al.*<sup>13</sup> indicate that the rate of the reaction is dependent on the concentration of the reactants and therefore the rate decreases as the reaction progresses [4].

$$u = k[\text{ArNO}_2][\text{SnCl}_2][\text{HCl}]_{\text{st}}^{0.5} \quad [4]$$

While the addition of further tin catalyst throughout the reaction proved ineffective due to the difficulty in removing the tin salts during workup, the addition of extra aliquots of diethyl ether/HCl throughout the course of the reaction noticeably improved the yields of amine product. Basification of the reaction at completion served to release the aromatic amine from any complex amine chlorostannate which was formed during the reaction as shown in equation [5].<sup>7</sup>



Hydrogenation with 10%Pd/C was used to reduce the nitro containing mesylate compound **(9)**.<sup>14</sup> This catalyst was chosen because of its heightened activity at slightly elevated temperatures and pressures. Furthermore, the procedure provided a very clean reaction from which the product was easily isolated.<sup>15</sup> A mixture of the nitro compound **(9)**, 10%Pd/C and THF were placed in a parr hydrogenator and left to agitate for 12 hours at 3 atmospheres.<sup>14</sup> The resultant product was filtered through celite and the solvent removed under high vacuum. Flash chromatography (10% MeOH/DCM) was used to purify the compound which was then converted to the hydrochloride salt **(10)** by the method outlined below, in 86% yield.

It was important that each of the target compounds synthesized were prepared as the hydrochloride salt because of the advantage of a water-soluble compound in *in vitro* antitumor testing. The hydrochloride salt of the amines was produced by reaction of **(3)**, **(5)** and **(9)** with anhydrous diethyl ether saturated with HCl gas.<sup>7</sup>

The ether/HCl solution was prepared by using the apparatus shown in Figure 37. A solution of 38% HCl was added dropwise from a pressure-equalizing dropping funnel into a RB flask containing 98% sulphuric acid, with rapid stirring. The liberated HCl gas was passed through an oil bubbler, which was connected to the dropping funnel, into a conical flask containing diethyl ether and solid MgSO<sub>4</sub>. This solution was filtered into a conical flask containing the amine dissolved in chloroform. The resulting precipitate, as the hydrochloride salt, was filtered and dried under high vacuum.

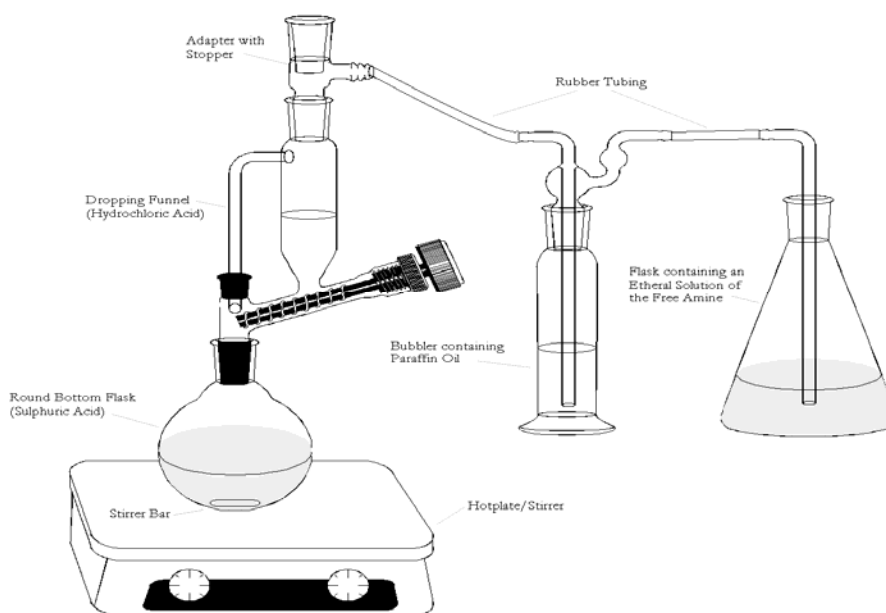
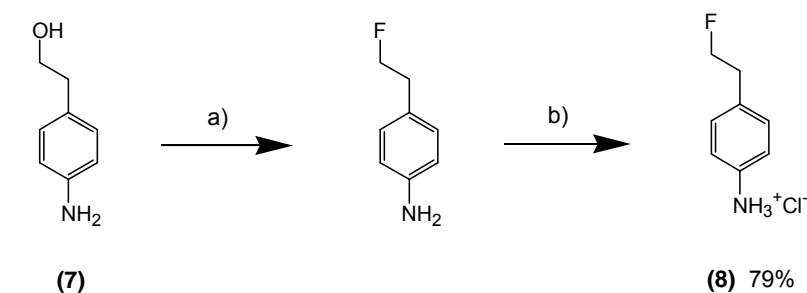


*Figure 37 – Apparatus Used in the Production of HCl Gas*

Initially, the yield of amine hydrochloride produced was low, and may have been attributed to the presence of water in the diethyl ether, or partial solubility of the end product in chloroform/diethyl ether. The addition of a drying agent ( $\text{MgSO}_4$ ) during HCl saturation to ensure minimal water absorption and the use of minimal amounts of chloroform/ether-HCl, produced higher yields of the hydrochlorides **(4)**, **(6)** and **(10)** in 65%, 71% and 86% yield respectively. It was envisaged that these compounds would to some degree possess antitumor activity via  $\text{S}_{\text{N}}2$  alkylation and subsequent inhibition of DNA synthesis.

The addition of acetic anhydride to the amine compounds **(4)** and **(6)** dissolved in  $\text{CHCl}_3$  was used in the synthesis of the acetamides, **(11)** and **(12)**, to give yields of 94 and 75% respectively.<sup>16</sup> Acetic anhydride was employed because of its facile reaction with amines. The acetamide formed readily in the absence of heating and precipitated with the addition of water. The products were recrystallized in ethanol and isolated pure, as yellow crystals, without the need for chromatography. The acetamides, **(11)** and **(12)**, were synthesized in order to assess the effect of the amide nitrogen's decreased electron availability, on the  $\text{S}_{\text{N}}2$  alkylation of DNA.

**2.2 SCHEME 2: SYNTHESIS OF 4-AMINOPHENETHYL FLUORIDE HYDROCHLORIDE (8)**

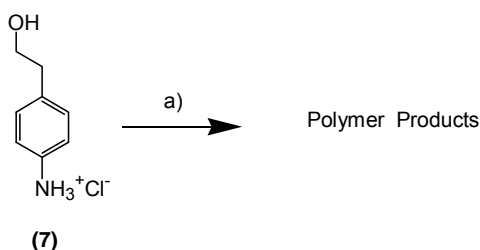


Reagents: a) DAST b) Ether/HCl

**Scheme 2**

Scheme 2 details the synthesis of 4-aminophenethyl fluoride hydrochloride (**8**). Fluorination of 4-aminophenethyl alcohol (**7**) was carried out using an equimolar amount of diethylaminosulfur trifluoride (DAST) in CHCl<sub>3</sub> under nitrogen. 4-Aminophenethyl alcohol was added at -78°C, the reaction warmed to room temperature and stirred for three hours.<sup>17</sup> Dilution with water, extraction with CHCl<sub>3</sub> and flash chromatography produced pure fluorinated compound which was converted to the hydrochloride salt via the methods previously outlined. Recrystallization from ethanol gave (**8**) in an overall yield of 79% as yellow crystals. This compound was envisaged to possess some antitumor activity through the S<sub>N</sub>2 alkylation of DNA.

**2.3 SCHEME 3: 1<sup>ST</sup> ATTEMPTED SYNTHESIS OF 4-AMINOPHENETHYL IODIDE HYDROCHLORIDE**



Reagents: a) HI

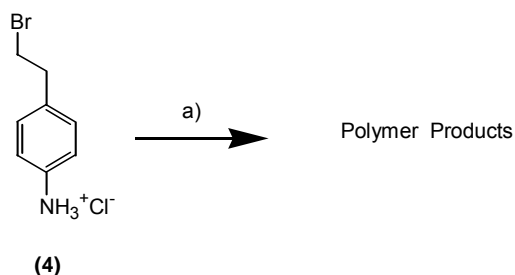
**Scheme 3**

Scheme 3 outlines the attempted synthesis of 4-aminophenethyl iodide hydrochloride following reaction of the hydrochloride salt of **(7)** with two equivalents of hydriodic acid at 60°C for two hours.<sup>18</sup>

Attempts to isolate the title compound from the crude material included titration from chloroform, followed by flash chromatography using 10% MeOH/CHCl<sub>3</sub> solution. Unfortunately these attempts were unsuccessful given the propensity of the end product to undergo polymerization, forming a multiple of products which proved very difficult to isolate.

Subsequent attempts employed decreased reaction times and temperature however gas chromatography results had failed to detect appreciable quantities of the monomeric product, 4-aminophenethyl iodide hydrochloride, irrespective of these changes.

**2.4 SCHEME 4: 2<sup>ND</sup> ATTEMPTED SYNTHESIS OF 4-AMINOPHENETHYL IODIDE HYDROCHLORIDE**



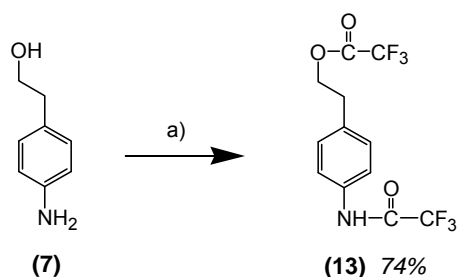
Reagents: a) NaI

**Scheme 4**

Scheme 4 outlines the attempted synthesis of 4-aminophenethyl iodide hydrochloride using the hydrochloride salt of **(4)** together with 5 equivalents of NaI in acetone (40 mL). The solution was stirred for 6 hours at 80°C under nitrogen. The reaction was reduced under pressure and the residue extracted with two portions of ethyl acetate. The organic layers were washed with brine and dried over magnesium sulphate. Reduction of the solvent under reduced pressure afforded a black oil.

Unfortunately, analysis showed that these conditions did little to stabilize the end product which again appeared to be a mixture of polymeric products. Given the obvious reactivity of 4-aminophenethyl iodide, it was suspected that the analogue if eventually isolated may still demonstrate a propensity to undergo nonproductive solvolysis in serum thereby making it a less attractive target.

**2.5 SCHEME 5: SYNTHESIS OF 2-{4-[2,2,2-TRIFLUOROACETYL]AMINO}PHENYL}-ETHYL TRIFLUOROACETATE (13)**

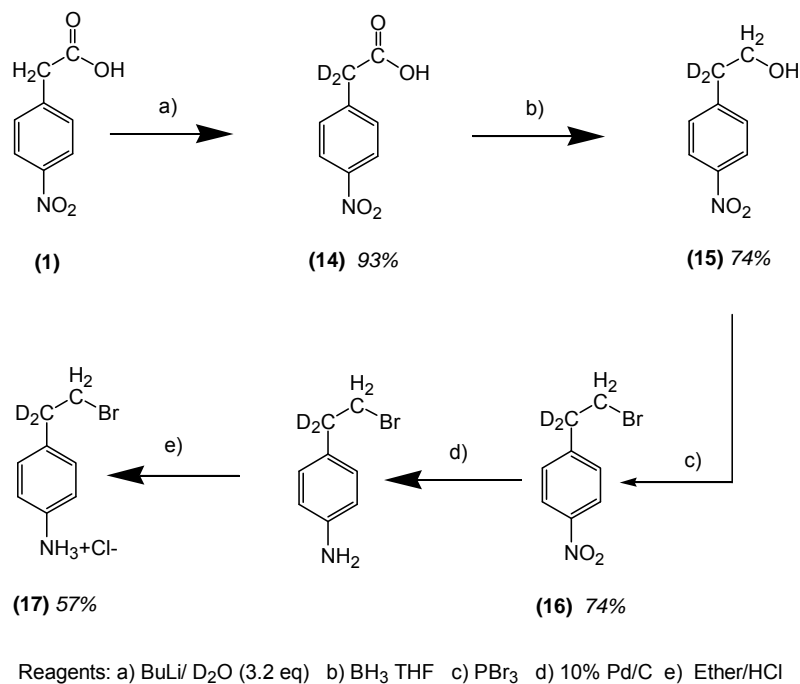


Reagents: a) Trifluoroacetic anhydride

**Scheme 5**

Scheme 5 details the successful synthesis of (13) following reaction of (7) with 2.5 equivalents of trifluoroacetic anhydride for ten minutes.<sup>20</sup> Titration of the crude material using diethyl ether afforded the product as a white powder in 74% yield.

**2.6 SCHEME 6: SYNTHESIS OF 4-AMINOPHEN-2(2D<sub>2</sub>)-ETHYL BROMIDE HYDROCHLORIDE (17)**



**Scheme 6**

Scheme 6 outlines the synthesis of 4-aminophen-2(2d<sub>2</sub>)-ethyl bromide hydrochloride (**17**). Preparation of the deuterated analogue of 4-aminophenethyl bromide began with selective deuteration at the alpha carbon of 4-nitrophenylacetic acid. This was carried out via deprotonation with BuLi (3 equivalents) at 0°C for 1.5 hours. The addition of deuterium oxide for a further hour produced the desired product as a precipitate which was filtered to give (**14**) as an orange powder in 93% yield.<sup>22</sup> These initial conditions provided an excellent yield of the desired product (93%) and therefore experimental variation was not required.

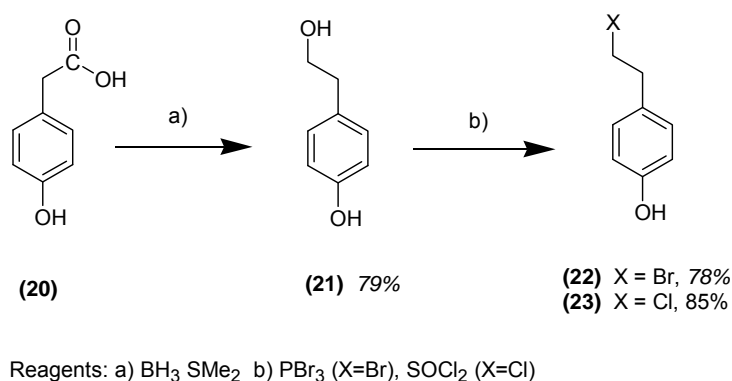
Reduction of a solution of the acid (**14**) in diethyl ether was carried out with borane dimethyl sulphide (3 equivalents) for 24 hours at room temperature under nitrogen.<sup>2</sup> The Vigreux column method previously discussed (Section 2.1) was employed in order to maximize product yield. Quenching of the reaction with water, extraction of the product into chloroform and

recrystallization in ethanol provided the pure compound **(15)** as yellow salts. A reasonable yield of 74% was obtained in the initial reaction, and therefore experimental variation was not required.

The reaction of **(15)** with three equivalents of phosphorous tribromide in chloroform at reflux for 24 hours yielded crude material.<sup>7</sup> Purification using flash chromatography (10% Methanol in DCM) provided the product **(16)** as orange crystals (74% yield).

Reduction of the nitro group of **(16)** was achieved via hydrogenation in THF using 10% palladium on charcoal, at 3 atmospheres for 12 hours.<sup>14</sup> Easy purification was facilitated through removal of the catalyst by filtration through celite, followed by evacuation of the solvent to provide the product as an orange oil. Conversion of the free amine to the hydrochloride salt was achieved by the addition of a HCl saturated solution of diethyl ether to the compound dissolved in chloroform.<sup>7</sup> The precipitated HCl salts were dried and recrystallized in ethanol to give pure product **(17)** as a white powder in 57% yield. The moderate yield may be attributed to the presence of water in the ether and polymerization of the non-protected intermediate. The experimental procedure was not repeated as sufficient quantities of material were obtained for NMR kinetic analysis.

## 2.7 SCHEME 7: SYNTHESIS OF 4-HYDROXYPHENETHYL HALIDES



**Scheme 7**

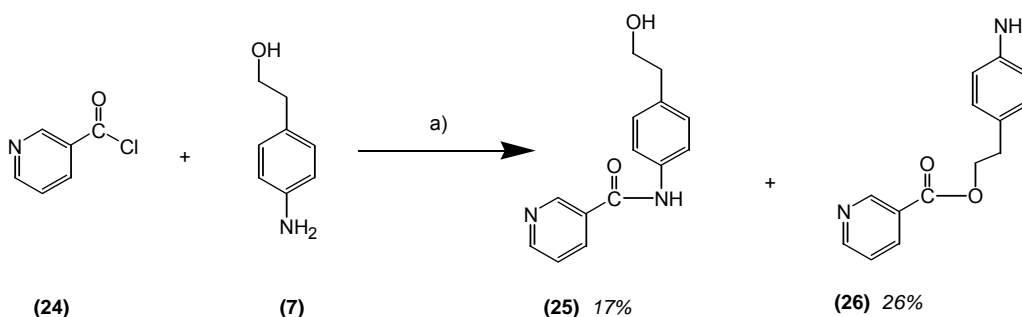
Scheme 7 details the synthesis of 4-hydroxyphenethyl bromide (**22**) and 4-hydroxyphenethyl chloride (**23**). These compounds were synthesized in order to conduct a comparative study of the antitumor activity expressed by 4-hydroxy versus 4-amine analogues.

The alcohol was synthesized via reaction of 4-hydroxyphenylacetic acid with borane dimethyl sulfide (2 eq) in ether at room temperature for 24 hours.<sup>2,3</sup> Aqueous workup and recrystallization in chloroform yielded (**21**) in 79% yield as yellow crystals.

Bromination of 4-hydroxyphenethyl alcohol (**21**) was carried out with phosphorous tribromide (7 eq, reflux, 48 hours) in chloroform.<sup>7</sup> Aqueous workup and purification via flash chromatography (10% MeOH in DCM) provided the pure product (**22**) as orange crystals in 78% yield.

The preparation of 4-hydroxyphenethyl chloride was achieved via the reaction of (**21**) dissolved in chloroform with thionyl chloride (3 eq, reflux, 24 hours).<sup>10</sup> Aqueous workup, extraction with chloroform and purification of the product via flash chromatography (10% MeOH in DCM) yielded the product (**23**) as yellow crystals (85% yield).

**2.8 SCHEME 8: 1<sup>ST</sup> ATTEMPTED SYNTHESIS OF 4-(2-CHLOROETHYL)-N-(3-PYRIDINYLMETHYL)ANILINE DIHYDROCHLORIDE (36)**



Reagents: a)  $K_2CO_3$  (s)/THF

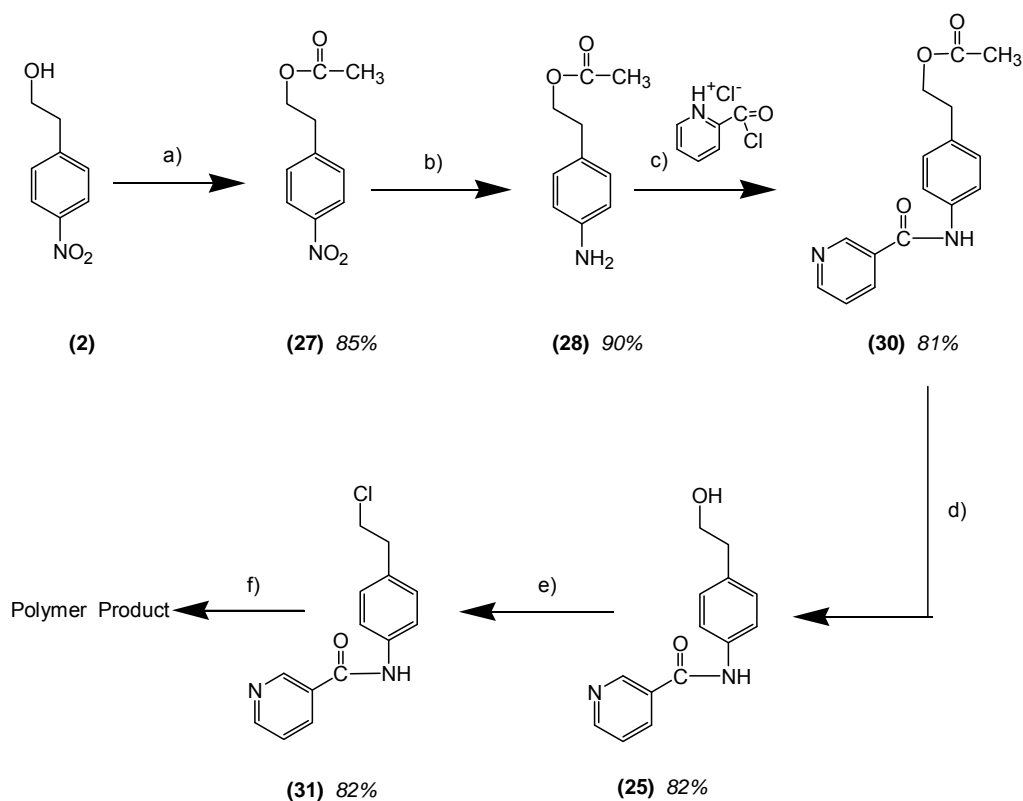
**Scheme 8**

Scheme 8 details the initial step undertaken in attempting synthesis of 4-(2-chloroethyl)-N-(3-pyridinylmethyl)aniline dihydrochloride. It was envisaged that this molecule and its counterparts (see Schemes 12-15) would, similarly to CC-1065, confer antitumor activity through both covalent and non-covalent interaction with DNA.

Initial attempts to synthesis the amide (**25**) employed the acid chloride (**24**) with 1 equivalent of 4-aminophenethyl alcohol (**7**) in a heterogeneous mixture of solid  $K_2CO_3$  and THF (reflux, 72 hours) under nitrogen. This method is a modification of the Schottman-Bauman procedure in which an aqueous solution of base is used in place of solid  $K_2CO_3$ .

Purification via flash chromatography provided the required amide (**25**) as yellow crystals, together with ester, (**26**). Due to the low yield of amide (17%), an alternative scheme (Scheme 2.9) involving alcohol protection, reaction of the amine with acid chloride and subsequent deprotection of the alcohol, was devised in order to minimize the loss of material in the initial steps of the scheme.

**2.9 SCHEME 9: 2<sup>ND</sup> ATTEMPTED SYNTHESIS OF 4-(2-CHLOROETHYL)-*N*-(3-PYRIDINYLMETHYL)ANILINE DIHYDROCHLORIDE (36)**



Reagents: a) Acetic anhydride b) 10% Pd/C c) K<sub>2</sub>CO<sub>3</sub> d) K<sub>2</sub>CO<sub>3</sub>/MeOH e) SOCl<sub>2</sub> f) BH<sub>3</sub> SMe<sub>2</sub>

**Scheme 9**

Scheme 9 details the attempted synthesis of 4-(2-chloroethyl)-*N*-(3-pyridinylmethyl)aniline dihydrochloride (**36**) which involved the protection and subsequent deprotection of the hydroxy functionality of 4-aminophenethyl alcohol. As envisaged, this scheme minimized the loss of intermediary products through a quick and efficient route.

Protection of the alcohol group of 4-aminophenethyl alcohol as the acetamide was via neat reaction at room temperature for 24 hours with acetic anhydride (2 eq).<sup>16</sup> Purification of product to give an 85% yield of yellow crystalline solid (**27**), was via partitioning between K<sub>2</sub>CO<sub>3</sub> and chloroform.

Reduction of the nitro group of **(27)** to the amine was carried out with 10% palladium on charcoal (w/w 1:10) using catalytic hydrogenation, over a period of 12 hours at 3 atmospheres.<sup>14</sup> Filtration of the resultant product through celite to remove catalyst together with flash chromatography (10% MeOH/DCM) successfully separated the amine product **(28)** from the starting material as an orange oil in 90% yield.

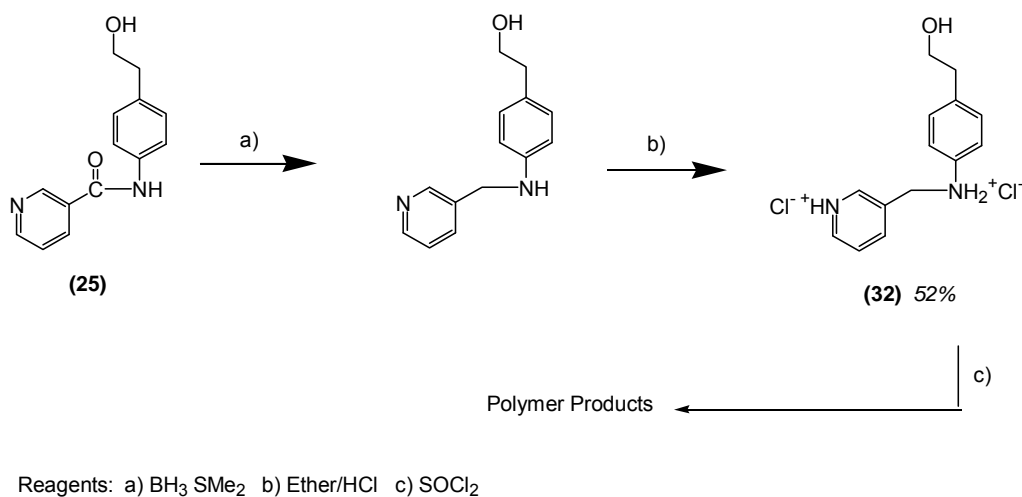
Reaction of the amine **(28)** with 1 equivalent of nicotinoyl chloride hydrochloride via the modified *Schottman-Baumann* procedure discussed above<sup>23,25</sup> (reflux, 72 hours) produced the target amide **(30)** in 81% yield as yellow crystals. Reaction conditions employed solid phase  $K_2CO_3$  as an HCl trap, which was subsequently removed via filtration.<sup>24,24</sup> Starting material was removed from the reaction residue via flash chromatography (10% MeOH in DCM) to give the amide in 81% yield.

Deprotection of **(30)** to give **(25)** in 82% yield was achieved via reaction with MeOH ( $w_{(30)}/v_{MeOH}$ , 1:5) in aqueous  $K_2CO_3$  ( $w_{(30)}/w_{K_2CO_3}$ , 1:1) at reflux for 24 hours.<sup>25</sup> Extraction into diethyl ether produced the target compound **(25)** as a white powder in 82% yield. This gave an overall yield of the alcohol of 52% from **(2)**, a substantial improvement from the former synthesis (Section 2.8) of 17%.

Initial chlorination attempts of **(25)** utilised thionyl chloride (10 eq) in refluxing chloroform for twelve hours under nitrogen. Extraction into chloroform provided the target product **(31)** as yellow crystals however, the reaction residue contained starting material in significant amounts (31%). A more desirable procedure involved the use of neat thionyl chloride (5 equivalents) at reflux for two hours.<sup>26,27</sup> Purification via flash chromatography (10% MeOH in DCM) gave **(31)** in 82% yield.

The attempted synthesis of **(36)** was via reduction of the carbonyl group of **(31)** with borane dimethyl sulphide (3 eq, room temperature, 24 hours).<sup>2,3</sup> Aqueous workup, extraction into chloroform and flash chromatography failed to isolate a single product. Mass spectroscopy and NMR indicated the formation of polymerization products.

**2.10 SCHEME 10: THIRD ATTEMPTED SYNTHESIS OF 4-(2-CHLOROETHYL)-*N*-(3-PYRIDINYLMETHYL)ANILINE DIHYDROCHLORIDE (36)**



**Scheme 10**

Scheme 10 outlines the attempted synthesis of 4-(2-chloroethyl)-*N*-(3-pyridinylmethyl)aniline dihydrochloride (**36**). It was envisaged that reduction of the carbonyl group of (**25**) prior to chlorination would be a more efficient route to the target molecule (**36**). It was hoped that the acidic environment of the chlorination reaction would assist in stabilizing the molecules as its amine salt, thereby hindering polymerization of the molecule.

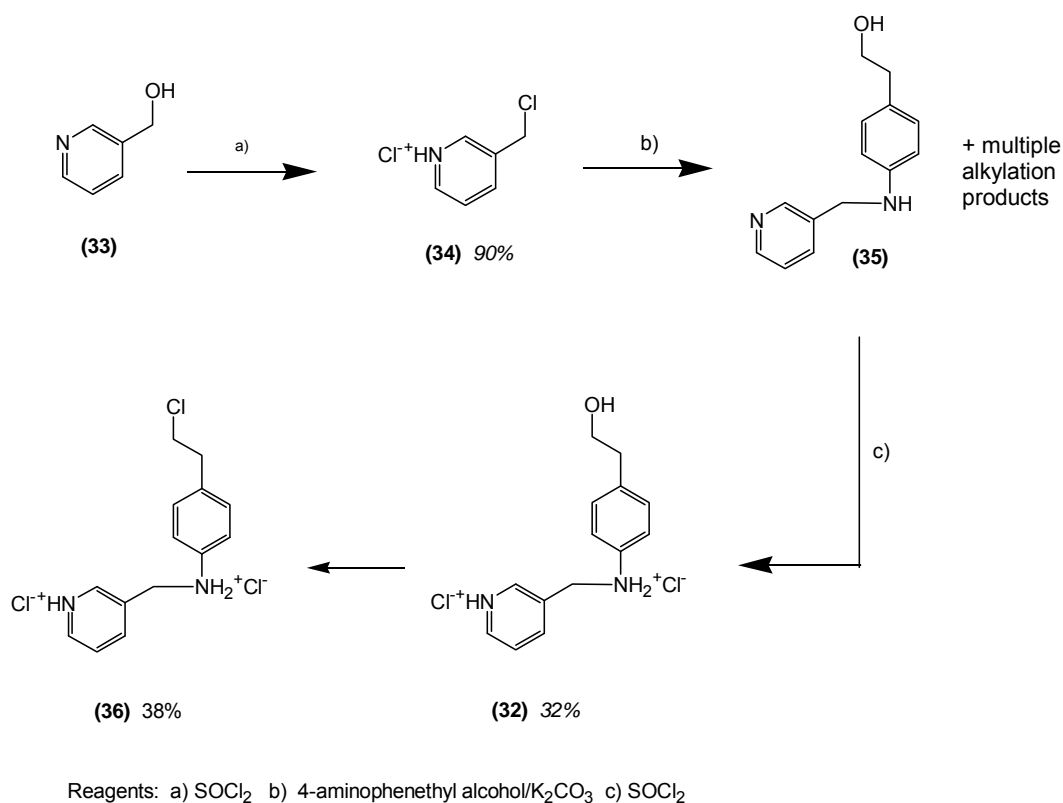
Reduction of (**25**) was carried out with borane dimethyl sulphide in diethyl ether (3 equivalents, reflux, 48 hours) under nitrogen.<sup>2,3</sup> Aqueous workup, extraction into diethyl ether and conversion to the HCl salt afforded the target compound (**32**) in 52% yield as a white solid.

Subsequent chlorination of (**32**) with neat thionyl chloride for two hours at reflux under nitrogen failed to produce a single target product.<sup>26,27</sup> Mass spectroscopy and NMR indicated that polymerization had occurred.

While small traces of the monomeric product were able to be isolated using flash chromatography, the quantity isolated was insufficient for analysis and therefore further synthesis was required.

Rather than trying to optimize the reaction conditions set out in Scheme 10, a decision was made to employ starting materials which had become newly available and could provide the title compound (**36**) following 3 simple synthetic steps (Scheme 11).

**2.11 SCHEME 11: SYNTHESIS OF 4-(2-CHLOROETHYL)-N-(3-PYRIDINYLMETHYL) ANILINE DIHYDROCHLORIDE (36)**



**Scheme 11**

Scheme 11 details the alternative 3-step synthesis of 4-(2-chloroethyl)-N-(3-pyridinylmethyl)aniline dihydrochloride (**36**). Chlorination of 3-pyridyl carbinol (**33**) was via the use of neat thionyl chloride (3 eq) at reflux for four hours.<sup>26,27</sup> Distillation of excess thionyl chloride, titration of the reaction mixture with hexane several times and removal of residual thionyl chloride under high vacuum provided crude product. The product was purified via flash chromatography (1% TEA/10% MeOH/DCM) and converted to the hydrochloride salt in 90% yield.

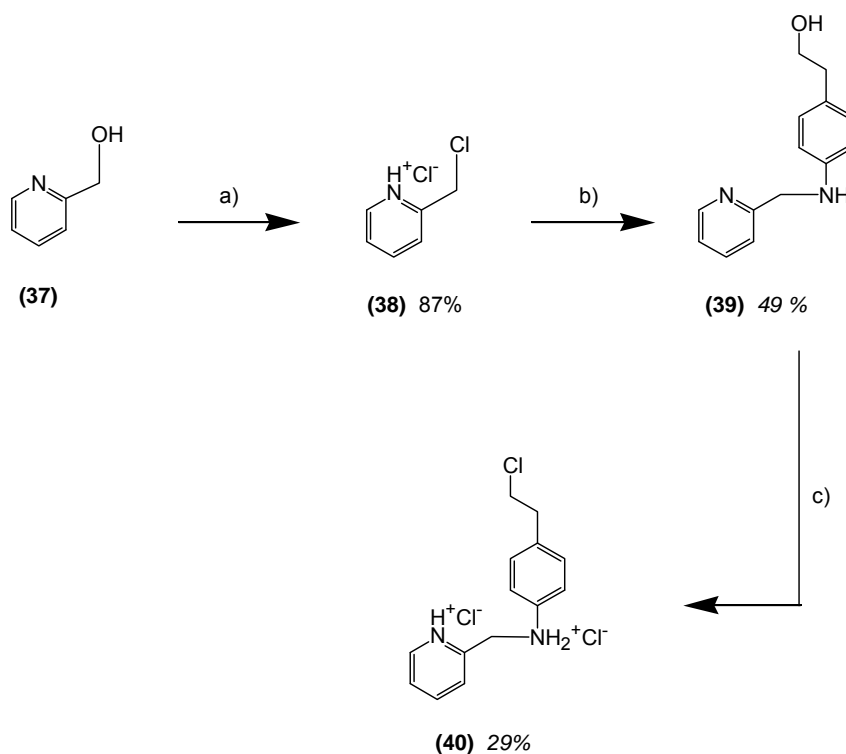
Compound (**34**) was coupled with 4-aminophenethyl alcohol (**7**)<sup>23,24</sup> in a refluxing heterogeneous solution of K<sub>2</sub>CO<sub>3</sub> and THF for 12 hours. The reaction mixture predominantly

contained the tertiary and quaternary amines, yielding only a relatively small proportion of compound **(35)**. This was not unexpected due to the increased nucleophilicity of amines with increased substitution. However, the monoalkylated product **(35)** was our preferred product and purification (32% yield) was achieved using flash chromatography (10% MeOH/CHCl<sub>3</sub>).

Chlorination of the hydrochloride salt of **(35)** with thionyl chloride (10 equivalents, 2 hours, reflux) yielded crude material.<sup>26,27</sup> Cleanup via conversion to the HCl salt and recrystallization of the salt in ethanol provided **(36)** as a pale brown powder in 38% yield.

Because of the simplicity and success of this synthetic route additional molecules of this type were designed (Schemes 2.12 – 2.15).

**2.12 SCHEME 12: SYNTHESIS OF 4-(2-CHLOROETHYL)-*N*-(2-PYRIDINYLMETHYL) ANILINE DIHYDROCHLORIDE (40)**



Reagents: a)  $\text{SOCl}_2$  b) 4-aminophenethyl alcohol/ $\text{K}_2\text{CO}_3(\text{s})$  c)  $\text{SOCl}_2$

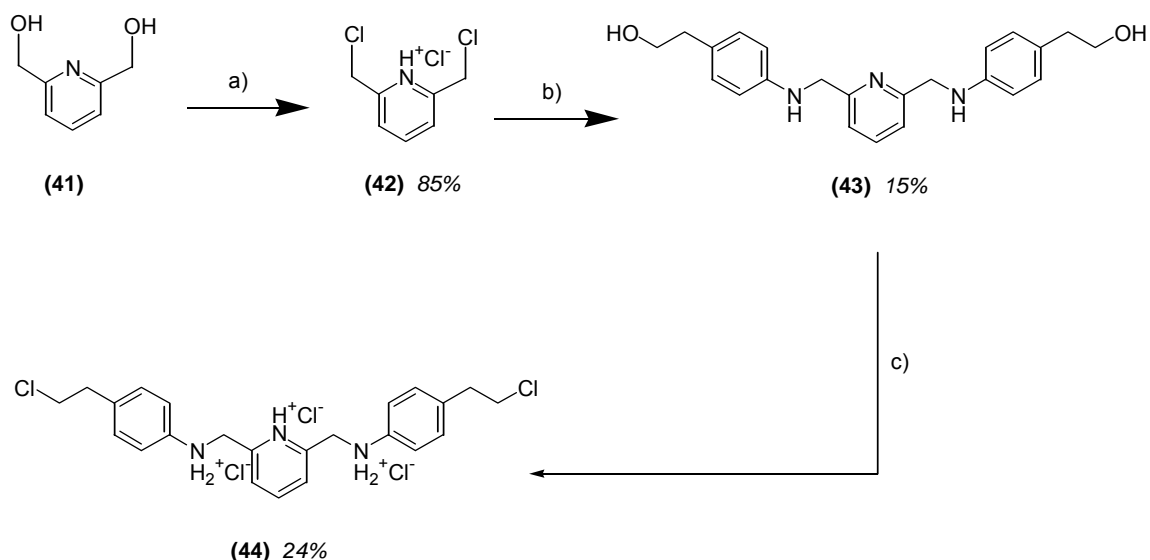
**Scheme 12**

The above scheme details the synthesis of 4-(2-chloroethyl)-*N*-(2-pyridinylmethyl)aniline dihydrochloride (**40**). Chlorination of 2-pyridyl carbinol (**37**) was via reaction with three equivalents of thionyl chloride at reflux for two hours under nitrogen.<sup>26,27</sup> Purification via flash chromatography (1% TEA/10% MeOH/DCM) and conversion to the hydrochloride salt afforded (**38**) in 87% yield.

The amine coupling reaction was carried out in a heterogeneous mixture of THF and  $\text{K}_2\text{CO}_3(\text{s})$  at reflux for 12 hours. The solid phase of the reaction was filtered off and the THF removed under vacuum to give crude material which was purified via flash chromatography (10% MeOH/ $\text{CHCl}_3$ ) to provide (**39**) as a white powder in 49% yield.

Chlorination of the hydrochloride salt of **(39)** in chloroform was carried out using thionyl chloride (10 eq) for 2 hours at reflux.<sup>26,27</sup> Basification with  $K_2CO_3$ , followed by extraction into chloroform and recrystallization in ethanol gave pure product **(40)** as yellow crystals (29% yield).

**2.13 SCHEME 13: SYNTHESIS OF N,N'-BIS[4-(2-CHLOROETHYL)PHENYL]-2,6-PYRIDINEDIMETHYLAMINE**



Reagents: a)  $\text{SOCl}_2$  b) 4-aminophenethyl alcohol/ $\text{K}_2\text{CO}_3(\text{s})$  c)  $\text{SOCl}_2$

**Scheme 13**

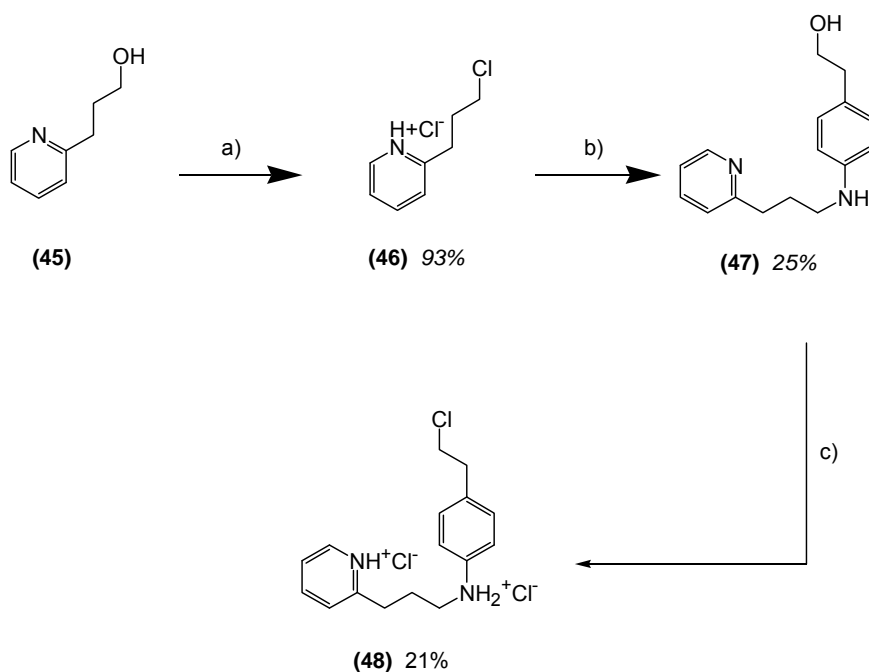
Scheme 13 details the synthesis of N,N'-bis[4-(2-chloroethyl)phenyl]-2,6-pyridinedimethylamine (**44**). Chlorination of the diol (**41**) employed thionyl chloride (4 eq) at reflux for 4 hours under nitrogen.<sup>26,27</sup> Trituration with hexane and column chromatography (1% TEA/10% MeOH/DCM) afforded pure product (**42**) as a white powder (85% yield).

Amine coupling via the use of a heterogeneous system employing (**42**) and (**7**) dissolved in THF and solid  $\text{K}_2\text{CO}_3$  at reflux for 12 hours, followed with purification via flash chromatography (10% MeOH/ $\text{CHCl}_3$ ) afforded (**43**) in a yield of 15% as a white solid. As for compound **43**, the majority of the crude reaction material contained tertiary and quaternary amine products, however as these were not the compounds of interest they were neither isolated nor characterized in full.

Initial attempts at the chlorination of (**43**) employed thionyl chloride in chloroform, at reflux for two hours. These conditions however, gave only small quantities of the desired product

which proved difficult to isolate from the polymeric mass. Successful bischlorination of **(43)** with thionyl chloride (10 eq) for four hours at room temperature under nitrogen provided the desired product together with a reduced amount of polymer product.<sup>26,27</sup> The target compound **(44)** was purified via flash chromatography (10% MeOH/CHCl<sub>3</sub>) and precipitated as the hydrochloride salt. The salt was recrystallized in ethanol to provide pure product as yellow crystals in 24% yield.

**2.14 SCHEME 14: SYNTHESIS OF 4-(2-CHLOROETHYL)-N-[3-(2-PYRIDINYL)PROPYL]ANILINE DIHYDROCHLORIDE (48)**



Reagents: a)  $\text{SOCl}_2$  b) 4-aminophenethyl alcohol/ $\text{K}_2\text{CO}_3(\text{s})$  c)  $\text{SOCl}_2$

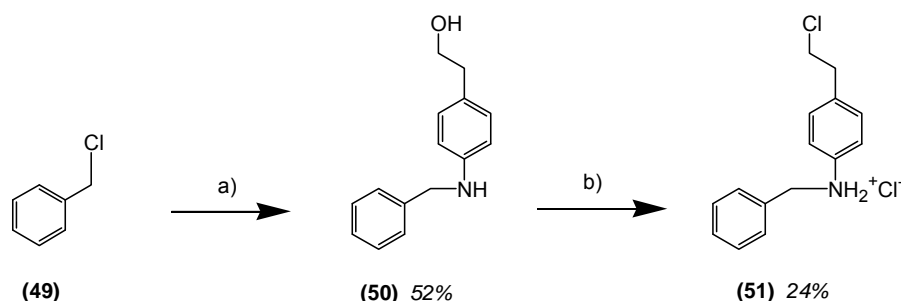
**Scheme 14**

Scheme 15 outlines the synthesis of 4-(2-chloroethyl)-N-[3-(2-pyridinyl)propyl]aniline dihydrochloride (**48**). Chlorination of (**45**) with neat thionyl chloride (4 eq) at reflux for four hours under nitrogen afforded compound (**46**).<sup>26,27</sup> The excess thionyl chloride was removed from the reaction via distillation. The crude material was triturated with hexane and converted to the hydrochloride salt which was subsequently recrystallized in ethanol to provide pure compound (**46**) as a pale brown powder in 93% yield.

The addition of the hydrochloride salt of 4-aminophenethyl alcohol (**7**) to (**46**) (1 eq), via a modified Schottman-Bauman procedure, in a mixture of THF and aqueous  $\text{K}_2\text{CO}_3$  for 12 hours at reflux yielded (**47**).<sup>23,24</sup> Workup via extraction into chloroform and recrystallization in ethanol yielded the pure compound in 25% yield as a white crystalline solid.

Compound **(48)** was prepared via chlorination of **(47)** with thionyl chloride (10 eq) in chloroform at reflux for 4 hours under nitrogen.<sup>26,27</sup> Basification with  $K_2CO_3$  followed by extraction into chloroform and recrystallization in ethanol provided **(48)** as yellow crystals in 21% yield.

**2.15 SCHEME 15: SYNTHESIS OF *N*-BENZYL-4-(2-CHLOROETHYL)ANILINE HYDROCHLORIDE (51)**



Reagents: a) 4-aminophenethyl alcohol/ $K_2CO_3(s)$  b)  $SOCl_2$

**Scheme 15**

Scheme 16 details the synthesis of *N*-benzyl-4-(2-chloroethyl)aniline hydrochloride (**51**). Compound (**50**) was prepared via a modified Schottman-Bauman coupling of (**7**) (1 eq) with (**49**) in a heterogeneous solution of THF and solid  $K_2CO_3$  at reflux for 12 hours.<sup>23,24</sup> Flash chromatography (1% TEA/10% MeOH/ $CHCl_3$ ) afforded (**50**) as a pale yellow solid in 52% yield.

The end product (**51**) was prepared via chlorination with neat thionyl chloride (10 eq) in chloroform under nitrogen for three hours.<sup>26,27</sup> Basification with  $K_2CO_3$  followed by extraction into chloroform and recrystallization in ethanol provided the target product as yellow crystals in 24% yield.

## 2.16 MECHANISTIC STUDIES OF 4-AMINOPHENETHYL-2D<sub>2</sub>-BROMIDE (19)

Research directed toward the development of prodrugs has uncovered that *seco*-CPI agents demonstrate alkylation profiles identical to that of their putative (cyclised) counterparts. This observation suggests that *seco*-CPI agents undergo facile ring closure, forming the cyclopropyl intermediate (Figure 38) prior to the event of DNA alkylation.<sup>28-30</sup>

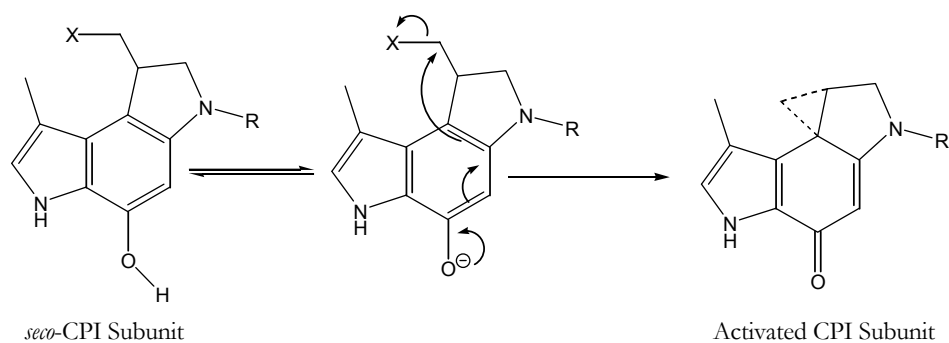


**Figure 38 – Ring Cyclisation of the *seco*-CPI Analogues**

Experiments performed by Winstein *et al.*<sup>31</sup> have confirmed that 4-hydroxyphenethyl halides undergo facile ring closure in a manner similar to *seco*-CPI adducts (Figure 39). More importantly, these simple molecules are also known to exhibit alkylation profiles characteristic of CPI-analogues and the natural product, CC-1065.

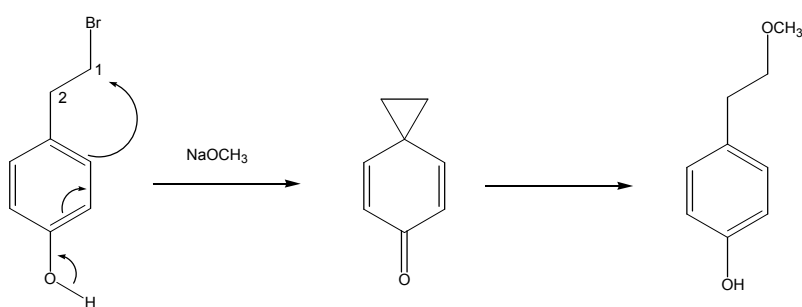


**Figure 39 – Formation of an Intermediary Spirodienone via Reaction of 4-Hydroxyphenethyl Alcohol with Sodium Methoxide**

Previously, we reported that 4-aminophenethyl halides exert a 2.5 fold increase in cytotoxic activity when compared to their 4-hydroxy counterparts. This has been attributed to an increase in non-covalent adduct stabilization arising from interactions between the 4-amino group and AT rich sequences within the minor groove.

The simplicity of the 4-aminophenethyl halide model makes it an attractive vantage point for our current study, where structural modifications would enable us to distinguish features pertinent to DNA-adduct formation.

Given the significance of this model, it was important to confirm that 4-aminophenethyl halides undergo facile ring closure in a manner consistent with that previously observed for the 4-hydroxyphenethyl halides. Although formation of the spirocyclopropylcyclohexadienyl imine intermediate is widely assumed, there has never been a study that was able to discount that DNA alkylation occurred through direct S<sub>N</sub>2 elimination at the C<sub>1</sub>-methyl halide carbon prior to ring cyclisation.

The current study has been able to determine this through a series of NMR experiments that monitored the introduction of sodium azide to a solution 4-aminophenethyl-2(2*d*<sub>2</sub>)-bromide **(19)** in D<sub>2</sub>O.

Sodium azide was selected to represent the N<sub>3</sub>-adenine function, as alkyl azides are poor nucleophiles resulting in di- and trialkylated byproducts that could possibly lead to misinterpretation of the results.<sup>32</sup>

While adenine may have been a more appropriate nucleophile to use in this mechanistic study it was not readily available in the lab. Hence, the lack of availability of adenine, coupled with project time constraints, necessitated the substitution of sodium azide for adenine in this project. (Note: The project has recently been assigned to another student and the results will be published in due course).

The deuterium analogue served to distinguish the C<sub>1</sub> and C<sub>2</sub> centres without altering the molecule's symmetry about the vertical axis, thus ensuring that nucleophilic attack at the C<sub>1</sub> and C<sub>2</sub> centres would remain indiscriminate should pathway B prevail (Figure 41).

### 2.16.1 Pathway A: Alkylation via direct $S_N2$ attack onto the $C_1$ -methyl halide carbon

Pathway A was expected to prevail in the event that 4-aminophenethyl-2-( $2d_2$ )-bromide (**19**) demonstrated a poor propensity to undergo ring closure, or the  $C_1$ -methyl halide carbon proved particularly susceptible to nucleophilic attack. The results here would indicate a large product ratio, with exclusive formation of the 4-aminophenethyl-2-( $2d_2$ )-azide (isomer A) (Figure 40) following direct  $S_N2$  attack onto the  $C_1$ -methyl halide carbon.

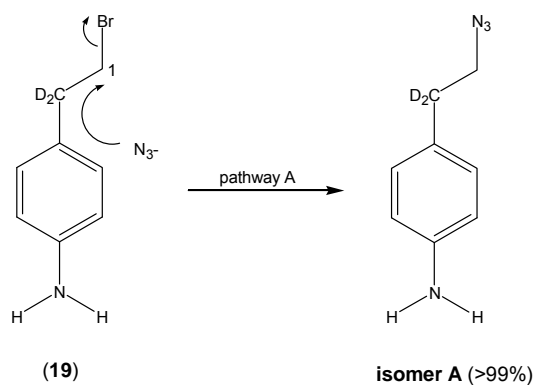


*Figure 40 – Direct  $S_N2$  attack by  $N_3^-$  at  $C_1$*

### 2.16.2 Pathway B: $Ar_{1,3}$ cyclisation followed by $S_N2$ attack onto the $C_1$ or $C_2$ centre

Pathway B was expected to prevail in the event that 4-aminophenethyl-2-( $2d_2$ )-bromide (**19**) readily underwent facile ring closure to form the cyclopropyl function, or the  $C_1$ -methyl halide carbon proved particularly stable to nucleophilic attack.

The results here would indicate a small product ratio, where almost equal amounts of the 4-aminophenethyl-2-( $2d_2$ )-azide (isomer A) (Figure 41) and 4-aminophenethyl-1-( $2d_2$ )-azide (isomer B) (Figure 41) are expected to be produced.

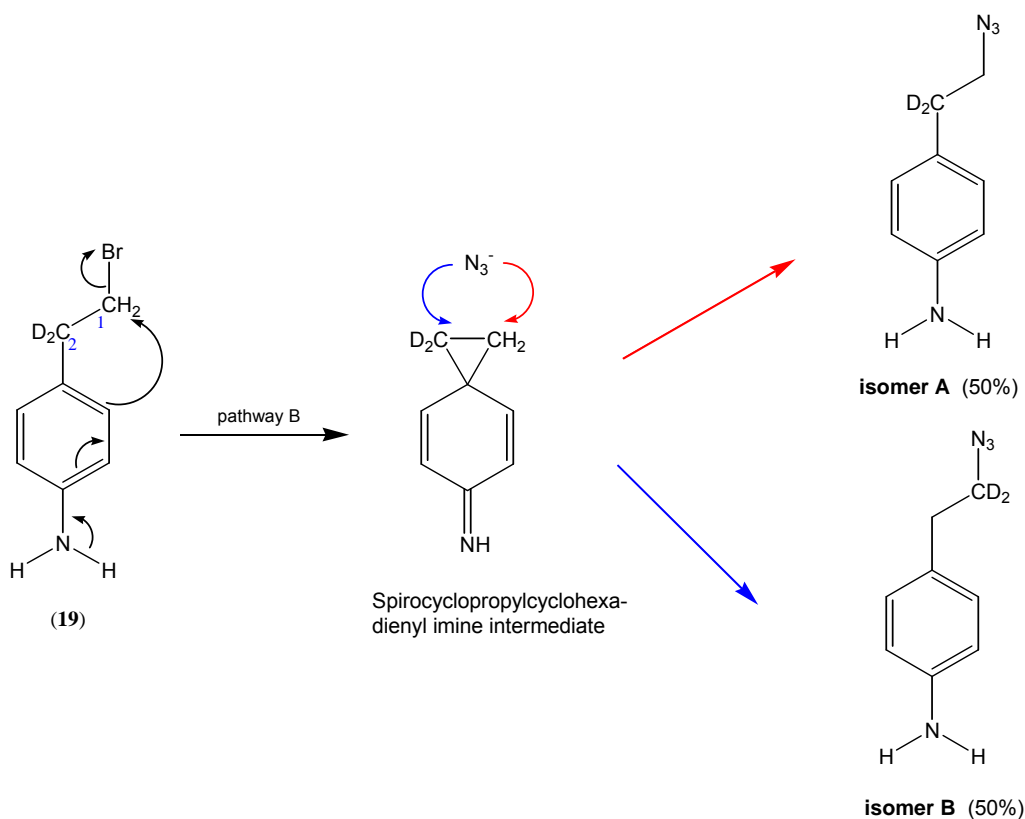


**Figure 41 –  $Ar_{1,3}$  Cyclisation**

### 2.16.3 Nuclear Magnetic Resolution Studies

Spectrum A (Figure 42) was recorded 15 minutes after the introduction of 4-aminophenethyl-2( $2d_2$ )-bromide ( $\sim 95\%$  deuterium) to a solution of acetone- $d_6$  /  $D_2O$  (5M, 10%) at room temperature (Figure 39). The proton spectrum shows a singlet at  $\delta$  3.43 ppm, indicating a single analogue. The chemical shift is indicative of cyclopropyl methylene protons, however the stable presence of 4-aminophenethyl-2( $2d_2$ )-bromide (19) can not be discounted.

Spectrum B (Figure 43) was taken following the introduction of sodium azide (1M, 1 hr) to the solution recorded in Spectrum A. Difficulties in shimming the reaction mixture due to the rapidly proceeding reaction within the NMR tube resulted in a decrease in the quality of the spectrum, however the spectrum recorded was considered sufficient to indicate what was occurring within the reaction mixture. The spectrum clearly shows two singlets of equal

intensity at  $\delta$  2.85 ppm and  $\delta$  3.57 ppm, indicating the presence 4-aminophenethyl-1-(2*d*<sub>2</sub>)-azide (Isomer B) and 4-aminophenethyl-2-(2*d*<sub>2</sub>)-azide (Isomer A).

A comparison of these two spectra allowed us to deduce that the species in Spectrum A was in fact the spirocyclopropylcyclohexadienyl imine intermediate, hence confirming that facile ring closure precedes alkylation thereby generating the two expected isomers, (Isomer A) and (Isomer B), in approximately equal molar amounts.

The propensity for 4-aminophenethyl halides to undergo facile ring closure can be attributed to an increase in 4-amino Ar<sub>1,3</sub> participation compared to that of their 4-hydroxy counterparts. This difference is believed to account for the superior activity observed for 4-aminophenethyl halides, where ready conversion to the active intermediate is expected to render them more susceptible to N3-adenine attack.

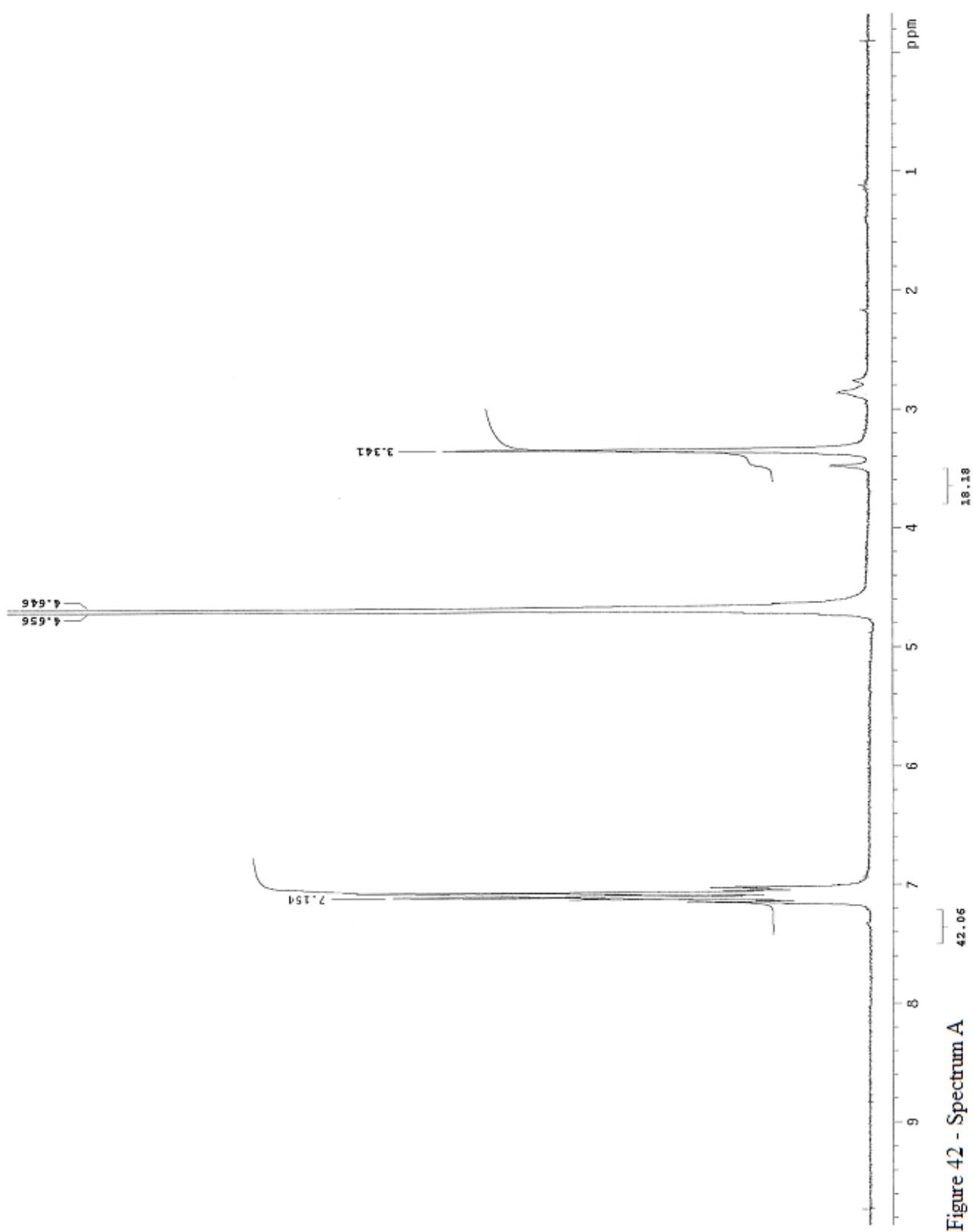


Figure 42 - Spectrum A

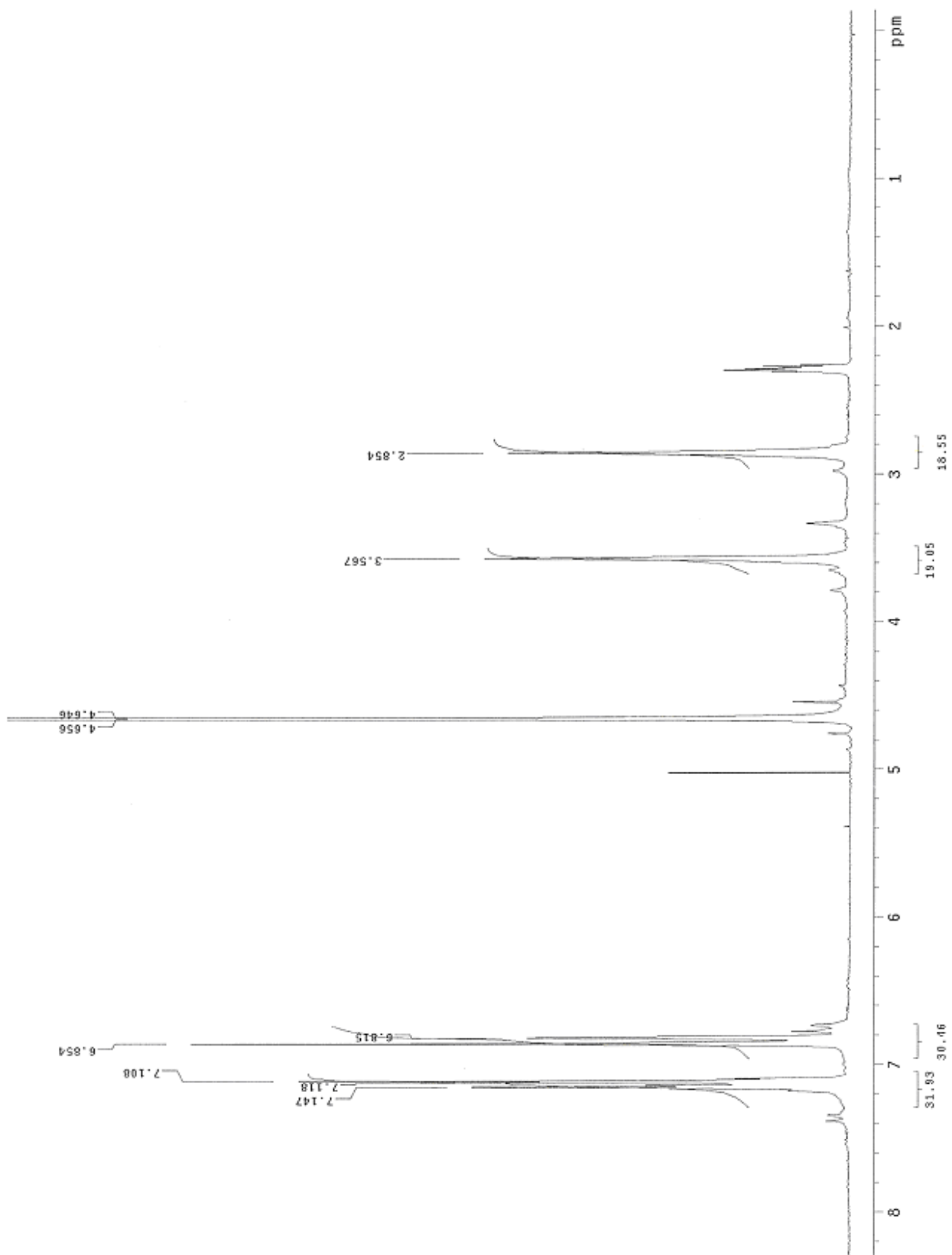


Figure 43 - Spectrum B

## **2.17 REFERENCES**

1. Pizey, J. S. *Synthetic Reagents (Vol 3)*. John Wiley and Sons Inc. New York. 1977. Vol 3, 53-63.
2. Krishnamurthy, S. *Tetrahedron Lett.*, **1982**, 23(33), 3315-3318.
3. Crochet, R. A., Blanton, C. D. *Syn.*, **1974**, 55-56.
4. Brown, H. C., Choi, Y. M., Narasimhan, S. *J. Org. Chem.*, **1982**, 47, 3153-3163.
5. Brown, H. C., Stocky, T. P. *JACS*, **1977**, 99(25), 8218-8226.
6. Casey, M., Leonard, J., Lygo, B., Procter, G. *Advanced Practical Organic Chemistry*. Chapman and Hall, New York, 1990, 129-136.
7. Vogel, A. I. *Textbook of Practical Organic Chemistry (5<sup>th</sup> ed.)*. Longman Scientific and Technical, New York, 1989, 412-417.
8. Lin, C. H., Aristoff, P. A., Johnson, P. D., McGrath, J. P., Timko, J. M., Robert, A. *J. Org Chem.*, **1987**, 52(25), 5594-601.
9. Bennett, G. M. and Hafez, M. M. *J. Chem Soc., Abstracts*, **1941**, 652-659.
10. Pizey, J. S. *Synthetic Reagents (Vol 1)*. John Wiley and Sons Inc. New York. 1974. Vol 1, 323-331.
11. Valu, K. K., Gourdie, T. A., Boritzki, T. J., Gravatt, G. L., Baguley, B. C., Wilson, W. R., Wakelin, L. Denny, W. A. *J. Med. Chem*, **1990**, 33, 3014-319.
12. Clarke, H. T. and Hartman W. W. *Organic Synthesis (Collective Volume 1)*, **1932**, 455-456.
13. Xing, W. and Ogata, Y. *J. Org Chem.*, **1982**, 47, 3577-3581.
14. Terpko, M. O., Heck, R. F. *J. Org. Chem.*, **1980**, 45, 4992-4993.
15. Vogel, A. *Textbook of Practical Organic Chemistry (5<sup>th</sup> ed.)*. Longman Scientific and Technical, New York, **1989**, 356-360.
16. Greene, T. *Protective Groups in Organic Synthesis (1<sup>st</sup> ed.)*. Wiley-Interscience Publications, New York, **1991**, 212-213.
17. Middleton, W. *J. Org Chem.*, **1975**, 40(5), 574-578.
18. Cheng, C. S., Ferber, C, Bashford, R. I., Grillot, G. F. *JACS*, **1951**, 73(3), 4081-4084.
19. Darzac, M., Brotin, T., Rousset-Arzel, T., Bouchu, D., Dutasta, J. *New J.Chem.*, **2004**, 28(4), 502-512.
20. Strazzolini, P., Verardo, G., Giumanini, G. *J. Org. Chem.* 1988, 53, 3321-3325.
21. Onaka, M., Ishikawa, K., Izumi, Y. *Chem. Lett.*, **1982**, 11, 1783-1786,

22. Herbert, R.B. and Knaggs, A.R. *J. Chem. Soc. Perkin Tran 1*, **1992**, 1903-1907.
23. Oshiro, K., Ogata, T., Yoshida, H., Inokawa, S. *Nippon Kagaku Zasshi*, **1968**, 89(2), 211-213.
24. Blanke, S., Blanke, R. *J. Anal. Toxicology*, **1984**, 8(5), 231-233.
25. Greene, T. and Wuts, P. *Protective Groups in Organic Synthesis (3<sup>rd</sup> ed.)*. Wiley-Interscience Publications, New York, **1999**, 289-292.
26. Trost, B. M., Fleming, I. *Comp. Org Chem*, **1993**, 6, 204-205.
27. Cope, A. C., Ciganek, E. *Organic Syntheses*, **1959**, 339.
28. White, R. H., Parsons, P. G., Prakash, A. S., Young, D. J. *Bioorganic and Medicinal Chem. Lett.*, **1995**, 5(16), 1869-1874.
29. Boger, D. L., Nishi, T., Teegarden, B. R. *J. Org. Chem.*, **1994**, 59, 4943-4949.
30. Boger, D. L., Ishizaki, T., Zarrinmayeh, H., Munk, S. A., Kitos, P. A., Suntornwat, O. *J. Am. Chem. Soc.*, **1990**, 112, 8961-8971.
31. Baird, R., Winstein, S. *J. Am. Chem. Soc.*, **1963**, 85, 567-575.
32. McMurry, J. *Organic Chemistry*, **1992**, Brooks/Cole Publishing Company, California, 972.

## **CHAPTER 3 – ORGANIC SYNTHESIS:**

### **EXPERIMENTAL**

#### **3.1 GENERAL PREPARATION**

##### **3.1.1 Experimental Setup for Moisture/Oxygen Sensitive Reactions**

Reactions requiring the exclusion of moisture and/or oxygen were conducted under an inert atmosphere of nitrogen or argon. All glassware was oven or flame dried prior to use.

##### **3.1.2 Solvents**

Tetrahydrofuran (THF), diethyl ether and dichloromethane (DCM) were distilled under a nitrogen atmosphere. THF and diethyl ether were distilled from sodium/benzophenone. DCM was distilled from calcium hydride. All deuterated solvents were supplied by Cambridge Isotope Laboratories (CIL) and were used without further purification.

##### **3.1.3 Reagents**

Acetic anhydride was supplied by AJAX Chemicals. All other reagents were supplied by the Aldrich Chemical Co. Thionyl chloride was distilled prior to use. All other chemicals were used without any further purification.

#### **3.2 INSTRUMENTATION**

##### **3.2.1 NMR Spectroscopy**

Proton ( $^1\text{H}$ ) nmr spectra were obtained on a Gemini 200, Varian Unity 400, or Bruker 600 spectrometer at 200 MHz, 400 MHz and 600 MHz respectively. Carbon ( $^{13}\text{C}$ ) nmr spectra were obtained on a Gemini 200, Varian Unity 400, or Bruker 600 spectrometer at 50 MHz, 100 MHz and 150 MHz respectively.

All spectra were internally referenced to TMS (0.0). Chemical shifts were recorded in parts per million (ppm) and peaks denoted as singlet (s), doublet (d), doublet of doublets (dd), doublet of triplets (dt), triplet (t), multiplet (m) or broad (br).

### **3.2.2 Microanalysis**

Microanalyses were performed by the Microanalytical Units of the University of Queensland, the Australian National University and the University of Auckland.

### **3.2.3 Melting Points**

Melting Points were determined on a Gallenkamp Electrothermal Digital Melting Point Apparatus and are uncorrected.

### **3.2.4 Mass Analysis**

Mass Spectrometry was performed on a VG PLATFORM2 Quadrupole mass spectrometer, using Electrospray Ionisation (ESI).

### **3.2.5 UV Absorption**

UV spectra were obtained on a BGBC 916 UV/VIS dual beam Scanning spectrometer, recording within a wavelength range of 200 and 500 micrometres and employing a compound concentration of  $10^{-4}$  g/L.

## **3.3 CHROMATOGRAPHY TECHNIQUES**

All thin layer chromatography (TLC) was performed on Merck TLC Aluminium silica gel 60 sheets ( $F_{254}$ ), visualized under ultraviolet light and the retention factors (RF) of individually observed components recorded.

Flash chromatography was performed under positive air pressure using Kieselgel (200-430 mesh) 60 Å silica using either 32 mm or 50 mm diameter columns and employing a silica to sample ratio of approximately 25:1. A layer of clean acid washed sand was employed as a silica stabilizer.

High performance liquid chromatography (HPLC) was performed using a Waters™600 pump and controller and a Waters™ 486 tunable absorbance detector at 282 nm. Components were separated on a normal phase silica Waters PrepLC 25 mm column using a 1:1 mixture of hexane and ethyl acetate at a flow rate of 15 mL/minute.

### **3.4 THE SYNTHESIS OF SIMPLE DNA ALKYLATING CPI ANALOGUES**

#### **3.4.1 Synthesis of 4-Aminophenethyl bromide Hydrochloride\_(4)**

##### **i) 4-Nitrophenethyl Alcohol (2)**

To a dry 250mL flask equipped with a septum cap and stirrer bar was added a solution of 4-nitrophenylacetic acid ((**1**), 8.0g, 48.4 mmol) in THF (100mL) under nitrogen. The solution was cooled in ice and 2M borane dimethyl sulfide in 2.0 M THF (48.4 mL, 96.8 mmol) was added dropwise via a syringe. The reaction was stirred at room temperature for 12 hours.<sup>1,2</sup> After this time, the reaction was quenched with water and all solvents removed under reduced pressure. The desired product was extracted into chloroform, dried (MgSO<sub>4</sub>), filtered and the solvent removed under vacuum. The solid was recrystallized from 10% water/ethanol and dried under high vacuum to give (**2**) as yellow crystals (2.46 g, 30% yield): mpt 63-65 °C (lit<sup>3</sup> 63°C).

$\delta_{\text{H}}$  (CDCl<sub>3</sub>, 200 MHz)  $\delta$  1.72 (1H, s, OH), 2.98 (2H, t,  $J_{2,1}$  7.3 Hz, H-2), 3.93 (2H, t,  $J_{1,2}$  7.3 Hz, H-1), 7.43 (2H, d,  $J_{2',3'}$  and  $J_{6',5'}$  8.4 Hz, H-2' and H-6'), 8.14 (2H, d,  $J_{3',2'}$  and  $J_{5',6'}$  8.4 Hz, H-3' and H-5').  $\delta_{\text{C}}$  (CDCl<sub>3</sub>, 50 MHz)  $\delta$  39.2 (CH<sub>2</sub>, C-2), 64.8 (CH<sub>2</sub>, C-1), 118.2 (2CH, Ar), 129.7 (2CH, Ar), 129.8 (quat., Ar), 154.8 (quat., Ar)

##### **ii) Modified reduction of 4-nitrophenylacetic acid to 4-nitrophenethyl alcohol (2)**

An oven dried flask (250 mL) containing a stirrer bar and capped with a septum was equipped with a Vigreux column and maintained under an inert atmosphere of nitrogen. The flask was charged with a solution of 4-nitrophenylacetic acid ((**1**), 8.0g, 48.4 mmol) in THF (100mL). The solution was cooled in ice and a 2M solution of borane dimethyl sulfide in THF (24.2 mL, 48.4 mmol) was added dropwise via a syringe and then stirred at reflux until the distillation of dimethyl sulfide was complete (ie. 4 hours). The flask was brought to room temperature and

the reaction quenched with water.<sup>4,5</sup> The desired product was extracted into chloroform, dried ( $\text{MgSO}_4$ ), filtered and the solvent removed under vacuum. The solid was recrystallized from 10% water/ethanol and dried under high vacuum to give **(2)** as yellow crystals (7.37 g, 91% yield): mpt 63-65 °C (lit<sup>3</sup> 63°C). (Refer to section 4.4.1 (i)).

### iii) 4-Nitrophenethyl Bromide (3)

To a dry flask equipped with stirrer bar and reflux condenser was added **(2)** (6.3 g, 37.7 mmol) in chloroform (40 mL) under nitrogen. Phosphorous tribromide (3.58 mL, 37.7 mmol) was added dropwise with stirring and the reaction refluxed for 12 hours.<sup>6,7</sup> After this period, the reaction was quenched with water and the aqueous layer extracted with further chloroform (3 x 30 mL). The combined organic layers were dried ( $\text{MgSO}_4$ ) and condensed under vacuum. The residue was purified by flash chromatography (10% methanol in DCM) to provide **(3)** as orange crystals (4.95 g, 57% yield): mpt 67 – 68 °C (lit<sup>8</sup> 68 – 70 °C, lit<sup>9</sup> 68-69).

$\delta_{\text{H}}$  ( $\text{CDCl}_3$ , 200 MHz)  $\delta$  3.20 (2H, t,  $J_{2,1}$  7.0 Hz, H-2), 3.69 (2H, t,  $J_{1,2}$  7.0 Hz, H-1), 7.42 (2H, d,  $J_{2',3'}$  and  $J_{6',5'}$  9.2 Hz, H-2' and H-6'), 8.21 (2H, d,  $J_{3',2'}$  and  $J_{5',6'}$  9.2 Hz, H-3' and H-5').  $\delta_{\text{C}}$  ( $\text{CDCl}_3$ , 50 MHz)  $\delta$  34.9 ( $\text{CH}_2$ , C-2), 38.0 ( $\text{CH}_2$ , C-1), 128.5 (2CH, Ar), 135.9 (2CH, Ar), 139.1 (quat., Ar), 141.6 (quat., Ar).

### iv) 4-Aminophenethyl Bromide Hydrochloride (4)

To a flask equipped with a stirrer bar and reflux condenser was added **(3)** (4.9 g, 21.3 mmol) in anhydrous diethyl ether (30 mL) under nitrogen. Tin powder (8.72 g, 73.5 mmol) was added to the reaction with rapid stirring.<sup>10</sup> Diethyl ether (30 mL) saturated with HCl was dried ( $\text{MgSO}_4$ ) and filtered into the reaction vessel. The reaction was refluxed over two days. During this period two additional aliquots of HCl in diethyl ether (30 mL) were added to the reaction. After this time, the reaction was neutralized with a saturated solution of  $\text{K}_2\text{CO}_3$ (aq) (2 mL) and filtered. The filtrate was extracted with chloroform (3 x 30 mL) and dried ( $\text{MgSO}_4$ ). The solvent was removed under reduced pressure and the residue purified by flash chromatography (10% MeOH/DCM) to give a light brown powder. To a dry flask was added a solution of this compound (2.0 g, 9.99 mmol) in chloroform (10 mL). Diethyl ether saturated with HCl was dried ( $\text{MgSO}_4$ ) and added. The precipitate was filtered to give **(4)** as yellow crystals (3.3 g, 65% yield): mpt 208 – 210 °C (lit<sup>11</sup> 212 – 213 °C); (Found C 40.30, H 4.48, N 5.65,  $\text{C}_8\text{H}_{11}\text{BrClN}$  requires C 40.62, H 4.69, N 5.92).

$\delta_{\text{H}}$  ( $\text{D}_2\text{O}$ , 200 MHz)  $\delta$  3.23 (2H, t,  $J_{2,1}$  6.9 Hz, H-2), 3.72 (2H, t,  $J_{1,2}$  6.9 Hz, H-1), 7.35 (2H, d,  $J_{2,3}$  and  $J_{6,5}$  8.8 Hz, H-2' and H-6'), 7.47 (2H, d,  $J_{3,2}$  and  $J_{5,6}$  8.8 Hz, H-3' and H-5').  $\delta_{\text{C}}$  ( $\text{D}_2\text{O}$ , 50 MHz) 32.1 ( $\text{CH}_2$ , C-2), 43.1 ( $\text{CH}_2$ , C-1), 116.1 (2CH, Ar), 127.3 (2CH, Ar), 135.2 (quat., Ar), 150.4 (quat., Ar).

### 3.4.2 Synthesis of 4-Aminophenethyl Chloride Hydrochloride (6)

#### i) 4-Nitrophenethyl Chloride (5)

To a dry flask equipped with a stirrer bar and reflux condenser was added **(2)** (4.76 g, 28.4 mmol) in chloroform (40 mL) under nitrogen. Thionyl chloride (6.21 mL, 85.2 mmol) was added dropwise and the reaction refluxed for 24 h.<sup>12,13</sup> After this time, the reaction was quenched with a saturated solution of  $\text{K}_2\text{CO}_3(\text{aq})$  (4 mL) and extracted with chloroform (3 x 30 mL). The extract was dried ( $\text{MgSO}_4$ ) and the solvent removed *in vacuo*. The residue was purified by flash chromatography (10% methanol in DCM) to give **(5)** as a brown oil (3.53 g, 67% yield).

$\delta_{\text{H}}$  ( $\text{CDCl}_3$ , 200 MHz) 3.17 (2H, t,  $J_{2,1}$  7.0 Hz, H-2), 3.77 (2H, t,  $J_{1,2}$  7.0 Hz, H-1), 7.40 (2H, d,  $J_{2,3}$  and  $J_{6,5}$  8.8 Hz, H-2' and H-6'), 8.15 (2H, d,  $J_{3,2}$  and  $J_{5,6}$  8.8 Hz, H-3' and H-5').  $\delta_{\text{C}}$  ( $\text{CDCl}_3$ , 50 MHz) 38.6 ( $\text{CH}_2$ , C-2), 44.2 ( $\text{CH}_2$ , C-1), 123.8 (2CH, Ar), 129.9 (2CH, Ar), 145.8 (quat., Ar), 147.1 (quat., Ar).

#### ii) 4-Aminophenethyl Chloride Hydrochloride (6)

a) To a dry flask equipped with a stirrer bar and reflux condenser was added **(5)** (3.0 g, 16.2 mmol) in anhydrous diethyl ether (30 mL) under nitrogen. Tin powder (5.77 g, 48.6 mmol) was added to the reaction with rapid stirring.<sup>10</sup> Diethyl ether (30 mL) saturated with HCl was dried ( $\text{MgSO}_4$ ) and filtered into the reaction vessel. The reaction was refluxed over two days. During this period two additional aliquots of HCl in diethyl ether (30 mL) were added to the reaction. After this time, the reaction was neutralized with a saturated solution of  $\text{K}_2\text{CO}_3(\text{aq})$  (2 mL) and filtered. The filtrate was extracted with chloroform (3 x 30 mL) and dried ( $\text{MgSO}_4$ ). The solvent was removed under reduced pressure to afford a brown oil which was purified by flash chromatography (10% Methanol/DCM). To a dry flask was added a solution of this oil (1.0 g, 6.42 mmol) in chloroform (10 mL). Diethyl ether saturated with HCl was

dried ( $\text{MgSO}_4$ ) and added. The precipitate was filtered to give **(6)** as light yellow crystals (2.2 g, 71% yield): 208 – 210 °C (lit<sup>14</sup> 209 – 210 °C); (Found C 49.89, H 5.83, N 7.14,  $\text{C}_8\text{H}_{11}\text{Cl}_2\text{N}$  requires C 50.02, H 5.77, N 7.29).

$\delta_{\text{H}}$  ( $\text{D}_2\text{O}$ , 200 MHz) 3.07 (2H, t,  $J_{2,1}$  7.0 Hz, H-2), 3.80 (2H, t,  $J_{1,2}$  7.0 Hz, H-1), 7.27 (2H, d,  $J_{2,3'}$  and  $J_{6',5'}$  8.2 Hz, H-2' and H-6'), 7.41 (2H, d,  $J_{3',2'}$  and  $J_{5',6'}$  8.2 Hz, H-3' and H-5').  $\delta_{\text{C}}$  ( $\text{D}_2\text{O}$ , 50 MHz) 52.2 ( $\text{CH}_2$ , C-2), 60.2 ( $\text{CH}_2$ , C-1), 137.8 (2CH, Ar), 143.4 (quat., Ar), 145.4 (2CH, Ar), 154.3 (quat., Ar).

### 3.4.3 Synthesis of 4-Aminophenethyl Fluoride Hydrochloride (**8**)

To a dry flask equipped with a stirrer bar and reflux condenser was added a solution of diethylaminosulfur trifluoride (3 mL, 22.7 mmol) in  $\text{CHCl}_3$  under nitrogen.<sup>15</sup> The flask was cooled to  $-78^\circ\text{C}$  and a solution of 4-aminophenethyl alcohol (**(7)**, 3.11 g, 22.6 mmol) in DCM (40 mL) was added dropwise. The reaction was warmed to room temperature and stirred for a further three hours. After this time water was added to the reaction mixture (20 mL) and the organic layer separated ( $\text{CHCl}_3$  3 x 30 mL) dried ( $\text{MgSO}_4$ ) and the solvent removed under vacuum. The residue was purified by flash chromatography (10% methanol in DCM) to give a brown oil. To a dry flask was added a solution of this oil (1.0 g, 6.42 mmol) in chloroform (10 mL). Diethyl ether saturated with HCl was dried ( $\text{MgSO}_4$ ) and added. The precipitate was filtered and recrystallized in ethanol to give **(8)** as light yellow crystals (3.14 g, 79% yield): mpt 207 – 209 °C; (Found C 54.67, H 6.38, N 7.70  $\text{C}_8\text{H}_{11}\text{ClFN}$  requires C 54.71, H 6.31, N 7.98);

$\delta_{\text{H}}$  ( $\text{D}_2\text{O}$ , 200 MHz)  $\delta$  2.98 (2H, t,  $J_{2,1}$  7.2 Hz, H-2), 3.12 (2H, t,  $J_{1,2}$  7.2 Hz, H-1), 7.33 (2H, d,  $J_{2,3'}$  and  $J_{6',5'}$  8.8 Hz, H-2' and H-6'), 7.42 (2H, d,  $J_{3',2'}$  and  $J_{5',6'}$  8.8 Hz, H-3' and H-5').  $\delta_{\text{C}}$  ( $\text{D}_2\text{O}$ , 50 MHz) 51.4 ( $\text{CH}_2$ , C-2), 55.3 ( $\text{CH}_2$ , C-1), 138.2 (2CH, Ar), 140.0 (2CH, Ar), 142.8 (quat., Ar), 154.0 (quat., Ar).

### 3.4.4 1<sup>st</sup> Attempted Synthesis of 4-Aminophenethyl Iodide Hydrochloride

To a flask equipped with a stirrer bar was added the hydrochloride salt of **(7)** (2.0 g, 14.6 mmol). The flask was cooled to  $-10^\circ\text{C}$  and aqueous hydriodic acid (57%) added (6.6 mL, 29.2 mmol). The reaction was slowly heated to  $60^\circ\text{C}$  and stirred for 2 hours.<sup>16</sup> After this time, the reaction was quenched with a saturated solution of  $\text{K}_2\text{CO}_3(\text{aq})$  (4 mL) and extracted with

chloroform (3 x 30 mL). The extract was dried ( $\text{MgSO}_4$ ) and the solvent removed *in vacuo* to provide a viscous gel.

#### 3.4.5 2<sup>nd</sup> Attempted Synthesis of 4-Aminophenethyl Iodide Hydrochloride

To a flask equipped with a solution of **(4)** (3.5 g, 14.6 mmol) in acetone was added sodium iodide (10.94 g, 73.0 mmol). The solution was stirred for 6 hours at 80°C under nitrogen.<sup>17</sup> The solvent was removed by rotary evaporation and the residue dissolved in chloroform and washed with brine (x 3). The organic layer was dried ( $\text{MgSO}_4$ ) and the solvent removed under vacuum to provide a viscous gel.

#### 3.4.6 Synthesis of 4-Aminophenethyl Mesylate Hydrochloride (**10**)

##### (i) 4-Nitrophenethyl Mesylate (**9**)

To a dry flask equipped with a stirrer bar and reflux condenser was added **(2)** (3.0 g, 17.9 mmol) in chloroform (40 mL) under nitrogen. Methane sulfonyl chloride (6.1 mL, 35.8 mmol) was added dropwise and the reaction refluxed for 6 h.<sup>18</sup> After this time, the reaction was quenched with a saturated solution of  $\text{K}_2\text{CO}_3(\text{aq})$  (4 mL) and extracted with chloroform (3 x 30 mL). The extract was dried ( $\text{MgSO}_4$ ) and the solvent removed *in vacuo*. The residue was purified by flash chromatography (10% methanol in DCM) to give **(9)** as an orange oil (3.72 g, 85% yield):

$\delta_{\text{H}}$  ( $\text{CDCl}_3$ , 200 MHz)  $\delta$  2.27 (3H, s,  $\text{CH}_3\text{SO}_2$ ), 3.03 (2H, t,  $J_{2,1}$  7.2 Hz, H-2), 3.75 (2H, t,  $J_{1,2}$  7.2 Hz, H-1), 7.42 (2H, d,  $J_{2',3'}$  and  $J_{6',5'}$  8.6 Hz, H-2' and H-6'), 8.12 (2H, d,  $J_{3',2'}$  and  $J_{5',6'}$  8.6 Hz, H-3' and H-5').  $\delta_{\text{C}}$  ( $\text{CDCl}_3$ , 50 MHz)  $\delta$  37.6 ( $\text{CH}_3$ ), 38.7 ( $\text{CH}_2$ , C-2), 45.6 ( $\text{CH}_2$ , C-1), 123.2 (2CH, Ar), 130.8 (2CH, Ar), 140.1 (quat., Ar), 157.0 (quat., Ar).

##### (ii) 4-Aminophenethyl Mesylate Hydrochloride (**10**)

A suspension of **(9)** (3.5 g, 14.3 mmol) and 10% Pd/C (0.35 g) in THF was placed inside a hydrogenation flask. The flask was fitted to a parr hydrogenator, evacuated, purged with hydrogen (3 atm) and left to agitate for a period of 12 hours.<sup>19</sup> The resultant suspension was filtered through celite, dried and reduced under pressure. The residue was purified by flash chromatography (10% methanol in DCM) to give a yellow oil. To a dry flask was added a solution of this oil (1.0 g, 6.42 mmol) in chloroform (10 mL). Diethyl ether saturated with HCl

was dried ( $\text{MgSO}_4$ ) and added. The resultant precipitate was filtered to give **(10)** as a white powder (3.11 g, 86% yield): mpt 183 – 185 °C; (Found C 42.76, H 5.57, N 5.40, O 19.37  $\text{C}_9\text{H}_{14}\text{ClNO}_3\text{S}$  requires C 42.94, H 5.61, N 5.56, O 19.07).

$\delta_{\text{H}}$  ( $\text{D}_2\text{O}$ , 200 MHz) 2.74 (3H, s,  $\text{CH}_3\text{SO}_2^-$ ), 3.03 (2H, t,  $J_{2,1}$  7.0 Hz, H-2), 3.75 (2H, t,  $J_{1,2}$  7.0 Hz, H-1), 7.31 (2H, d,  $J_{2',3'}$  and  $J_{6',5'}$  8.8 Hz, H-2' and H-6'), 7.40 (2H, d,  $J_{3',2'}$  and  $J_{5',6'}$  8.8 Hz, H-3' and H-5').  $\delta_{\text{C}}$  ( $\text{D}_2\text{O}$ , 50 MHz)  $\delta$  37.6 ( $\text{CH}_3$ ), 38.7 ( $\text{CH}_2$ , C-2), 45.6 ( $\text{CH}_2$ , C-1), 123.2 (2CH, Ar), 130.8 (2CH, Ar), 140.1 (quat., Ar), 157.1 (quat., Ar).

#### 3.4.7 4-Acetamidophenethyl Bromide (11)

To a solution of the free amine of **(4)** (2.56 g, 12.8 mmol) in  $\text{CHCl}_3$  (10 mL) was added acetic anhydride (5 mL, 53.0 mmol) with rapid stirring.<sup>20</sup> After 20 minutes the precipitate was filtered, washed with ether. Recrystallization from ethanol gave **(11)** as yellow crystals. (2.92 g, 94 % yield): mpt 139 – 141 °C (lit<sup>21</sup> 140 – 142 °C); (Found C 49.55, H 4.98, N 5.65, O 6.49  $\text{C}_{10}\text{H}_{12}\text{BrNO}$  requires C 49.61, H 5.00, N 5.79, O 6.61).

$\delta_{\text{H}}$  (Acetone- $d_6$ , 200 MHz)  $\delta$  2.94 (3H, s,  $\text{CH}_3\text{CO}-$ ), 3.09 (2H, t,  $J_{2,1}$  7.7 Hz, H-2), 3.62 (2H, t,  $J_{1,2}$  7.7 Hz, H-1), 7.14 (2H, d,  $J_{2',3'}$  and  $J_{6',5'}$  8.0 Hz, H-2' and H-6'), 7.58 (2H, d,  $J_{3',5'}$  and  $J_{5',6'}$  8.0 Hz, H-3' and H-5'), 9.08-9.31 (1H, br s,  $\text{NHCO}$ ).  $\delta_{\text{C}}$  (Acetone- $d_6$ , 50 MHz)  $\delta$  24.6 ( $\text{CH}_3\text{CO}-$ ), 33.3 ( $\text{CH}_2$ , C-2), 38.9 ( $\text{CH}_2$ , C-1), 120.5 (2CH, Ar), 129.3 (2CH, Ar), 135.0 (quat., Ar), 169.0 (quat., Ar).

#### 3.4.8 Synthesis of 4-Acetamidophenethyl Chloride (12)

To a solution of the free amine of **(6)** (2.2 g, 14.3 mmol) in  $\text{CHCl}_3$  (10 mL) was added acetic anhydride (5 mL, 53.0 mmol) with rapid stirring.<sup>20</sup> After 10 minutes the precipitate was filtered and washed with ether. Recrystallization from ethanol gave **(12)** as yellow crystals. (2.11 g, 75% yield): mpt 119 - 121 °C (lit<sup>22</sup> 123 – 124 °C). (Found C 60.71, H 6.05, N 7.24, O 7.94  $\text{C}_{10}\text{H}_{12}\text{ClNO}$  requires C 60.76, H 6.12, N 7.09, O 8.09).

$\delta_{\text{H}}$  (DMSO, 200 MHz)  $\delta$  2.06 (3H, s,  $\text{CH}_3\text{CO}-$ ), 2.99 (2H, t,  $J_{2,1}$  7.4 Hz, H-2), 3.84 (2H, t,  $J_{1,2}$  7.4 Hz, H-1), 7.25 (2H, d,  $J_{2',3'}$  and  $J_{6',5'}$  8.1 Hz, H-2' and H-6'), 7.51 (2H, d,  $J_{3',2'}$  and  $J_{5',6'}$  8.1 Hz, H-3' and H-5'), 9.95 (1H, br s,  $\text{NHCO}$ ).  $\delta_{\text{C}}$  ( $\text{CDCl}_3$ , 200 MHz)  $\delta$  24.8 ( $\text{CH}_3\text{CO}-$ ), 33.7 ( $\text{CH}_2$ , C-2), 48.1 ( $\text{CH}_2$ , C-1), 120.0 (2CH, Ar), 127.1 (2CH, Ar), 135.7 (quat., Ar), 141.2 (quat., Ar).

### 3.4.9 Synthesis of 2-{4-[2,2,2-Trifluoroacetyl]amino}phenyl}ethyl Trifluoroacetate (13)

To a solution of **(7)** (2.0 g, 14.6 mmol) in  $\text{CHCl}_3$  (10 mL) was added trifluoroacetic anhydride (5 mL, 35.4 mmol) with rapid stirring.<sup>23</sup> After 10 minutes the precipitate was filtered, washed with diethyl ether and dried under vacuum to give **(13)** as a white powder. (3.54 g, 74% yield): mpt 122 – 124 °C; (Found C 43.91, H 2.73, N 4.28, O 14.34  $\text{C}_{12}\text{H}_9\text{F}_6\text{NO}_3$  requires C 43.78, H 2.76, N 4.25, O 14.58).

$\delta_{\text{H}}$  (DMSO, 200 MHz)  $\delta$  3.00 (2H, t,  $J_{2,1}$  6.6 Hz, H-2) 4.57 (2H, t,  $J_{1,2}$  6.6 Hz, H-1), 7.29 (2H, d,  $J_{2,3}$  and  $J_{6,5}$  8.8 Hz, H-2' and H-6'), 7.59 (2H, d,  $J_{3,2}$  and  $J_{5,6}$  8.8 Hz, H-3' and H-5'), 11.22 (s, 1H, NH).  $\delta_{\text{C}}$  (DMSO, 50 MHz)  $\delta$  33.29 ( $\text{CH}_2$ , C-2), 68.47 ( $\text{CH}_2$ , C-1), 111.63 (C=O), 112.97 ( $\text{CF}_3$ ), 117.23 (HN-CO), 118.76 ( $\text{CF}_3$ ), 121.17 (2CH, Ar), 129.36 (2CH, Ar), 134.16 (quat., Ar), 135.11 (quat., Ar).

### **3.5 MECHANISTIC STUDIES INVOLVING 4-AMINOPHENETHYL-2D<sub>2</sub>-BROMIDE (19)**

#### **3.5.1 Synthesis of 4-Aminophenethyl-2d<sub>2</sub>-bromide (19)**

##### **(i) 4-Nitrophenyl-2d<sub>2</sub>-acetic Acid (14)**

To a dry flask equipped with a stirrer bar and purged with nitrogen was added a solution of butyllithium (36.75 ml, 59 mmol) in diethyl ether (60 mL). The solution was cooled to 0°C and **(1)** (5.0 g, 30.3 mmol) was added and stirred for 90 minutes. After this time, deuterium oxide (2.40 g, 120.0 mmol) was introduced dropwise and the resultant suspension stirred for a further 60 minutes.<sup>24</sup> The precipitate was filtered and dried under vacuum. Recrystallization from ethanol gave **(14)** as an orange powder (4.71 g, 93%): mpt 152 – 154 °C (lit<sup>24</sup> 153 – 154 °C).

$\delta_{\text{H}}$  ((10%) Actone-d<sub>6</sub> / D<sub>2</sub>O, 200 MHz)  $\delta$  7.37 (2H, d,  $J_{3', 2'}$  and  $J_{5', 6'}$  8.8 Hz, H-3' and H-5'), 8.14 (2H, d,  $J_{2', 3'}$  and  $J_{6', 5'}$  8.8 Hz, H-2' and H-6').  $\delta_{\text{C}}$  ((10%) Actone-d<sub>6</sub> / D<sub>2</sub>O, 50 MHz)  $\delta$  37.1 (CD<sub>2</sub>, C-2), 123.8 (2CH, Ar), 129.7 (2CH, Ar), 145.8 (quat., Ar), 147.1 (quat., Ar), 167.4 (CO).

##### **(ii) 4-Nitrophenethyl-2d<sub>2</sub>-alcohol (15)**

To a dry flask equipped with a stirrer bar was added **(14)** (4.5 g, 26.9 mmol) under nitrogen. The solution was cooled in ice and a 10M solution of borane dimethyl sulfide in diethyl ether (7.65 mL, 80.7 mmol) was added dropwise via a syringe and then stirred at room temperature for 24 h.<sup>1</sup> After this time, the reaction was quenched with water and all solvents removed under reduced pressure. The residue was dissolved in chloroform, dried (MgSO<sub>4</sub>), filtered and the solvent removed *in vacuo*. Recrystallization from ethanol provided **(15)** as yellow crystals (3.39 g, 74% yield): mpt 63 – 65 °C (lit<sup>3</sup> 63 °C).

$\delta_{\text{H}}$  ((10%) Actone-d<sub>6</sub> / D<sub>2</sub>O, 200 MHz)  $\delta$  1.88 (1H, br s, OH), 2.74 (2H, s, H-1), 7.37 (2H, d,  $J_{3', 2'}$  and  $J_{5', 6'}$  8.8 Hz, H-3' and H-5'), 8.17 (2H, d,  $J_{2', 3'}$  and  $J_{6', 5'}$  8.8 Hz, H-2' and H-6').  $\delta_{\text{C}}$  ((10%) Actone-d<sub>6</sub> / D<sub>2</sub>O, 50 MHz)  $\delta$  38.6 (CD<sub>2</sub>, C-2), 61.2 (CH<sub>2</sub>, C-1), 122.3 (2CH, Ar), 128.4 (2CH, Ar), 144.8 (quat., Ar), 146.3 (quat., Ar).

**(iii) 4-Nitrophenethyl-2d<sub>2</sub>-bromide (16)**

To a flask equipped with stirrer bar and reflux condenser was added **(15)** (3.0 g, 17.7 mmol) in chloroform (30 mL). Phosphorous tribromide (5.13 mL, 54.0 mmol) was added dropwise with stirring and the reaction refluxed for 24 h.<sup>6</sup> After this period, the reaction was quenched with water and the aqueous layer extracted with further chloroform (3 x 30 mL). The combined organic layers were dried (MgSO<sub>4</sub>) and condensed under vacuum. The residue was purified by flash chromatography (10% methanol in DCM) to provide **(16)** as orange crystals (3.03 g, 74% yield): mpt 66 – 68 °C (lit<sup>8</sup> 68 – 70 °C, lit<sup>9</sup> 68-69°C).

$\delta_{\text{H}}$  ((10%) Actone-d<sub>6</sub> / D<sub>2</sub>O, 200 MHz)  $\delta$  2.94 (2H, s, H-1), 7.41 (2H, d,  $J_{3',2'}$  and  $J_{5',6'}$  8.4 Hz, H-3' and H-5'), 8.15 (2H, d,  $J_{2',3'}$  and  $J_{6',5'}$  8.4 Hz, H-2' and H-6').  $\delta_{\text{C}}$  ((10%) Actone-d<sub>6</sub> / D<sub>2</sub>O, 50 MHz)  $\delta$  36.7 (CD<sub>2</sub>, C-2), 39.0 (CH<sub>2</sub>, C-1), 122.2 (2CH, Ar), 129.8 (2CH, Ar), 145.6 (quat., Ar), 147.0 (quat., Ar).

**(iv) 4-Aminophenethyl-2d<sub>2</sub>-bromide Hydrochloride (17)**

A suspension of **(16)** (3.0 g, 12.9 mmol) and 10% Pd/C (0.30 g) in THF was placed inside a hydrogenation flask. The flask was fitted to a parr hydrogenator, evacuated, purged with hydrogen (3 atm) and left to agitate for a period of 12 hours.<sup>19</sup> The resultant suspension was filtered through celite, dried and reduced under pressure. The residue was purified by flash chromatography (10% methanol in DCM) to give an orange oil. To a dry flask was added a solution of this oil (2.0 g, 9.9 mmol) in chloroform (20 mL). Diethyl ether saturated with HCl was dried (MgSO<sub>4</sub>) and added. The resultant precipitate was filtered to give **(17)** as a white powder (1.76 g, 57% yield): mpt 204 – 206 °C; (Found C 40.10, H 5.56, N 5.65, O 3.34 C<sub>8</sub>H<sub>9</sub>D<sub>2</sub>BrClN requires C 40.28, H 5.49, N 5.87).

$\delta_{\text{H}}$  ((10%) Actone-d<sub>6</sub> / D<sub>2</sub>O, 200 MHz)  $\delta$  3.43 (2H, s, H-1), 7.23 (2H, d,  $J_{3',2'}$  and  $J_{5',6'}$  8.0 Hz, H-3' and H-5'), 7.32 (2H, d,  $J_{2',3'}$  and  $J_{6',5'}$  8.0 Hz, H-2' and H-6').  $\delta_{\text{C}}$  ((10%) Actone-d<sub>6</sub> / D<sub>2</sub>O, 50 MHz)  $\delta$  37.1 (CD<sub>2</sub>, C-2), 40.1 (CH<sub>2</sub>, C-1), 123.3 (2CH, Ar), 128.8 (quat., Ar), 130.2 (2CH, Ar), 144.7 (quat., Ar).

**(v) 4-Aminophenethyl-1(2*d*)-azide (18) and 4-Aminophenethyl-2(2*d*)-azide (19)**

To a 10 mL RBF was added **(4)** (30 mg, 0.13 mmol). A solution of NaN<sub>3</sub> (150 mg, 1.89 mmol), D<sub>2</sub>O (1.8 mL) and acetone-*d*<sub>6</sub> (0.2 mL) was added with rapid stirring and gentle warming for 1 hour. Evaporation of the solvent under reduced pressure followed by aqueous workup afforded the title compounds, **(18)** and **(19)**, in approximately equal molar amounts (8.24 mg, 32% and 8.76, 34%).

**(18)**: mpt 208 – 210 °C (lit<sup>11</sup> 212 – 213 °C); (Found C 48.29, H 5.62, N 28.15 C<sub>8</sub>H<sub>11</sub>ClN<sub>4</sub> requires C 48.37, H 5.58, N 28.20).

$\delta_{\text{H}}$  ((10%) Actone-*d*<sub>6</sub> / D<sub>2</sub>O, 200 MHz)  $\delta$  2.85 (2H, s, H-2), 6.82 (2H, d,  $J_{3',2'}$  and  $J_{5',6'}$  8.4 Hz, H-3' and H-5'), 7.11 (2H, d,  $J_{2',3'}$  and  $J_{6',5'}$  7.8 Hz, H-2' and H-6').  $\delta_{\text{C}}$  ((10%) Actone-*d*<sub>6</sub> / D<sub>2</sub>O, 50 MHz)  $\delta$  27.6 (CH<sub>2</sub>, C-2), 46.1 (CD<sub>2</sub>, C-1), 109.2 (2CH, Ar), 120.2 (quat., Ar), 122.8 (2CH, Ar), 138.0 (quat., Ar).

**(19)**: mpt 208 – 210 °C (lit<sup>11</sup> 212 – 213 °C); (Found C 48.29, H 5.62, N 28.15 C<sub>8</sub>H<sub>11</sub>ClN<sub>4</sub> requires C 48.37, H 5.58, N 28.20).

$\delta_{\text{H}}$  ((10%) Actone-*d*<sub>6</sub> / D<sub>2</sub>O, 200 MHz)  $\delta$  3.57 (2H, s, H-1), 6.82 (2H, d,  $J_{3',2'}$  and  $J_{5',6'}$  8.4 Hz, H-3' and H-5'), 7.11 (2H, d,  $J_{2',3'}$  and  $J_{6',5'}$  7.8 Hz, H-2' and H-6').  $\delta_{\text{C}}$  ((10%) Actone-*d*<sub>6</sub> / D<sub>2</sub>O, 50 MHz)  $\delta$  27.6 (CH<sub>2</sub>, C-2), 46.1 (CD<sub>2</sub>, C-1), 109.2 (2CH, Ar), 120.2 (quat., Ar), 122.8 (2CH, Ar), 138.0 (quat., Ar).

### 3.5.2 Synthesis of 4-Hydroxyphenethyl Bromide (22)

**i) 4-Hydroxyphenethyl Alcohol (21)**

To a dry flask equipped with a stirrer bar was added 4-hydroxyphenylacetic acid (**(20)**, 4.0 g, 29.4 mmol) in chloroform (30 mL) under nitrogen. The solution was cooled in ice and a 10M solution of borane dimethyl sulfide in ether (5.2 mL, 58.8 mmol) was added dropwise via a syringe and then stirred at room temperature for 24 hours.<sup>1</sup> After this time, the reaction was quenched with water and all solvents removed under reduced pressure. The residue was dissolved in chloroform, dried (MgSO<sub>4</sub>) and filtered and removed *in vacuo*. Recrystallization from chloroform provided **(21)** as yellow crystals (3.2 g, 79% yield): mpt 89-91 °C (lit<sup>25</sup> 89-92 °C).

$\delta_{\text{H}}$  (CDCl<sub>3</sub>, 200 MHz)  $\delta$  2.55 (2H, t,  $J_{2,1}$  6.8 Hz, H-2), 3.50 (2H, t,  $J_{1,2}$  6.8 Hz, H-1), 7.45 (2H, d,  $J_{2',3'}$  and  $J_{6',5'}$  8.3 Hz, H-2' and H-6'), 6.66 (1H, br s, OH), 7.00 (2H, d,  $J_{3',2'}$  and  $J_{5',6'}$  8.3 Hz, H-3' and H-5').  $\delta_{\text{C}}$  (CDCl<sub>3</sub>, 50 MHz)  $\delta$  36.2 (CH<sub>2</sub>, C-2), 59.5 (CH<sub>2</sub>, C-1), 118.0 (2CH, Ar), 129.7 (2CH, Ar), 154.3 (quat., Ar), 164.2 (quat., Ar).

#### ii) 4-Hydroxyphenethyl Bromide (22)

To a flask equipped with stirrer bar and reflux condenser was added (21) (1.5 g, 10.9 mmol) in chloroform (40 mL). Phosphorous tribromide (7.15 mL, 75.3 mmol) was added dropwise with stirring and the reaction refluxed for 48 hours.<sup>6</sup> After this period, the reaction was quenched with water and the aqueous layer extracted with further chloroform (3 x 30 mL). The combined organic layers were dried (MgSO<sub>4</sub>) and condensed under vacuum. The residue was purified by flash chromatography (10% methanol in DCM) to provide (22) as orange crystals (1.7 g, 78% yield): mpt 54-55°C; (Found C 47.71, H 4.76, O 8.04 C<sub>8</sub>H<sub>9</sub>BrO requires C 47.79, H 4.51, O 7.96).

$\delta_{\text{H}}$  (CDCl<sub>3</sub>, 200 MHz) 3.21 (2H, t,  $J_{2,1}$  6.9 Hz, H-2), 3.67 (2H, t,  $J_{1,2}$  6.9 Hz, H-1), 6.92 (2H, d,  $J_{2',3'}$  and  $J_{6',5'}$  8.2 Hz, H-2' and H-6'), 7.15 (2H, d,  $J_{3',2'}$  and  $J_{5',6'}$  8.2 Hz, H-3' and H-5').  $\delta_{\text{C}}$  (CDCl<sub>3</sub>, 50 MHz) 34.6 (CH<sub>2</sub>, C-2), 38.0 (CH<sub>2</sub>, C-1), 116.7 (2CH, Ar), 130.6 (2CH, Ar), 154.8 (quat., Ar), 166.6 (quat., Ar).

#### 3.5.3 Synthesis of 4-Hydroxyphenethyl Chloride (23)

To a flask equipped with stirrer bar and reflux condenser was added (21) (1.5 g, 10.9 mmol) in chloroform (40 mL). Thionyl chloride (2.40 mL, 32.7 mmol) was added dropwise with stirring and the reaction refluxed for 24 hours.<sup>12,13</sup> After this period, the reaction was quenched with water and the aqueous layer extracted with further chloroform (3 x 30 mL). The combined organic layers were dried (MgSO<sub>4</sub>) and condensed under vacuum. The residue was purified by flash chromatography (10% methanol in DCM) to provide (23) as yellow crystals (1.45 g, 85% yield): mpt 54 - 56 °C; (Found C 61.33, H 5.82, O 10.25 C<sub>8</sub>H<sub>9</sub>ClO requires C 61.35, H 5.79, O 10.22).

$\delta_{\text{H}}$  (CDCl<sub>3</sub>, 200 MHz)  $\delta$  3.09 (2H, t,  $J_{2,1}$  7.0 Hz, H-2), 3.69 (2H, t,  $J_{1,2}$  7.0 Hz, H-2), 6.82 (2H, d,  $J_{2',3'}$  and  $J_{6',5'}$  8.2 Hz, H-2' and H-6'), 7.12 (2H, d,  $J_{3',2'}$  and  $J_{5',6'}$  8.2 Hz, H-3' and H-5').  $\delta_{\text{C}}$

(CDCl<sub>3</sub>, 50 MHz)  $\delta$  38.5 (CH<sub>2</sub>, C-2), 45.5 (CH<sub>2</sub>, C-1), 115.6 (2CH, Ar), 130.16 (2CH, Ar), 154.4 (quat., Ar), 167.5 (quat., Ar).

### **3.6 SYNTHESIS OF MONO- AND BISALKYLATORS INCORPORATING PYRIDYL/BENZYL NONCOVALENT BINDING SUB UNITS**

#### **3.6.1 1<sup>st</sup> Attempted synthesis of 4-(2-Chloroethyl)-*N*-(3-pyridinylmethyl)aniline Dihydrochloride (36)**

##### **(i) *N*-[4-(2-Hydroxyethyl)phenyl]nicotinamide (25) and 2-(4-aminophenyl)ethyl Nicotinate (26)**

To a dry flask (250 mL) equipped with a stirrer bar and reflux condenser was added 4-aminophenethyl alcohol ((**7**), 4.12 g, 30.0 mmol) in anhydrous THF (60 mL) and solid K<sub>2</sub>CO<sub>3</sub> (6.0 g) under nitrogen. A solution of nicotinoyl chloride hydrochloride ((**24**), 4.23 g, 30.0 mmol) in THF (40 mL) was added dropwise to the reaction which was then refluxed for 72 hours.<sup>26,27</sup> After this time, the reaction was filtered to remove residual K<sub>2</sub>CO<sub>3</sub>, dried (MgSO<sub>4</sub>) and the solvent condensed under vacuum to give a white residue. This crude material was then purified by flash chromatography (10% Methanol/DCM) to give the required compound (**25**) as yellow crystals (1.24 g, 17% yield) and 2-(4-aminophenyl)ethyl nicotinate (**26**) as a white powder (1.89 g, 26% yield).

**25:** mpt 156 – 158 °C; (Found C 69.44, H 5.96, N 11.71, O 13.37 C<sub>14</sub>H<sub>14</sub>N<sub>2</sub>O<sub>2</sub> requires C 69.41, H 5.82, N 11.56, O 13.21).

$\delta_{\text{H}}$  (Acetone-d<sub>6</sub>, 200 MHz) 2.74(2H, t,  $J_{2,1}$  6.6 Hz, H-2), 3.37 (1H, br s, OH), 3.79 (2H, t,  $J_{1,2}$  6.6 Hz, H-1), 7.19 (2H, d,  $J_{3',2'}$  and  $J_{5',6'}$  8.5 Hz, H-3' and H-5'), 7.53-7.58 (1H, m, H-5'), 7.74 (2H, d,  $J_{2',3'}$  and  $J_{6',5'}$  8.4 Hz, H-2' and H-6'), 8.27 (1H, d,  $J_{4',5'}$  6.6 Hz, H-4'), 8.74 (1H, d,  $J_{6',5'}$  4.4 Hz, H-6'), 9.11 (1H, s, H-2'), 10.39 (1H, br s, NH).  $\delta_{\text{C}}$  (Acetone-d<sub>6</sub>, 50 MHz)  $\delta$  38.6 (CH<sub>2</sub>, C-2), 62.3 (CH<sub>2</sub>, C-1), 120.3 (2CH, Ar), 123.4 (CH, Ar), 129.0 (2CH, Ar), 130.6 (quat., Ar), 135.3 (CH, Ar), 136.6 (quat., Ar), 145.7 (quat., Ar), 148.5 (CH, Ar), 151.9 (CH, Ar), 163.7 (quat., C=O).

**26:** mpt 147-150°C (Found C 69.64, H 5.72, N 11.45, O 13.20 C<sub>14</sub>H<sub>14</sub>N<sub>2</sub>O<sub>2</sub> requires C 69.41, H 5.82, N 11.56, O 13.21).

$\delta_{\text{H}}$  (Acetone-d<sub>6</sub>, 200 MHz) 2.81(2H, t,  $J_{2,1}$  7.1 Hz, H-2), 3.76 (2H, t,  $J_{1,2}$  7.1 Hz, H-1), 7.25 (2H, d,  $J_{3',2'}$  and  $J_{5',6'}$  8.5 Hz, H-3' and H-5'), 7.47-7.58 (1H, m, H-5'), 7.72 (2H, d,  $J_{2',3'}$  and  $J_{6',5'}$  8.5 Hz, H-2' and H-6'), 8.27-8.39 (1H, d,  $J_{4',5'}$  6.5 Hz, H-4'), 8.71-8.82 (1H, d,  $J_{6',5'}$  4.4 Hz, H-6'), 9.17 (1H, s, H-2').  $\delta_{\text{C}}$  (Acetone-d<sub>6</sub>, 50 MHz)  $\delta$  39.1 (CH<sub>2</sub>, C-2), 63.7 (CH<sub>2</sub>, C-1), 121.8 (2CH, Ar), 126.7 (CH, Ar), 128.9 (2CH, Ar), 131.9 (quat., Ar), 137.2 (quat., Ar), 134.8 (CH, Ar), 137.3 (quat., Ar), 139.8 (quat., Ar), 147.9 (CH, Ar), 152.3 (CH, Ar), 162.4 (quat., CO<sub>2</sub>).

### 3.6.2 2<sup>nd</sup> Attempted Synthesis of 4-(2-Chloroethyl)-N-(2-pyridin-3-ylethyl)aniline Dihydrochloride (36)

#### (i) 4-Nitrophenethyl Acetate (27)

To a flask equipped with stirrer bar was added **(2)** (20 g, 119.7 mmol). To this was added acetic anhydride (22.6 mL, 239.5 mmol) which was subsequently stirred at room temperature for 24 hours.<sup>20</sup> After this time a saturated solution of K<sub>2</sub>CO<sub>3</sub> (40 mL) was added, the reaction mixture stirred for 4 hours and then extracted with chloroform (3 x 30 mL). The extract was dried (MgSO<sub>4</sub>) and the solvent removed *in vacuo* to give **(27)** as a yellow crystalline solid (21.3 g, 85% yield): mpt 78 – 79 °C (lit<sup>28</sup> 77 – 79 °C).

$\delta_{\text{H}}$  (Acetone-d<sub>6</sub>, 200 MHz)  $\delta$  1.98 (3H, s, CH<sub>3</sub>), 3.07 (2H, t,  $J_{2,1}$  6.8 Hz, H-2), 4.29 (2H, t,  $J_{1,2}$  6.8 Hz, H-1), 7.51 (2H, d,  $J_{2',3'}$  and  $J_{6',5'}$  8.7 Hz, H-2' and H-6'), 8.12 (2H, d,  $J_{3',2'}$  and  $J_{5',6'}$  8.7 Hz, H-3' and H-5').  $\delta_{\text{C}}$  (Acetone-d<sub>6</sub>, 50 MHz) 20.5 (CH<sub>3</sub>), 35.2 (CH<sub>2</sub>, C-2), 64.2 (CH<sub>2</sub>, C-1), 123.8 (2CH, Ar), 129.9 (2CH, Ar), 145.7 (quat., Ar), 146.5 (quat., Ar), 170.3 (CO).

#### (ii) 4-Aminophenethyl Acetate (28)

A suspension of **27** (20 g, 95.6 mmol) and 10% Pd/C (2.0 g) in THF (100 mL) was placed inside a hydrogenation flask. The flask was fitted to a parr hydrogenator, evacuated, purged with hydrogen (3 atm) and left to agitate for a period of 12 hours.<sup>19</sup> The resultant suspension was filtered through celite, dried and reduced under pressure. The residue was purified by

flash chromatography (10% methanol in DCM) to give **28** as an orange oil (15.3 g, 90% yield): mpt 198 - 201 °C (lit<sup>28</sup> 201 °C).

$\delta_{\text{H}}$  (CDCl<sub>3</sub>, 200 MHz)  $\delta$  2.03 (3H, s, CH<sub>3</sub>), 2.89 (2H, t,  $J_{2,1}$  7.0 Hz, H-2), 3.60 (br s, 2H, NH<sub>2</sub>), 4.22 (2H, t,  $J_{1,2}$  7.0 Hz, H-1), 6.66 (2H, d,  $J_{2,3}$  and  $J_{6,5}$  8.5 Hz, H-2' and H-6'), 7.02 (2H, d,  $J_{3,2}$  and  $J_{5,6}$  8.5 Hz, H-3' and H-5').  $\delta_{\text{C}}$  (CDCl<sub>3</sub>, 50 MHz) 20.7 (CH<sub>3</sub>), 35.2 (CH<sub>2</sub>, C-2), 64.4 (CH<sub>2</sub>, C-1) 121.1 (2CH, Ar), 129.9 (2CH, Ar), 146.2 (quat., Ar), 147.3 (quat., Ar).

### (ii) 2-{4-[(3-Pyridinylcarbonyl)amino]phenyl}ethyl acetate (**30**)

To a dry flask equipped with a stirrer bar and reflux condenser was added (**28**) (6.0 g, 33.5 mmol) in anhydrous THF (40 mL) and solid K<sub>2</sub>CO<sub>3</sub> (3.0 g) under nitrogen. A solution of nicotinoyl chloride hydrochloride (**29**, 6.0 g, 33.7 mmol) in THF (60 mL) was added dropwise to the reaction which was then refluxed for 72 hours.<sup>26,27</sup> After this time, the reaction was filtered to remove residual K<sub>2</sub>CO<sub>3</sub>, dried (MgSO<sub>4</sub>) and the solvent removed under vacuum to give a white residue. This was then purified by column chromatography (10% Methanol/DCM) to give (**30**) as yellow crystals (7.74 g, 81% yield): mpt 119 – 121 °C; (Found C 67.54, H 5.62, N 9.67, O 16.91 C<sub>16</sub>H<sub>16</sub>N<sub>2</sub>O<sub>3</sub> requires C 67.59, H 5.67, N 9.85, O 16.88).

$\delta_{\text{H}}$  (Acetone-d<sub>6</sub>, 200 MHz)  $\delta$  1.98 (3H, s, CH<sub>3</sub>), 2.92 (2H, t,  $J_{2,1}$  7.0 Hz, H-2), 4.24 (2H, t,  $J_{1,2}$  7.0 Hz, H-1), 7.27 (2H, d,  $J_{3,2}$  and  $J_{5,6}$  8.4 Hz, H-3' and H-5'), 7.50-7.53 (1H, m, H-5'), 7.78 (2H, d,  $J_{2,3}$  and  $J_{6,5}$  8.4 Hz, H-2' and H-6'), 8.29 (1H, d,  $J_{4',5'}$  6.6 Hz, H-4'), 8.73 (1H, d,  $J_{6',5'}$  4.4 Hz, H-6'), 9.17 (1H, s, H-2'), 9.63 (1H, br s, NH).  $\delta_{\text{C}}$  (Acetone-d<sub>6</sub>, 50 MHz)  $\delta$  20.9 (CH<sub>3</sub>), 35.2 (CH<sub>2</sub>, C-2), 65.4 (CH<sub>2</sub>, C-1), 121.1 (2CH, Ar), 124.2 (CH, Ar), 130.1 (2CH, Ar), 131.8 (quat., Ar), 134.9 (quat., Ar), 135.9 (CH, Ar), 138.4 (quat., Ar), 149.5 (CH, Ar), 153.0 (CH, Ar), 164.8 (quat., C=O).

### (iii) N-[4-(2-Hydroxyethyl)phenyl]nicotinamide (**25**)

To a flask equipped with a stirrer bar and reflux condenser was added (**30**) (6.0 g, 21.1 mmol) in anhydrous THF (60 mL) and MeOH (30 mL). A solution of K<sub>2</sub>CO<sub>3</sub> (6.0 g) in H<sub>2</sub>O (30 mL) was added to the reaction which was then refluxed for 24 hours.<sup>29</sup> The resultant two-phase system was partitioned and the aqueous phase extracted with 3 portions of diethyl ether. The organic fractions were then combined, dried and removed under vacuum to give the title compound (**25**) as a white powder (4.2 g, 82% yield); mpt 156 – 158 °C. (Refer to section 4.5.1 (i) for compound characterization).

**(iv) N-[4-(2-Chloroethyl)phenyl]nicotinamide (31)**

To a dry flask equipped with a stirrer bar and reflux condenser was added **(25)** (4.0 g, 16.5 mmol) under nitrogen. Thionyl chloride (6.0 mL, 82.3 mmol) was added dropwise and the reaction refluxed for 2 hours.<sup>12,13</sup> After this time, the reaction was quenched with a saturated solution of K<sub>2</sub>CO<sub>3</sub>(aq) (15 mL) and extracted with chloroform (3 x 30 mL). The extract was dried (MgSO<sub>4</sub>) and the solvent removed *in vacuo*. The reaction residue was purified by flash chromatography (10% methanol in DCM) to give **(31)** as yellow crystals (3.53 g, 82 % yield): mpt 148 – 150 °C; (Found C 64.67, H 5.04, N 10.64, O 6.12 C<sub>14</sub>H<sub>13</sub>ClN<sub>2</sub>O requires C 64.49, H 5.03, N 10.74, O 6.14).

$\delta_{\text{H}}$  (Acetone-d<sub>6</sub>, 400 MHz) 3.03 (2H, t,  $J_{2,1}$  7.2 Hz, H-2), 3.78 (2H, t,  $J_{1,2}$  7.2 Hz, H-1), 7.31 (2H, d,  $J_{3',2'}$  and  $J_{5',6'}$  8.5 Hz, H-3' and H-5'), 7.48-7.55 (1H, m, H-5'), 7.80 (2H, d,  $J_{2',3'}$  and  $J_{6',5'}$  8.5 Hz, H-2' and H-6'), 8.32 (1H, d,  $J_{4',5'}$  6.6 Hz, H-4'), 8.74 (1H, d,  $J_{6',5'}$  4.4 Hz, H-6'), 9.17 (1H, s, H-2'), 9.72 (1H, br s, NH).  $\delta_{\text{C}}$  (Acetone-d<sub>6</sub>, 100 MHz) 39.2 (CH<sub>2</sub>, C-2), 46.0 (CH<sub>2</sub>, C-1), 121.2 (2CH, Ar), 124.2 (CH, Ar), 130.1 (2CH, Ar), 132.0 (quat., Ar), 135.0 (quat., Ar), 135.9 (CH, Ar), 138.4 (quat., Ar), 149.5 (CH, Ar), 153.0 (CH, Ar), 167.2 (quat., C=O).

**(v) Attempted Synthesis of 4-(2-Chloroethyl)-N-(3-pyridinylmethyl)aniline (36)**

To a dry flask equipped with a stirrer bar was added **(31)** (3.5 g, 13.4 mmol) under nitrogen. The solution was cooled in ice and a 10M solution of borane dimethyl sulfide in ether (3.78 mL, 42.5 mmol) was added dropwise via a syringe and then stirred at room temperature for 24 hours.<sup>1</sup> After this time, the reaction was quenched with water and the product extracted into chloroform (3 x 30 mL) which was subsequently removed under reduced pressure. Attempts to purify the product via flash chromatography (10% MeOH/DCM) failed due to polymerization of the title compound, as indicated by mass spectroscopy and NMR.

### 3.6.3 3<sup>rd</sup> Attempted Synthesis of 4-(2-Chloroethyl)-*N*-(2-pyridin-3-ylethyl)aniline Dihydrochloride.

#### (i) 2-{4-[(3-Pyridinylmethyl)amino]phenyl}ethanol Dihydrochloride (**32**)

To a dry flask equipped with a stirrer bar was added (**25**) (4.2 g, 17.3 mmol) in ether (30 mL) under nitrogen. The solution was cooled in ice and a 2.0 M solution of borane dimethyl sulfide (27.4 mL, 54.8 mmol) was added dropwise via a syringe and then stirred at reflux for 48 hours.<sup>1</sup> After this time, the reaction was quenched with water and extracted with diethyl ether (6 x 30 mL). A solution of HCl saturated diethyl ether was added with stirring and the resultant precipitate filtered to give (**32**) as a white powder (2.7 g, 52% yield): mpt 198 – 200 °C; (Found C 55.84, H 6.22, N 6.13, O 5.38 C<sub>14</sub>H<sub>18</sub>Cl<sub>2</sub>N<sub>2</sub>O requires C 55.82, H 6.02, N 9.30, O 5.31).

$\delta_{\text{H}}$  (DMSO, 400 MHz)  $\delta$  2.82 (2H, t,  $J_{2,1}$  6.8 Hz, H-2), 3.31 (2H, s, -CH<sub>2</sub>N), 3.71 (2H, t,  $J_{1,2}$  6.8 Hz, H-1), 4.80 (1H, br s, OH), 5.41 (1H, br s, NH), 7.10 (2H, d,  $J_{3',2'}$  and  $J_{5',6'}$  8.2 Hz, H-3' and H-5'), 7.52-7.56 (1H, m, H-5'), 7.78 (2H, d,  $J_{2',3'}$  and  $J_{6',5'}$  8.2 Hz, H-2' and H-6'), 8.29 (1H, d,  $J_{4',5'}$  6.8 Hz, H-4'), 8.77 (1H, d,  $J_{6',5'}$  4.4 Hz, H-6').  $\delta_{\text{C}}$  (DMSO, 100 MHz)  $\delta$  39.3 (CH<sub>2</sub>, C-2), 48.7 (-CH<sub>2</sub>N), 64.9 (CH<sub>2</sub>, C-1), 120.0 (2CH, Ar), 123.2 (CH, Ar), 129.3 (2CH, Ar), 131.1 (quat., Ar), 135.9 (CH, Ar), 137.7 (quat., Ar), 145.2 (quat., Ar), 148.5 (CH, Ar), 152.0 (CH, Ar).

#### (ii) Attempted Synthesis of 4-(2-Chloroethyl)-*N*-(3-pyridinylmethyl)aniline Dihydrochloride (**36**)

To a dry flask equipped with a stirrer bar and reflux condenser was (**32**) (2.5 g, 9.96 mmol) under nitrogen. Thionyl chloride (6.0 mL, 82.3 mmol) was added dropwise and the reaction refluxed for 2 hours.<sup>12,13</sup> After this time, the reaction was quenched with a saturated solution of K<sub>2</sub>CO<sub>3</sub>(aq) (15 mL) and extracted with chloroform (3 x 30 mL). The extract was dried (MgSO<sub>4</sub>) and the solvent removed *in vacuo*. Attempts to purify the residue by flash failed due to polymerization of the title compound.

### 3.6.4 Synthesis of 4-(2-Chloroethyl)-*N*-(3-pyridinylmethyl)aniline Dihydrochloride (36)

#### (i) 3-Pyridine Methylchloride (34)

To a dry flask equipped with a stirrer bar and reflux condenser was added 3-pyridyl carbinol (**(33)**, 6.0 g, 55.0 mmol) under nitrogen. Thionyl chloride (12.0 mL, 164.6 mmol) was added dropwise and the reaction refluxed for 4 hours.<sup>12,13</sup> After this time the excess thionyl chloride was distilled from the reaction mixture. The crude reaction product was triturated with hexane (10 mL) and the residual thionyl chloride was removed under high vacuum. The residue was dissolved in chloroform and a solution of dried (MgSO<sub>4</sub>) diethyl ether saturated with HCl was added. The precipitated hydrochloride salt was triturated in ethanol and filtered to give **(34)** as a pale brown powder (8.1 g, 90% yield): mpt 138 – 140 °C (lit<sup>28</sup> – 137-143 °C).

$\delta_{\text{H}}$  (DMSO, 200 MHz)  $\delta$  4.95 (2H, s, H-1), 7.57-7.61 (1H, m, H-5'), 8.31 (1H, d,  $J_{4',5'}$  6.6 Hz, H-4'), 8.73 (1H, d,  $J_{6',5'}$  4.4 Hz, H-6'), 9.09 (1H, s, H-2').  $\delta_{\text{C}}$  (DMSO, 50 MHz)  $\delta$  42.1 (CH<sub>2</sub>, C-1), 123.3 (CH, Ar), 135.7 (CH, Ar), 145.8 (quat., Ar), 148.2 (quat., Ar), 142.1 (CH, Ar), 151.1 (CH, Ar).

#### (ii) 2-{4-[(3-Pyridinylmethyl)amino]phenyl}ethanol (35)

To a flask equipped with a stirrer bar and condenser was added **(34)** (5.0 g, 30.7 mmol). A heterogeneous solution of **7** (5.31 g, 38.7 mmol) and K<sub>2</sub>CO<sub>3</sub> (10.0 g) in THF (100 mL) was added to the flask and refluxed for 72 hours with rapid stirring.<sup>26,27</sup> After this time the reaction mixture was filtered to remove residual K<sub>2</sub>CO<sub>3</sub>, dried (MgSO<sub>4</sub>) and the solvent removed under vacuum. The product was purified by flash chromatography (10% MeOH/CHCl<sub>3</sub>) to yield **(35)** as a white powder which was converted to the hydrochloride salt to yield **(32)** (2.25 g, 32% yield). (Refer to section 4.5.3(i) for compound characterization).

#### (iii) 4-(2-Chloroethyl)-*N*-(3-pyridinylmethyl)aniline Dihydrochloride (36)

To a dry flask equipped with a stirrer bar was added **(32)** (1.0 g, 3.32 mmol) in chloroform (20 mL) under nitrogen. Thionyl chloride (3.0 mL, 41.1 mmol) was added dropwise and the reaction stirred at reflux for 2 hours.<sup>12,13</sup> After this time, the reaction was quenched with a saturated solution of K<sub>2</sub>CO<sub>3</sub>(aq) (15 mL) and extracted with chloroform (3 x 30 mL). A HCl saturated solution of diethyl ether was added to the extract to precipitate the product as the

hydrochloride salt. The precipitate was filtered and recrystallized in ethanol to provide **(36)** as a pale brown powder (0.4 g, 38% yield): mpt 235–237°C; (Found C 52.84, H 5.24, N 8.74 C<sub>14</sub>H<sub>17</sub>Cl<sub>3</sub>N<sub>2</sub> requires C 52.60, H 5.36, N 8.76).

$\delta_{\text{H}}$  (DMSO, 400 MHz)  $\delta$  2.98 (2H, t,  $J_{2,1}$  6.6 Hz, H-2), 3.36 (2H, s, -CH<sub>2</sub>N), 3.64 (2H, t,  $J_{1,2}$  6.6 Hz, H-1), 5.44 (1H, br s, NH), 7.11 (2H, d,  $J_{3',2'}$  and  $J_{5',6'}$  8.2 Hz, H-3' and H-5'), 7.50-7.55 (1H, m, H-5'), 7.78 (2H, d,  $J_{2',3'}$  and  $J_{6',5'}$  8.2 Hz, H-2' and H-6'), 8.28 (1H, d,  $J_{4',5'}$  6.6 Hz, H-4'), 8.79 (1H, d,  $J_{5',6'}$  4.5 Hz, H-6'), 9.10 (1H, s, H-2').  $\delta_{\text{C}}$  (DMSO, 100 MHz)  $\delta$  38.2 (CH<sub>2</sub>, C-2), 48.4 (-CH<sub>2</sub>N), 45.2 (CH<sub>2</sub>, C-1), 120.7 (2CH, Ar), 123.5 (CH, Ar), 129.3 (2CH, Ar), 131.0 (quat., Ar), 135.6 (CH, Ar), 137.2 (quat., Ar), 144.9 (quat., Ar), 148.4 (CH, Ar), 151.8 (CH, Ar).

### 3.6.5 Synthesis of 4-(2-Chloroethyl)-*N*-(2-pyridinylmethyl)aniline Dihydrochloride (**40**)

#### (i) 2-Pyridine Methylchloride (**38**)

To a dry flask equipped with a stirrer bar and reflux condenser was added 2-pyridyl carbinol (**(37)**, 6.0 g, 55.0 mmol) under nitrogen. Thionyl chloride (12.0 mL, 164.5 mmol) was added dropwise and the reaction refluxed for 2 hours.<sup>12,13</sup> After this time the excess thionyl chloride was removed from the reaction via distillation. The crude material was then triturated with hexane (10 mL) and any residual thionyl chloride removed under high vacuum. The residue was dissolved in chloroform and a solution of dried (MgSO<sub>4</sub>) diethyl ether saturated with HCl was added. The precipitated hydrochloride salt was triturated in ethanol and filtered to give **(38)** as a pale brown powder (7.8 g, 87% yield): mpt 120-122 (Lit<sup>28</sup> 120-124).

$\delta_{\text{H}}$  (DMSO, 200 MHz)  $\delta$  5.01 (2H, s, H-1), 7.99-8.06 (1H, m, H-5'), 8.10 (1H, d,  $J_{3'',4''}$  8.0 Hz, H-3''), 8.56-8.64 (1H, m, H-4''), 8.75 (1H, d,  $J_{6'',5''}$  5.8 Hz, H-6'').  $\delta_{\text{C}}$  (DMSO, 50 MHz)  $\delta$  42.9 (CH<sub>2</sub>, C-1), 138.7 (CH, Ar), 139.7 (CH, Ar), 143.4 (quat., Ar), 146.3 (CH, Ar), 148.1 (CH, Ar).

**(ii) 2-{4-[(2-Pyridinylmethyl)amino]phenyl}ethanol (39)**

To a flask equipped with a stirrer bar and condenser was added **(38)** (5.0 g, 30.7 mmol) in THF (40 mL). A heterogeneous solution of **7** (5.3 g, 30.7 mmol) and  $K_2CO_3$  (5.0 g) in THF (60 mL) was added to the flask and refluxed for 72 hours with rapid stirring.<sup>26,27</sup> After this time the reaction mixture was filtered to remove  $K_2CO_3$ , dried ( $MgSO_4$ ) and the solvent removed under vacuum. The residue was purified via flash chromatography (10%MeOH/ $CHCl_3$ ) to yield **(39)** as a white powder (3.43 g, 64% yield): 133-135°C (Found C 73.87, H 7.13, N 12.45, O 6.98  $C_{14}H_{16}N_2O$  requires C 73.66, H 7.06, N 12.27, O 7.01).

$\delta_H$  (DMSO, 400 MHz)  $\delta$  2.79 (2H, t,  $J_{2,1}$  6.8 Hz, H-2), 3.39 (2H, s,  $-CH_2N$ ), 3.79 (2H, t,  $J_{1,2}$  6.8 Hz, H-1), 4.79 (1H, br s, OH), 5.44 (1H, br s, NH), 7.08 (2H, d,  $J_{3',2'}$  and  $J_{5',6'}$  8.2 Hz, H-3' and H-5'), 7.72 (2H, d,  $J_{2',3'}$  and  $J_{6',5'}$  8.2 Hz, H-2' and H-6'), 7.99-8.06 (1H, m, H-5''), 8.10 (1H, d,  $J_{3'',4''}$  8.0 Hz, H-3''), 8.56-8.64 (1H, m, H-4''), 8.75 (1H, d,  $J_{6'',5''}$  5.8 Hz, H-6'').  $\delta_C$  (DMSO, 100 MHz)  $\delta$  39.7 ( $CH_2$ , C-2), 48.9 ( $-CH_2N$ ), 64.2 ( $CH_2$ , C-1), 120.1 (2CH, Ar), 129.0 (2CH, Ar), 131.0 (quat., Ar), 138.0 (CH, Ar), 139.6 (CH, Ar), 137.2 (quat., Ar), 143.9 (quat., Ar), 146.4 (CH, Ar), 148.3 (CH, Ar).

**(iii) 4-(2-Chloroethyl)-N-(2-pyridinylmethyl)aniline Dihydrochloride (40)**

To a dry flask equipped with a stirrer bar and reflux condenser was added **(39)** (1.0 g, 4.38 mmol) in chloroform under nitrogen. Thionyl chloride (3.0 mL, 41.1 mmol) was added dropwise and the reaction refluxed for 2 hours.<sup>12,13</sup> After this time, the reaction was neutralized with a saturated solution of  $K_2CO_3$ (aq) (20 mL). The target product was extracted into chloroform (3 x 30 mL) and dried ( $MgSO_4$ ). The solvent was removed under reduced pressure to give crude product which was in ethanol to provide **(40)** as yellow crystals (0.4 g, 29% yield): mpt 245-247°C; (Found C 52.73, H 5.38, N 8.61  $C_{14}H_{17}Cl_3N_2$  requires C 52.60, H 5.36, N 8.76).

$\delta_H$  (DMSO, 400 MHz)  $\delta$  2.99 (2H, t,  $J_{2,1}$  6.6 Hz, H-2), 3.39 (2H, s,  $-CH_2N$ ), 3.68 (2H, t,  $J_{1,2}$  6.6 Hz, H-1), 5.44 (1H, br s, NH), 7.08 (2H, d,  $J_{3',2'}$  and  $J_{5',6'}$  8.2 Hz, H-3' and H-5'), 7.72 (2H, d,  $J_{2',3'}$  and  $J_{6',5'}$  8.2 Hz, H-2' and H-6'), 7.99-8.06 (1H, m, H-5''), 8.10 (1H, d,  $J_{3'',4''}$  8.0 Hz, H-3''), 8.56-8.64 (1H, m, H-4''), 8.75 (1H, d,  $J_{6'',5''}$  5.8 Hz, H-6'').  $\delta_C$  (DMSO, 100 MHz)  $\delta$  37.7 ( $CH_2$ , C-2), 48.9 ( $-CH_2N$ ), 45.5 ( $CH_2$ , C-1), 120.1 (2CH, Ar), 129.0 (2CH, Ar), 131.0 (quat., Ar),

138.0 (CH, Ar), 139.6 (CH, Ar), 137.2 (quat., Ar), 143.9 (quat., Ar), 146.4 (CH, Ar), 148.3 (CH, Ar).

### 3.6.6 Synthesis of *N,N'*-[Pyridine-2,6-diyl-di(methylene)]bis[4-(2-chloroethyl)aniline] Trihydrochloride (**44**)

#### (i) 2,6-Bis(chloromethyl)pyridine (**41**)

To a dry flask equipped with a stirrer bar and reflux condenser was added 2,6-pyridine dimethanol (**41**), 6.0 g, 43.1 mmol) under nitrogen. Thionyl chloride (12.0 mL, 164.5 mmol) was added dropwise and the reaction refluxed for 4 hours.<sup>12,13</sup> After this time the excess thionyl chloride was removed from the reaction via distillation. The crude material was then triturated with hexane (10 mL) and any residual thionyl chloride removed under high vacuum. The crude material was dissolved in chloroform and a solution of dried (MgSO<sub>4</sub>) diethyl ether saturated with HCl was added. The precipitated hydrochloride salt was triturated in ethanol and filtered to provide (**42**) as a white powder (7.8 g, 85% yield): mpt 75-77 °C; (Found C 39.58, H 3.91, N 6.34 C<sub>7</sub>H<sub>8</sub>Cl<sub>3</sub>N requires C 39.56, H 3.79, N 6.59).

$\delta_{\text{H}}$  (Acetone-d<sub>6</sub>, 400 MHz)  $\delta$  4.34 (4H, s, CH<sub>2</sub>OH), 5.19 (2H, s, OH), 7.10 (2H, d,  $J_{3'',4''}$  and  $J_{5'',3''}$  8.0 Hz, H-3'' and H-5''), 7.60 (1H, dd,  $J_{4'',3''}$  8.0 Hz and  $J_{4'',5''}$  8.0 Hz, H-4'').  $\delta_{\text{C}}$  (Acetone-d<sub>6</sub>, 100 MHz)  $\delta$  64.3 (CH<sub>2</sub>, C-1), 118.4 (2CH, Ar), 137.1 (CH, Ar), 160.8 (2 quat., Ar).

#### (ii) 2,2'-[2,6-Pyridinediylbis(methyleneimino-4,1-phenylene)]diethanol (**43**)

To a flask equipped with a stirrer bar and condenser was added (**42**) (7.0 g, 32.9 mmol). A heterogeneous mixture of (**7**) (9.03 g, 65.8 mmol) and solid K<sub>2</sub>CO<sub>3</sub> (10.0 g) in THF (30mL) was added to the flask and refluxed for 72 hours with rapid stirring.<sup>26,27</sup> After this time the reaction mixture was extracted with chloroform (3 x 30 mL), the extracts combined, dried and the solvent removed under vacuum. The residue was purified via flash chromatography (10% MeOH/CHCl<sub>3</sub>) to yield (**43**) as a white powder (1.9 g, 15% yield): mpt 164-166 °C; (Found C 73.27, H 7.07, N 11.21, O 8.43 C<sub>23</sub>H<sub>27</sub>N<sub>3</sub>O<sub>2</sub> requires C 73.18, H 7.21, N 11.13, O 8.48).

$\delta_{\text{H}}$  (Acetone-d<sub>6</sub>, 400 MHz)  $\delta$  2.82 (4H, t,  $J_{2,1}$  6.4 Hz, H-2), 3.46 (4H, s, -CH<sub>2</sub>NH), 3.64 (4H, t,  $J_{1,2}$  6.4 Hz, H-1), 4.71 (2H, br s, OH), 7.27 (4H, d,  $J_{3',2'}$  and  $J_{5',6'}$  7.4 Hz, H-3' and H-5'), 7.82 (4H, d,  $J_{2',3'}$  and  $J_{6',5'}$  7.4 Hz, H-2' and H-6'), 8.27-8.30 (1H, m, H-4'), 8.37 (2H, d,  $J_{5'',4''}$  and

$J_{3'',4''}$  6.6 Hz, H-5'' and H-3'), 6.23 (2H, br s, NH),  $\delta_C$  (Acetone- $d_6$ , 100 MHz)  $\delta$  38.7 (2CH<sub>2</sub>, C-2), 40.9 (-2CH<sub>2</sub>NH), 62.3 (2CH<sub>2</sub>, C-1), 121.2 (4CH, Ar), 125.2 (2quat., Ar), 129.1 (4CH, Ar), 135.7 (2CH, Ar), 139.8 (1CH, Ar), 148.9 (2 quat., Ar), 161.5 (2quat., Ar).

**(iii) *N,N'*-[2,6-Pyridinediylbis(methylene)]bis[4-(2-chloroethyl)aniline] Trihydrochloride (44)**

To a dry flask equipped with a stirrer bar and reflux condenser was added **(43)** (1.5 g, 3.97 mmol) in chloroform under nitrogen. Thionyl chloride (3.0 mL, 41.1 mmol) was added dropwise and the reaction stirred at room temperature for 4 hours.<sup>12,13</sup> After this time, the reaction was neutralized with a saturated solution of K<sub>2</sub>CO<sub>3</sub>(aq) (20 mL). The target product was extracted into chloroform (3 x 30 mL) and dried (MgSO<sub>4</sub>). The solvent was removed under reduced pressure to give crude product which was purified via flash chromatography (10% MeOH/CHCl<sub>3</sub>), converted to the HCl salt by the methods previously mentioned in ethanol to give **(44)** as yellow crystals (0.5 g, 24% yield): mpt decomp. 336 °C; (Found C 52.78, H 5.45, N 7.94 C<sub>23</sub>H<sub>27</sub>Cl<sub>5</sub>N<sub>3</sub> requires C 52.85, H 5.21, N 8.04).

$\delta_H$  (D<sub>2</sub>O, 400 MHz)  $\delta$  2.96 (4H, t,  $J_{2,1}$  6.6 Hz, H-2), 3.49 (4H, s, -CH<sub>2</sub>NH), 3.69 (4H, t,  $J_{1,2}$  6.6 Hz, H-1), 7.31 (4H, d,  $J_{3',2'}$  and  $J_{5',6'}$  7.4 Hz, H-3' and H-5'), 7.86 (4H, d,  $J_{2',3'}$  and  $J_{6',5'}$  7.4 Hz, H-2' and H-6'), 8.31-8.34 (1H, m, H-4'), 8.42 (2H, d,  $J_{3'',4''}$  and  $J_{5'',4''}$  6.6 Hz, H-5'' and H-3''), 6.34 (2H, br s, NH),  $\delta_C$  (D<sub>2</sub>O, 100 MHz)  $\delta$  37.6 (2CH<sub>2</sub>, C-2), 41.3 (-2CH<sub>2</sub>NH), 45.6 (2CH<sub>2</sub>, C-1), 121.7 (4CH, Ar), 125.9 (2quat., Ar), 129.8 (4CH, Ar), 136.1 (2CH, Ar), 140.2 (1CH, Ar), 149.2 (2 quat., Ar), 161.7 (2quat., Ar).

**3.6.7 Synthesis of 4-(2-Chloroethyl)-*N*-[3-(2-pyridinyl)propyl]aniline Dihydrochloride (48)**

**(i) 2-Pyridine Propylchloride (46)**

To a dry flask equipped with a stirrer bar and reflux condenser was added 2-pyridine propyl alcohol (**(45)**, 6.0 g, 43.7 mmol) under nitrogen. Thionyl chloride (12.0 mL, 218.5 mmol) was added dropwise and the reaction refluxed for 4 hours.<sup>12,13</sup> After this time the excess thionyl chloride was removed from the reaction via distillation. The crude material was then triturated with hexane (10 mL) and any residual thionyl chloride removed under high vacuum. The

crude material was dissolved in chloroform and a solution of dried ( $\text{MgSO}_4$ ) diethyl ether saturated with HCl was added. The precipitated hydrochloride salt was triturated in ethanol and filtered to give **(46)** as a pale brown powder (7.8 g, 93% yield): mpt 121 – 124 °C (lit<sup>3</sup> 120-124°C); (Found C 49.82, H 5.87, N 7.14  $\text{C}_8\text{H}_{11}\text{Cl}_2\text{N}$  requires C 50.02, H 5.77, N 7.29).

$\delta_{\text{H}}$  (DMSO, 200 MHz)  $\delta$  2.87 (2H, m, H-2), 2.94 (2H, t,  $J_{3,2}$  6.8 Hz, H-3), 3.71 (2H, t,  $J_{1,2}$  6.8 Hz, H-1), 8.01-8.09 (1H, m, H-5'), 8.13 (1H, d,  $J_{3'',4''}$  8.0 Hz, H-3'), 8.57-8.64 (1H, m, H-4'), 8.78 (1H, d,  $J_{6'',5''}$  5.8 Hz, H-6').  $\delta_{\text{C}}$  (DMSO, 50 MHz)  $\delta$  34.8 ( $\text{CH}_2$ , C-2), 36.4 ( $\text{CH}_2$ , C-3), 46.1 ( $\text{CH}_2$ , C-1), 138.7 (CH, Ar), 139.7 (CH, Ar), 143.4 (quat., Ar), 146.3 (CH, Ar), 148.1 (CH, Ar).

**(ii) 2-(4-{{3-(2-Pyridinyl)propyl}amino}phenyl)ethanol (47)**

To a flask equipped with a stirrer bar and condenser was added **(46)** (7.0 g, 36.4 mmol) in THF (50 mL). A solution of **7** (5.0 g, 36.4 mmol) in THF (50 mL) was added to the flask together with solid  $\text{K}_2\text{CO}_3$  (8.0 g) and the reaction mixture refluxed for 72 hours with rapid stirring.<sup>26,27</sup> After this time the reaction mixture was filtered to remove the  $\text{K}_2\text{CO}_3$  and the solvent was then removed under vacuum. The residue was recrystallized in ethanol to yield **(47)** as a white solid (6.2 g, 67% yield): mpt 141 - 144 °C; (Found C 74.83, H 7.98, N 10.89, O 5.98  $\text{C}_{16}\text{H}_{20}\text{N}_2\text{O}$  requires C 74.97, H 7.86, N 10.93, O 6.24).

$\delta_{\text{H}}$  (Acetone- $d_6$ , 400 MHz)  $\delta$  2.82-2.89 (4H, m, H-2 and H-3), 2.90-2.94 (2H, m, H-4 and H-5), 3.62 (br s, 2H,  $\text{NH}_2$ ), 4.12 (2H, t,  $J_{1,2}$  7.0 Hz, H-1), 6.71 (2H, d,  $J_{2',3'}$  and  $J_{6',5'}$  8.5 Hz, H-2' and H-6'), 7.11 (2H, d,  $J_{3',2'}$  and  $J_{5',6'}$  8.5 Hz, H-3' and H-5'), 8.01-8.09 (1H, m, H-5'), 8.13 (1H, d,  $J_{3'',4''}$  8.0 Hz, H-3'), 8.57-8.64 (1H, m, H-4'), 8.78 (1H, d,  $J_{6'',5''}$  5.8 Hz, H-6').  $\delta_{\text{C}}$  (Acetone- $d_6$ , 100 MHz)  $\delta$  35.0 ( $\text{CH}_2$ , C-2), 35.2 ( $\text{CH}_2$ , C-3), 36.8 ( $\text{CH}_2$ , C-5), 48.4 ( $\text{CH}_2$ , C-3), 64.4 ( $\text{CH}_2$ , C-1), 121.1 (2CH, Ar), 129.9 (2CH, Ar), 138.9 (CH, Ar), 140.1 (CH, Ar), 143.6 (quat., Ar), 146.2 (quat., Ar), 146.8 (CH, Ar), 147.3 (quat., Ar), 148.7 (CH, Ar).

**(iii) 4-(2-Chloroethyl)-N-[3-(2-pyridinyl)propyl]aniline Dihydrochloride (48)**

To a dry flask equipped with a stirrer bar and reflux condenser was added **(47)** (2.0 g, 7.80 mmol) in chloroform under nitrogen. Thionyl chloride (6.0 mL, 82.2 mmol) was added dropwise and the reaction refluxed for 2 hours.<sup>12,13</sup> After this time, the reaction was neutralized with a saturated solution of  $\text{K}_2\text{CO}_3$ (aq) (20 mL). The target product was extracted into chloroform (3 x 30 mL) and dried ( $\text{MgSO}_4$ ). The solvent was removed under reduced

pressure to give crude product which was in ethanol to yield the free amine of **(48)**. A HCl saturated solution of ether was added to the compound dissolved in  $\text{CHCl}_3$ , to afford the title compound **(48)** as a white powder (0.57 g, 21% yield): 276-278 °C; (Found C 55.03, H 6.21, N 8.04  $\text{C}_{16}\text{H}_{21}\text{Cl}_3\text{N}_2$  requires C 55.27, H 6.09, N 8.06).

$\delta_{\text{H}}$  ( $\text{D}_2\text{O}$ , 400 MHz)  $\delta$  2.82-2.85 (2H, m, H-3), 2.90-2.94 (6H, m, H-2, H-4 and H-5), 3.58 (2H, br s,  $\text{NH}_2$ ), 3.86 (2H, t,  $J_{1,2}$  7.0 Hz, H-1), 6.72 (2H, d,  $J_{2,3}$  and  $J_{6,5}$  8.5 Hz, H-2' and H-6'), 7.14 (2H, d,  $J_{3,2}$  and  $J_{5,6}$  8.5 Hz, H-3' and H-5'), 8.07-8.12 (1H, m, H-5'), 8.13 (1H, d,  $J_{3',4'}$  8.0 Hz, H-3'), 8.53-8.60 (1H, m, H-4'), 8.77 (1H, d,  $J_{6',5'}$  5.8 Hz, H-6').  $\delta_{\text{C}}$  ( $\text{D}_2\text{O}$ , 100 MHz)  $\delta$  35.4 ( $\text{CH}_2$ , C-3), 36.0 ( $\text{CH}_2$ , C-4), 36.4 ( $\text{CH}_2$ , C-2), 36.6 ( $\text{CH}_2$ , C-5), 36.8 ( $\text{CH}_2$ , C-5), 63.8 ( $\text{CH}_2$ , C-1), 120.9 (2CH, Ar), 130.4 (2CH, Ar), 139.0 (CH, Ar), 140.2 (CH, Ar), 143.9 (quat., Ar), 146.7 (quat., Ar), 147.1 (CH, Ar), 147.4 (quat., Ar), 148.9 (CH, Ar).

### 3.6.8 Synthesis of *N*-benzyl-4-(2-chloroethyl)aniline Hydrochloride (**51**)

#### (i) 2-[4-(Benzylamino)phenyl]ethanol (**50**)

To a flask equipped with a stirrer bar and condenser was added benzyl chloride (**(49)**, 5.0 g, 39.5 mmol). A solution of **(7)** (5.42 g, 39.5 mmol) in THF (40 mL) was added to the flask followed by solid  $\text{K}_2\text{CO}_3$  (5.0 g). The reaction was then refluxed for 72 hours with rapid stirring.<sup>26,27</sup> After this time, the reaction was filtered to remove  $\text{K}_2\text{CO}_3$ , and the solvent was subsequently removed under vacuum. Purification of the crude material by flash chromatography (10% MeOH/ $\text{CHCl}_3$ ) afforded **(50)** as a pale yellow powder (4.68 g, 52% yield): mpt 119-122°C; (Found C 79.20, H 7.62, N 6.15, O 7.07  $\text{C}_{15}\text{H}_{17}\text{NO}$  requires C 79.26, H 7.54, N 6.16, O 7.04).

$\delta_{\text{H}}$  (Acetone- $d_6$ , 400 MHz) 2.78 (2H, t,  $J_{2,1}$  6.6 Hz, H-2), 3.80 (2H, t,  $J_{1,2}$  6.6 Hz, H-1), 4.21 (2H, s,  $\text{CH}_2\text{NH}$ ), 4.23 (1H, br s, NH), 7.02 (2H, d,  $J_{3,2}$  and  $J_{5,6}$  8.0 Hz, H-3' and H-5'), 7.27 (2H, dd,  $J_{5'',6''}$  and  $J_{3'',2''}$  7.2 Hz,  $J_{5'',4''}$  and  $J_{3'',4''}$  7.1 Hz, H-5'' and H-3'), 7.29 (1H, dd,  $J_{4'',5''}$  and  $J_{4'',3''}$  7.1 Hz,  $J_{4'',6''}$  and  $J_{4'',2''}$  1.8 Hz, H-4'), 7.33 (2H, dd,  $J_{6'',5''}$  and  $J_{2'',3''}$  7.2 Hz,  $J_{6'',4''}$  and  $J_{2'',4''}$  1.8 Hz, H-6'' and H-2'), 7.67 (2H, d,  $J_{2,3}$  and  $J_{6,5}$  8.0 Hz, H-2' and H-6').  $\delta_{\text{C}}$  (Acetone- $d_6$ , 100 MHz) 38.9 ( $\text{CH}_2$ , C-2), 47.9 ( $\text{CH}_2$ , NH), 63.3 ( $\text{CH}_2$ , C-1), 121.8 (2CH, Ar), 127.1 (2CH, Ar), 127.7 (quat., Ar), 128.0 (CH, Ar), 128.3 (2CH, Ar), 128.6 (2CH, Ar), 137.3 (quat., Ar), 148.4 (quat., Ar).

**(ii) N-Benzyl-4-(2-chloroethyl)aniline Hydrochloride (51)**

To a dry flask equipped with a stirrer bar and reflux condenser was added **(50)** (2.0 g, 8.80 mmol) in chloroform under nitrogen. Thionyl chloride (7.0 mL, 95.9 mmol) was added dropwise and the reaction refluxed for 3 hours.<sup>12,13</sup> After this time, the reaction was neutralized with a saturated solution of  $K_2CO_3$ (aq) (20 mL). The target product was extracted into chloroform (3 x 30 mL) and dried ( $MgSO_4$ ). The solvent was removed under reduced pressure to give crude material which was recrystallized from ethanol to give the free amine as yellow crystals. This was converted to the HCl salt via the methods previously outlined, to afford the title compound **(51)** as a white powder (0.6 g, 24% yield): 222-224°C; (Found C 63.67, H 6.14, N 4.84  $C_{15}H_{17}Cl_2N$  requires C 63.84, H 6.07, N 4.96).

$\delta_H$  ( $D_2O$ , 400 MHz) 2.99 (2H, t,  $J_{2,1}$  6.6 Hz, H-2), 3.58 (2H, t,  $J_{1,2}$  6.6 Hz, H-1), 4.23 (2H, s,  $CH_2NH$ ), 4.28 (1H, br s, NH), 7.05 (2H, d,  $J_{3',2'}$  and  $J_{5',6'}$  8.0 Hz, H-3' and H-5'), 7.27 (2H, dd,  $J_{5'',6''}$  and  $J_{3'',2''}$  7.2 Hz,  $J_{5'',4''}$  and  $J_{3'',4''}$  7.1 Hz, H-5'' and H-3''), 7.27 (1H, dd,  $J_{4'',5''}$  and  $J_{4'',3''}$  7.1 Hz,  $J_{4'',6''}$  and  $J_{4'',2''}$  1.8 Hz, H-4''), 7.31 (2H, dd,  $J_{6'',5''}$  and  $J_{2'',3''}$  7.2 Hz,  $J_{6'',4''}$  and  $J_{2'',4''}$  1.8 Hz, H-6'' and H-2''), 7.69 (2H, d,  $J_{2',3'}$  and  $J_{6',5'}$  8.0 Hz, H-2' and H-6').  $\delta_C$  ( $D_2O$ , 100 MHz) 38.2 ( $CH_2$ , C-2), 47.6 ( $CH_2$ , NH), 44.9 ( $CH_2$ , C-1), 120.5 (2CH, Ar), 126.8 (2CH, Ar), 127.3 (quat., Ar), 127.9 (CH, Ar), 128.4 (2CH, Ar), 128.7 (2CH, Ar), 137.8 (quat., Ar), 147.9 (quat., Ar).

### **3.7 REFERENCES:**

1. Krishnamurthy, S. *Tetrahedron Lett.* **1982**, 23(33), 3315-3318.
2. Crochet, R. A., Blanton, C. D. *Syn.*, **1974**, 55-56.
3. *Aldrich Catalogue Handbook of Fine Chemicals*, **1996**, 1086.
4. Brown, H. C., Choi, Y. M., Narasimhan, S. *J. Org. Chem.*, **1982**, 47, 3153-3163.
5. Brown, H. C., Stocky, T. P. *JACS*, **1977**, 99(25), 8218-8226.
6. Pizey, J. S. *Synthetic Reagents (Vol 1)*. John Wiley and Sons Inc. New York. 1974. Vol 1, 323-331.
7. Lin, C. H., Aristoff, P. A., Johnson, P. D., McGrath, J. P., Timko, J. M., Robert, A. *J. Org Chem.*, **1987**, 52(25), 5594-601.
8. Eliel, E. *J. Org. Chem.*, **1961**, 26, 518-5190.
9. Blackwell, L. F., Jolley, K. W., MacGibbon, A. K. *J. C. S. Perkin (II)*, **1973**, 171.
10. Clarke, H. T., Hartman, W. W. *Organic Syntheses*, **1932**, *Collective Vol. 1*, 455.
11. Ashley, J., Berber, H., Ewins, A., Newbery, G. *J. Chem Soc.*, **1942**, 103, 115.
12. Trost, B. M., Fleming, I. *Comp. Org Chem*, **1993**, 6, 204-205.
13. Cope, A. C., Ciganek, E. *Organic Syntheses*, **1959**, 339.
14. Braun, V. *J. Ber.*, **1912**, 45, 1279.
15. Middleton, W. *J. Org Chem.*, **1975**, 40(5), 574-578.
16. Cheng, C. S., Ferber, C., Bashford, R. I., Grillot, G. F. *JACS*, **1951**, 73(3), 4081-4084.
17. Darzac, M., Brotin, T., Rousset-Arzel, L., Bouchu, D., Dutasta, J. *New J. Chem.*, **2004**, 28(4), 502-512.
18. Valu, K. K., Gourdie, T. A., Boritzki, T. J., Gravatt, G. L., Baguley, B. C., Wilson, W. R., Wakelin, L. *J. Med. Chem*, **1990**, 33, 3014-319.
19. Terpko, M. O., Heck, R. F. *J. Org. Chem.*, **1980**, 45, 4992-4993.
20. Greene, T. and Wuts, P. *Protective Groups in Organic Synthesis*. Wiley-Interscience Publications, New York., **1991**, 112 - 114.
21. Patent: May and Baker Ltd, *Chem Abstr.*, **1960**, 61, 6994d.
22. Carnmalm, B., Gyllander, J., Jonsson, N. A., Mikiver, L. *Acta. Pharm. Suecicia*, **1974**, 11, 33-48.
23. Strazzolini, P., Verardo, G., Giumanini, G. *J. Org. Chem.* **1988**, 53, 3321-3325.
24. Herbert, R.B. and Knaggs, A.R. *J. Chem. Soc. Perkin Tran 1*, **1992**, 1903-1907.

25. *Aldrich Catalogue Handbook of Fine Chemicals*, **1996**, 514.
26. Oshiro, K., Ogata, T., Yoshida, H., Inokawa, S. *Nippon Kagaku Zasshi*, **1968**, 89(2), 211-213.
27. Blanke, S., Blanke, R. *J. Anal. Toxicology*, **1984**, 8(5), 231-233.
28. *Aldrich Catalogue Handbook of Fine Chemicals*, **2004**, 491.
29. Greene, T. and Wuts, P. *Protective Groups in Organic Synthesis*. Wiley-Interscience Publications, New York., **1991**, 320-324.

## **CHAPTER 4 – CYTOTOXICITY STUDIES – RESULTS AND DISCUSSION**

### **4.1 INTRODUCTION**

Cancer is the name for a group of more than 100 diseases resulting from rapid and abnormal cellular growth, that afflict millions of people worldwide each year, presenting as the second highest cause of death in the first world after cardiovascular disease.<sup>1,2,3</sup> The American Cancer Society maintains that, of persons living in developed nations, half of all men and one-third of all women in the United States will develop cancer during their lifetimes.<sup>3,4</sup> Globally, the most common cancers are lung (~1.2 million cases per year), breast (~1.05 million cases per year), colorectal (~950,000 cases per year), stomach (~880,000 cases per year), and liver (~560,000 cases per year).<sup>4,5</sup>

The above profile varies greatly between populations, however the risk of developing most types of cancer can be reduced by changes in a person's lifestyle including limiting alcohol intake, avoiding tobacco, exercising regularly, maintaining a healthy diet and avoiding excessive exposure to UV rays.<sup>6-12</sup> Furthermore, detecting tumors early through enhanced detection methods has resulted in a better overall prognosis for patients.

While the number of deaths from cancer have been decreasing by, on average, 2.1% per annum due to more efficient treatment regimens<sup>3</sup> and early detection, the incidence in the number of cases of cancer has increased in the population over the past thirty years. It is not surprising that approximately 77% of all cancers are diagnosed in persons aged 55 or older, as increased cell damage occurs throughout a lifetime with increased exposure to toxins and harmful UV rays. As such, the enhanced longevity of the population contributes markedly to the increasing incidence of cancer diagnosis in developed nations.<sup>3,4,6-12</sup>

The incidence and type of cancer varies according to sex, race and age, with the most commonly affected sites being the breasts, lungs, prostate, stomach, colon, liver and rectum.<sup>1,4,5</sup> While the disease symptoms and patient prognosis depend upon the organ affected, four similar features characterize all cancers.<sup>1,2</sup> These include:

- excessive cell proliferation,
- a loss of tissue specific characteristics,
- the ability to grow into adjacent tissues (invasiveness), and
- the ability to spread to new sites via blood vessels and lymph nodes, or across body cavities from one organ to another (metastasis).

Billions of dollars are spent on research each year, however, cancer still poses a formidable challenge. Cancer is not a single disease and requires different approaches depending on the cancer in question.

## **4.2 TREATMENT**

Modern medicine utilizes three main techniques in the treatment of cancer, either alone or in combination. Broadly categorized, these techniques fall under the headings of

- chemotherapy,
- radiation, and
- surgery.

Much of the scope of this thesis encompasses the theory behind chemotherapy however, radiation and surgery still remain important as first lines of defense against cancer.<sup>3</sup>

Most drug research will generally fall into one of the following broad categories:

- cytotoxic agents (i.e. alkylating, intercalating or groove binding analogues and their prodrugs);
- cell abrogating agents;
- hormone manipulators/immunotherapy (i.e. interferon stimulating); or
- combination/multi-drug therapy

#### 4.2.1 Cytotoxic Agents –

**(a) DNA Alkylating Agents** – This class consists of some of the earliest drugs used in the treatment of cancer. While CC-1065 has been extensively reviewed in Chapter 1, this class consists of other compounds, each very different in structure and efficacy. The first widely used group of alkylators were the aliphatic nitrogen mustards (i.e. mustine – Figure 44) whose high chemical reactivity and limited specificity cause a wide range of toxic side effects. However, with the introduction of milder, aromatic nitrogen mustards (melphalan – Figure 44) that were able to be administered orally, the effectiveness of treatment against lymphoblastic leukemia, malignant lymphoma and tumors of the breast and ovary was enhanced, particularly when administered in conjunction with mitotic inhibitors such as vinblastine.<sup>13-17</sup>

The nitrosoureas, more recent alkylating agents with lipophilic properties, are active against tumors of the brain and cerebrospinal fluid. Clinically useful drugs in this group include cisplatin, carmustine (i.v. administration) and lomustine which are orally administered.<sup>13-17</sup>

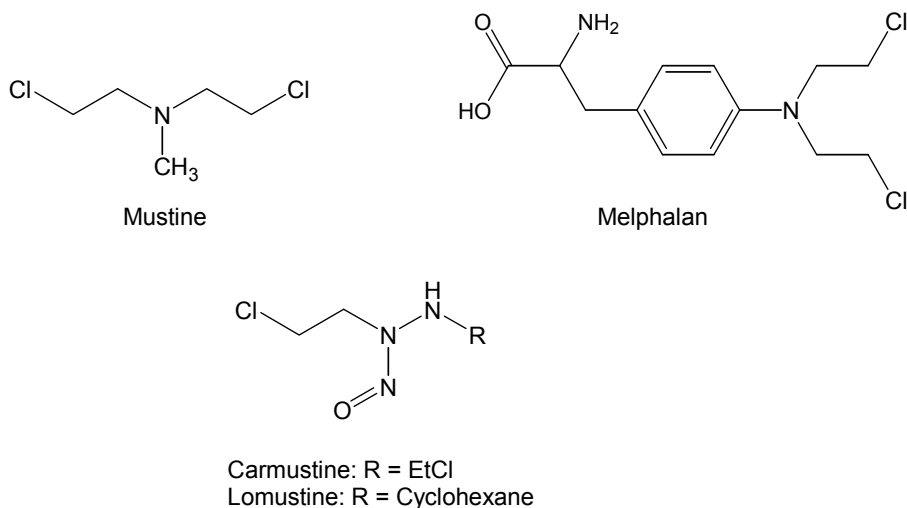


**Figure 44 – Clinically Applicable Alkylating Agents**

Similar to CC-1065, nitrogen mustards readily react with the N-7 of guanine, under physiological conditions via a neighboring group assisted nucleophilic substitution (Figure 45).

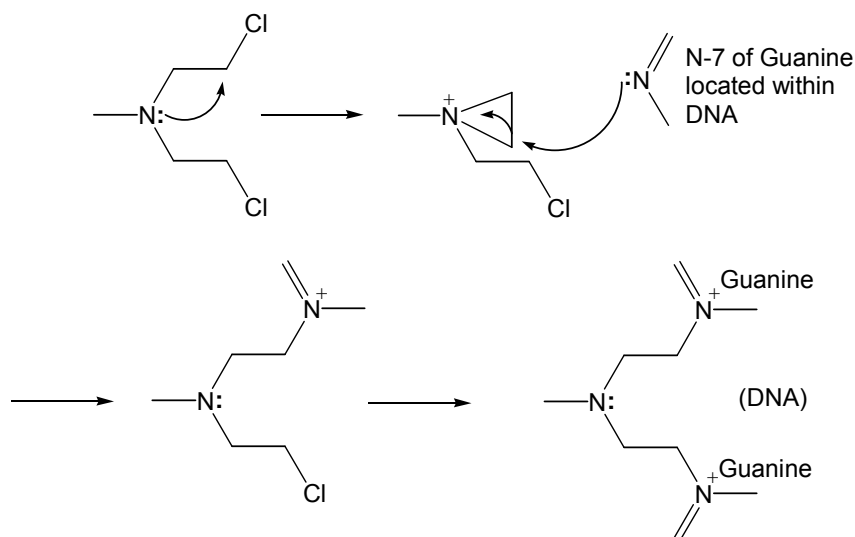


**Figure 45 – The Alkylation of DNA by the Nitrogen Mustard Mustine**

The examples cited serve as a model for most alkylating agents. While there are numerous other alkylating compounds currently in clinical use (i.e. hydrazine derivatives) they lie outside the scope of this thesis.

**(b) Intercalating Agents** – Intercalating agents are cytotoxic to cell populations that are proliferating rather than quiescent and generally prevent progression past the G<sub>2</sub>/M phase of the cell cycle. They also induce chromosomal abnormalities, condense chromatin and inhibit DNA and RNA synthesis. However, central to the action of intercalating agents is their ability to inhibit the activity of topoisomerase II which is essential for DNA repair.<sup>13-17</sup>

Intercalating agents all share a related structure, consisting of a fused, generally tricyclic system, which is required for insertion between the base pairs of the DNA helix. This group makes up a considerable number of clinically administered drugs and includes the:

- acridines,

- anthracyclins,
- ellipticines and
- quinoxalines.

The aminoacridines were the earliest recognized DNA intercalators and are powerful frameshift mutagens that are active against a broad spectrum of cancers. Amsacrine is used to fight leukemias and malignant lymphomas while a second acridine, nitracrine was shown to be active against mammary and ovarian carcinomas (Figure 46).<sup>13-17</sup>

The anthracyclins, comprising adriamycin and daunomycin (Figure 46) are the most commonly used intercalating agents. Both possess a broad spectrum of activity, inhibiting DNA and RNA synthesis and causing single strand breaks. Interestingly, daunomycin's mechanism of intercalation has been well studied and involves rapid external attachment to the helix, followed by insertion and monomolecular rearrangement.<sup>13-17</sup>

The ellipticines (9-Hydroxy-N-methylellipticinum – Figure 46) are also good intercalating agents and inhibit topoisomerase II, the action of which is essential for DNA repair and thus, cellular survival.<sup>13-17</sup>

The quinoxaline antibiotics are a group of polyintercalating compounds, the most recognized being echinomycin and triostin A. They intercalate into DNA with the rings lying parallel to one another, spanning two base pairs in the complex. These compounds are highly sequence selective and show specificity toward CG rich DNA sequences.<sup>13-17</sup>

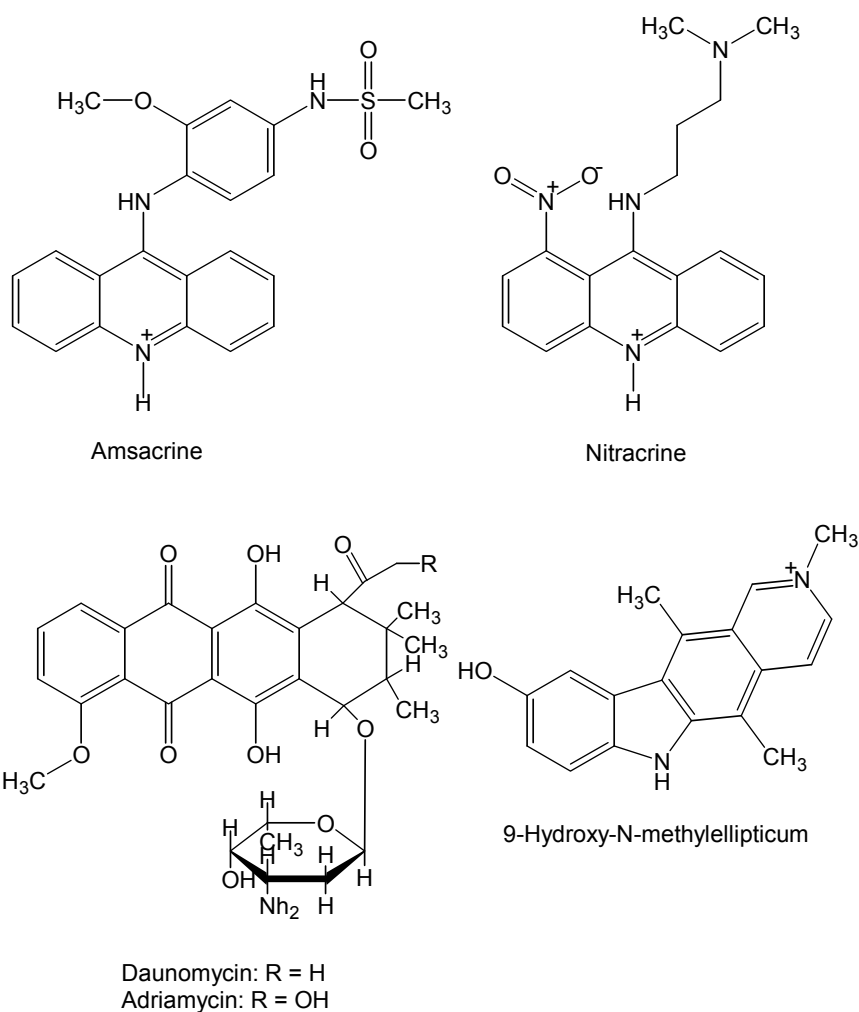


**Figure 46 – Conventional Intercalating Agents**

#### 4.2.2 Cell Abrogation Compounds –

The eukaryotic cell cycle is tightly regulated by protein tyrosine kinases and as such represents an important target for the development of anticancer drugs.

Activation of the cdc2-cyclin B complex is a crucial element in the regulation of the cell cycle's G<sub>2</sub>/M transition. The complex is activated by phosphorylation at Thr-161 and inhibited by phosphorylation at both Thr-14 and Tyr-15.<sup>18-20</sup>

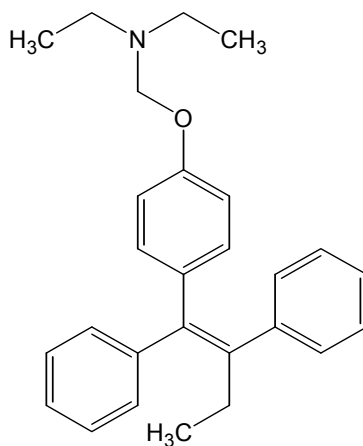
The protein kinases Wee1 and Myt1 are responsible for the inhibitory phosphorylations and are the main target of research groups involved in developing cell abrogation compounds. The

inhibition of one or both of these enzymes by targeted drugs prevents the activation of the cdc2-cyclin B complex, thereby averting the entry of the cell into mitosis<sup>18-20</sup> and eventually resulting in cell death.

#### 4.2.3 Hormone Manipulation –

Modification of the hormonal environment in which a tumor exists can often result in regression of the cellular mass. Tamoxifen, (Figure 47) belonging to the anti-oestrogen class of drugs, is used in the treatment of breast cancer and in some cases of endometrial cancer. This drug competes with endogenous oestrogens for their receptors in breast tissue and inhibits the transcription of oestrogen-responsive genes that contribute to tumor proliferation. It also induces the production of transforming growth factor- $\beta$  which inhibits the growth of malignant cells.<sup>18,21</sup>

Generally, Tamoxifen and most other endocrine treatments are used separately from cytotoxic drugs, as there is no evidence to support that giving them in combination offers any additional benefit.<sup>21</sup>



Tamoxifen

*Figure 47 – Tamoxifen*

### **4.3 CELL TYPES**

The detailed study of mammalian cells *in vivo* is complicated and so in order to study the activity of cell lines under controlled conditions, cells are typically cultured in an artificially standardized environment. Cancer cells are relatively simple to study in culture because of their ability to divide indefinitely. While normal cells propagate for only a limited number of cycles, cancer cells possess one or more mutations that allow them to proliferate in an immortal manner, providing a genetically homogeneous source of cells.<sup>2</sup>

The required cell lines were supplied adhered to the glass surface of a flat bottomed culture vessel in a medium containing 5% fetal calf serum (FCS) which provides the necessary growth factors for cell proliferation and survival (i.e. PDGF). Additional amino acids (required in protein synthesis), vitamins (ie. nicotinamide), salts, antibiotics (to inhibit bacterial growth, ie. streptomycin and penicillin) and glucose were also incorporated into the medium. The cells were incubated at 37°C in an atmosphere of 5% CO<sub>2</sub>/air until required in culture experiments. While normal cells (i.e. NFF) are inhibited by crowding and generally only form a single layer in culture flasks, cancer cells do not exhibit this density dependent inhibition.<sup>16</sup> As a result, the cell density (represented by cell count) of the cancer lines provided was several times more than that of the control (ie. non-tumor) cell lines used.

The main cell types that were utilized in the experimental (Chapter 6), and that are commonly used in cancer research include HeLa, MM96L and NFF. While both the HeLa and MM96L cell lines are tumor derived, NFF are normal fibroblastic cells that act as a control group, enabling us to compare the activity of various chemotherapeutic drugs in both tumor and non-tumor cell lines. Some of these cell lines are described below (4.3.1-4.3.7).<sup>22,23</sup>

#### **4.3.1 HeLa –**

HeLa is a fast growing epithelial cell line that was isolated from a human cervical carcinoma in 1952. This was the first continuous line of cells established and is still commonly used today in cancer research. HeLa cells are capable of growth both in suspension and on a solid medium.

#### **4.3.2 MM96L –**

The MM96L cell line is a continuous line of human metastatic melanoma cells. These cells are highly invasive but sensitive to oxygen radicals and nucleosides.

#### **4.3.3 MM418c5 –**

This is a heavily pigmented human melanoma that is sensitive to GSH depletion.

#### **4.3.4 DU145 and PC3**

Both the DU-145 and PC3 cell lines originate from human prostate cancer.

#### **4.3.5 NFF –**

Neonatal foreskin fibroblasts (NFF) have a limited life-span of several months in culture and therefore are not regarded as a continuous line of cells. NFF cells are inhibited by crowding and only form a single layer in cell culture.

#### **4.3.6 HaCat –**

This immortalised human keratinocyte cell line while not tumorigenic, exhibits altered characteristics to normal skin cells. While the cell line is not continuous it exhibits a longer life-span than normal fibroblastic cell lines. Furthermore, HaCat cells do not exhibit the degree of density dependent inhibition displayed by NFF cells lines.

**4.3.7 293 –** An adenovirus transformed human kidney cell line.

### **4.4 CELL SURVIVAL STUDIES**

The fundamental dilemma in the treatment of cancer is the limited specificity displayed by many of the drugs used in conventional chemotherapy. While most of the cancerous growth can frequently be removed by surgery, it is often difficult to eradicate all of the tumor cells, particularly if metastasis has occurred. Therefore it is often desirable to seek a second form of therapy (ie. radiation or chemotherapy). Neither of these methods has been particularly specific to date, however the advent of new protocols in drug research has seen some startling developments in chemotherapeutic drug regimens in recent years.

Recent developments in drug research have relied more heavily on rational design, rather than trial and error or guesswork, and focus on the differences between normal and neoplastic cells (ie. proliferation rate, metabolism and radiosensitivity). Furthermore, certain cancers depend on the presence of hormones and may possess recognizable antibodies on their cell surface, providing further possibilities for anticancer vaccine development, however, future work is expected to largely encompass combination and multi-drug therapy.

#### 4.4.1 Necrosis and Programmed Cell Death<sup>24,25</sup> –

Cells exhibit one of two distinct morphologies during cell death following treatment with cytotoxic compounds (Figure 48). Cellular death can occur via one of two mechanisms: necrosis or programmed cell death.

- (a) **Necrosis** – This occurs as a consequence of trauma, for example exposure to toxins or heat, and disease. Cells undergoing necrosis display characteristic morphological features, beginning with plasma membrane changes that result in a loss in the sodium and calcium ion balance, followed by acidosis, osmotic shock, chromatin clumping and nuclear condensation. These changes are accompanied by mitochondrial phospholipase activation and decreased RNA, protein and ATP synthesis. The end result is a reduced homeostatic balance and subsequent cell death.<sup>24</sup>
  
- (b) **Programmed cell death or apoptosis** – This phenomenon is morphologically distinct from necrosis and occurs as a result of the ignition of a programmed genetic signal. Apoptosis is the method via which cells counterbalance mitosis, hence maintaining the size and shape of tissues and organs. This mechanism of cell death is characterized by shrinkage and condensation of cells, margination and blebbing of chromatin and increased RNA and protein synthesis, which declines following death.<sup>24</sup>

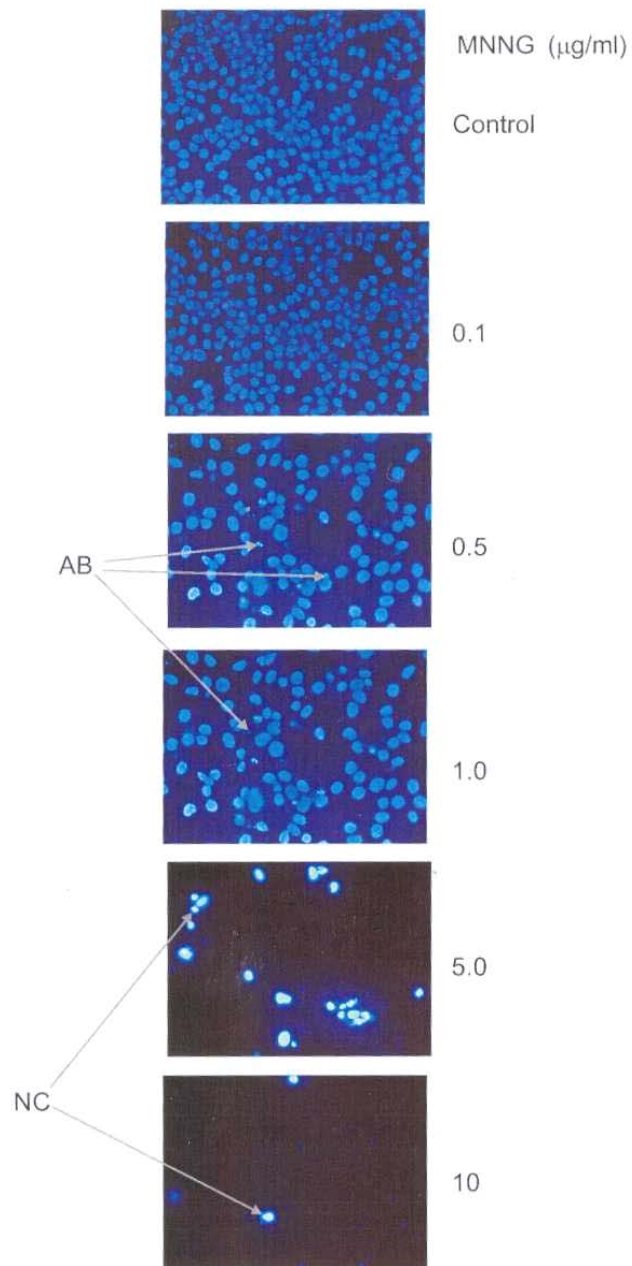


*Figure 48 – The Effect of Varying Concentrations of MNNG (a DNA alkylating compound) on the morphology of MM96L cells (400x) following staining with Hoechst 33258, a fluorescent nuclear stain. Apoptotic Bodies (AB) and Nuclear Chromatin Condensation (C) are shown (Taken from Reference 17).*

#### 4.4.2 The Effect of Varying Concentrations of Synthesized Alkylating Compound on Various Cell Lines –

Prior studies conducted by White *et al.*,<sup>26</sup> incorporating the compounds illustrated in Figure 49(a) demonstrated that the simple 4-hydroxyphenethyl halide analogues (Figure 49(a)) possessed the minimal structural requirements for alkylating DNA with  $Ar_{1,3}$  participation (Figure 49(b)).

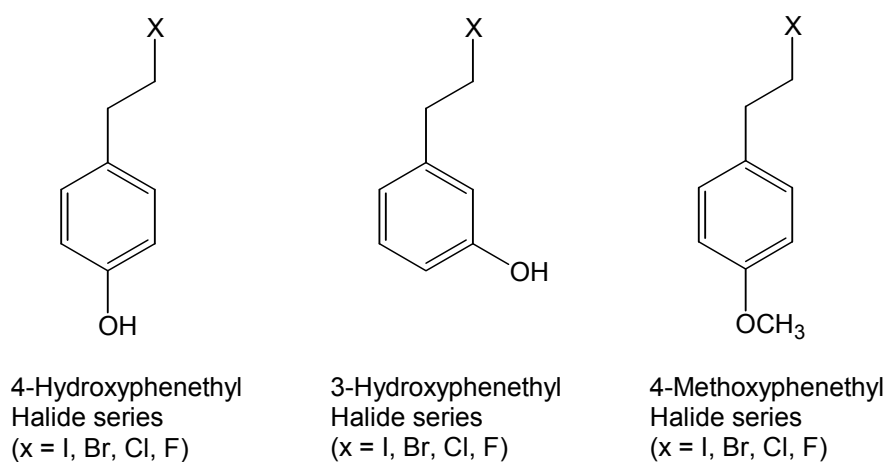


**Figure 49(a) – 4-Hydroxyphenethyl, 3-Hydroxyphenethyl and 4-Methoxyphenethyl halide series**

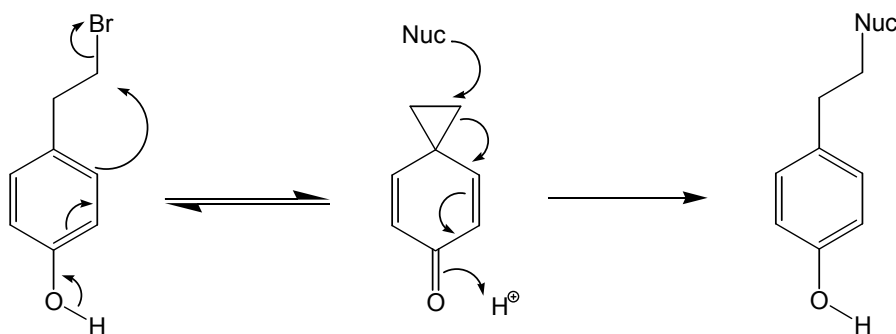


**Figure 49(b) –  $Ar_{1,3}$  Ring Cyclisation of 4-Hydroxyphenethyl Bromide**

This study, involving the compounds shown in the scheme above revealed the following relationships:

- (a) The relative cytotoxicities of the 3-hydroxyphenethyl and 4-methoxyphenethyl halides correlated with leaving group ability (ie.  $I > Br > Cl$ ) in line with  $S_N2$  alkylation.
- (b) The relative cytotoxicities of the 4-hydroxyphenethyl halides was found to be  $Br > I > Cl$  although this difference in cytotoxicity was much less pronounced than that of 3-hydroxyphenethyl and 4-methoxyphenethyl halides.
- (c) The 4-hydroxyphenethyl halides demonstrated higher levels of DNA alkylation than the 3-hydroxyphenethyl and 4-methoxyphenethyl halides.
- (d) The intensity of the DNA alkylation exhibited by the 4-hydroxyphenethyl halide analogues was of the following order:  $Br > I > Cl$  which corresponds with the relative cytotoxicity of these compounds.
- (e) 4-Hydroxyphenethyl bromide demonstrated some sequence selectivity toward runs of A and T. However, this selectivity for AT rich DNA was markedly lower than that of CC-1065, indicating the importance of the non-covalent binding subunits of CC-1065 in directing sequence selectivity.

From the above observations it can be deduced that the greater potency of 4-hydroxyphenethyl chloride and bromide relative to the corresponding 3-hydroxy and 4-methoxy derivatives is related to the enhanced DNA alkylating capabilities by virtue of  $Ar_{1,3}$  participation. Furthermore, the cytotoxicity of these compounds was found to be proportional to the electropositive nature of the leaving group and is therefore consistent with the theory that ring closure is rate determining.

Given the above, we hypothesized that 4-aminophenethyl halide derivatives would exhibit even greater cytotoxic activity than their hydroxyl counterparts because of the enhanced ability of  $Ar_{1,3}$  participation via the improved electron donating capability of the amine functionality. As such, the following project was designed in order to deduce whether:

- (a) The 4-aminophenethyl halides would exhibit greater cytotoxicity than their 4-hydroxyphenethyl halide counterparts in the corresponding order:  $Br > Cl > F$ . (Note: 4-aminophenethyl iodide was synthetically inaccessible due rapid to polymerization of the subunit).
- (b) The addition of electron withdrawing functionality to the 4-amine would limit  $Ar_{1,3}$  cyclisation and hence diminish the cytotoxicity of the compound.

- (c) The addition of simple subunits to 4-aminophenethyl halide analogues would enhance the cytotoxicity of the compound through non-covalent binding with DNA.

In order to compare the cytotoxicity of our synthesized compounds toward both non-tumor and tumor cell lines, we applied varied concentrations of drug to a range of cell lines as shown in Figures 50 - 61. The cells were incubated with drug for two hours at 37°C.

An incubation time of two hours was commonly used in the Parson's lab where particularly reactive compounds were involved. Preliminary studies conducted by Shalders *et al.*<sup>27</sup> demonstrated that 4-aminophenethyl bromide is completely hydrolyzed in buffer between 30 and 60 minutes and its reaction with DNA is complete within 5 minutes. This phenomenon was confirmed in drug stability studies (Chapter 5.2). For this reason, a two hour incubation time was deemed appropriate.

Following incubation with drug, the plates were washed and incubated with fresh medium for a further 3 days at 37°C. The plates were then washed, fixed, stained with sulforhodamine B and analyzed via spectrophotometric methods, as described in Section 6.2.1. The results are as summarised in Figures 50 – 61 and Table 16.

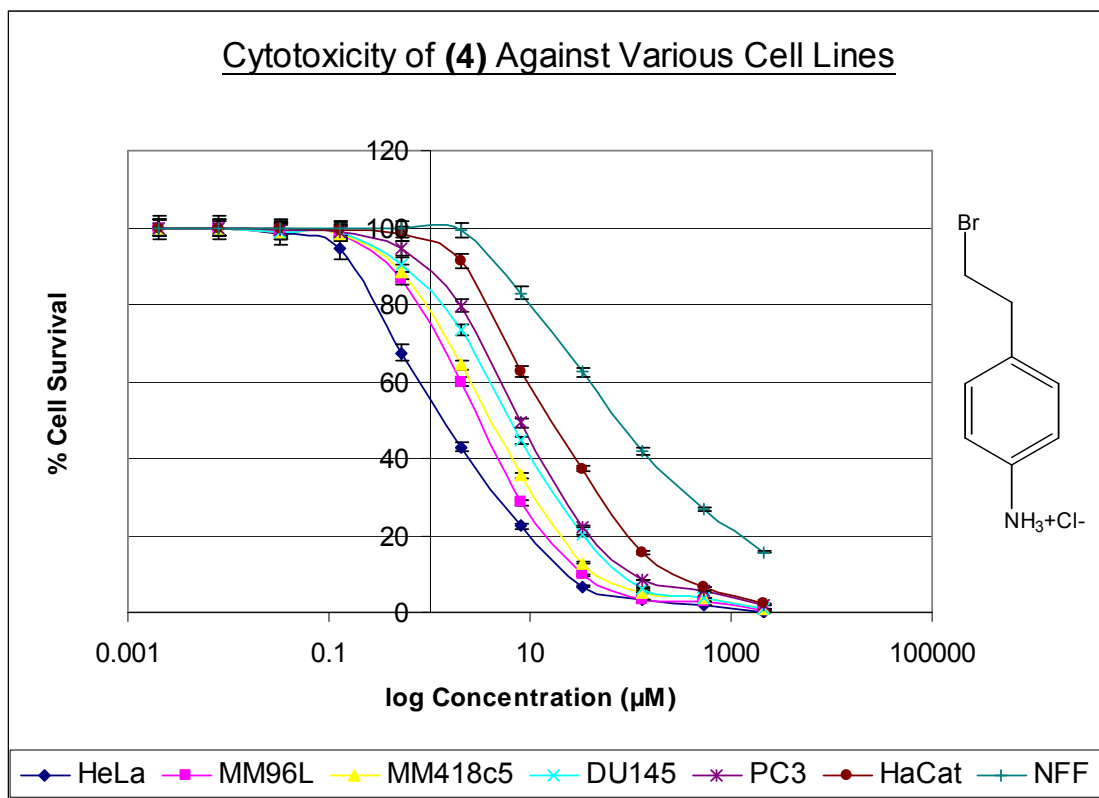


*Figure 50 – The Cytotoxicity of Compound (4) Toward DU145, HeLa, HaCat, MM96L, MM418c5, NFF and PC3 Cell Lines.*

	DU145	HeLa	HaCat	MM418c5	MM96L	NFF	PC3
<b>D<sub>37</sub></b>	20.1 ± 0.6	4.82 ± 0.2	52.3 ± 1.6	18.5 ± 0.7	12.3 ± 0.4	801 ± 24	28.4 ± 0.9
<b>D<sub>50</sub></b>	5.15 ± 0.2	1.94 ± 0.1	10.5 ± 0.3	3.56 ± 0.1	3.14 ± 0.9	126 ± 3.8	6.73 ± 0.2

**Table 4:** D<sub>37</sub> and D<sub>50</sub> values (µM) for (4) Against Various Cell Lines.

The relative cytotoxicity of (4) toward various cell lines as determined by D<sub>37</sub> values is:

HeLa>MM96L>MM418c5>DU145>PC3>HaCat>NFF

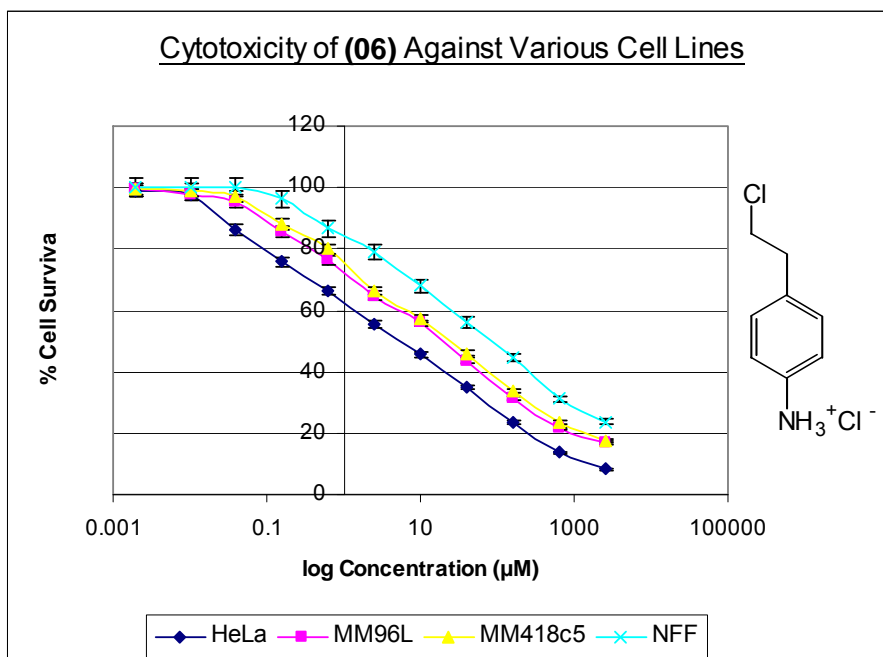


**Figure 51** – The Cytotoxicity of Compound (6) Toward HeLa, MM418c5, MM96L and NFF Cell Lines.

	HeLa	MM418c5	MM96L	NFF
D <sub>37</sub>	32.3 ± 1.3	160 ± 6.1	116 ± 4.2	785 ± 31
D <sub>50</sub>	5.82 ± 0.2	26.3 ± 1.2	18.5 ± 0.6	110 ± 4.4

**Table 5:** D<sub>37</sub> and D<sub>50</sub> values (µM) for Compound (6) Against Various Cell Lines.

The relative cytotoxicity of (6) toward various cell lines as determined by D<sub>37</sub> values is: HeLa>MM96L> MM418c5>NFF

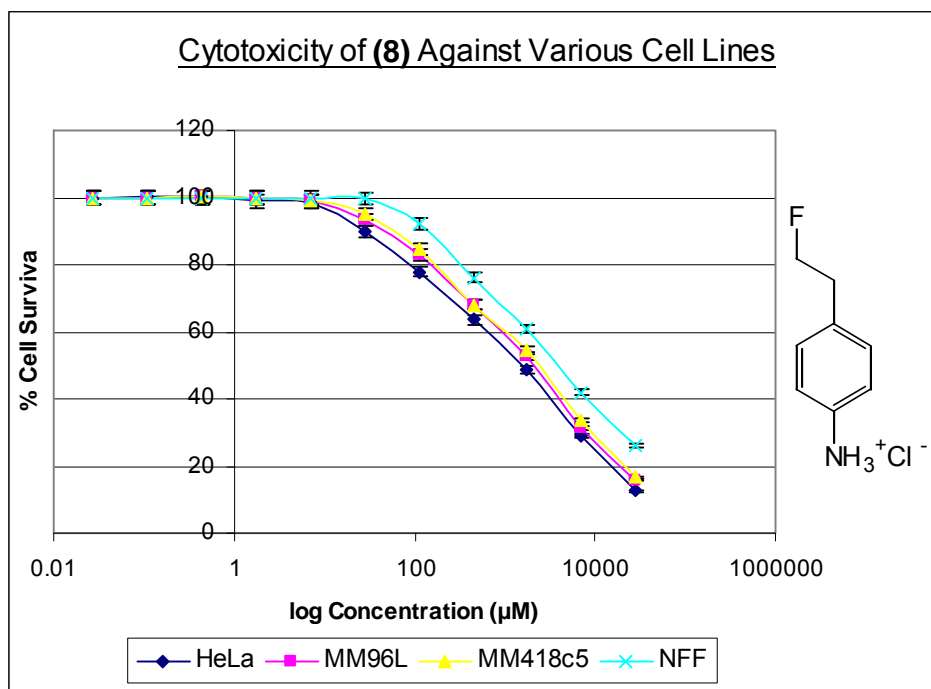


*Figure 52 – The Cytotoxicity of Compound (8) Toward HeLa, MM96L, MM418c5 and NFF Cell Lines.*

	HeLa	MM418c5	MM96L	NFF
<b>D<sub>37</sub></b>	>500	>500	>500	>500
<b>D<sub>50</sub></b>	>500	>500	>500	>500

**Table 6:** D<sub>37</sub> and D<sub>50</sub> values ( $\mu\text{M}$ ) for Compound (8) Against Various Cell Lines.

The relative cytotoxicity of (8) toward various cell lines as determined by D<sub>37</sub> values is:  
 HeLa > MM96L > MM418c5 > NFF

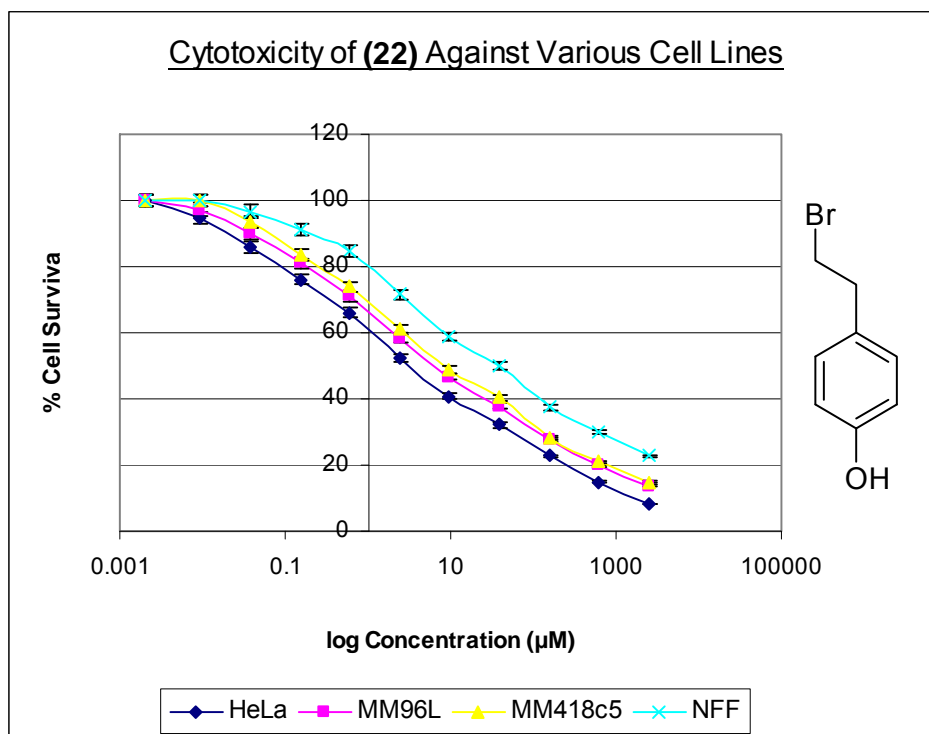


*Figure 53 – The Cytotoxicity of (22) Toward HeLa, MM418c5, MM96L and NFF Cell Lines.*

	HeLa	MM418c5	MM96L	NFF
$D_{37}$	$23.8 \pm 0.8$	$69.8 \pm 3.1$	$52.3 \pm 2.0$	$309 \pm 14$
$D_{50}$	$4.17 \pm 0.1$	$11.7 \pm 0.4$	$8.13 \pm 0.4$	$41.8 \pm 1.9$

**Table 7:**  $D_{37}$  and  $D_{50}$  values ( $\mu\text{M}$ ) for Compound (22) Against Various Cell Lines.  $D_{37}$  is the dose ( $\mu\text{M}$ ) Required to Reduce Cell Survival to 37%.  $D_{50}$  is the dose ( $\mu\text{M}$ ) Required to Reduce Cell Survival to Half.

The relative cytotoxicity of (22) toward various cell lines as determined from  $D_{37}$  values is:  
 HeLa > MM96L > MM418c5 > NFF

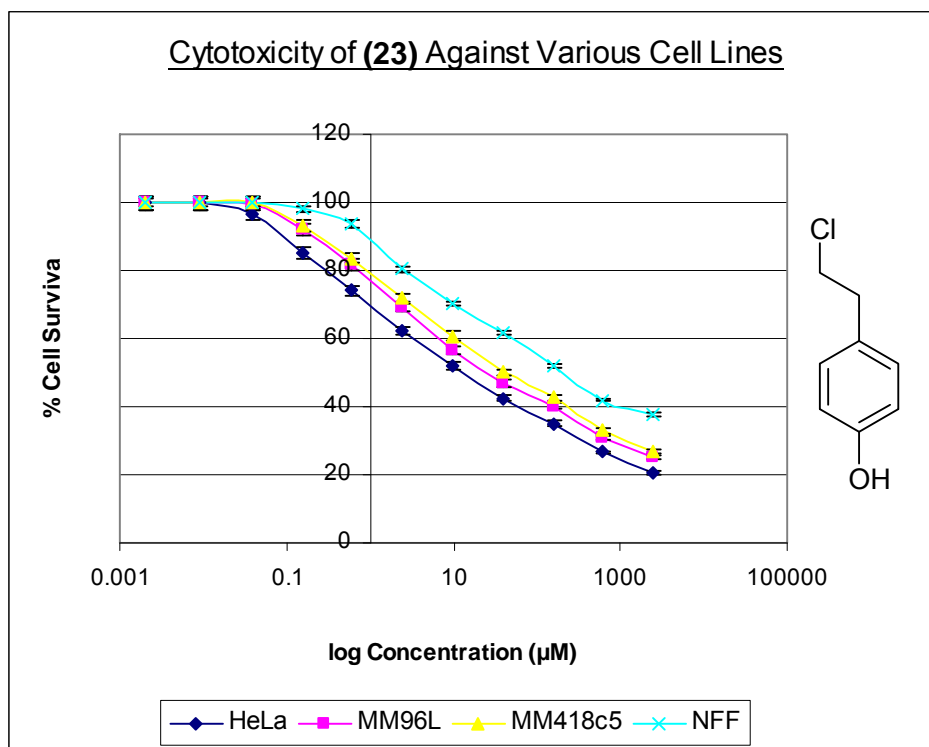


*Figure 54 – The Cytotoxicity of (23) Toward HeLa, MM418c5, MM96L and NFF Cell Lines.*

	HeLa	MM418c5	MM96L	NFF
$D_{37}$	$119 \pm 5.1$	$503 \pm 17$	$309 \pm 15$	>500
$D_{50}$	$20.7 \pm 0.8$	$61.3 \pm 2.1$	$39.9 \pm 2.0$	$399 \pm 15$

**Table 8:**  $D_{37}$  and  $D_{50}$  values ( $\mu\text{M}$ ) for Compound (23) Against Various Cell Lines.  $D_{37}$  is the dose ( $\mu\text{M}$ ) Required to Reduce Cell Survival to 37%.  $D_{50}$  is the dose ( $\mu\text{M}$ ) Required to Reduce Cell Survival to Half.

The relative cytotoxicity of (23) toward various cell lines as determined from  $D_{37}$  values is:

HeLa > MM96L > MM418c5 > NFF

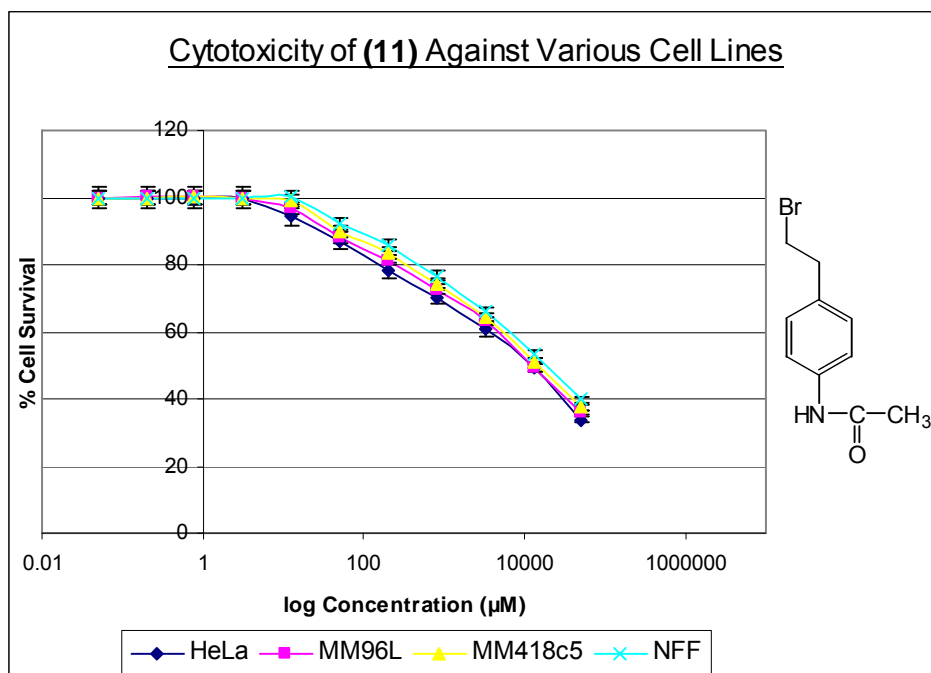


**Figure 55** – The Cytotoxicity of (11) Toward HeLa, MM418c5, MM96L and NFF Cell Lines.

	HeLa	MM418c5	MM96L	NFF
<b>D<sub>37</sub></b>	>500	>500	>500	>500
<b>D<sub>50</sub></b>	>500	>500	>500	>500

**Table 9:** D<sub>37</sub> and D<sub>50</sub> values (µM) for Compound (11) Against Various Cell Lines. D<sub>37</sub> is the dose (µM) Required to Reduce Cell Survival to 37%. D<sub>50</sub> is the dose (µM) Required to Reduce Cell Survival to Half.

The relative cytotoxicity of (11) toward various cell lines as determined from D<sub>37</sub> values is:  
 HeLa>MM418c5> MM96L>NFF

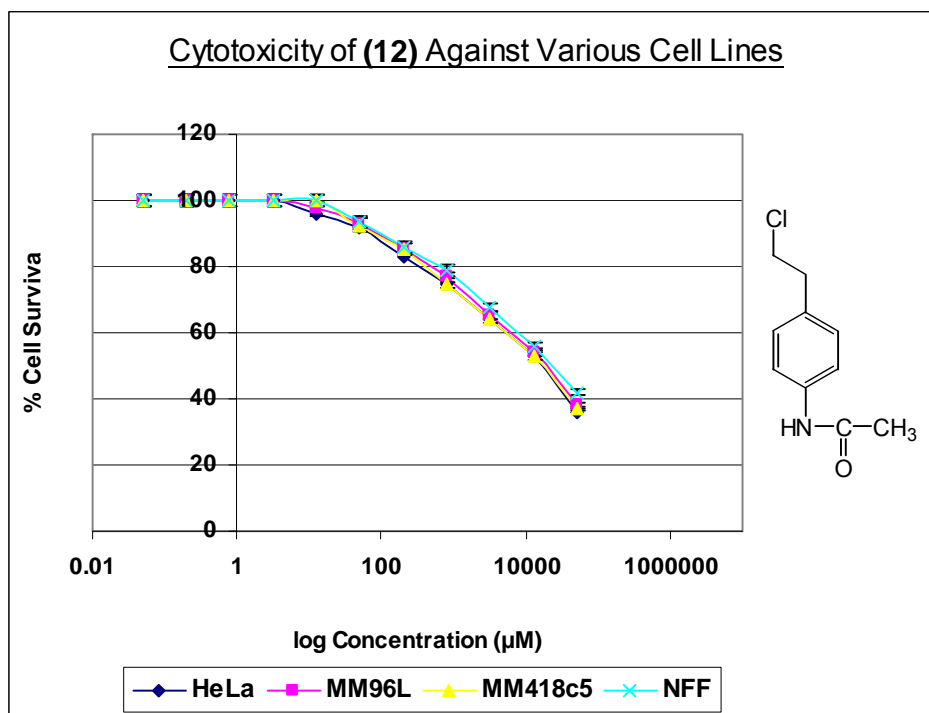


**Figure 56 – The Cytotoxicity of (12) Toward HeLa, MM418c5, MM96L and NFF Cell Lines.**

	HeLa	MM418c5	MM96L	NFF
<b>D<sub>37</sub></b>	>500	>500	>500	>500
<b>D<sub>50</sub></b>	>500	>500	>500	>500

**Table 10:** D<sub>37</sub> and D<sub>50</sub> values ( $\mu\text{M}$ ) for Compound (12) Against Various Cell Lines. D<sub>37</sub> is the dose ( $\mu\text{M}$ ) Required to Reduce Cell Survival to 37%. D<sub>50</sub> is the dose ( $\mu\text{M}$ ) Required to Reduce Cell Survival to Half.

The relative cytotoxicity of (12) is: HeLa>MM418c5>MM96L>NFF

Attempts to evaluate the cytotoxicity of the parent 4-nitrophenethyl halide analogues failed due to their insolubility in biological medium even with the addition of 1% DMSO. Given that DMSO displays an intrinsic cytotoxicity at concentrations greater than 1% in medium we were unable to provide an accurate assessment of the 4-nitrophenethyl halides cytotoxicity toward tumor cells.

4.4.3 – The cytotoxicity of Mono- and bis-Alkylators Incorporating pyridyl/benzyl noncovalent binding sub units against various cell lines.

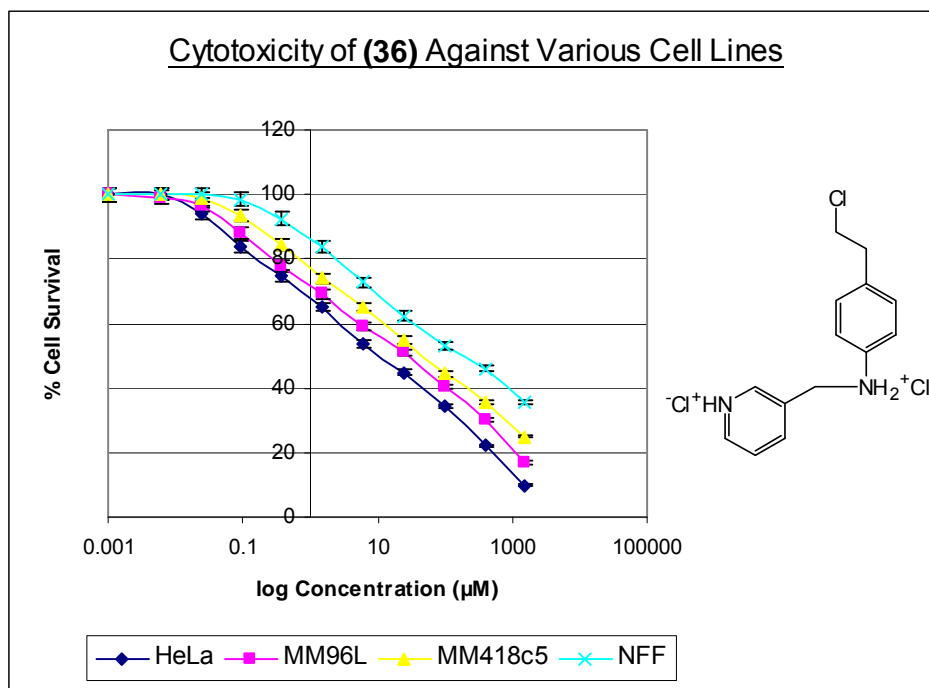
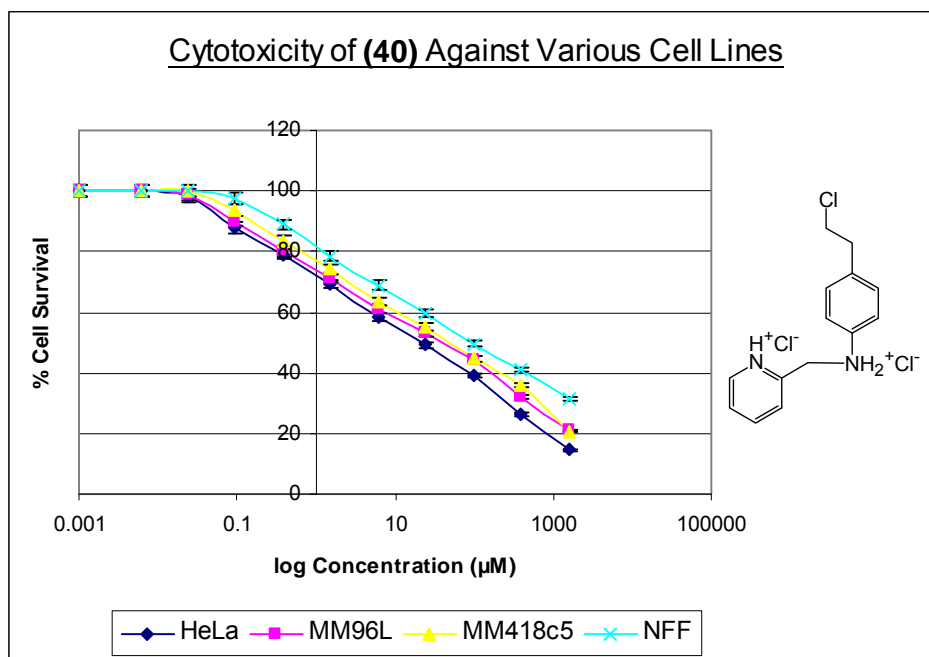


Figure 57 – The Cytotoxicity of (36) Toward HeLa, MM418c5, MM96L and NFF Cell Lines.

	HeLa	MM418c5	MM96L	NFF
<b>D<sub>37</sub></b>	60.8 ± 1.9	481 ± 19	171 ± 7.3	>500
<b>D<sub>50</sub></b>	8.95 ± 0.3	55.6 ± 2.2	20.1 ± 0.9	355 ± 16

**Table 11:** D<sub>37</sub> and D<sub>50</sub> values (µM) for Compound (36) Against HeLa cells. D<sub>37</sub> is the dose (µM) Required to Reduce Cell Survival to 37%. D<sub>50</sub> is the dose (µM) Required to Reduce Cell Survival to Half.

The relative cytotoxicity of (36) toward various cell lines as determined from D<sub>37</sub> values is:  
HeLa > MM96L > MM418c5 > NFF



**Figure 58 – The Cytotoxicity of (40) Toward HeLa, MM418c5, MM96L and NFF Cell Lines.**

	HeLa	MM418c5	MM96L	NFF
<b>D<sub>37</sub></b>	110 ± 2.8	380 ± 13	275 ± 8.5	>500
<b>D<sub>50</sub></b>	18.4 ± 0.5	50.4 ± 1.7	36.5 ± 1.1	166 ± 7.1

**Table 12:** D<sub>37</sub> and D<sub>50</sub> values (µM) for Compound (40) Against MM96L cells. D<sub>37</sub> is the dose (µM) Required to Reduce Cell Survival to 37%. D<sub>50</sub> is the dose (µM) Required to Reduce Cell Survival to Half.

The relative cytotoxicity of (40) toward various cell lines as determined from D<sub>37</sub> values is:

HeLa > MM96L > MM418c5 > NFF

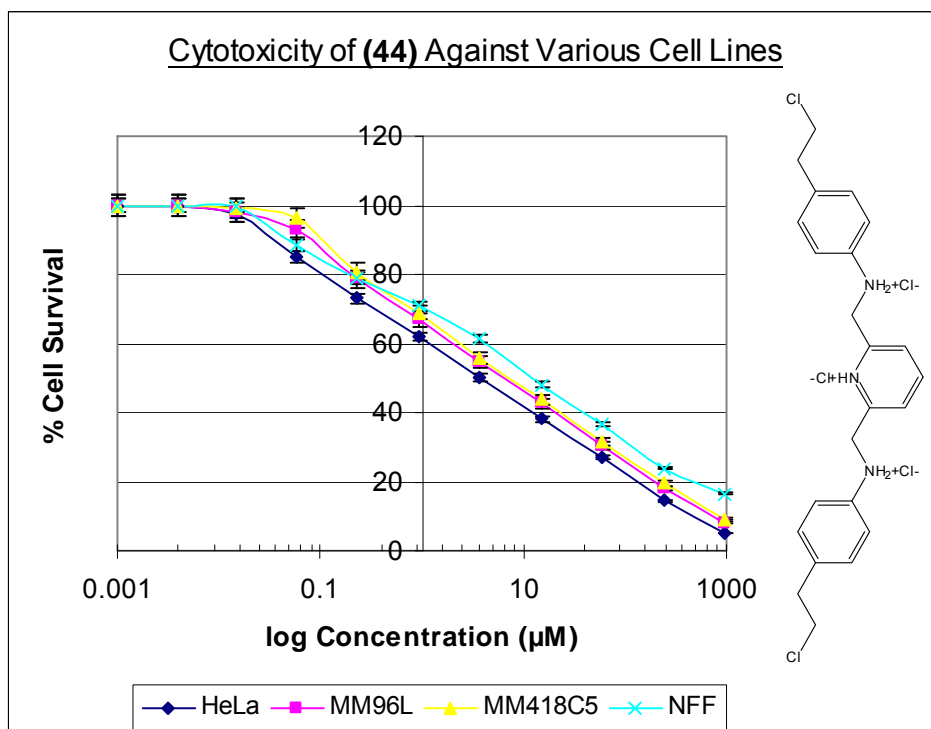


**Figure 59** – The Cytotoxicity of (44) Toward HeLa, MM418c5, MM96L and NFF Cell Lines.

	HeLa	MM418c5	MM96L	NFF
<b>D<sub>37</sub></b>	17.6 ± 0.8	40.3 ± 1.6	33.1 ± 1.3	80.9 ± 3.6
<b>D<sub>50</sub></b>	3.17 ± 0.1	6.88 ± 0.3	5.06 ± 0.2	10.0 ± 0.5

**Table 13:** D<sub>37</sub> and D<sub>50</sub> values (µM) for Compound (44) Against NFF cells. D<sub>37</sub> is the dose (µM) Required to Reduce Cell Survival to 37%. D<sub>50</sub> is the dose (µM) Required to Reduce Cell Survival to Half.

The relative cytotoxicity of (44) toward various cell lines as determined from D<sub>37</sub> values is:  
 HeLa > MM96L > MM418c5 > NFF

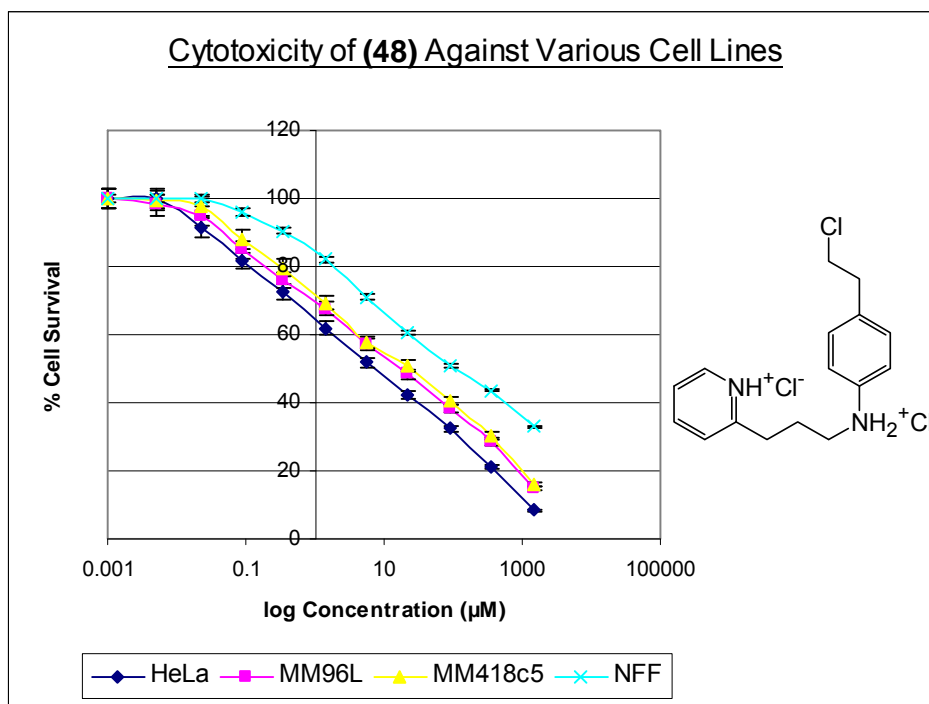


*Figure 60 – The Cytotoxicity of (48) Toward HeLa, MM418c5, MM96L and NFF Cell Lines.*

	HeLa	MM418c5	MM96L	NFF
<b>D<sub>37</sub></b>	40.1 ± 1.6	155 ± 6.2	115 ± 5.4	>500
<b>D<sub>50</sub></b>	6.75 ± 0.3	22.3 ± 0.9	10.1 ± 0.5	201 ± 6.0

**Table 14:** D<sub>37</sub> and D<sub>50</sub> values (µM) for Compound (48) Against NFF cells. D<sub>37</sub> is the dose (µM) Required to Reduce Cell Survival to 37%. D<sub>50</sub> is the dose (µM) Required to Reduce Cell Survival to Half.

The relative cytotoxicity of (48) toward various cell lines as determined from D<sub>37</sub> values is:  
HeLa>MM96L>MM418c5>NFF

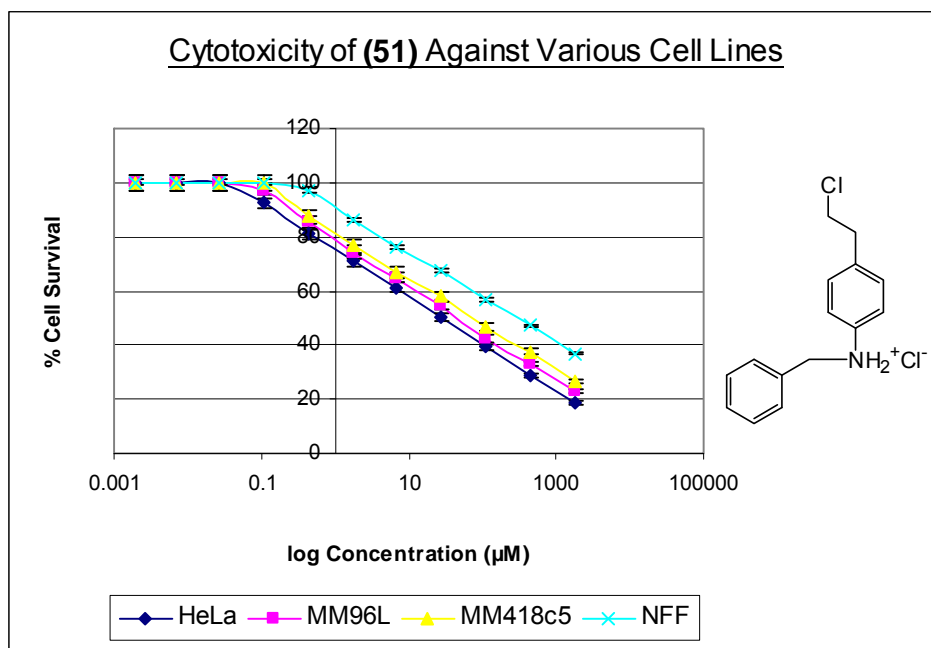


*Figure 61 – The Cytotoxicity of (51) Toward HeLa, MM418c5, MM96L and NFF Cell Lines.*

	HeLa	MM418c5	MM96L	NFF
$D_{37}$	$189 \pm 5.1$	$731 \pm 25$	$391 \pm 11$	$>500$
$D_{50}$	$29.9 \pm 0.8$	$108 \pm 3.7$	$57.6 \pm 1.7$	$719 \pm 22$

**Table 15:**  $D_{37}$  and  $D_{50}$  values ( $\mu\text{M}$ ) for Compound (51) Against NFF cells.  $D_{37}$  is the dose ( $\mu\text{M}$ ) Required to Reduce Cell Survival to 37%.  $D_{50}$  is the dose ( $\mu\text{M}$ ) Required to Reduce Cell Survival to Half.

The relative cytotoxicity of (51) toward various cell lines as determined from  $D_{37}$  values is:  
 HeLa>MM96L>MM418c5>NFF

#### 4.4.4 Summary of Results –

Compound		HeLa	MM418c5	MM96L	NFF
(4)	D <sub>37</sub>	4.82 ± 0.2	18.5 ± 0.7	12.3 ± 0.4	801 ± 24
	D <sub>50</sub>	1.94 ± 0.1	3.56 ± 0.1	3.14 ± 0.9	126 ± 3.8
(6)	D <sub>37</sub>	32.3 ± 1.3	160 ± 6.1	116 ± 4.2	785 ± 31
	D <sub>50</sub>	5.82 ± 0.2	26.3 ± 1.2	18.5 ± 0.6	110 ± 4.4
(8)	D <sub>37</sub>	>500	>500	>500	>500
	D <sub>50</sub>	>500	>500	>500	>500
(11)	D <sub>37</sub>	>500	>500	>500	>500
	D <sub>50</sub>	>500	>500	>500	>500
(12)	D <sub>37</sub>	>500	>500	>500	>500
	D <sub>50</sub>	>500	>500	>500	>500
(22)	D <sub>37</sub>	23.8 ± 0.8	69.8 ± 3.1	52.3 ± 2.0	309 ± 14
	D <sub>50</sub>	4.17 ± 0.1	11.7 ± 0.4	8.13 ± 0.4	41.8 ± 1.9
(23)	D <sub>37</sub>	119 ± 5.1	503 ± 17	309 ± 15	>500
	D <sub>50</sub>	20.7 ± 0.8	61.3 ± 2.1	39.9 ± 2.0	399 ± 15
(36)	D <sub>37</sub>	60.8 ± 1.9	481 ± 19	171 ± 7.3	>500
	D <sub>50</sub>	8.95 ± 0.3	55.6 ± 2.2	20.1 ± 0.9	355 ± 16
(40)	D <sub>37</sub>	110 ± 2.8	380 ± 13	275 ± 8.5	>500
	D <sub>50</sub>	18.4 ± 0.5	50.4 ± 1.7	36.5 ± 1.1	166 ± 7.1
(44)	D <sub>37</sub>	17.6 ± 0.8	40.3 ± 1.6	33.1 ± 1.3	80.9 ± 3.6
	D <sub>50</sub>	3.17 ± 0.1	6.88 ± 0.3	5.06 ± 0.2	10.0 ± 0.5
(48)	D <sub>37</sub>	40.1 ± 1.6	155 ± 6.2	115 ± 5.4	>500
	D <sub>50</sub>	6.75 ± 0.3	22.3 ± 0.9	10.1 ± 0.5	201 ± 6.0
(51)	D <sub>37</sub>	189 ± 5.1	731 ± 25	391 ± 11	>500
	D <sub>50</sub>	29.9 ± 0.8	108 ± 3.7	57.6 ± 1.7	719 ± 22

- Cell line of lowest resistance to drug of interest
- Cell line of highest resistance to drug of interest

**Table 16:** D<sub>37</sub> and D<sub>50</sub> values in μM (for compounds (4), (6), (8), (11), (12), (22), (23), (36), (40), (44), (48) and (51)) Against Various Cell Lines. D<sub>37</sub>: the dose required to reduce cell survival to 37%. D<sub>50</sub>: the dose required to reduce cell survival to half.

The results in Table 16 demonstrate the following:

- (a) 4-Aminophenethyl bromide hydrochloride (ie. Compound (4)) is the most potent of all of the compounds synthesized, including the more complex non-covalent subunit containing compounds (ie. (36), (40), (44), (48) and (51)).

- (b) The bisalkylating compound **(44)** shows marked potency toward HeLa cells, but less than that of 4-aminophenethyl bromide **(4)**;
- (c) The amide containing compounds **(11)** and **(12)** show remarkably poor cytotoxicity against all cell lines as expected;
- (d) Compounds **(36)**, **(40)** and **(51)** displayed diminished cytotoxicity to all cell lines tested relative to the simple monoalkylating analogue **(6)**. Compound **(36)** displayed enhanced cytotoxicity to all cell lines tested relative to its structural analogue **(40)**.
- (e) Compound **(48)** also showed similar cytotoxicity toward HeLa, MM96L and MM418c5 cells when compared to the monoalkylating compound **(6)** but enhanced cytotoxicity toward NFF when compared to **(6)**.
- (f) All of the compounds exhibited specificity toward HeLa relative to the other cell lines tested;
- (g) All compounds show markedly diminished cytotoxicity toward the NFF cell line when compared to that shown toward HeLa, MM418c5 and MM96L;

The marked differences in potency between the above compounds can be explained as follows:

- (a) 4-Aminophenethyl bromide hydrochloride **(4)** exhibits enhanced potency toward tumor cells when compared to that of its hydroxyl counterpart. This can be attributed to the enhanced electron donating ability of the amine nitrogen relative to that of the hydroxyl oxygen, enabling superior DNA alkylating capabilities by virtue of  $Ar_{1-3}$  participation.
- (b) The bisalkylating compound **(44)** displays enhanced cytotoxicity when compared to that of the simpler monoalkylating compound 4-aminophenethyl chloride **(6)**, but diminished activity relative to **(4)**. It is proposed that this compound reacts with DNA in a similar fashion to Bizelesin through the formation of interstrand crosslinks within DNA and subsequent cessation of the DNA replication process, thereby making it a potent cytotoxic compound. Given this data, the bromide derivative of **(44)** is hypothesized to exhibit ever greater cytotoxicity than the simple monoalkylating compound **(4)**, however its synthesis and isolation was not achieved due to the formation of polymer product during the reaction.

- (c) As expected, the amide compounds **(22)** and **(23)** exhibited decreased activity. While a limited degree of alkylation may have occurred via an S<sub>N</sub>2 reaction, DNA alkylation by virtue of Ar<sub>1-3</sub> participation is retarded due to the limited electron donating ability of the amide nitrogen, thereby resulting in diminished cytotoxicity.
- (d) Compound **(36)** exhibits enhanced cytotoxicity relative to its structural analogue **(40)**. The only structural difference between these two molecules is the placement of the pyridine nitrogen, the positioning of which in compound **(36)** may serve to provide additional stabilization in the DNA groove.
- (e) Tumor cells generally have a greater proportion of cells in active cell division compared with normal cells. Tumor cells which are actively undergoing the cell cycle are more susceptible to alkylating compounds as the DNA in such cells is relatively exposed during cell division.<sup>8</sup> The enhanced proliferative rate, along with the highly permeable vasculature of tumor cells explains the preferential activity of the DNA alkylating compounds tested toward HeLa, MM96L and MM418c5 when compared to the normal neonatal foreskin fibroblast (NFF) cell line.<sup>28-30</sup> That is, the DNA of the tumor cell lines is more accessible to the reactive alkylating compounds tested, rendering them more susceptible to alkylation and hence cell death.

To summarise, of the compounds tested, 4-aminophenethyl bromide **(4)** shows the most promise as an antitumor agent due to its potent cytotoxicity against tumor cells relative to a normal cell line *in vitro* and ease of synthesis.

#### **4.5 REFERENCES**

1. Smith, H. J and Williams, H. *Introduction to the Principles of Drug Design (3<sup>rd</sup> ed.)*. Harwood Academic Publishers, Sydney, 1998, 367-369.
2. Kumar, V., Cotran, R. S., Robbins, S. L. *Basic Pathology(5<sup>th</sup> ed.)*. W. B. Saunders Company, Philadelphia, 1992, 219-226.
3. Australian Cancer Council Website (About Cancer):  
<http://www.cancer.org.au/AboutCancer/CancerTypes.htm>, Date Accessed: 15/01/2008.
4. Jemal, A., Tiwari, R., Murray, T., Ghafour, A., Samuels, A., Ward, E., Feuer, E. J., Thun M. J. *CA*, **2004**, 54(1), 8-29.
5. Parkin, D. M. *Lancet Onc.*, **2001**, 2(9), 533-543.
6. Dossus, L. and Kaaks, R. *Clin. Endocrinology & Met.*, **2008**, 22(4), 551-571.
7. Navarro-Alarcon, M. and Cabrera-Vique, C. *Sc. Total. Env.*, **2008**, 400(1-3), 115-141
8. Nasterlack, M. *Int. J. Hyg. Env. Health*, **2007**, 210(5), 645-657.
9. Ceschi, M., Gutzwiller, F., Moch, H., Eichholzer, M., Probst-Hensch, N. M. *Swiss Med. Weekly*, **2007**, 137(3/4), 50-56.
10. Cowey, S., Hardy, R. W. *Am. J. Path.*, **2006**, 169(5), 1505-1522.
11. Adhami, V. M., Aziz, M. H., Ahmad, N., Mukhtar, H. *Phytopharm. Can. Chemoprev.*, **2005**, 389-426.
12. Hecht, Stephen S. *Env. Mol. Mut.*, **2002**, 39(2/3), 119-126.
13. Rajski, J. and Williams, H. *Chemical Reviews*, **1998**, 98(8), 2726 – 2795.
14. Yang, X. and Wang, A. *Pharm. Therapeutics*, **1999**, 83, 181 – 215.
15. Smith, H. and Williams, H. *Introduction to the Principles of Drug Design (3<sup>rd</sup> ed.)*. Harwood Academic Publishers, Sydney, **1998**, 166 – 194.
16. Alberts, B, Bray, D., Lewis, J., Raff, M., Roberts, K., Watson, J. D. *Molecular biology of the Cell (3<sup>rd</sup> ed.)*. Garland Publishing Inc., New York, **1994**, 401-409.
17. Campbell, N. A. *Biology (3<sup>rd</sup> ed.)*. The Benjamin/Cummings Publishing Company Inc., California, 1993, 171-215.
18. Papageorgiou, C., Camenisch, G., Borer, X. *Bioorg. Med. Chem. Lett.*, **2001**, 11, 1549-1552.
19. Goes, F. S. and Martin, J. *Eur. J. Biochem.*, **2001**, 268(8), 2281-2289.

20. Nakanishi, M., Ando, H., Watanabe, N., Kitamura, K., Ito, K., Okayama, H., Miyamoto, T., Agui, T., Sasaki, M. *Genes to Cells*, **2000**, 5, 839-847.
21. Rang, H. P., Dale, M. M., Ritter, J. M. *Pharmacology (3<sup>rd</sup> ed)*. Churchill Livingstone, Edinburgh, **1995**, 696-717.
22. <http://www.biotech.ist.unige.it/cldb/cname-lc.html>, Date Accessed: 27/03/2005.
23. <http://crisp.cit.nih.gov/theasaurus/index.htm>, Date Accessed: 29/03/2005.
24. Evans, G. *Chem. Biol.*, **1994**, 1, 137-141.
25. Gambhir, S. S., Barrio, J. R., Herschman, H. R., Phelps, M. E. *Nuclear Med. Biol.*, **1999**, 26, 481-490.
26. White, R. H., Parsons, P. G., Prakash, A. S., Young, D. J. *Bioorg. Med. Chem. Lett.*, **1994**, 5(16), 1869-1874.
27. Shalders, R. L., Blanch, G., Brown, C. L., Prakash, A. S., Young, D. J. *Chem. Biol. Interact.*, **1999**, 117(1), 83-94.
28. Nugent, L. J. and Jain, R. K. *Cancer Res.*, **1995**, 55, 3552-3756.
29. Maeda, H. A. *A Polymeric Site-Specific Pharmacotherapy*. J. Wiley, New York, **1994**, 95-116.
30. Yuan, F., Dellian, M., Fukumura, D., Leunig, M., Berk, D. A., Torchilin, V. P., Jain, R. K. *Cancer Res.*, **1995**, 55, 3552-3756.

## **CHAPTER 5 – FURTHER PRELIMINARY BIOLOGICAL STUDIES – RESULTS AND DISCUSSION**

### **5.1 REPORTER ASSAYS**

The sequence selectivity of DNA alkylating compounds is an important consideration in cancer therapeutics. Previous DNA alkylation studies that were conducted by Shalders *et al.*<sup>1</sup> involved the observation of AT and CG rich DNA that had been incubated with 4-aminophenethyl halide. The fragmentation of the DNA observed on polyacrylamide gel demonstrated that 4-aminophenethyl bromide exhibited specificity for AT rich sequences of DNA, alkylating in a similar fashion to CC-1065 at the N7 of adenine. Molecular modeling by the same author supported this observation and confirmed that steric repulsion, groove width and non-covalent interactions all played key roles in the binding and stabilization of 4-aminophenethyl halide in the AT rich minor groove.

In order to substantiate these previous studies a further method of investigation employing  $\beta$ -galactosidase assays was utilized. The CPR- $\beta$ -galactosidase and pOct-Luciferase assays were used to probe for specificity toward AT and CG rich DNA sequences respectively. These assays were chosen for their simplicity and low inter-assay variation<sup>2-5</sup> Furthermore, neither required the use of radioactive labelling, were less labor intensive, and relatively fast and inexpensive when compared to other reporter assays (i.e. chloramphenicol acetyl transferase (CAT))<sup>6,7</sup>

#### **5.1.1 Probing for AT selectivity: The $\beta$ -Galactosidase reporter Assay –**

The  $\beta$ -Galactosidase reporter assay utilized MM96L cells that had been transfected (infected) with a recombinant, replication defective adenovirus. The adenoviral genome contained the gene *lacZ* which encodes for  $\beta$ -galactosidase, an enzyme that can be quantified colourimetrically at 680 nm. The  $\beta$ -galactosidase gene was flanked by an AT rich cytomegalovirus enhancer-promoter (Figure 62) that regulates the transcription of the  $\beta$ -galactosidase gene.<sup>3</sup>

When determining whether the drugs of interest exhibit any specificity for either AT or CG rich DNA the following is assumed:

- (a) Compounds that show no AT sequence specificity will not bind to the cytomegalovirus enhancer-promotor and hence the  $\beta$ -galactosidase gene will be readily transcribed. The transcribed  $\beta$ -galactosidase will react enzymatically with CPRG upon its addition to the plate to produce a blue colouration that can be quantified colourmetrically.
- (b) Compounds which are AT sequence specific will inhibit transcription of the  $\beta$ -galactosidase gene at a magnitude correlating to their affinity for the AT rich cytomegalovirus enhancer-promotor. The decrease in levels of  $\beta$ -galactosidase levels results in diminished activity toward CPRG and hence lower absorbency readings.

Put simply, the higher the absorbancy readings obtained, the less specific the drug for AT rich sequences of DNA. Conversely, the lower the absorbancy readings obtained, the greater the specificity of the drug for AT rich DNA sequences.

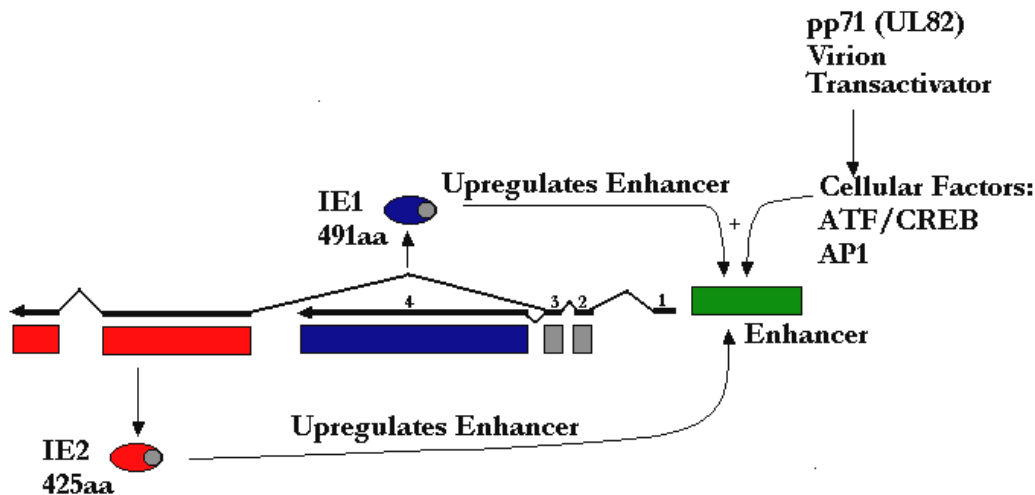


**Figure 62 – The CMV *ie1/ie2* Promoter-Enhancer Region Which Flanks the *lacZ* gene**

The transcription of the  $\beta$ -Galactosidase gene is dependent on the host cell's transcription machinery. The mechanism is as follows:

1. Following transfection of the MM96L cells by adenovirus, several virion proteins (ie. pp71), together with host cellular factors initiate the transcription of the *ie1/ie2* promoter-enhancer region (Figure 62), resulting in the production of the proteins IE1<sub>491aa</sub>, IE2<sub>425aa</sub> and IE2<sub>579aa</sub>.<sup>3,8</sup>
2. The IE1<sub>491aa</sub> and IE2<sub>425aa</sub> proteins act to upregulate the *ie1/ie2* enhancer and initiate transcription of the  $\beta$ -Galactosidase gene.

Given the above information, the transcription of  $\beta$ -Galactosidase can be inhibited by either:

- (i) binding of the drug to the AT rich promoter enhancer,
- (ii) direct binding of the drug to the lacZ gene, **or**
- (iii) binding of the drug to the genes responsible for the expression of the enhancer proteins (IE1 and IE2).

In order to probe for AT selectivity **(4)**, **(6)**, **(22)**, **(43)** and **(44)** were incubated at 37°C with viral infected MM96L cells for 3 days. After this time, CPRG reagent was added to each of the 96 well plates, which were then incubated for a further 30 minutes at 37°C. The intensity of the blue colouration from reaction of the CPRG with  $\beta$ -galactosidase, is indicative of the amount of  $\beta$ -galactosidase transcribed in the cell. That is, the greater the level of  $\beta$ -galactosidase in the cell, the greater the intensity of the colour. In order to quantitate the level of transcription, the absorbance of each well was read at 680 nm on a BioRad microplate reader 3550. The cellular survival of each sample was also measured at this timepoint using the SRB method described in Chapter 4 in order to determine whether or not any decrease in  $\beta$ -galactosidase transcription resulted from a decrease in cell number. The results were graphed as percentage of control versus log concentration ( $\mu$ M) (Figures 63 – 67, Table 17).

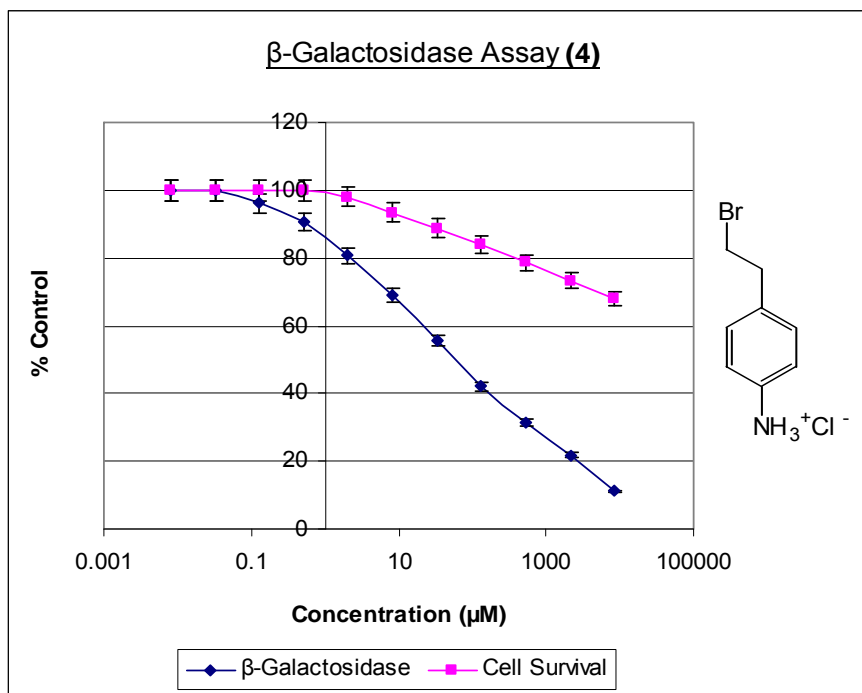


*Figure 63 – Plot of  $\beta$ -Galactosidase Production (% Control) Versus Concentration of (4) ( $\mu\text{M}$ ) in MM96L Cells.*

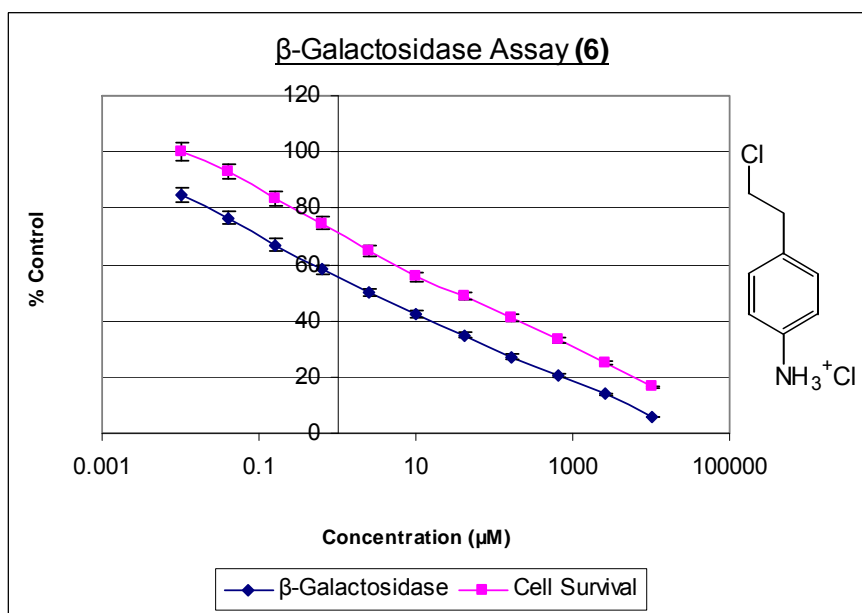


*Figure 64 – Plot of  $\beta$ -Galactosidase Production (% Control) Versus Concentration of (6) ( $\mu\text{M}$ ) in MM96L Cells.*

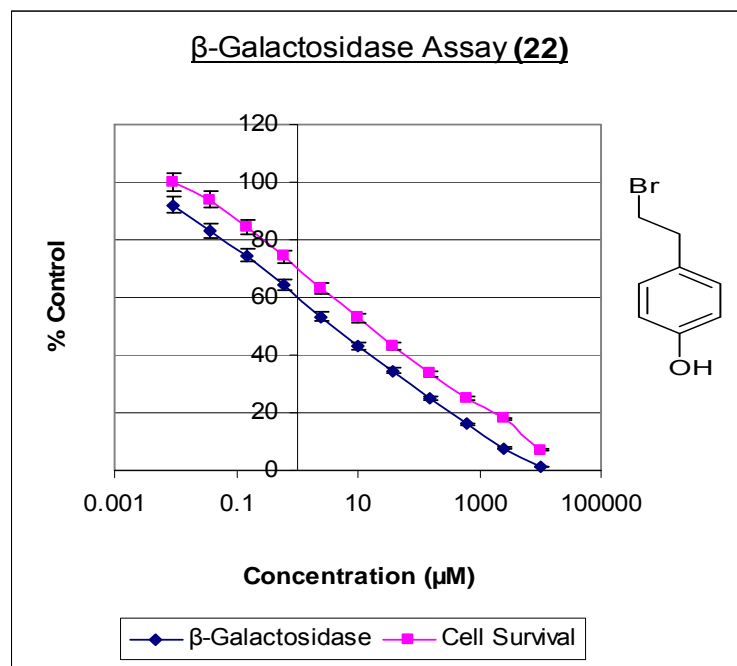


*Figure 65 – Plot of  $\beta$ -Galactosidase Production (% Control) Versus Concentration of (22) ( $\mu\text{M}$ ) in MM96L Cells.*

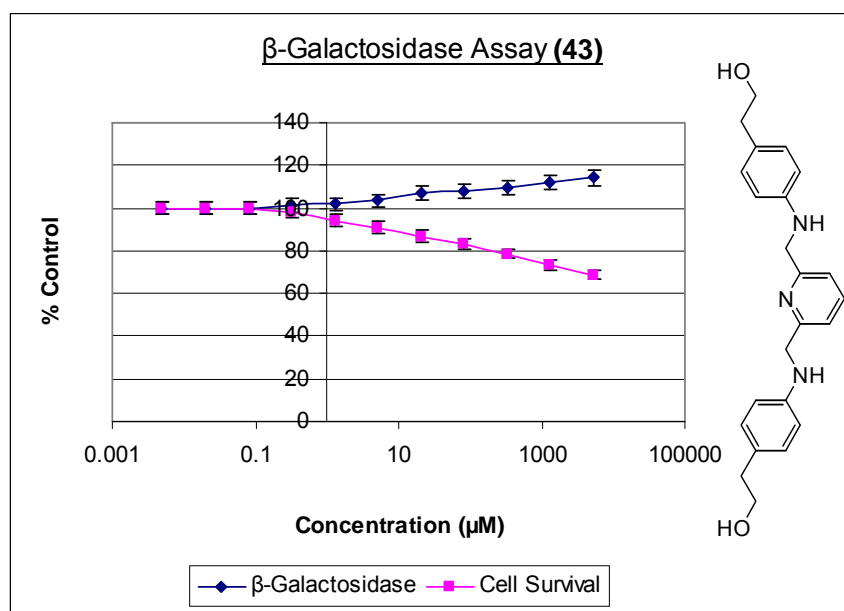


*Figure 66 – Plot of  $\beta$ -Galactosidase Production (% Control) Versus Concentration of (43) ( $\mu\text{M}$ ) in MM96L Cells.*

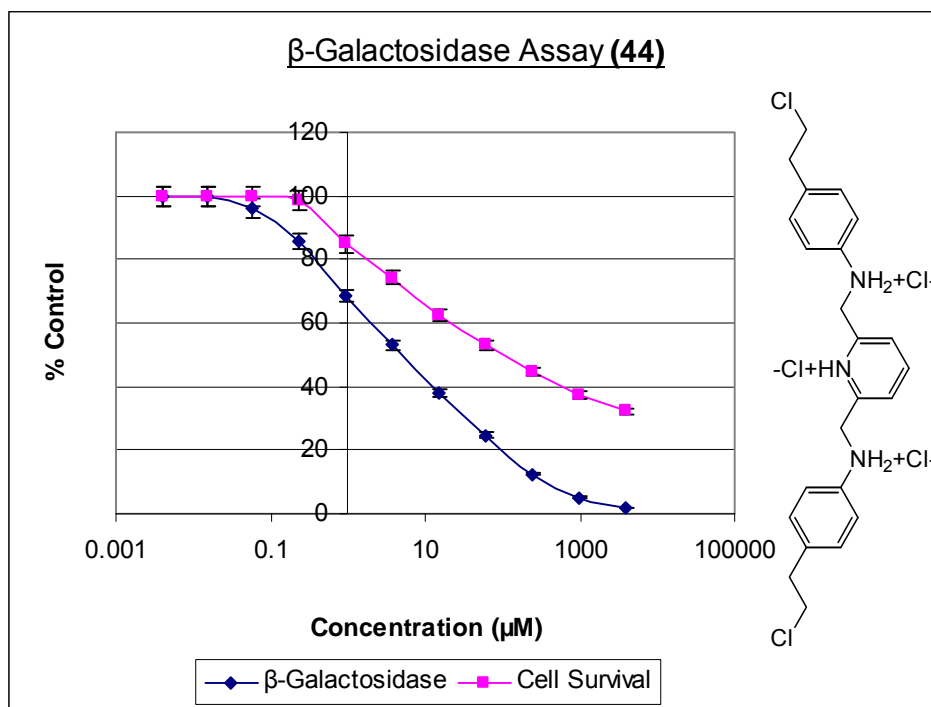


**Figure 67 – Plot of  $\beta$ -Galactosidase Production (% Control) Versus Concentration of (44) ( $\mu\text{M}$ ) in MM96L Cells.**

Compound	Cell Survival		$\beta$ -Galactosidase	
	Rate of Cell Decline (Gradient)	ID <sub>50</sub> ( $\mu\text{M}$ )	Rate of Cell Decline (Gradient)	ID <sub>50</sub> ( $\mu\text{M}$ )
(4)	2.43	>500	7.03	55.3 $\pm$ 1.8
(6)	6.06	30.3 $\pm$ 0.9	5.65	4.92 $\pm$ 0.2
(23)	6.86	19.2 $\pm$ 0.6	6.75	4.81 $\pm$ 0.1
(43)	2.39	>500	-1.09	>500
(44)	5.72	181 $\pm$ 5.4	8.39	7.06 $\pm$ 0.2

**Table 17:** ID<sub>50</sub> values ( $\mu\text{M}$ ) and relative rate of cellular decline as compared to the rate of  $\beta$ -galactosidase decline. These values are calculated from the line of best fit.

The results can be summarized as follows:

- (a) Compounds **(4)** and **(6)** elicit an appreciable decline in the transcription of the  $\beta$ -Galactosidase enzyme in adenoviral infected MM96L cells. This decline becomes even more marked as the drug concentration increases.
- (b) The decline in transcription of the  $\beta$ -Galactosidase enzyme observed for incubation with compound **(4)** cannot be explained by decreases in cell number. The relative rate of decline in  $\beta$ -galactosidase (Gradient=-7.03) is markedly higher than the rate of decline in cell number (Gradient=-2.43) (Table 17).
- (c) The decline in transcription of the  $\beta$ -Galactosidase enzyme observed for incubation with compound **(6)** cannot be explained by decreases in cell number. The relative rate of decline in  $\beta$ -galactosidase (Gradient=-5.65) is greater than the rate of decline in cell number (Gradient=-6.06) (Table 17).
- (d) Compound **(22)** appears to affect a reduction in the transcription of the  $\beta$ -Galactosidase enzyme. However, this can be correlated with a decline in cell numbers. The relative rate of decrease of cell number (Gradient=-6.86) corresponds to that of the relative rate of decline in  $\beta$ -galactosidase transcription (Gradient=-6.74).
- (e) Compound **(43)** affected an increase in the production of  $\beta$ -galactosidase at each concentration used. (Figure 66).
- (f) The decline in transcription of the  $\beta$ -Galactosidase enzyme observed for incubation with compound **(44)** cannot be explained by decreases in cell number. The relative rate of decline in  $\beta$ -galactosidase (Gradient=-8.39) is greater than the rate of decline in cell number (Gradient=-5.72) (Table 17).

The following observations can be made with respect to these results:

- (a) Compounds **(4)**, **(6)** and **(44)** exhibit specificity toward AT rich sequences of DNA. This correlates with the results obtained from prior research that was conducted by Shalders *et al.*<sup>1</sup>
- (b) Surprisingly, 4-hydroxyphenethyl chloride **(22)** did not exhibit any AT sequence selectivity as observed for its amine counterpart **(6)**;

- (c) It is unclear why an increase in production of  $\beta$ -Galactosidase should occur on incubation with compound (43). It may be that this compound binds to the crs region (Figure 67). Given that the gene product IE2<sub>579aa</sub> contributes to the repression of  $\beta$ -galactosidase transcription by binding to the crs region of the promoter-enhancer (Figure 67),<sup>3</sup> the binding of drug to either the crs region, or the IE2<sub>579aa</sub> protein would block this repression, resulting in an increase in  $\beta$ -galactosidase transcription.<sup>3</sup>

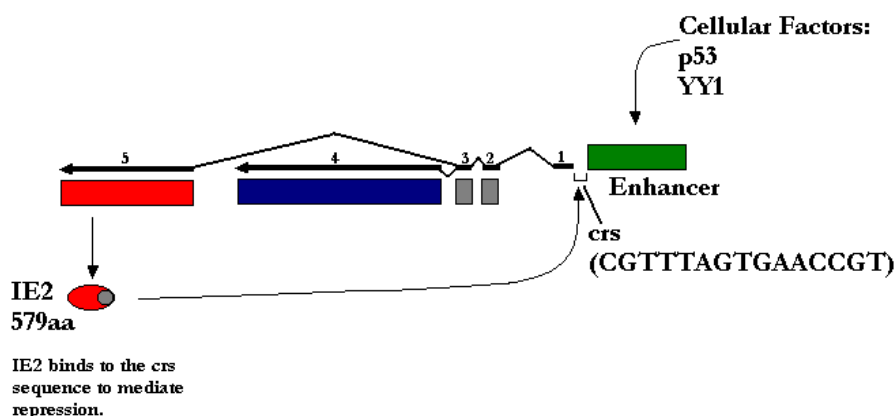


*Figure 67 – Repression of IE1/IE2 Gene Expression*

### 5.1.2 Probing for CG selectivity: The Luciferase reporter Assay –

In order to determine whether the drugs of interest demonstrated specificity towards CG rich DNA sequences the luciferase (LUC) reporter assay was utilized.<sup>7,5</sup> The advantage of this assay over similar reporter assays is that the results are not affected by cell storage time, baseline expression of undamaged plasmids or expressions of damaged plasmids and as such, the LUC assay is not affected by variation in transfection efficiencies.<sup>7</sup>

Similar to the  $\beta$ -galactosidase reporter assay, the LUC assay utilizes a recombinant, replication defective adenovirus which was transfected into MM96L cells. The recombinant genome contains the gene for luciferase, an enzyme that can be quantified colourmetrically at 680nm, and is similarly flanked by a cytomegalovirus immediate promoter and enhancer.<sup>7</sup>

This assay assumes that:

- (a) Compounds lacking CG sequence specificity will not bind to the cytomegalovirus enhancer-promotor and hence the luciferase gene will be readily transcribed. The luciferase will react enzymatically with luciferin substrate upon its addition to the plate to produce an orange colouration, the luminosity of which can be quantified in terms of light units (counts/second).
- (b) Compounds which are CG sequence specific will inhibit transcription of the luciferase gene to a magnitude correlating to their affinity for the CG rich cytomegalovirus enhancer-promotor. The decrease in levels of luciferase will result in diminished activity toward luciferin and hence lower counts/second.

Compounds **(4)**, **(6)**, **(22)**, **(43)** and **(44)** were diluted in triplicate and incubated with MM96L cells for 3 days. Luciferin substrate (see Appendix 1) was used to quantify the amount of luciferase transcribed and the results were graphed as percentage of control versus concentration (Figures 68 – 72, Table 18).

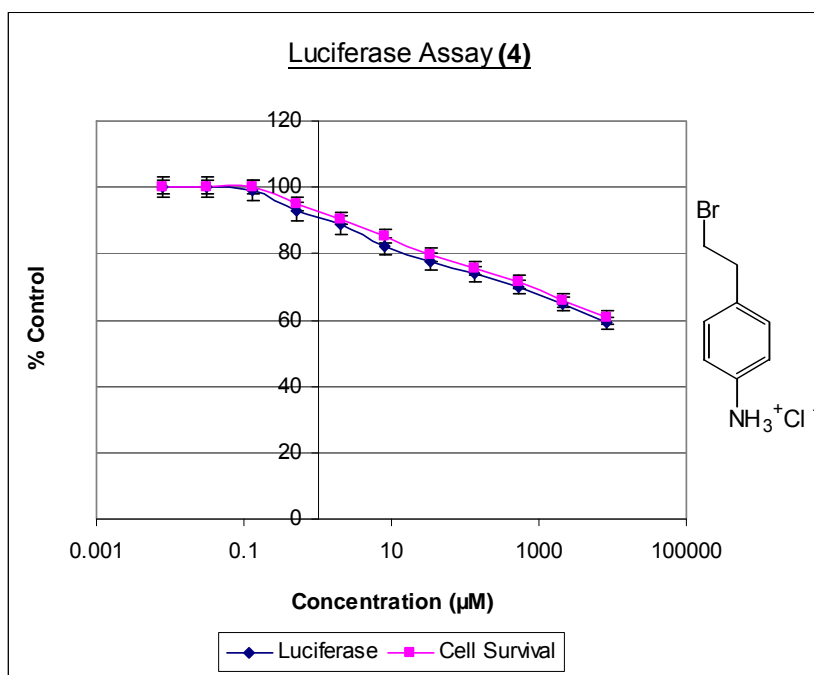


**Figure 68 – Plot of Luciferin Production (% Control) Versus Concentration of (4) ( $\mu\text{M}$ ) in MM96L Cells.**

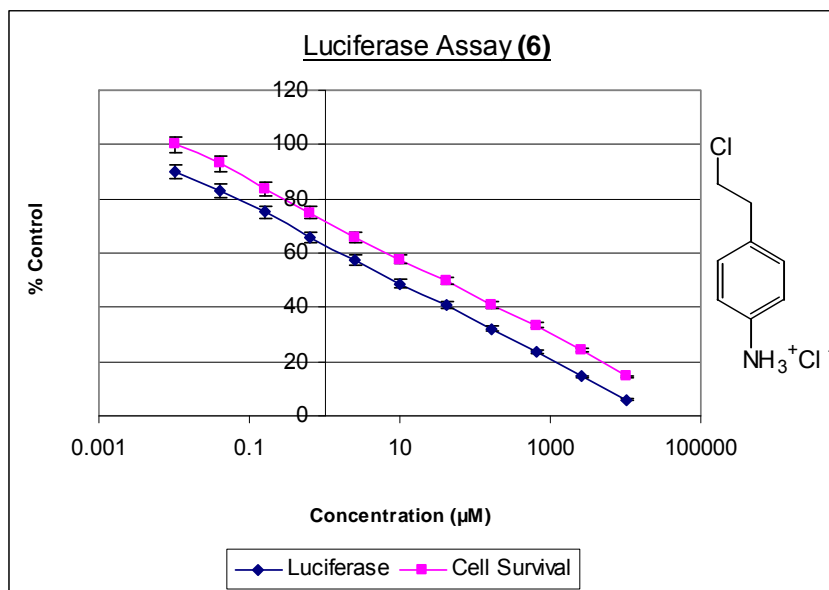


*Figure 69 – Plot of Luciferin Production (% Control) Versus Concentration of (6) (µM) in MM96L Cells.*

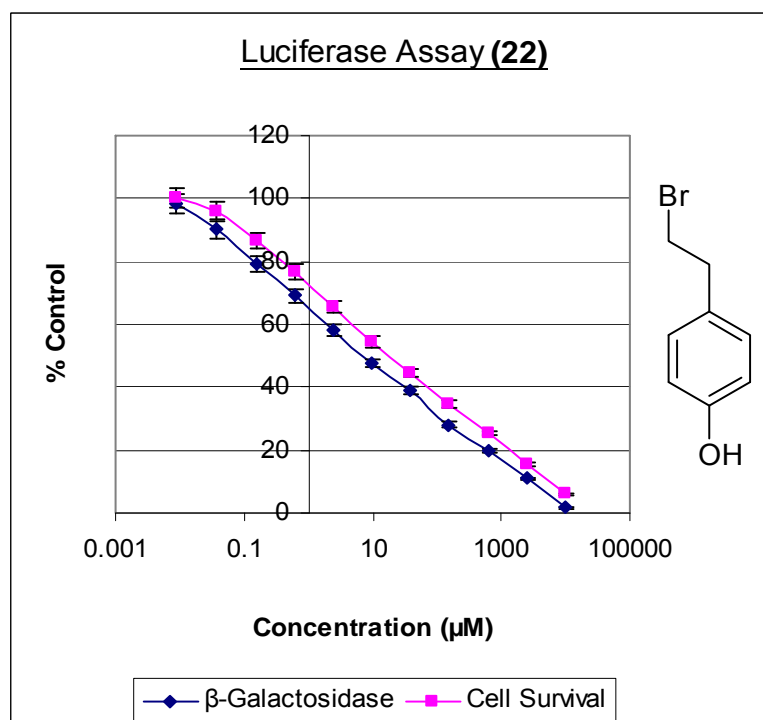


*Figure 70 – Plot of Luciferin Production (% Control) Versus Concentration of (22) (µM) in MM96L Cells.*

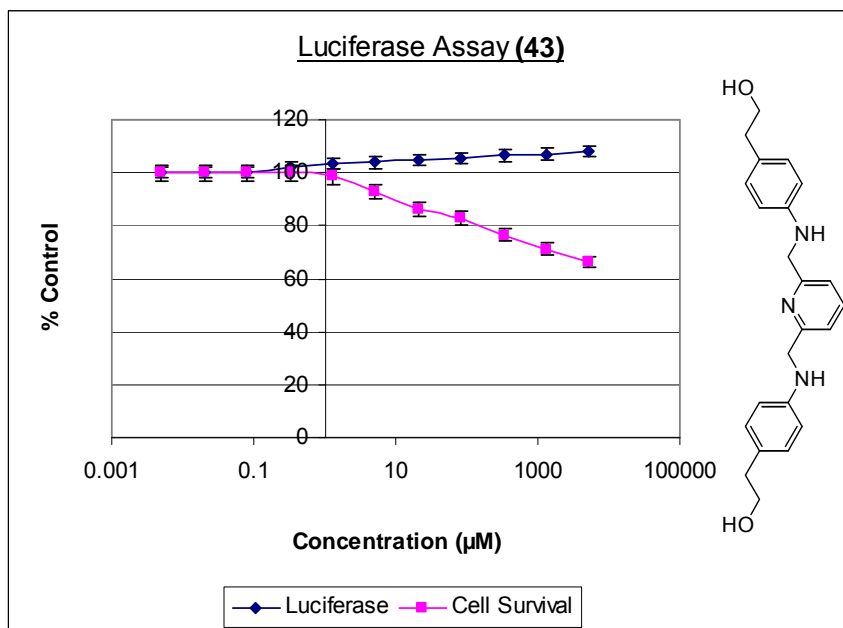


*Figure 71 – Plot of Luciferin Production (% Control) Versus Concentration of (43) (µM) in MM96L Cells.*

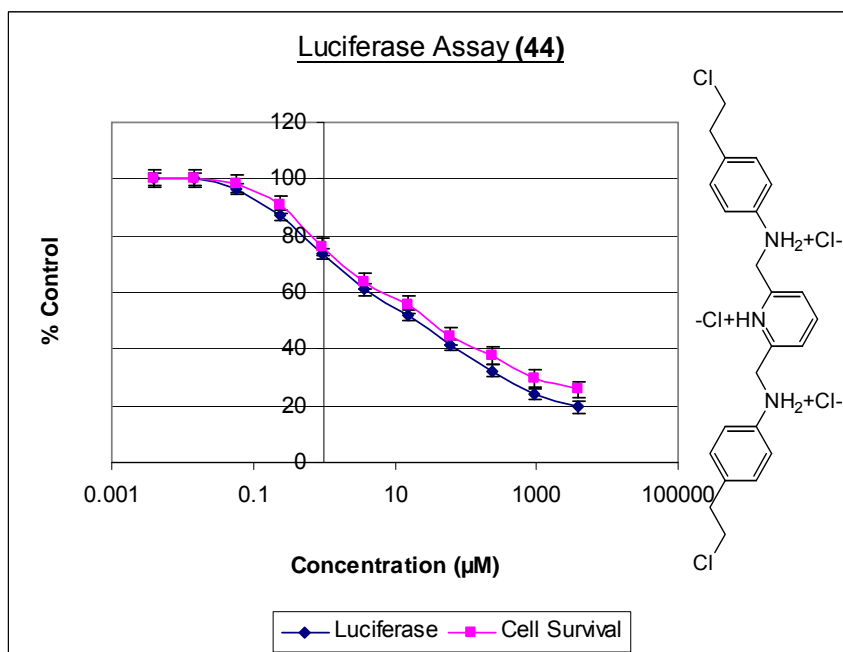


*Figure 72 – Plot of Luciferin Production (% Control) Versus Concentration of (44) (µM) in MM96L Cells.*

Compound	Cell Survival		Luciferase	
	Rate of Cell Decline (Gradient)	ID <sub>50</sub> (μM)	Rate of Cell Decline (Gradient)	ID <sub>50</sub> (μM)
<b>(4)</b>	3.06	>500	3.15	>500
<b>(6)</b>	6.15	46.3 ± 1.4	6.12	10.2 ± 0.3
<b>(23)</b>	7.08	20.2 ± 0.7	7.06	10.1 ± 0.4
<b>(43)</b>	2.63	>500	-0.62	>500
<b>(43)</b>	6.23	58.2 ± 1.7	6.66	58.2 ± 1.9

**Table 18:** ID<sub>50</sub> values (μM) and relative rate of cellular decline as compared to the rate of Luciferase decline.

These values are calculated from the line of best fit.

These results can be summarized as follows:

- (a) Compounds **(4)**, **(6)** and **(22)** elicit an appreciable decline in the transcription of the luciferase enzyme in adenoviral infected MM96L cells which becomes even more marked as the drug concentration increases. This apparent decrease can however, be attributed to a decline in cell number. In each case, the relative rate of decrease of cell number corresponds to the relative rate of decline in luciferase transcription (Table 18).
- (b) Compound **(43)** affected an increase in the production of luciferase (Figure 71). Initial cytotoxicity studies with these compounds showed **(43)** to have limited alkylation capability. This increased transcription may, therefore, be attributed to the noncovalent interaction of drug with genes or proteins that are normally involved in the repression of transcription.
- (c) The decline in transcription of Luciferase observed with incubation of compound **(44)** cannot be explained by decreases in cell number. The relative rate of decline in Luciferase (Gradient=-6.66) is slightly greater than the rate of decline in cell number (Gradient=-6.23) (Table 18). Compound **(44)** may display very limited specificity for CG rich sequences of DNA.

## **5.2 DRUG STABILITY**

There are many factors that influence the oral bioavailability of a compound, including aqueous solubility and stability.

### **5.2.1 Compound Solubility –**

Poor aqueous solubility is likely to result in absorption problems. Absorption across the intestine is proportional to the concentration gradient of the drug between the intestinal lumen and the blood.<sup>9</sup> There are two methods which are commonly used to enhance bioavailability in this respect:

- (i) The formulation of a drug with a vehicle that enhances its delivery to the targeted site.
- (ii) The conversion of groups such as amines and carboxylic acids into water soluble salts. Each of the amine compounds synthesized in this study were converted to the corresponding hydrochlorides. Compounds that were insoluble in medium (ie. those lacking an amine group) were dissolved in a solution of 1%DMSO/medium before testing.

While it is possible to fine-tune the solubility of compounds *in vivo* using the method's described above, there are limits to what can realistically be achieved.

Lipinski's rule of five states that drug-like compound possess  $\leq 5$  hydrogen bond donating groups,  $\leq 10$  hydrogen bond accepting groups, have a molecular weight  $\leq 500$  and a  $\log P \leq 5$ .<sup>9,10</sup> Compounds which do not meet at least two of these criteria are generally not viable as drugs due to either problems associated with permeability, or the possession of groups which act as substrates for transporters that actively passage the compounds across a membrane.<sup>9</sup> This model has been enhanced to include filters that limit the number of rotatable bonds or the molecules polar surface area.<sup>10</sup> Of the compounds tested in this study, all satisfied at least three out of four of the "Rule of Five" criteria, indicating that they possess "drug-like" qualities.

### **5.2.2 Compound Stability –**

While the "Rule of Five" and other similar prognostic models are useful for predicting the bioavailability of drugs, a compound is of no value if it is found to be unstable under the conditions employed. Solvolytic stability (i.e. stability of the compound *en route* to the target) is

an important point to consider in the design of DNA alkylating antitumor compounds. One of the most common dilemmas within this group of compounds is their removal from solution (i.e. either culture medium *in vitro* and blood *in vivo*) by reaction with nucleophiles, *viz.* non-productive solvolysis. A degree of fine-tuning in drug functionality is required to maintain an appropriate balance between reactivity and stability.

### 5.2.3 Assessment of Drug Stability Following Incubation with Various of Nucleophiles

In order to assess their stability, compounds (4) and (6) were exposed to a panel of nucleophiles, generally found both *in vitro* or *in vivo*. Each compound was incubated (37°C) at three different concentrations with various nucleophiles for 1.5 hours, 3 hours and 6 hours. Following incubation, each of the samples (drug + nucleophile) were added in quadruplicate to 96 well plates containing MM96L cells, at the concentrations shown in Figures 72 - 77. The plates were then incubated at 37°C for two hours.

The plates were subsequently washed with PBS and fixed and stained with sulforhodamine B, a commonly used cell stain. Figures 73 – 78 show only three time points because of the technical limitation of cultures cooling down and changes in pH (due to loss of CO<sub>2</sub>) upon removing the 96-well plate from the incubator in order to add the next dose of drug. It was thus not possible to add drugs more frequently during the informative time period of drug decomposition without significantly disturbing reaction conditions. Nor was it necessary at this stage to more closely resolve the time course, due to the large differences in stability that were found between compounds.

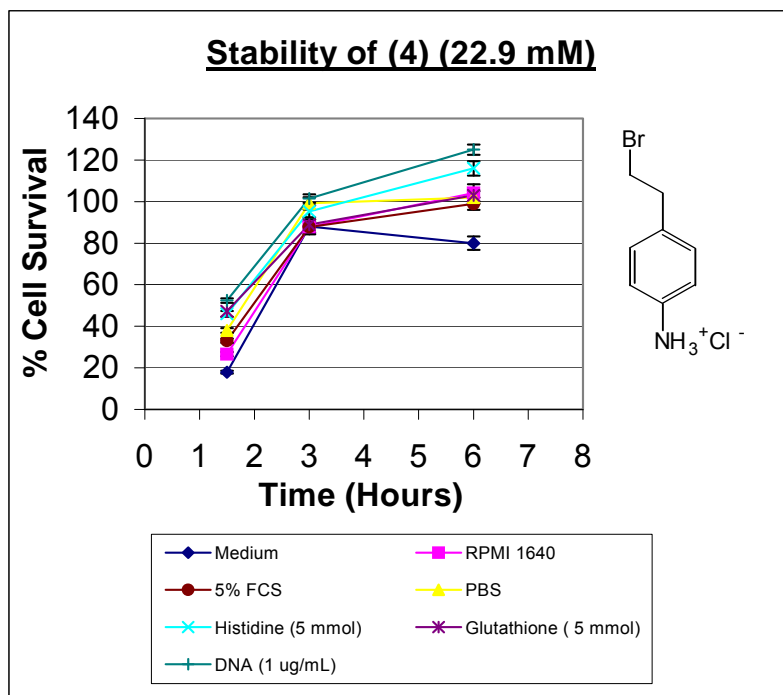


*Figure 73 – Graph of % Cell Survival Versus Time of Incubation of (4) (at 22.9 mM) with Various Nucleophiles.*

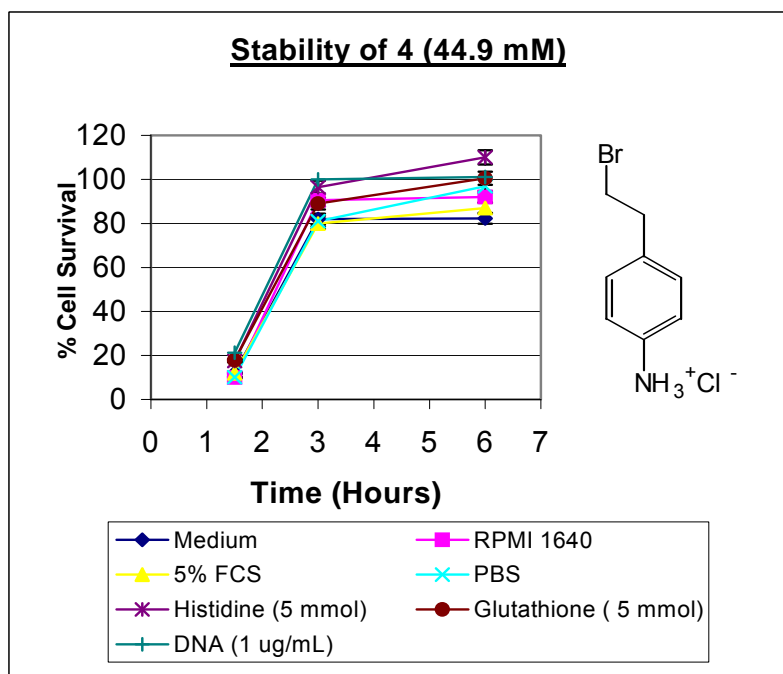


*Figure 74 – Graph of % Cell Survival Versus Time of Incubation of (4) (at 44.9 mM) with Various Nucleophiles.*

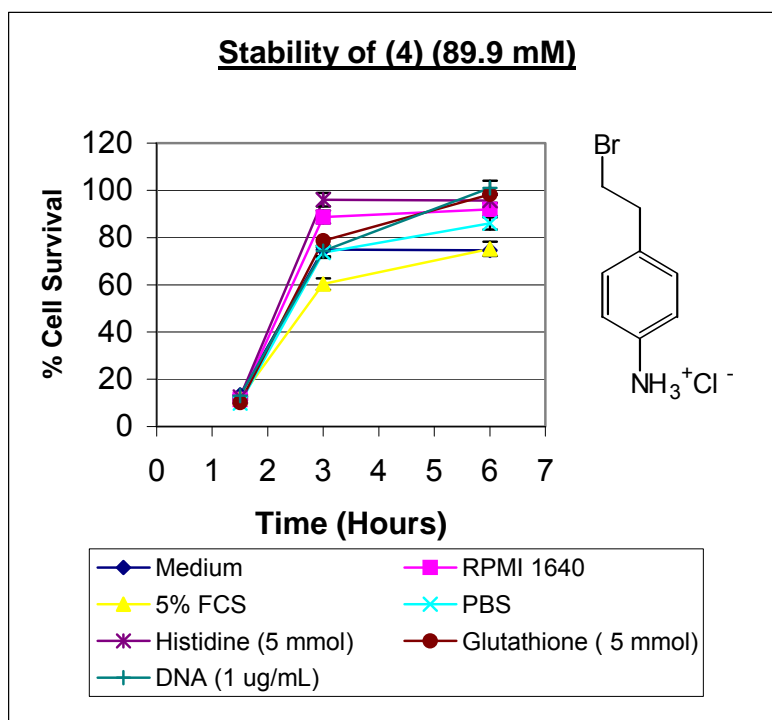


*Figure 75 – Graph of % Cell Survival Versus Time of Incubation with (4) (at 89.9 mM) with Various Nucleophiles.*

Nucleophiles	22.5 mM	44.9 mM	89.9 mM
Medium	17.9	12.1	13.5
RPMI	26.6	10.0	11.4
5% FCS	33.1	11.9	12.0
PBS	38.0	10.1	9.9
Histidine (5 mmol)	46.0	17.5	12.5
Glutathione (5 mmol)	47.2	17.9	10.2
DNA (1 µg/mL)	52.4	21.3	13.1

**Table 19:** Stability (% Cell Survival) of (4) Following a 1.5 hr Incubation with Various Nucleophiles

<b>Nucleophiles</b>	<b>22.5 mM</b>	<b>44.9 mM</b>	<b>89.9 mM</b>
Medium	88.0	82.0	75.0
RPMI	87.8	90.5	88.7
5% FCS	87.8	79.9	60.3
PBS	99.2	81.0	73.6
Histidine (5 mmol)	95.3	96.5	96.0
Glutathione (5 mmol)	89.0	89.0	78.6
DNA (1 µg/mL)	101.5	100.0	74.3

**Table 20:** Stability (% Cell Survival) of **(4)** Following a 3.0 hr Incubation with Various Nucleophiles

<b>Nucleophiles</b>	<b>22.5 mM</b>	<b>44.9 mM</b>	<b>89.9 mM</b>
Medium	80.0	82.3	74.6
RPMI	104.2	92.0	92.0
5% FCS	99.0	87.0	75.2
PBS	102.0	96.8	86.0
Histidine (5 mmol)	116.0	110.0	95.6
Glutathione (5 mmol)	103.0	100.5	98.2
DNA (1 µg/mL)	125.0	101.0	101.0

**Table 21:** Stability (% Cell Survival) of **(4)** Following a 6.0 hr Incubation with Various Nucleophiles

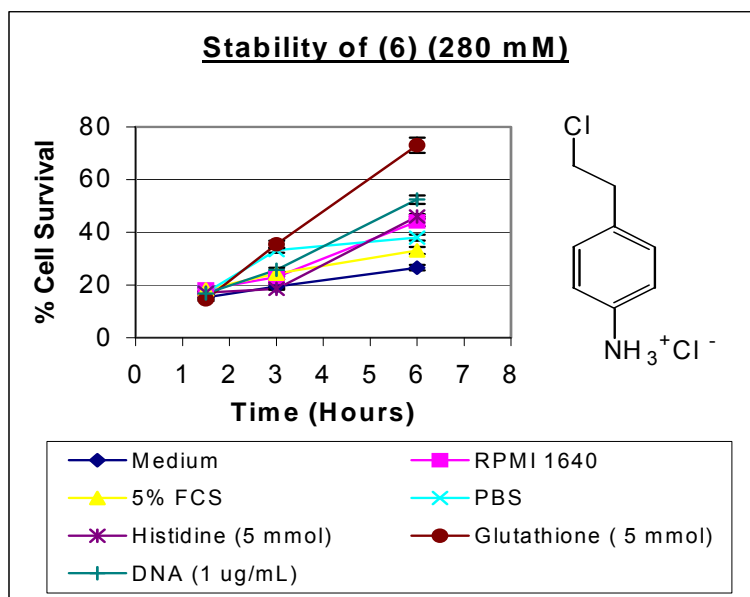


*Figure 76 – Graph of % Cell Survival Versus Time of Incubation with Compound (6) (280 mM) with Various Nucleophiles.*

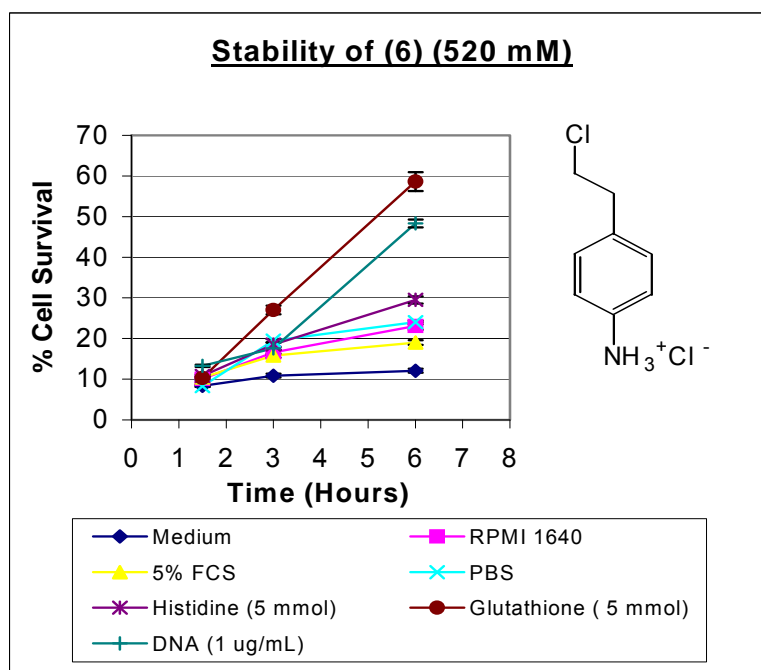


*Figure 77 – Graph of % Cell Survival Versus Time of Incubation with (6) (at 520 mM) with Various Nucleophiles.*

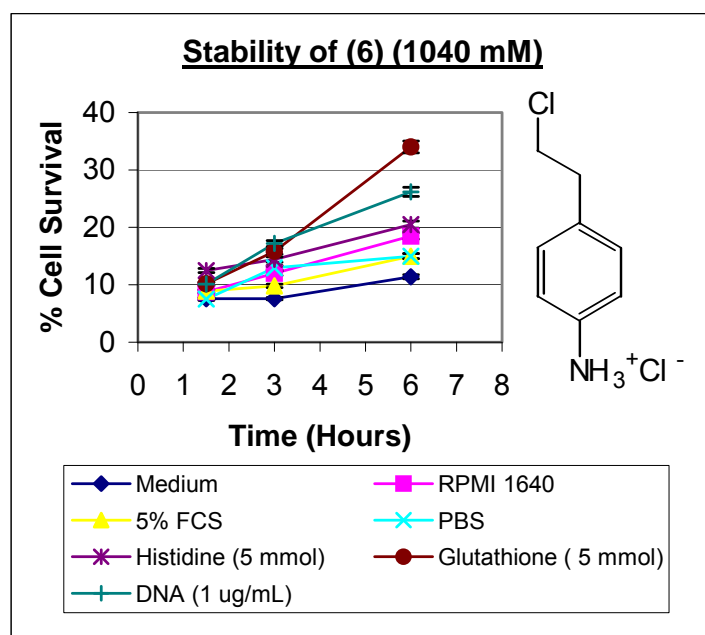


*Figure 78 – Graph of % Cell Survival Versus Time of Incubation with (6) (at 1040 mM) with Various Nucleophiles.*

Nucleophiles	280 mM	520 mM	1040 mM
Medium	15.3	8.4	7.6
RPMI	18.3	10.1	8.8
5% FCS	18.3	10.4	8.9
PBS	17.1	8.3	7.5
Histidine (5 mmol)	17.1	10.8	12.5
Glutathione (5 mmol)	14.6	10.3	10.2
DNA (1 µg/mL)	16.8	13.3	10.1

**Table 22:** Stability (% Cell Survival) of (6) Following a 1.5 hr Incubation with Various Nucleophiles

Nucleophiles	280 mM	520 mM	1040 mM
Medium	19.5	10.9	7.6
RPMI	23.0	16.6	12.0
5% FCS	24.3	15.8	9.8
PBS	33.2	19.5	13.0
Histidine (5 mmol)	18.6	18.5	14.4
Glutathione (5 mmol)	35.4	27.0	15.8
DNA (1 µg/mL)	25.8	17.6	17.2

**Table 23:** Stability (% Cell Survival) of (6) Following a 3.0 hr Incubation with Various Nucleophiles

Nucleophiles	280 mM	520 mM	1040 mM
Medium	26.6	12.1	11.4
RPMI	44.1	23.1	18.5
5% FCS	33.1	19.0	15.0
PBS	38.0	24.0	15.0
Histidine (5 mmol)	46.0	29.5	20.5
Glutathione (5 mmol)	73.0	58.6	34.0
DNA (1 µg/mL)	52.4	48.3	26.2

**Table 24:** Stability (% Cell Survival) of (6) Following a 6.0 hr Incubation with Various Nucleophiles

The results were as follows:

- (a) Compound **(4)** demonstrated considerable reactivity towards three of the nucleophiles in the order DNA>Glutathione>Histidine. This correlated with results obtained in the cell cytotoxicity assays.
- (b) Likewise, compound **(6)** demonstrated considerable reactivity toward the same three nucleophiles, although was less discriminating between the three, also corresponding with the results obtained in cell cytotoxicity assays.
- (c) Not surprisingly, MM96L cell survival increased as the drug-nucleophile incubation time was increased for both compounds **(4)** and **(6)**.

### **5.3 CELL CYCLE STUDIES**

Cells progress through an orderly sequence of events known as the cell cycle many times in a lifetime in order to grow and proliferate. The four phases of the mammalian cell cycle (Mitosis,  $G_1$ , S and  $G_2$ ) must be exactly coordinated in order for the cell to divide into two typically functioning daughter cells. The synchronization of this cycle is tightly regulated by the cyclin-CDK family of protein kinase complexes.<sup>11,12</sup>

#### **5.3.1 The Eukaryotic Cell Cycle –**

The cell cycle is a series of events that take place in a eukaryotic cell that lead to its replication. These events can be divided in two brief periods: interphase, during which the cell grows, accumulating nutrients needed for mitosis and duplicating its DNA, and the mitotic (M) phase, during which the cell splits itself into two distinct cells, often called "daughter cells".<sup>9,12,13</sup>

The cell cycle consists of four distinct phases:  $G_1$  phase, the DNA synthesis phase (ie. S phase) and  $G_2$  phase (collectively known as interphase) and M phase. The activation of each phase is dependent on the proper progression and completion of the previous one. Cells that have temporarily or reversibly stopped dividing are said to have entered a state of quiescence called  $G_0$  phase.

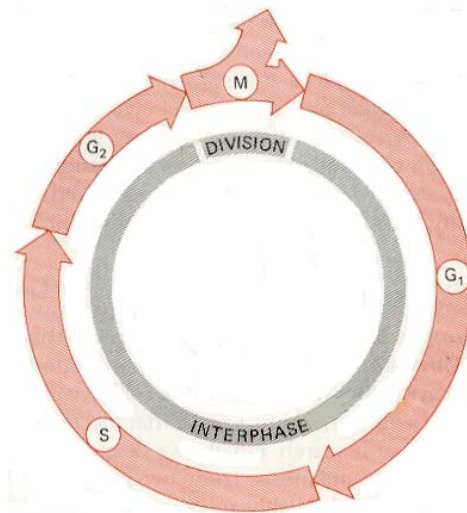


***Figure 79 – The Eukaryotic Cell Cycle (Taken From Reference 11)***

(I) M phase - The relatively brief M phase is composed of two tightly coupled processes: mitosis, in which the cell's chromosomes are divided between two daughter cells, and cytokinesis, in which the cell's cytoplasm divides resulting in two distinct cells.<sup>9,12</sup>

(II) Interphase - Following mitosis, the daughter cells enter into the beginning of a new cycle called interphase. Although the various stages of interphase (ie. G<sub>1</sub>, S and G<sub>2</sub>) are not usually morphologically distinguishable, each phase of the cell cycle has a distinct set of specialized biochemical processes that prepare the cell for initiation of cell division.

(i) G<sub>1</sub> phase

The first phase within interphase, from the end of the previous M phase till the beginning of DNA synthesis is called G<sub>1</sub> (G indicating *gap* or *growth*). During this phase the biosynthetic activities of the cell, which had been considerably slowed down during M phase, resume at a high rate. This phase is marked by synthesis of various enzymes that are required in S phase, mainly those needed for DNA replication. The duration of G<sub>1</sub> is highly variable, even among different cells of the same species.<sup>14</sup>

(ii) The DNA synthesis phase (ie. S phase)

The ensuing S phase begins with the commencement of DNA synthesis; when it is complete, all of the chromosomes have been replicated, ie., each chromosome has two chromatids. Thus, during this phase, the amount of DNA in the cell has effectively doubled, though the ploidy of the cell remains the same. The rates of RNA transcription and protein synthesis are very low during this phase.<sup>15,16</sup> The duration of S phase is relatively constant among cells of the same species.<sup>17</sup>

(iii) G<sub>2</sub> phase

Following the S phase the cell enters the G<sub>2</sub> phase, which lasts until the cell enters mitosis. Again, significant protein synthesis occurs during this phase, mainly involving the production of microtubules, which are required during the process of mitosis. The inhibition of protein synthesis during G<sub>2</sub> phase prevents the cell from undergoing mitosis.

### 5.3.2 Protein Kinases and Regulation of the Cell Cycle –

The regulation of the cell cycle involves steps that are crucial to the cell, including the detection and repair of genetic damage, and the provision of various checks to prevent uncontrolled cell division. The steps that control the cell cycle are ordered and directional and it is impossible to "reverse" the cycle.

Two key classes of regulatory molecules, cyclins and cyclin-dependent kinases (CDKs), determine a cell's progress through the cell cycle.<sup>18</sup> Cyclins form the regulatory subunits and CDKs the catalytic subunits of an activated heterodimer. The CDKs are all serine/threonine kinases ranging from 30 – 36 kDa which are completely dependent on binding of a cyclin partner for protein kinase activity. Within any phase of the cycle only a specific cyclin-CDK complex will be present in the cell.<sup>12,13</sup> Importantly, cyclins have no catalytic activity and CDKs are inactive in the absence of a partner cyclin. When activated by a bound cyclin, CDKs perform a common biochemical reaction called phosphorylation that activates or inactivates target proteins to coordinate entry into the next phase of the cell cycle. Different cyclin-CDK combinations determine the downstream proteins targeted. It is important to note that CDKs are expressed constitutively in the cell, whereas cyclins are synthesised at specific stages of the cell cycle in response to various molecular signals.<sup>19</sup>

### 5.3.3 Specific cyclin-CDK complexes

Cyclin D is the first cyclin produced in the cell cycle in response to extracellular signals (eg. growth factors). Cyclin D binds to CDK4, forming the active cyclin D-CDK4 complex which, in turn, phosphorylates the retinoblastoma susceptibility protein (RB). Once phosphorylated, RB dissociates from the E2F/DP1/RB complex activating E2F.<sup>14</sup> The activation of E2F results in the transcription of various genes such as cyclin E, cyclin A, DNA polymerase and thymidine kinase. Cyclin E subsequently binds to CDK2, forming the cyclin E-CDK2 complex, which pushes the cell from G<sub>1</sub> to S phase (G<sub>1</sub>/S transition). Cyclin A along with CDK2 forms the cyclin A-CDK2 complex, which initiates the G<sub>2</sub>/M transition. Cyclin B-CDK1 complex activation causes breakdown of nuclear envelope and initiation of prophase, and subsequently, its deactivation causes the cell to exit mitosis.<sup>14</sup>

## Regulation of cell cycle - Schematic

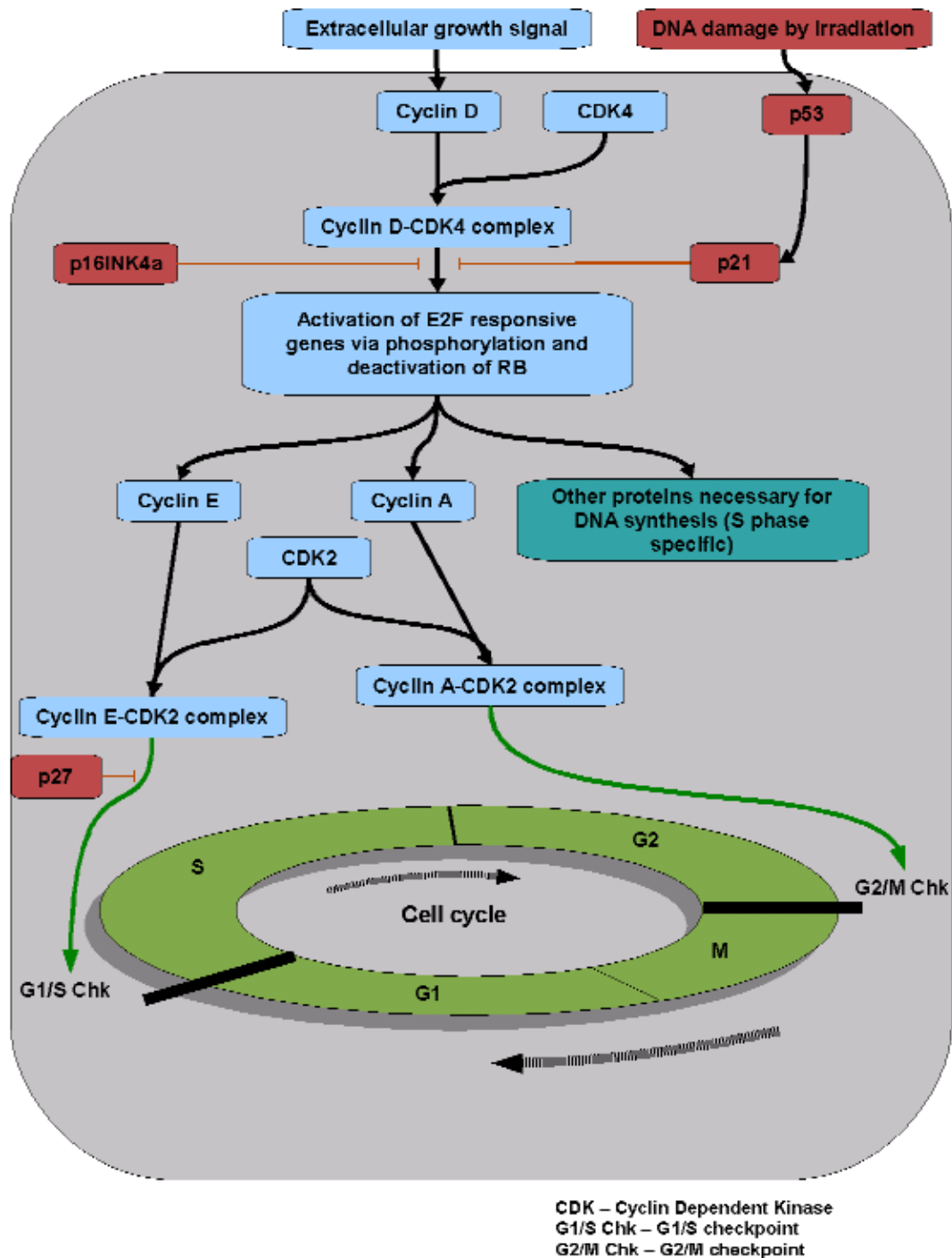


Figure 80 – The Eukaryotic Cell Cycle (Taken from Reference 11)

### 5.3.4 Cell Cycle Inhibitors

Two families of genes, the *cip/kip* family and the INK4a/ARF prevent the progression of the cell cycle. Because these genes are instrumental in the prevention of tumor formation, they are known as tumor suppressors.

The *cip/kip* family includes the genes p21, p27 and p57, which halt the cell cycle in G<sub>1</sub> phase, by binding to, and inactivating, cyclin-CDK complexes. Damage to DNA (e.g. due to radiation) activates p53 which, in turn, triggers the activation of p21.

The INK4a/ARF family includes p16INK4a, which binds to CDK4 and arrests the cell cycle in G<sub>1</sub> phase, and p14arf which prevents p53 degradation.

### 5.3.5 Checkpoints

Cell cycle checkpoints are used by the cell to monitor and regulate the progress of the cell cycle.<sup>15</sup> Checkpoints prevent cell cycle progression at specific points, allowing verification of necessary phase processes and repair of DNA damage. The cell cannot proceed to the next phase until checkpoint requirements have been met.

Several checkpoints are designed to ensure that damaged or incomplete DNA is not passed onto daughter cells. Two main checkpoints exist: the G<sub>1</sub>/S checkpoint and the G<sub>2</sub>/M checkpoint. G<sub>1</sub>/S transition is a rate-limiting step in the cell cycle and is also known as restriction point.<sup>134</sup>

### 5.3.6 Role of the Cell Cycle in Tumor Formation

Deregulation of the cell cycle components may result in the formation of tumors. As noted above, the mutation of certain genes such as the cell cycle inhibitors RB and p53 may cause the cell to multiply uncontrollably, resulting in a tumor. Although the duration of the cell cycle in tumor cells is equal to or longer than that of the normal cell cycle, the proportion of cells that are in active cell division (versus quiescent cells in G<sub>0</sub> phase) in tumor cells is greater than that of normal cells. Thus there is a net increase in cell number as the number of cells that die by apoptosis or senescence remains the same.

### 5.3.7 The Application of CDK Inhibition in Cancer Therapeutics –

The recognition in recent years that CDKs and their regulators are often the target of genetic modulations which result in cancer (ie. oncogenic alterations), has led to the development of a new class of cancer therapeutics: CDK inhibitors (CDI). These inhibitors work by either directly blocking the catalytic ability of the CDK or target the enzymes that regulate the phosphorylation state of CDKs (i.e. Cdc2 phosphatases, Wee1, Myt1).<sup>18-23</sup> Of the classes that have been defined, all exhibit a characteristic structure that allows them to occupy the ATP-binding pocket of the enzyme and therefore compete with ATP.<sup>18-23</sup>

The first Cdc2 inhibitor identified was 6-dimethyl aminopurine (DMAP;  $IC_{50} = 120 \mu M$ ).<sup>18-20,24</sup> Since then various other inhibitors of this type have been synthesized and tested producing some promising results with olomoucine ( $IC_{50} = 7 \mu M$ ) and roscovitine ( $IC_{50} = 0.7 \mu M$ ) (Figure 81). Both compounds inhibited Cdc2, Cdk2, Cdk5 and MAP kinase against a panel of 35 kinases, but did not affect Cdk4 or Cdk6, thereby providing some specificity within this class of compounds.<sup>25</sup> One of the more recent additions to this set however is purvalanol, which shows a 100 fold increase in potency ( $IC_{50} = 70 \text{ nM}$ ) against Cdk2/cyclin A when compared to roscovitine.<sup>26</sup> Each of these compounds exhibits its effects through binding in the ATP binding pocket of the CDK, however roscovitine and purvalanol derive their specificity through contacts made by the adenine side-chain at sites outside the conserved binding domain.<sup>25</sup>

Both roscovitine and olomoucine arrest a number of various cell types in the  $G_1$  and  $G_2$  phases both through different mechanisms. Roscovitine blocks phosphorylation of the Cdc2/cyclin B substrate; vimentin and olomoucine phosphorylates the Cdc2 substrates protein phosphatase I and elongation factors  $\alpha$  and  $\gamma$ .<sup>26-30</sup>

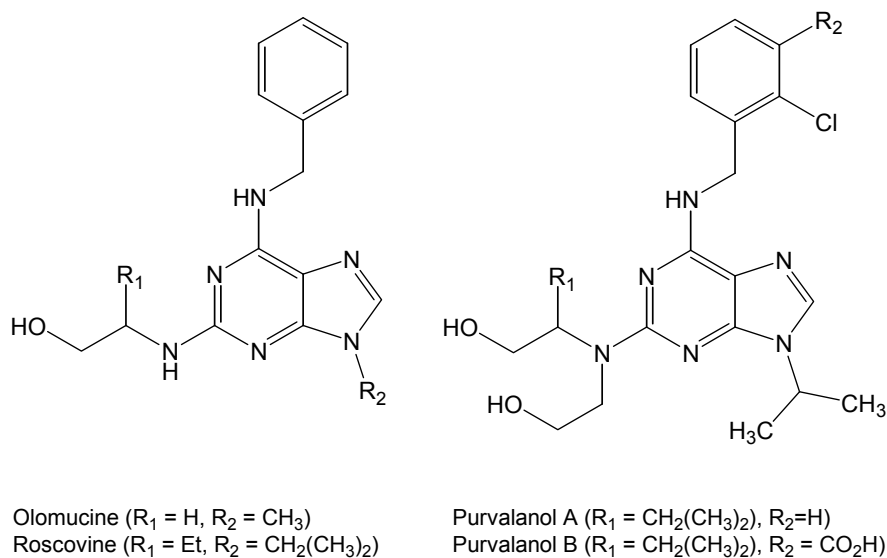


**Figure 81 – Trisubstituted Purine CDIs**

### 5.3.8 Determination of Cell Cycle Phase –

The aim of this part of the project was to determine whether the simple alkylating compounds used in this study interfered with the eukaryotic cell cycle and if they did, within what phase did this occur. We proposed that DNA alkylating compounds would interfere with the DNA synthesis stage of the cell cycle.

While there are several methods available to examine the cell cycle, flow cytometry was the method employed in the Parsons' lab. Flow Cytometry has the advantage that thymidine labelling of DNA, and therefore autoradiography, is not required.<sup>31</sup> Rather, our assay utilized the fluorescent marker propidium iodide, which is detectable at 680 nm using a fluorescence-2 detector.

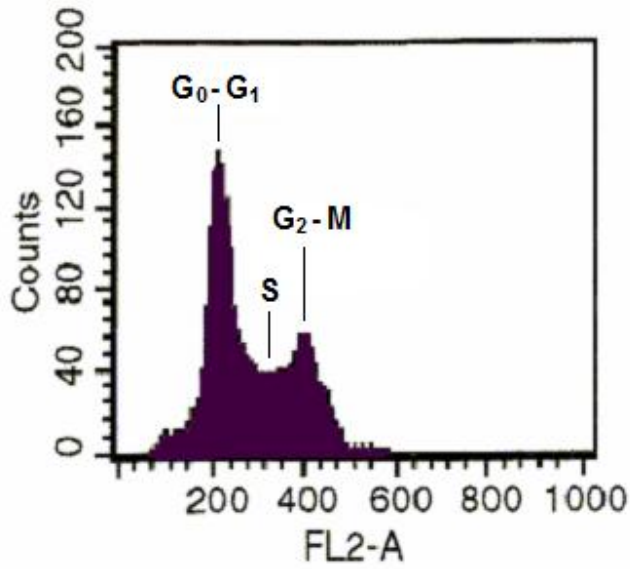
This study employed the use of the MM96L  $\beta$ -galactosidase, neonatal foreskin fibroblast (NFF) and 293 cell lines, which were added to 60 mm plates and then incubated overnight. Following overnight incubation, MNNG, MMS, **(4)**, **(6)** and **(23)** were added in triplicate to the each cell line at the concentrations shown in Figures 82 – 101 and incubated at 37°C for 30 minutes. Hydroxyurea (2 mM) and Albendazole (1  $\mu\text{g}/\text{mL}$ ) were added separately to four of the MM96L plates containing **(4)** at the concentrations shown in Figures 102-106. Following further incubation at 37°C for two hours, the old medium was washed from the plates and

replaced with fresh medium. The plates were subsequently incubated for another 24 hours at 37°C. The cells were then washed, resuspended in PBS, stained with propidium iodide solution and analyzed by flow cytometry using a FACSCalibur instrument.

Flow cytometry allows simultaneous measurement of multiple physical characteristics of up to fifty thousand cells per second. Determination of the cell cycle distribution is carried out by measuring the amount of DNA-bound probe in a cell. Cells in G<sub>2</sub>/M show twice the DNA content as cells in G<sub>0</sub>/G<sub>1</sub>, while the DNA content of cells in S phase is somewhere in between. As the DNA content of cells increases, the amount of DNA bound probe increases accordingly, enabling the measurement of DNA content and hence determination of the cell cycle distribution.

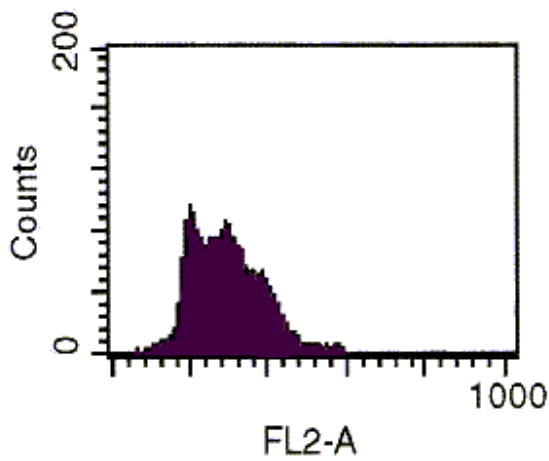
### **5.3.9 The Effect of Various DNA Alkylating Compounds on the MM96L Cell Cycle –**

Figures 82- 95 illustrate the effect of various DNA alkylating compounds on the MM96L cell cycle. Figure 82 illustrates a standard (control) cell cycle distribution, depicting both a minor and major peak which represent G<sub>0</sub>-G<sub>1</sub> and G<sub>2</sub>-M respectively as labeled. The DNA synthesis phase is represented by the area between the peaks. Normal cells cycle from G<sub>1</sub> through to mitosis. However, any event which inhibits the progression of the cell cycle past a particular check-point, will result in the accumulation of cells in the preceding phase which will be demonstrated by an increase in relevant peak area in the cell cycle distribution curve.



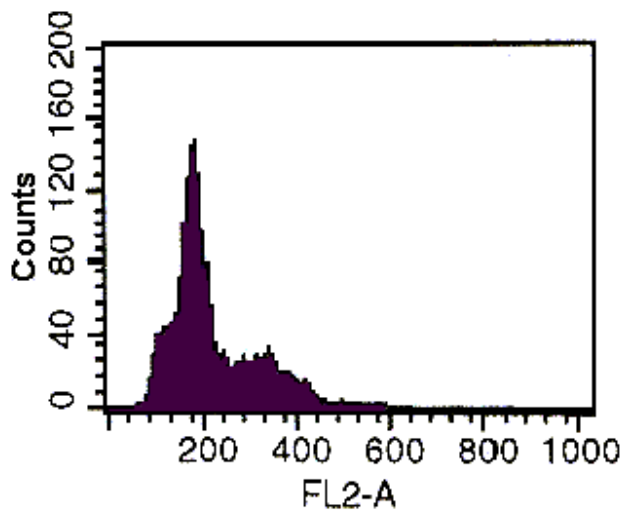
**Diploid Population: 100%**  
**G<sub>0</sub>-G<sub>1</sub>: 58.91 %**  
**G<sub>2</sub>-M: 8.09 %**  
**S: 33.00 %**  
**Debris: 0.34%**  
**Apoptosis/Necrosis: 11.44%**

*Figure 82 – MM96L Cell Cycle Control*



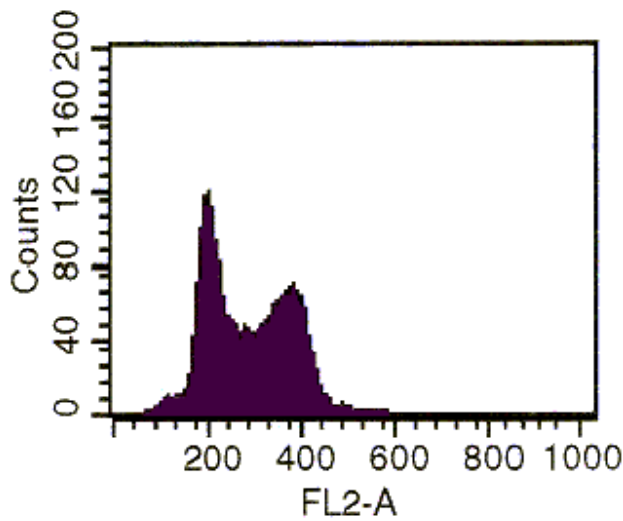
**Diploid Population: 100%**  
**G<sub>0</sub>-G<sub>1</sub>: 14.59 %**  
**G<sub>2</sub>-M: 0 %**  
**S: 85.41 %**  
**Debris: 0.62 %**  
**Apoptosis/Necrosis: 0.36 %**

*Figure 83 – MM96L Cell Cycle Following Incubation with 1.70 μM of MNNG*



**Diploid Population: 100%**  
**G<sub>0</sub>-G<sub>1</sub>: 56.23 %**  
**G<sub>2</sub>-M: 14.14 %**  
**S: 29.64 %**  
**Debris: 0.67%**  
**Apoptosis/Necrosis: 0.38 %**

*Figure 84 – MM96L Cell Cycle Following Incubation with 17.00 μM of MNNG*



**Diploid Population: 100%**  
**G<sub>0</sub>-G<sub>1</sub>: 26.68 %**  
**G<sub>2</sub>-M: 23.50 %**  
**S: 49.82 %**  
**Debris: 0 %**  
**Apoptosis/Necrosis: 2.71 %**

*Figure 85 – MM96L Cell Cycle Following Incubation with 227.00 μM of MMS*

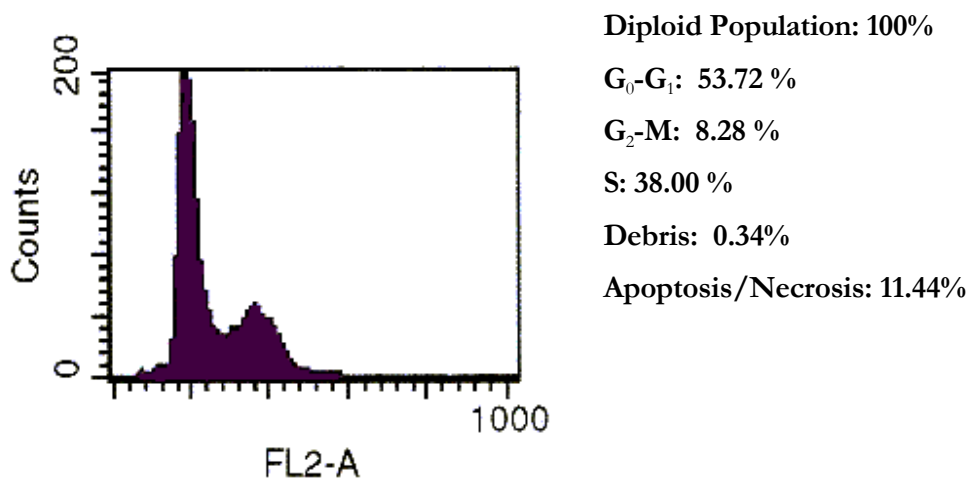


*Figure 86 – MM96L Cell Cycle Following Incubation with 2.27 mM of MMS*

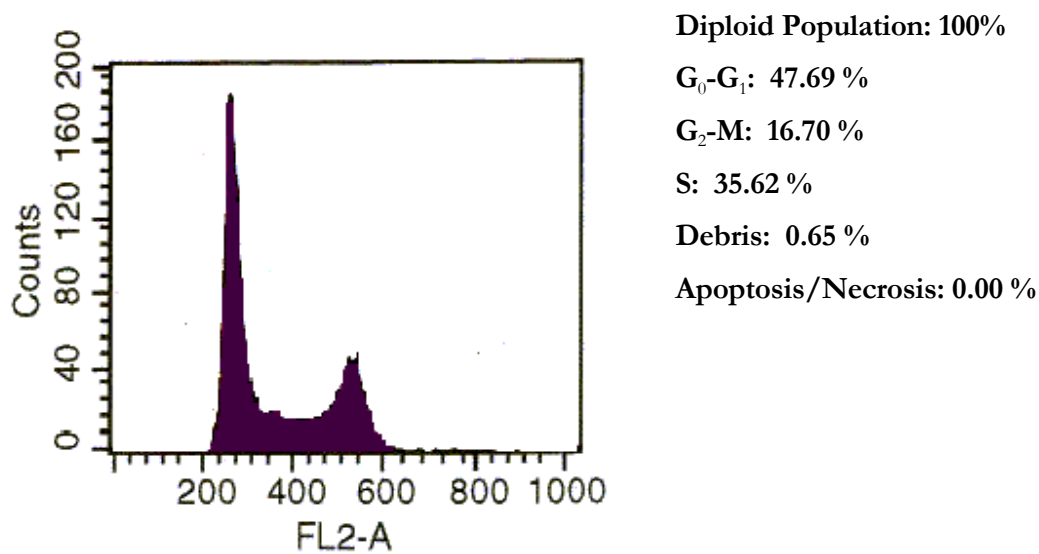
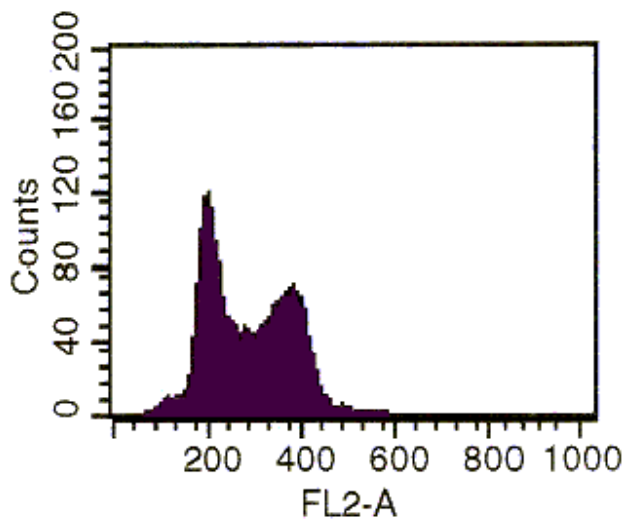
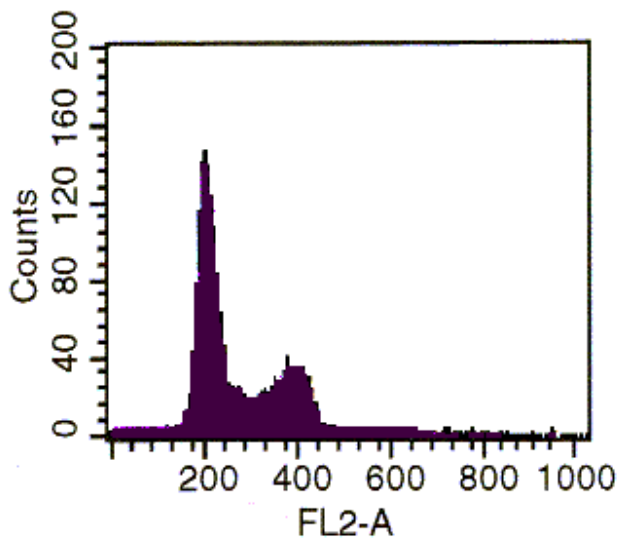


*Figure 87 – MM96L Cell Cycle Following Incubation with (4) at a conc. of 1.1 μM*



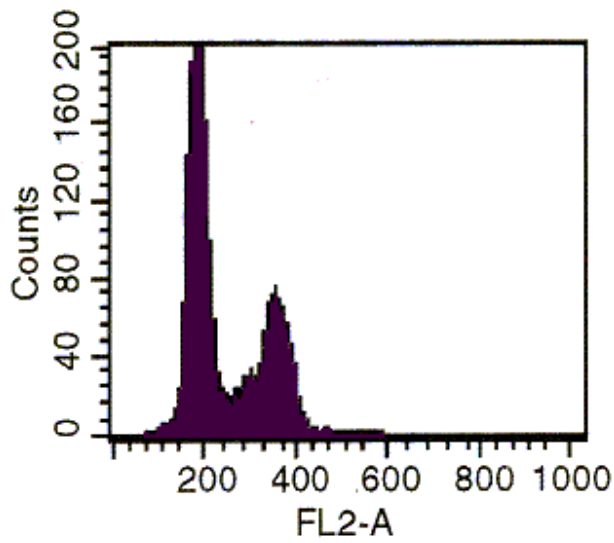
**Diploid Population: 100%**  
**G<sub>0</sub>-G<sub>1</sub>: 33.45 %**  
**G<sub>2</sub>-M: 20.78 %**  
**S: 45.77 %**  
**Debris: 1.35 %**  
**Apoptosis/Necrosis: 0.43 %**

*Figure 88 – MM96L Cell Cycle Following Incubation with (4) at a conc. of 2.1 μM*



**Diploid Population: 100%**  
**G<sub>0</sub>-G<sub>1</sub>: 51.71 %**  
**G<sub>2</sub>-M: 13.62 %**  
**S: 34.67 %**  
**Debris: 5.15 %**  
**Apoptosis/Necrosis: 5.25 %**

*Figure 89 – MM96L Cell Cycle Following Incubation with (4) at a conc. of 3.2 μM*



**Diploid Population: 100%**

**G<sub>0</sub>-G<sub>1</sub>: 56.03 %**

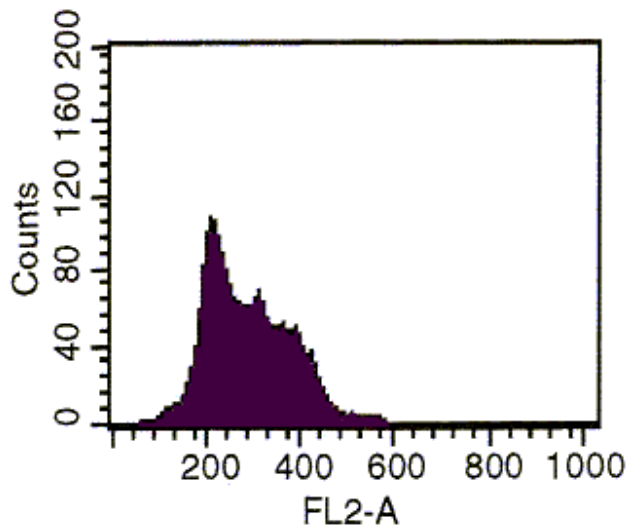
**G<sub>2</sub>-M: 17.07 %**

**S: 26.90 %**

**Debris: 0.48 %**

**Apoptosis/Necrosis: 2.06 %**

*Figure 90 – MM96L Cell Cycle Following Incubation with (4) at a conc. of 10.6 μM*



**Diploid Population: 100%**

**G<sub>0</sub>-G<sub>1</sub>: 29.02 %**

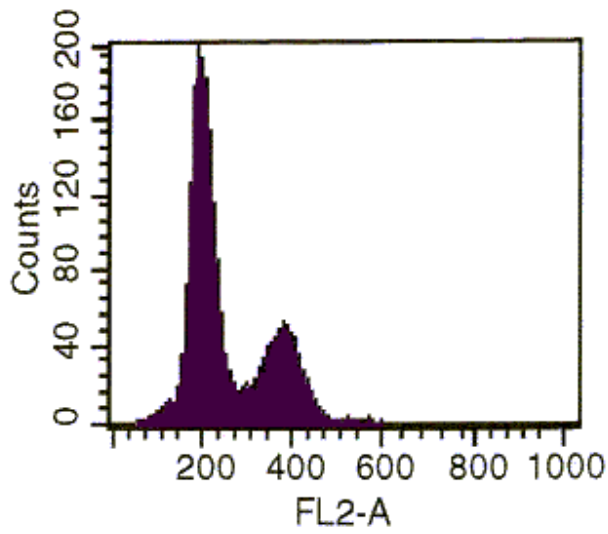
**G<sub>2</sub>-M: 14.27 %**

**S: 56.72 %**

**Debris: 0.37%**

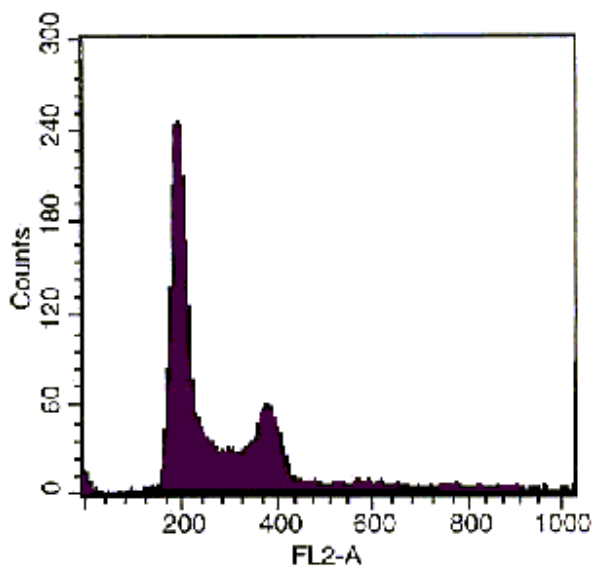
**Apoptosis/Necrosis: 0.73%**

*Figure 91 – MM96L Cell Cycle Following Incubation with (6) at a conc. of 26.0 μM*



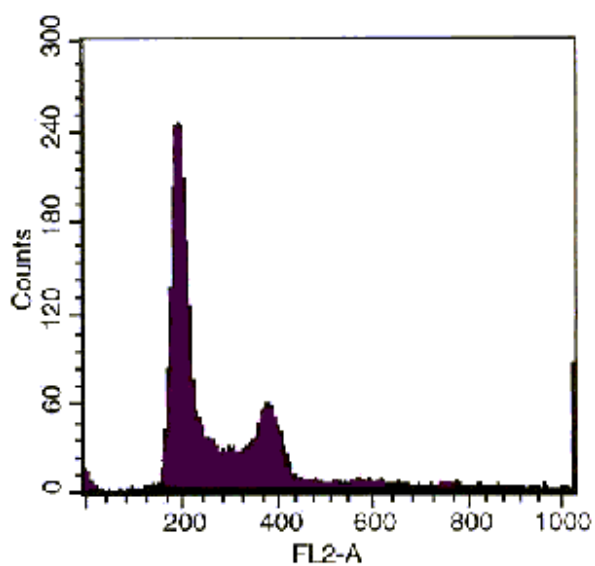
**Diploid Population: 100%**  
**G<sub>0</sub>-G<sub>1</sub>: 53.60 %**  
**G<sub>2</sub>-M: 21.13 %**  
**S: 25.28 %**  
**Debris: 0.00 %**  
**Apoptosis/Necrosis: 2.04%**

*Figure 92 – MM96L Cell Cycle Following Incubation with (6) at a conc. of 260.3 μM*



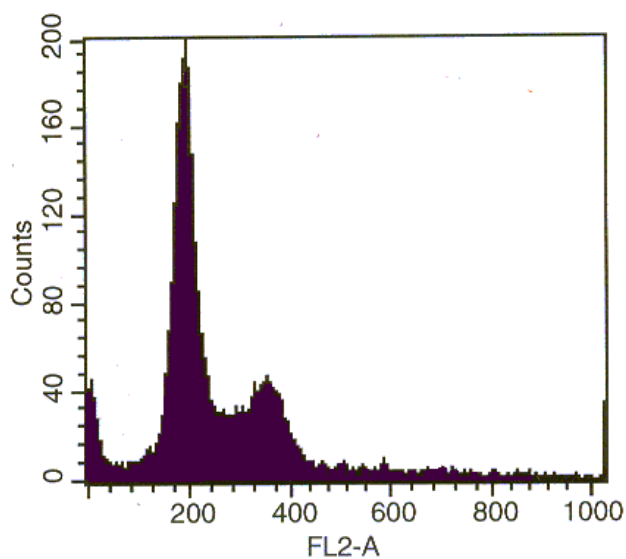
**Diploid Population: 100%**  
**G<sub>0</sub>-G<sub>1</sub>: 56.48 %**  
**G<sub>2</sub>-M: 22.01 %**  
**S: 21.51 %**  
**Debris: 0.49 %**  
**Apoptosis/Necrosis: 0.00 %**

*Figure 93 – MM96L Cell Cycle Following Incubation with (23) at a conc. of 40.0 μM*



**Diploid Population: 100%**  
**G<sub>0</sub>-G<sub>1</sub>: 37.45 %**  
**G<sub>2</sub>-M: 13.45 %**  
**S: 49.11 %**  
**Debris: 0.39%**  
**Apoptosis/Necrosis: 0.00%**

*Figure 94 – MM96L Cell Cycle Following Incubation with (23) at a conc. of 95.8 μM*



**Diploid Population: 100%**  
**G<sub>0</sub>-G<sub>1</sub>: 52.23 %**  
**G<sub>2</sub>-M: 22.43 %**  
**S: 25.34 %**  
**Debris: 2.56 %**  
**Apoptosis/Necrosis: 0.21 %**

*Figure 95 – MM96L Cell Cycle Following Incubation with (23) at a conc. of 319.3 μM*

5.3.10 The Effect of Compound 4 on Other Cell Lines –

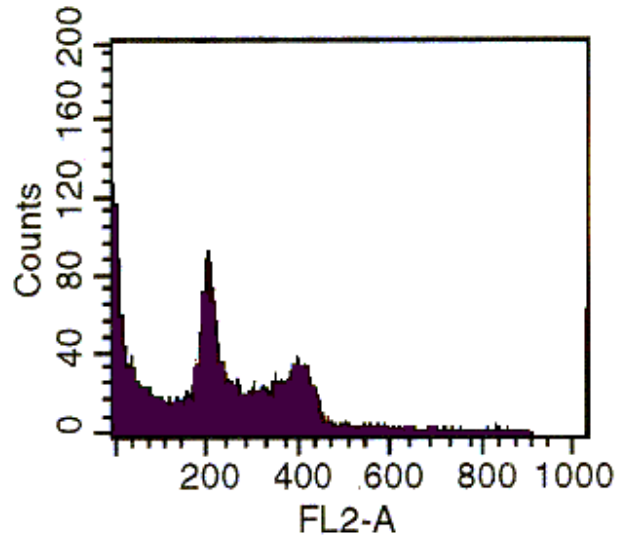


Figure 96 – 293 Cell Cycle Following Incubation with (4) at a conc. of 3.2  $\mu$ M

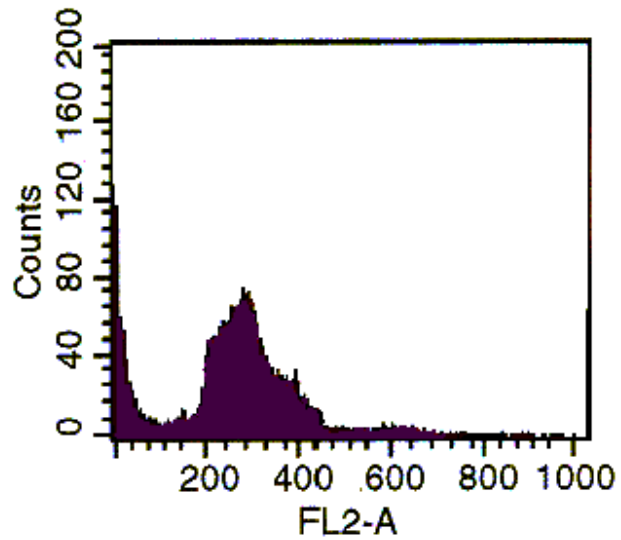
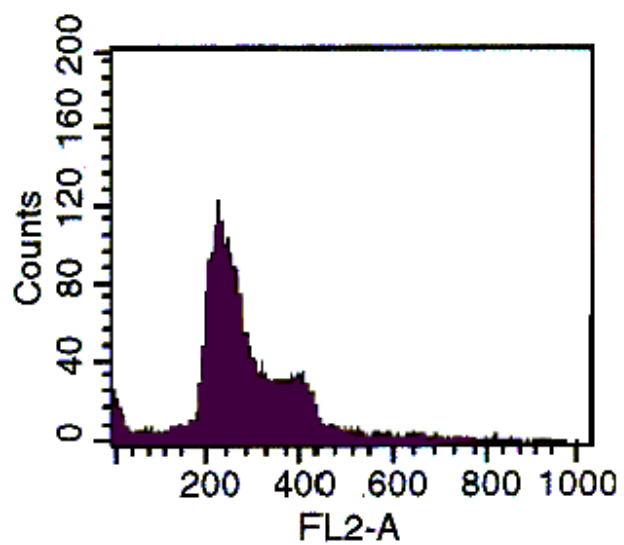
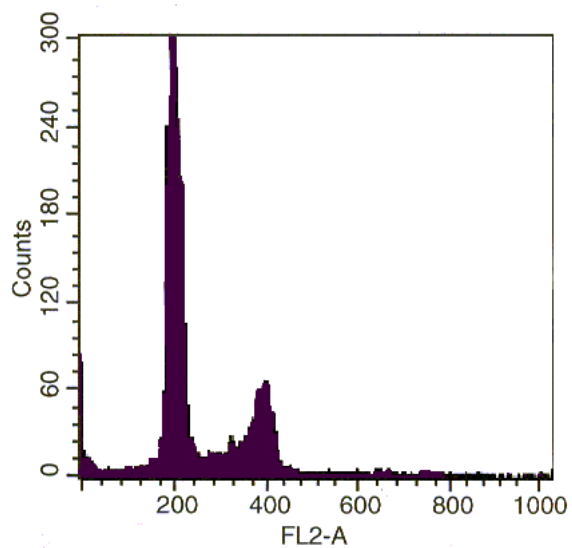


Figure 97 – 293 Cell Cycle Following Incubation with (4) at a conc. of 6.3  $\mu$ M



*Figure 98 – 293 Cell Cycle Following Incubation with (4) at a conc. of 10.6  $\mu$ M*



*Figure 99 – NFF Cell Cycle Following Incubation with (4) at a conc. of 3.3  $\mu$ M*

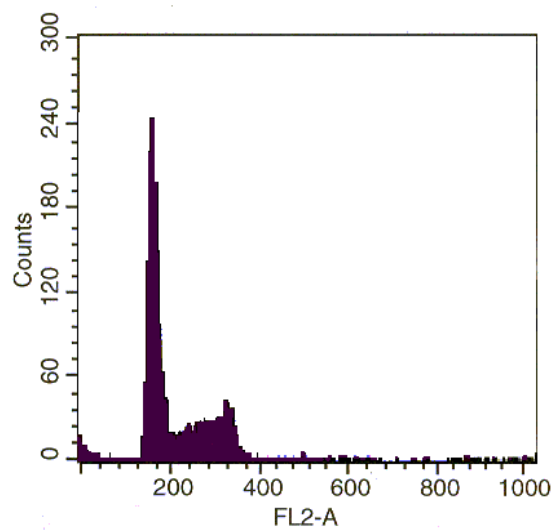


*Figure 100 – NFF Cell Cycle Following Incubation with (4) at a conc. of 6.3 μM*

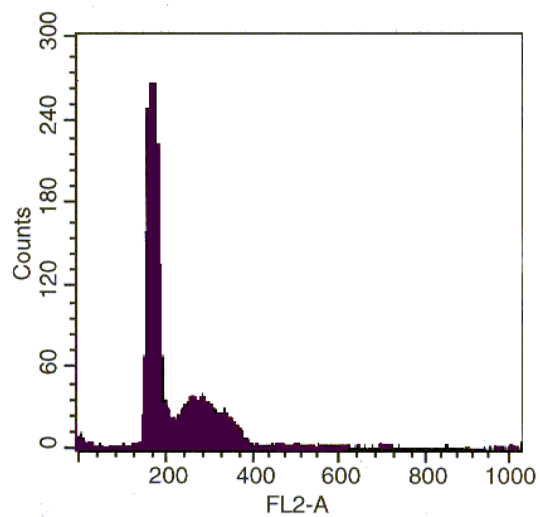


*Figure 101 – NFF Cell Cycle Following Incubation with (4) at a conc. of 10.6 μM*

5.3.11 The Effect on the Cell Cycle Following Treatment of MM96L Cells with Compound 4 in Combination with either Hydroxyurea (HU) or Albendazole (AB) –

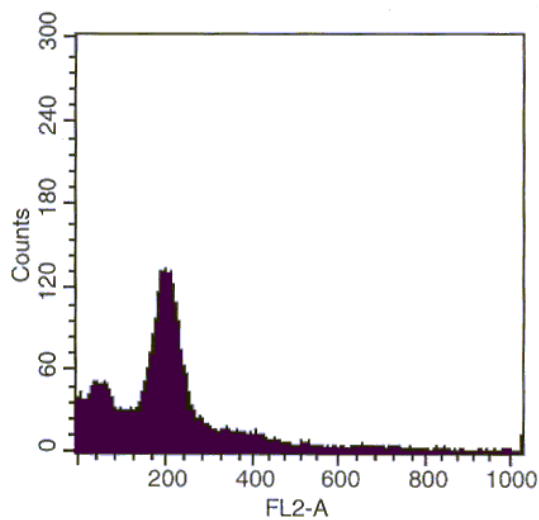


*Figure 102 – MM96L Cell Cycle Following Incubation with (4) at a conc. of 3.3 μM + HU*

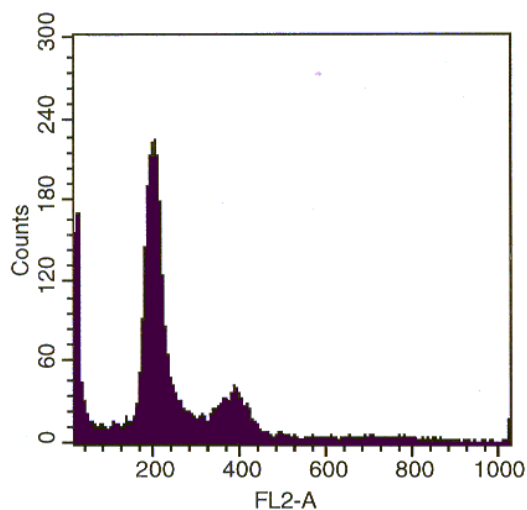


*Figure 103 – MM96L Cell Cycle Following Incubation with (4) at a conc. of 6.3 μM + HU*

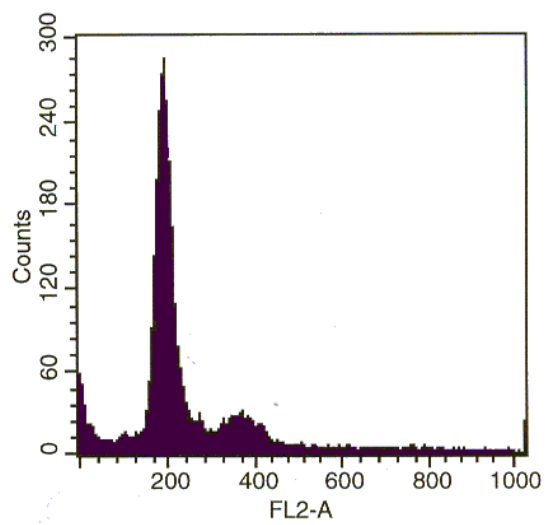


*Figure 104 – MM96L Cell Cycle Following Incubation with (4) at a conc. of 10.6  $\mu$ M + HU*

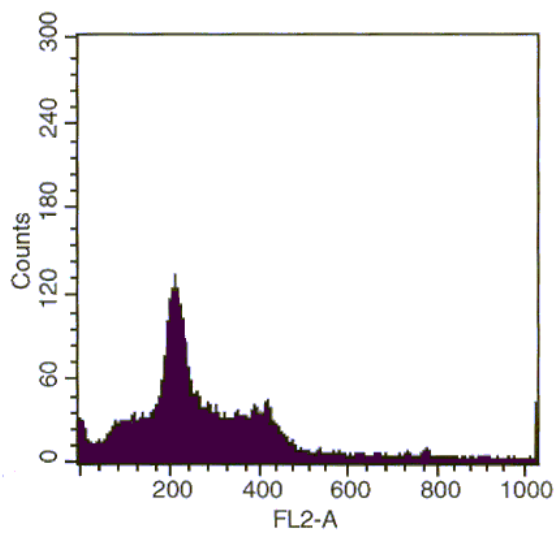


*Figure 105 – MM96L Cell Cycle Following Incubation with (4) at a conc. of 3.3  $\mu$ M + AB*

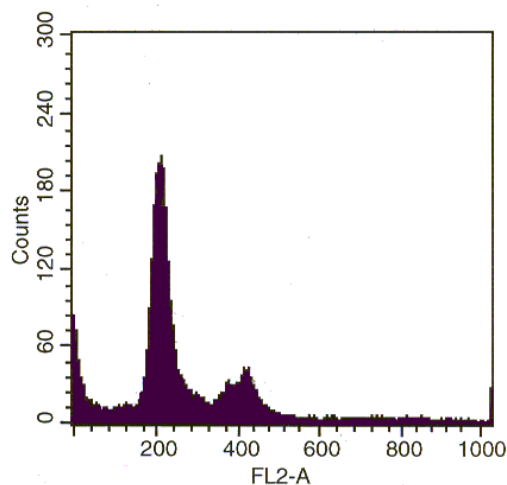


**Figure 106 – MM96L Cell Cycle Following Incubation with (4) at a conc. of 6.3  $\mu$ M + AB**

### 5.3.12 Cell Cycle Summary of Results –

These results can be summarized as follows:

- (a) In order to demonstrate the cell cycle distribution of MM96L cells following treatment with a known S-phase inhibitor, MNNG, a potent O-methylating agent and DNA synthesis inhibitor, was utilized. Figure 83 demonstrates that following treatment with 1.70  $\mu$ M of MNNG, the proportion of MM96L cells in the S-phase (ie. 85%) is greater than that found in the control cell cycle distribution (ie. 33% - Figure 82). As expected, we can conclude that MNNG has elicited an S-phase block.
- (b) At a concentration of 17  $\mu$ M MNNG appeared to have no affect on the MM96L cell cycle distribution (Figure 84).
- (c) In order to further demonstrate the effect of a known S-phase inhibitor on MM96L cells, MMS, which methylates DNA predominantly on the N-7 of guanine and inactivates DNA synthesis, was utilized.<sup>19,23</sup> The treatment of MM96L cells with 227  $\mu$ M of MMS (Figure 85) resulted in an increase in the S-phase fraction in the cellular distribution graph, indicating that MMS is also eliciting an S-phase block.

- (d) Similar to MNNG, the MM96L cell cycle distribution following treatment with 2.27 mM mg of MMS (Figure 86) resulted in a typical MM96L control distribution (Figure 82).
- (e) Compound **(4)** had no effect on the MM96L cell cycle at 1.1  $\mu\text{M}$  and but displayed a marked S-phase block at 2.1  $\mu\text{M}$  (Figure 88). The cell cycle distribution returned to that of the control distribution at concentrations of 3.2  $\mu\text{M}$  and 10.6  $\mu\text{M}$ .
- (f) Compound **(6)** exhibited a marked S-phase block at 26  $\mu\text{M}$  with 56% of cells blocked at the DNA synthesis phase of the cell cycle. Similarly to **(4)**, the cell cycle distribution returned to control values at a concentration of 260  $\mu\text{M}$ .
- (g) Compound **(23)** exhibited a slight G<sub>2</sub>-M block in MM96L cells at 40  $\mu\text{M}$  and a marked S-phase block at 95.8  $\mu\text{M}$ .
- (h) Compound **(4)** was a potent S-phase inhibitor in 293 cells at 3.2  $\mu\text{M}$  and 6.3  $\mu\text{M}$ , eliciting a return to a cell cycle distribution similar to control at 10.6  $\mu\text{M}$ .
- (i) At 3.3  $\mu\text{M}$  compound **(4)** had no effect on the cell cycle distribution of NFF cells, but resulted in a minor S-phase block at 6.3  $\mu\text{M}$ .
- (j) Compound **(4)**, in combination with hydroxyurea (HU) elicited a G<sub>0</sub>-G<sub>1</sub> block at 3.3  $\mu\text{M}$ . The cell cycle distribution returned to normal at 6.3  $\mu\text{M}$  and 10.6  $\mu\text{M}$  of **(4)** in the presence of HU.
- (k) At 3.3  $\mu\text{M}$ , compound **(4)** elicited a potent S-phase block in MM96L cells in combination with Albendazole (AB). The cell cycle distribution returned to a standard distribution at 6.3  $\mu\text{M}$  of compound **4** in the presence of Albendazole.

These results suggest the following:

- (a) Compound **(4)** exhibits a similar effect on the MM96L cell cycle distribution (Figure 87-89) as MNNG and MMS (known S-phase inhibitors), but differs in that it exhibits dramatic changes in activity over a small dose range. This is not surprising considering that **(4)** shows mild to considerable cellular damage over a limited dose in both the *in vitro* and *in vivo* studies (Section 5.5).

- (b) The apparent return to the control cell cycle distribution with increased concentrations of compound **(4)** (ie. 3.2  $\mu\text{M}$  and 10.6  $\mu\text{M}$ ) could result from one or more of the following factors:
- (i) saturating alkylation of DNA which prevents the transcription of proteins (ie. cyclins) that are required for the cell to progress through each of the cell cycle phases;
  - (ii) binding and inhibiting the catalytic activity of various CDKs that are required throughout the cell cycle; or
  - (iii) targeting the enzymes that regulate the phosphorylation state of CDKs (i.e. Cdc2 phosphatases, Wee1, Myt1).

As a result of this saturated binding by **(4)** at high concentrations, and hence inhibition of cellular components that are involved in each phase of the cell cycle, the cells appear to 'freeze' in a standard pattern of distribution. This phenomenon is known as cellular senescence and normally occurs in response to DNA damage or degradation.<sup>32</sup>

Cellular senescence is also demonstrated in 293 and NFF cell lines following treatment with compound **(4)**. However, given that NFF cells show a normal cellular metabolism compared to the MM96L and 293 cell lines, they are less susceptible to alkylation by **(4)** and hence only exhibit an S-phase block at higher concentrations of drug (ie. 6.3  $\mu\text{M}$ ). Again, the selectivity of **(4)** for tumor cells (c.f. normal NFF cells) makes it an interesting candidate for further studies.

- (c) Compound **(6)** is also an S-phase inhibitor at low concentrations, but exhibits the same phenomenon as compound **(4)** at higher concentrations (ie. 260  $\mu\text{M}$ ) for the reasons discussed above.
- (d) The G<sub>2</sub>-M phase block exhibited by compound **(23)** at 40  $\mu\text{M}$  may indicate that this compound binds and inactivates proteins (ie. cyclin A, CDK2) that are required in order for the cell cycle to progress through the G<sub>2</sub>-M checkpoint. This would indicate that **(23)** displays a decreased specificity for DNA compared to the amine counterparts **(4)** and **(6)**. This is supported by the results observed in Chapter 4 where compound **(23)** was found to have lower potency toward DNA than compounds **(4)** and **(6)**.

- (e) HU depletes deoxynucleotide pools via the inhibition of ribonucleotide reductase. This results in the inhibition of DNA synthesis, causing cells to accumulate in the S-phase.<sup>21</sup> However, in combination with compound **4**, HU appears to elicit a G<sub>0</sub>-G<sub>1</sub> block.
- (f) Albendazole (ABZ) inhibits microtubule polymerization by binding to  $\beta$ -tubulin.<sup>22</sup> Because microtubules play an important role in the formation of the mitotic spindle, the disruption of tubulin assembly by albendazole ultimately results in cellular death. Albendazole had been shown to inhibit the cell cycle at either G<sub>0</sub>-G<sub>1</sub> or G<sub>2</sub>-M. In combination with (**4**), ABZ inhibits the cell cycle block at G<sub>0</sub>-G<sub>1</sub>.

#### **5.4 ADENOVIRAL ASSAYS**

The adenovirus is commonly used for *in vitro* experiments involving human cell lines (tumor or normal) because of both its ability to replicate well in human cells, and its rapid quantification in as little as two days post infection.

Adenoviral assays are commonly used as *in vitro* probes for the chemosensitivity of short-term cultures of human tumors (i.e. melanoma cell lines and primary cultures of melanoma biopsies). A convenient immunoperoxidase method has been developed in the Parsons lab for quantifying viral replication two days after infection. Two different approaches were explored:<sup>33</sup>

- (a) Host Cell Reactivation assay (HCR) utilizing drug-treated virus. This method is commonly used to quantify the ability of a cell's repair machinery to fix and hence reactivate viral DNA that has been damaged by alkylating agents.
- (b) Viral capacity assay utilizing drug-treated cells. This assay quantifies the sensitivity/resistance of different cell lines to DNA alkylating agents by examining the ability of drug treated cells to replicate viral DNA. Higher replication rates indicate increased resistance/decreased sensitivity to a drug.

The results of these assays are shown in Figures 107-110.

#### 5.4.7 Host Cell Reactivation (HCR) Assays –

The therapeutic treatment of certain types of cancer (e.g. breast cancer) is at times problematic due to the presence of tumor populations with inherent or acquired resistance to drugs. Most drug combinations use at least one alkylating agent, however their effectiveness is limited by the presence of cell populations that are resistant to one or more of these drugs.

There are several mechanisms which lead to drug resistance in cell lines including:

- decreased drug accumulation resulting from enhanced DNA repair by the removal of various types of lesions (i.e. interstrand crosslinks created by bisalkylating compounds),
- altered drug transport,
- altered drug metabolism, and
- enhanced drug detoxification, generally by glutathione and/or glutathione S-transferases.<sup>22</sup>

The ability of various tumor cell lines to repair DNA which had been damaged by DNA alkylating agent, **(4)** was investigated. The host cell reactivation assay is a fundamental technique for investigating the efficiency of intrinsic DNA repair in sensitive and resistant tumor cells, (cells which are resistant to drug generally have a more efficient repair capacity than drug sensitive cell lines). Enhanced host cell reactivation is generally found in cell lines that are resistant to treatment with drugs. Figures 107, 108 and 109 illustrate the ability of MM96L and NFF cells respectively to reactivate adenovirus following treatment with compound **(4)**.

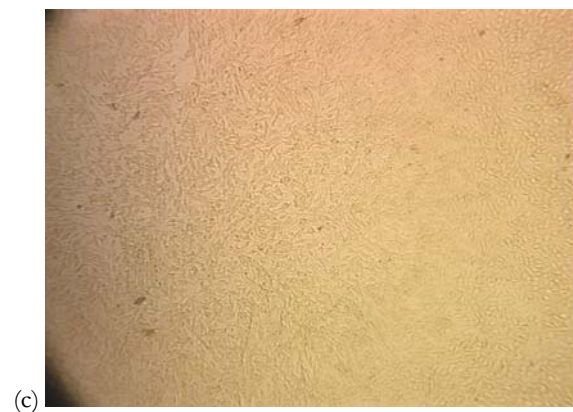


*Figure 107 –Reactivation of Virus in MM96L Cells (indicated by staining), Following Treatment with Compound (4) at: (a) 0, (b) 13.5 (c) 27.0 and (d) 44.9 mM.*

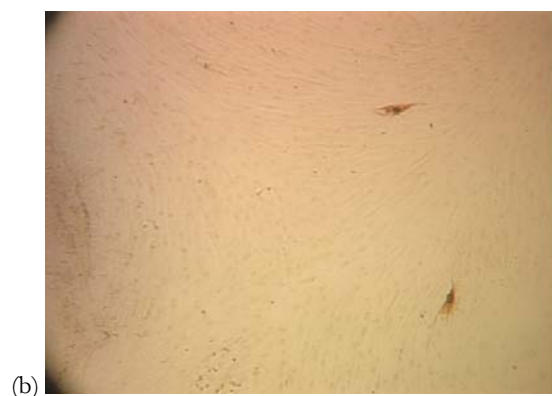


*Figure 108 – Reactivation of Virus in NFF cells (indicated by staining),  
Following Treatment with Compound (4) at: (a) 0, (b) 13.5 (c) 27.0 (d) 44.9 mM.*

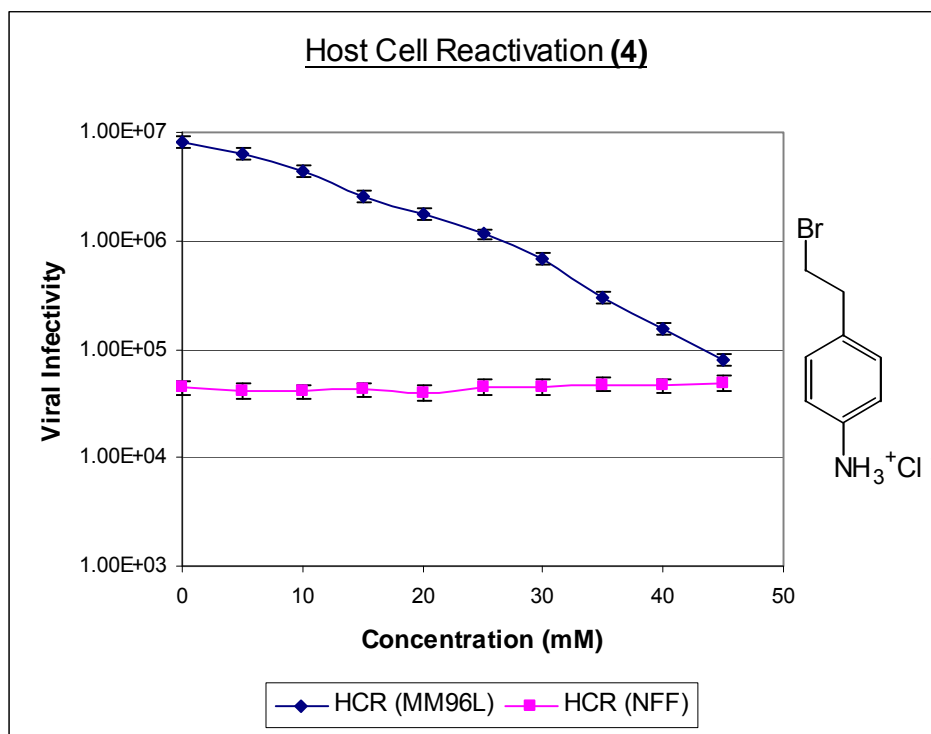


**Figure 109 – Host Cell Reactivation of Drug (4) Treated Virus (HCR of Drug Treated Virus is Inhibited in MM96L cells)**

The HCR assay employed both MM96L and NFF cells lines. Figure 109 demonstrates that as the concentration of (4) increases, the ability of the MM96L cell line to repair and hence reactivate the viral DNA decreases, indicating that MM96L cells possess a sensitivity toward (4). This is not surprising given that many tumor cell lines show a diminished ability to repair damaged DNA.

In comparison, the ability of NFF cells to reactivate virus is maintained even with increasing concentrations of drug. Similar to the cellular cytotoxicity assays, these results indicate that the NFF cell line shows an enhanced resistance to (4) compared to that exhibited by MM96L cells.

#### 5.4.2 Viral Capacity –

While HCR assays are a useful tool for investigating the intrinsic DNA repair ability of various tumor cell lines, viral capacity assays enable the rapid identification of cell lines that

are either sensitive or resistant toward various drugs. The inhibition of viral replication in drug-treated cells is indicative of cell lines that are sensitive to the drug administered.<sup>33</sup>

This approach has been used to detect the sensitivity of melanoma cell lines to a wide range of antitumor agents including hydroxyurea, deoxyadenosine, cytosine arabinoside, fluorouracil, vincristine, adriamycin, 6-mercaptopurine and ionizing radiation. As such, we expected this assay to be useful in demonstrating the sensitivity of MM96L cells and the resistance of NFF cells, to our simple monoalkylator, **(4)**.<sup>33</sup>

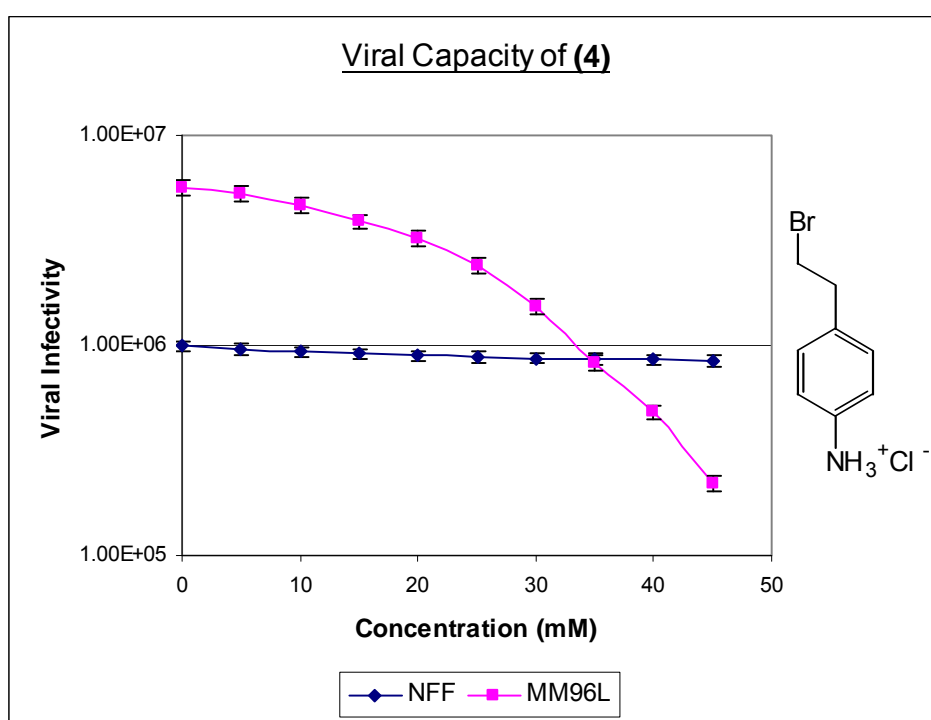


*Figure 110 – A Comparison of Viral Capacity in MM96L and NFF Cells Following Treatment with Compound (4) (0, 13.5, 27.0, 44.9 mM).*

The HCR assay examines the ability of drug treated cells to replicate viral DNA. In summary, the results indicate that the MM96L cell line is dramatically more sensitive to **(4)** than are NFF cells. This is demonstrated in Figure 110 in which viral replication decreased with increased concentrations of drug applied to the cells, indicating that MM96L cells have an inherent sensitivity to compound **(4)**. This correlates well with the previously demonstrated enhanced cytotoxicity of **(4)** toward the MM96L cell line.

Conversely, the NFF cell line did not exhibit this same decline in viral infectivity even at higher drug concentrations and as such is markedly more resistant to **(4)** than the MM96L cell line. The treatment of NFF cells with much higher concentrations of drug was required before any visible decrease in viral infectivity occurred.

#### **5.4.3 Adenoviral Assay Summary -**

The adenoviral assays indicate that MM96L cells have a decreased capacity to repair damaged DNA and as such are sensitive to the DNA alkylating compound **(4)**. Furthermore, the treatment of MM96L cells with drug inhibits their ability to replicate DNA, again indicating chemosensitivity to **(4)**.

As expected, NFF cells show resistance to **(4)**, even at higher drug concentrations. The selectivity of **(4)** toward non-tumor cells (c.f. tumor cells) makes it an attractive candidate for further investigation.

### **5.5 IN-VIVO STUDIES**

A preliminary investigation into the *in-vivo* activity of **(4)** in nude mice was performed by Professor Peter Parsons, at the Queensland Institute of Medical Research, Brisbane. In order to enable implantation of human tumor cells into the mouse host and prevent rejection of the subsequent tumor growth, nude mice (ie. immunocompromised mice) were used.

The procedure involved the subcutaneous injection of  $2 \times 10^6$  MM96L cells in 0.1 mL of medium, at four sites on the flanks of 8 week old female nude mice. After three weeks tumors with an average volume of  $20 \text{ mm}^3$  had developed. Each mouse was given 0.3 mg, 1 mg and 3 mg of **(4)** by intraperitoneal injection on three successive days. On the fourth day the treated mice appeared sluggish and thin, so treatment was discontinued. After seven weeks the tumor sizes were measured (Table 25).

8 sites in untreated mice	230 +/- 45 mm <sup>3</sup>
8 sites in treated mice	215 +/- 36 mm <sup>3</sup>

**Table 25:** Examination of tumor volume in treated versus untreated nude mice

While preliminary results indicate that **(4)** failed to demonstrate any significant decrease in tumor volume, changes to the drug regimen (ie. a decreased dosage administered tri-weekly over a 4 week period) may elicit better results.

Furthermore, the use of immunocompromised mice may have a dramatic effect on outcome of drug treatment. Therefore, as suggested by Dr Parsons, future studies using common lab mice with normal immune system function may elicit improved results.

## **5.6 CONCLUSIONS AND FUTURE WORK**

### **5.6.1 Reporter Assays –**

The  $\beta$ -galactosidase assay demonstrated that the amine derivatives **(4)** and **(6)** may possess moderate AT sequence specificity. The drugs interact with DNA in such a way as to inhibit the transcription of genes which are essential for the viability of the cell, thus contributing to cellular death. However, while it has been established that DNA is the primary target of the alkylating compounds tested, the exact mechanism of transcription inhibition is uncertain. In order to determine whether the inhibition results from binding specifically within the promoter, additional reporter assays need to be performed.

### **5.6.2 Drug Stability Studies –**

Results from stability studies indicate that **(4)** reacts with many nucleophiles commonly found in human serum, particularly DNA. This deactivation does not occur *in vitro* before the compound has an opportunity to exhibit its antitumor activity.

### 5.6.3 Cell Cycle Studies –

Cellular survival studies indicate that 4-aminophenethyl bromide shows the most promise as an anticancer candidate due to its high specificity for tumor cells *in-vitro* when compared to noncancerous cell lines (ie. NFF). Further investigation and quantification of the cytotoxic ability of both 4-amine derivatives ((**4**) and (**6**)) and the diamine analogue (**44**) is required before a firm evaluation can be made relating to the potential of each of these agents as clinical drugs. Furthermore, this technique does not allow us to determine the distinction between apoptotic and necrotic cell death as definitively as microscopy (ie. The use of Hoeschst 33258, a fluorescent nuclear stain, as shown in Figure 48, Page 129). As such, this technique shall be employed in future work in order to determine this.

### 5.6.4 Adenoviral Assays –

These assays indicate that the MM96L tumor cell line exhibits an inherent sensitivity to the DNA alkylating compound (**4**). Like many tumor types, MM96L cells show defective DNA repair ability following treatment with drugs. In contrast, normal NFF cells show resistance to (**4**). This result correlates well with that obtained in the cytotoxicity studies (Chapter 4). Having said this, a broader range of viral assays shall be utilized in future in order to determine that the phenomenon observed was a result of sensitivity to drug rather than a genetic anomaly within the adenovirus that altered the ability of cells to repair DNA.

### 5.6.5 *in-vivo* Studies –

The isolation of an *in vitro* model from the immune and metabolic systems of the host is advantageous because of the ease and accessibility with which this can be done; however it can also be a limitation. While the above *in vitro* results provide a basis for obtaining vital information at the tumor cell level, future integration with *in vivo* studies is required.<sup>19,34</sup>

As discussed above, the use of immunocompromised mice (ie. nude mice) may have a dramatic effect on the outcome of drug treatment. Therefore, future studies using common lab mice with normal immune system function may elicit improved results.

### 5.6.6 Synthetic Studies -

As discussed in this text, the incorporation of 4-aminophenethyl halide moieties with subunits that were envisaged to provide stability and assist in the non-covalent binding of DNA has shown moderately successful results.

Taking a different tact, the author would like to investigate the effectiveness of linking carborane molecules to the simple 4-aminophenethyl halide series investigated above. Carborane undergoes rapid fission in the presence of thermal neutrons to produce high linear energy transfer  $\text{Li}^{3+}$  and alpha particles, causing cell destruction over a limited distance. As such, the linking of this normally biologically inactive compound to our simple 4-aminophenethyl halide subunits is expected to provide some interesting and rewarding results.

## **5.7 REFERENCES**

1. Gambhir, S. S., Barrio, J. R., Herschman, H. R., Phelps, M. E. *Nuclear Med. Biol.*, **1999**, 26, 481-490.
2. Fields, B., Knipe, D., Howley, P., Chanock, R., Melnick, J., Roizman, B., Straus, S. *Virology*. Lippincott-Raven Publishers, New York, **1996**, 189-193.
3. Giacomini, A., Corich, V., Ollero, F., Squartini, A., Nuti, M. *FEMS Microbiol. Lett.*, **1992**, 100, 87-90.
4. Qiao, Y, Spitz, M. R., Guo, Z., Hadeyati, M., Grossman, L., Kraemer, K. H., Wei, Q. *Mut. Res.*, **2002**, 509, 165-174.
5. Goes, F. S. and Martin, J. *Eur. J. Biochem.*, **2001**, 268(8), 2281-2289.
6. Nakanishi, M., Ando, H., Watanabe, N., Kitamura, K., Ito, K., Okayama, H., Miyamoto, T., Agui, T., Sasaki, M. *Genes to Cells*, **2000**, 5, 839-847.
7. Sissons, J. G. P, Bain, M., Wills, M. R., Sinclair, J. H. *J. Infection*, **2002**, 44, 71-77.
8. Lipinski, C. A., Lombardo, F., Dominy, b. W., Feeney, P. J. *Adv. Drug Delivery Rev.*, **2110**, 46, 3-26.
9. Walters, W. P. and Murcko, M. A. *Adv. Drug Delivery Rev.*, **(2002)**, 54, 255-271.
10. Raven, P. H., Johnson, G. B. (1989) *Biology*. Times Mirror/Mosby College Publishing, St. Louis, 200-212.
11. <http://www.ndsu.kodak.edu/instruction/mcclean/plsc434/cellcycle/cellcycle1.htm>, Date Accessed 28/04/2005.
12. Pines, J. *Seminars in Cell Biology*. **1999**, 15, 399-408.
13. Smith, J. A. and Martin, L. *PNAS*, 70(4), 1263-1267.
14. Wu, S. and Bonner, W. M. *Cell*. **1981**, 27, 321-330.
15. Nelson, D. M. *Mol. Cell. Biol.*, **2002**, 22(21), 7459-7472.

16. Cameron, I. L. and Greulich, R. C. *J. Cell Biol.*, **2005**, 18, 31-40.
17. Garrett, M. D. and Fattaey, A. *Cur. Op. in Genetics and Dev.*. **1999**, 9, 104-111.
18. Parsons, P. G. and Brown, S. G. *AJEBAK*. **1979**, 57(2), 161-170.
19. Galli, A. G. and Schiestl. *Mut. Res.*, **1996**, 354, 69-75
20. Mutomba, M. C. and Wang, C. C. *Mol. Biochem. Parasitology*, **1996**, 80, 89-102.
21. Pourgholami, A. G., Woon, L., Amajd, R., Akhter, J., Bowery, P., Morris, D. L. *Cancer Lett.*, **2001**, 165, 43-49.
22. Plant, J. E. and Roberts, J. J. *Chem. Biol. Interact.* **1971**, 3, 337-342.
23. Neant, I., Guerrier, P. *Exp. Cell Res.*. **1988**, 176, 68-79.
24. Vesely, J, Havlicek, L., Stroad, M., Blow, J. J., Donella-Deana, A., Pinna, L., Letham, D. S., Kato, J., Detivaud, I., Leclerc, J. *Eur. J. Biochem.*, **1994**, 224, 771-786.
25. Gray, N. S., Wodicka, L., Thonnisen, A. M., Norman, T. C., Kwon, S., Espinoza, F. H., Morgan, D. O., Barnes, G., Leclerc, S., Meijer, L. *Science*. **1998**, 281, 533-538.
26. Abraham, R. T., Acquarone, M., Andersen, A., Aseni, A., Belle, R., Berger, F., Bergounioux, C., Brunn, G., Buquet-Fagot, C., Fagot, D. *Bio. Cell*, **1995**, 83, 105-120.
27. Meijer, L., Borgne, A., Mulner, O., Chong, J. P., Blow, J. J., Inajaki, N., Inagaki, M., Delcrois, J. G., Moulinoux, J. P. *Eur. J. Biochem.* **1997**, 243, 527-536.
28. Misteli, T. and Warren, G. *J. Cell Science*, **1996**, 108, 2715-2727.
29. Kwon, Y. G., Lee, S. Y., Choi, Y., Greengard, P., Naim, A.C. *Proc. Natl. Acad. Sci. USA*, **1997**, 94, 2168-2173.
30. Bhuyan, B. K. and Groppi, V. E. *Pharmac. Ther.* **1989**, 207-248.
31. Parsons, P., Carter, F., Morrison, L., Mary, R. *Cancer Res.*, **1981**, 41, 1525 – 1534.
32. Batist, G. S., Schecter, R. L. and Alaoui Jamali, M. A. *Principles of Cancer Drug Pharmacology*, Marcel Dekker Publications, **1996**, 245-251.

## **CHAPTER 6 – EXPERIMENTAL – BIOLOGICAL ACTIVITY**

### **6.1 GENERAL PREPARATIONS –**

The origin and properties of the human melanoma cell lines, MM96L, MM418c5, the cervical cancer cell line HeLa and the neonatal fibroblasts, NFF have been described in Chapter 3. Cells were cultured in 5% CO<sub>2</sub>/air at 37°C in culture medium containing 5% fetal calf serum (FCS), 3mM HEPES, 1mM pyruvate, 50 micromolar nicotinamide, 100IU/ml penicillin and 100 micrograms/ml streptomycin.

### **6.2 EXPERIMENTAL PROCEDURES –**

**6.2.1 Cell Survival Assay:** *In vitro* cytotoxicity testing employed the following cell lines: HeLa (3 x 10<sup>4</sup> cells/mL), MM96L (5 x 10<sup>4</sup> cells/mL), MM418c5 (7 x 10<sup>4</sup> cells/mL), NFF (7 x 10<sup>4</sup> cells/mL), HaCat (5 x 10<sup>4</sup> cells/mL) 293 (5 x 10<sup>4</sup> cells/mL). The diluted cell line was then added to each 6 mm well of a 96 well plate (100 µL/well). The plates were incubated overnight to ensure surface attachment of the cells.

Compounds **(4)**, **(6)**, **(8)**, **(36)**, **(40)**, **(44)**, **(48)**, and **(51)** were dissolved in 1 mL of H<sub>2</sub>O at concentrations of 2, 2, 20, 2, 2, 2, 2, and 2 mg/mL respectively and serially diluted into the plates at the concentrations shown (Chapter 4: Figures 50 – 52, 57 - 61). Compounds **(11)**, **(12)**, **(22)** and **(23)** were initially dissolved in 100 µL of DMSO, made up to 1 mL using H<sub>2</sub>O and serially diluted into the plates at the concentrations shown (Chapter 4 – Figures 53 - 56). Dilutions were carried out so that the final concentration of DMSO was no more than 1% and therefore did not interfere with the test results.

The plates were then incubated for 2 hours at 37°C. Following incubation the medium was removed, fresh medium was added and the plates incubated for a further 3 days at 37°C. After this time the plates were washed with PBS, fixed with methylated spirits for 5 minutes and washed twice with water. Sulforhodamine B (SRB) solution (50 µL of 0.4% in acetic acid) was added to each well of the plate and left at room temperature for 15 minutes. The SRB solution

was then removed and the plate washed two times with 1% acetic acid. One hundred microlitres of 10 mM Tris base (unbuffered, pH, >9) was added to each well and left to stand for 5 minutes. The plate was then read on an ELISA reader (570/450 nm ratio). The results were graphed as percentage of control versus concentration and are summarized in Table 16.

**6.2.2 CPR- $\beta$ -Galactosidase Assay:** This assay employed the use of the MM96L  $\beta$ -Galactosidase cell line, the properties of which are described in Chapter 5. The cell cultures were diluted with 5% FCS to give a cell number of approximately  $5 \times 10^5$  cells/mL. An aliquot of 100  $\mu$ L of the diluted cell line was then added to each 6 mm well of a 96 well plate. The plates were incubated overnight to allow attachment of the cells to the plate surface.

Compounds **(4)**, **(6)** and **(44)** were initially dissolved in 1 mL of H<sub>2</sub>O and then serially diluted into 96 well plates in quadruplicate, to the dilutions shown in Figures 63, 64 and 67. Compounds **(23)** and **(43)** were initially dissolved in 100  $\mu$ L of DMSO and 900  $\mu$ L of H<sub>2</sub>O and then serially diluted into the 96 well plate in quadruplicate, to the dilutions shown in Figures 65 and 66. Dilutions were carried out so that the final concentration of DMSO was approximately 1% and therefore did not interfere with the test results.

The plates were subsequently incubated for 4 days. After this time the media was removed from the plate and the surface washed with PBS. 100  $\mu$ L of 1X CPRG reagent was then added to each well of the plate and incubated at 37°C for 30 minutes to allow colour development. The absorbance was read at 570 nm on a BioRad microplate reader 3550. Results were graphed as percentage of control versus concentration (Chapter 5: Figures 63 - 67).

**6.2.3 Luciferase Assay:** This assay employed the used of the MM96L pOctL cell line described earlier. The cell cultures were diluted with 5% FCS to a cell number of approximately  $5 \times 10^5$  cells/mL. The diluted cell line was then added to each 6 mm well of a 96 well plate (100  $\mu$ L/well). The plates were incubated overnight to allow attachment of the cells to the plate surface.

Compounds **(4)**, **(6)** and **(44)** were initially dissolved in 1 mL of H<sub>2</sub>O and then serially diluted into the 96 well plate in quadruplicate to give the dilutions shown in Figures 68, 69 and 72.

Compounds **(23)** and **(43)** were initially dissolved in 100  $\mu\text{L}$  of DMSO and 900  $\mu\text{L}$  of  $\text{H}_2\text{O}$  and then serially diluted into the 96 well plate in quadruplicate to the dilutions shown in Figures 70 and 71. Dilutions were carried out so that the final concentration of DMSO was approximately 1% and therefore did not interfere with the test results.

The plates were then incubated for 4 days. After this time the media was removed from the plate and the surface washed with PBS. Luciferin substrate (20  $\mu\text{L}$ ) (see Appendix 1) was added and the luminosity measured in terms of light units. Results were graphed as percentage of control versus concentration (Chapter 5: Figures 68 - 72).

**6.2.4 Drug Stability:** This study employed the use of the MM96L cell line. Samples of **(4)** (2 mg/mL) and **(6)** (2 mg/mL) were each incubated with Medium, RPMI 1640, 5% FCS, PBS, Histidine (5 mmol), Glutathione (5 mmol) and DNA (1  $\mu\text{g}/\text{mL}$ ) for 0 hours (control), 1.5 hours, 3 hours and 6 hours at 37°C. Each sample was added in quadruplicate to 96 well plates at the concentrations shown in Figures 73 - 78. The plates were then incubated at 37°C for two hours.

After this time the medium was removed, fresh medium added and the plates incubated for a further three days. Following incubation the plates were washed with PBS, fixed with methylated spirits for 5 minutes and washed twice with water. Sulforhodamine B (SRB) (50  $\mu\text{L}$ ) solution (0.4% in acetic acid) was added to each well of the plate and left at room temperature for 15 minutes. The SRB solution was then removed and the plate washed two times with 1% acetic acid. Tris base (100  $\mu\text{L}$ ) (10mM, unbuffered, pH, >9) was added to each well and left to stand for 5 minutes. The plate was then read on an ELISA reader (570/450 nm ratio). The results were graphed as percentage of control versus concentration (Chapter 5: Figures 73 - 78).

**6.2.5 Cell Cycle Studies:** This study employed the use of the MM96L, 293 and NFF cell lines. The cell cultures were diluted with 5% FCS to give a cell number of approximately  $2.0 \times 10^5$  cells/mL. The diluted cell line (4 mL) was then added to 60 mm plates. The plates were incubated overnight to allow for the attachment of the cells to the plate surface.

Following overnight incubation, MNNG, MMS **(4)**, **(6)** and **(23)** were added in triplicate to the MM96L plates at the concentrations shown in Figures 82 - 95. Compound **(4)** was also

diluted in triplicate onto 293 and NFF cells at the dilutions shown in Figures 96 - 101. The plates were then incubated at 37°C for 30 minutes. After this time 2 mM hydroxyurea was added to four of the MM96L plates containing **(4)** at the concentrations shown in 101 - 103. Likewise, albendazole was added to four MM96L plates containing **(4)** as shown in Figures 105 and 106. The plates were incubated for a further two hours. After this time the plates were washed and incubated with fresh medium for a further 24 hours.

Following incubation the cells were detached with trypsin solution (0.2 mg/mL, 7.5 mM EDTA in Dulbecco's solution) and harvested into 10 mL centrifuge tubes. The pellets obtained following centrifuging were resuspended in PBS and repelleted (X2). The washed pellets were resuspended in 400 µL of PBS and pushed through a gauze tipped syringe. Propidium iodide solution (100 µL, 0.1 mg RNase A, 1 µL 10% Triton, 0.5 µL Propidium Iodide (10 mg/mL), 98.5 µL PBS) was added prior to analysis on a FACSCalibur instrument (Becton-Dickinson FACS systems, Sunnyvale California, USA) with a fluorescence-2 detector. Cell cycle distribution (as a percentage) was analyzed using Modfit software.

### **6.2.6 Adenoviral Assays:**

**6.2.6(a): Host Cell Reactivation (HCR)** - This assay employed the use of the MM96L and NFF cell lines. Each cell line was seeded into a 96 well plate at  $5 \times 10^4$  cells per well in 100 µL of medium and incubated overnight to allow attachment of the cells to the plate surface. The virus was diluted 1 in 10 in medium containing dilutions of **(4)** shown in Figure 109 and incubated for two hours prior to addition to the MM96L cell line. The damaged virus was then diluted in quadruplicate onto MM96L cells at concentration ranges of  $10^{-2}$  to  $10^{-7}$  for each dilution of **(4)**. The plates were incubated for 48 hours and the adenoviral replication detected using the immunoperoxidase assay (Section 6.2.6(c)).

**6.2.6(b): Viral Capacity (VC)** - This assay employed the use of the MM96L cell line. The cells were seeded into a 96 well plate at  $5 \times 10^3$  cells per well in 100 µL of medium and incubated overnight to allow surface attachment of cells. After this time, **(4)** was diluted onto the MM96L cell line at the concentrations shown in Figure 110. The drug treated cell line was incubated for two hours. Following incubation, the virus was diluted onto the drug treated

damaged cells at dilutions of  $10^{-2}$  to  $10^{-7}$ . The plates were then incubated for a further 48 hours. Adenoviral replication was then detected using the immunoperoxidase assay (see 6.2.6(c)).

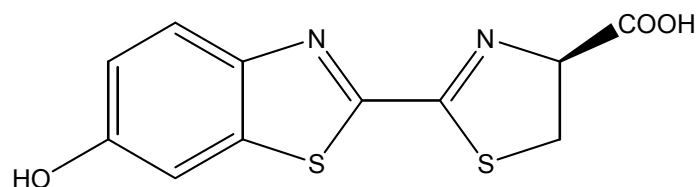
**6.2.6(c): Immunoperoxidase Detection of Adenovirus Replication** – Following 48 hours of viral infection, the medium was tipped from the plates and the well surface washed with PBS. The cells were then fixed by the addition of 200  $\mu\text{L}$  of methanol. After two minutes the methanol was tipped from the plates and the wells washed with PBS. PGP plasma (20  $\mu\text{L}$ ) was then added to each well and incubated for 30 minutes at  $37^{\circ}\text{C}$ . After this time the plates were washed two times with PBS and then 20  $\mu\text{L}$  of peroxidase-labelled protein A diluted to 5 mg/mL added each well. After 60 minutes the plates were washed once in PBS and once in peroxidase buffer (10mM Tris pH 7.4). Peroxidase buffer containing substrates (100  $\mu\text{L}$ ) was then added quickly to each well and the development of colour observed under the microscope over a period of 10 minutes. The plates were then washed twice with water and the number of stained cells per well counted, with counts over 200 being ignored. The results were graphed as infectious dose (ID) versus drug concentration (Chapter 5: Figures 109 and 110).

## APPENDIX 1 – COMMON REAGENTS USED IN BIOLOGICAL ASSAYS

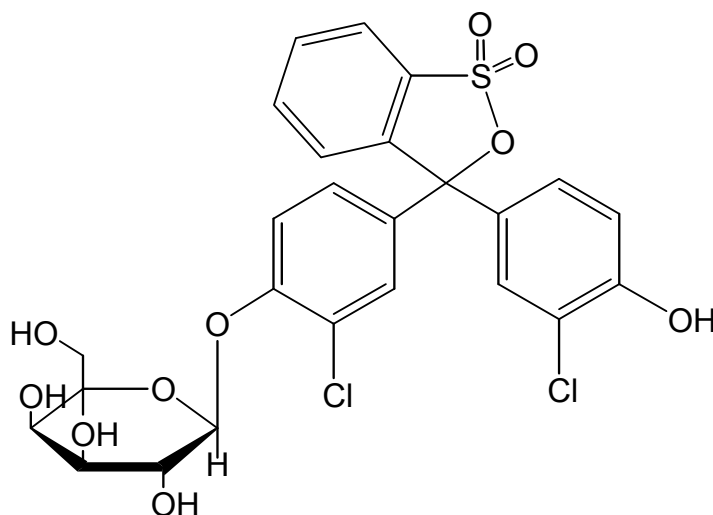
**Albendazole (Methyl-5-[propylthio]-2-benz-imidazolecarbamate):** a broad-spectrum antiparasitic that inhibits microtubule polymerization by binding to  $\beta$ -tubulin.<sup>1</sup>

**Hydroxyurea:** An antineoplastic compound which inhibits ribonuclease reductase and DNA replication.<sup>2</sup>

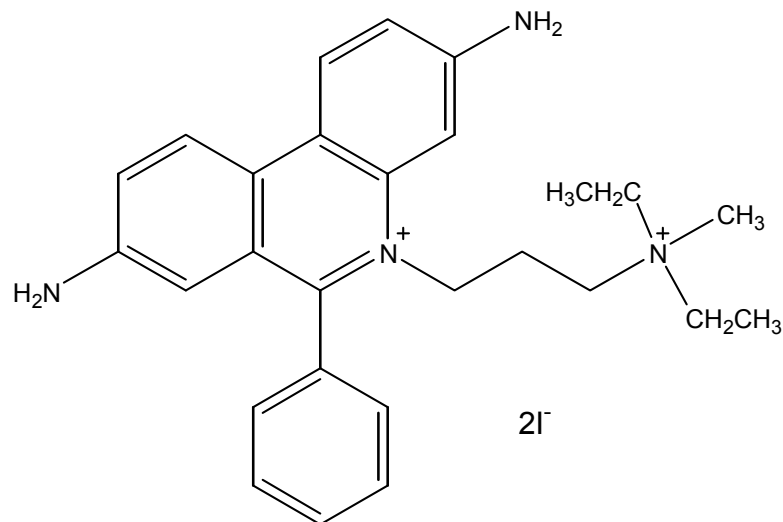
**D-Luciferin (4,5-Dihydro-2-[6-hydroxy-2-benzothiazolyl]-4-thiazole carboxylic acid):** a substrate for the enzyme Luciferase.<sup>3</sup>



**CPRG-Reagent:** Chlorophenol Red- $\beta$ -D-galactopyranoside.<sup>4</sup>



**Propidium Iodide:** a fluorescent stain for nucleic acids.<sup>5</sup>

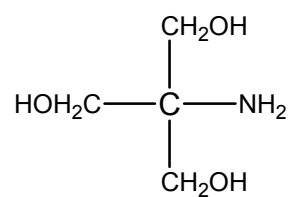


**Protein A:** A polypeptide isolated from *Staphylococcus aureus* that binds the Fc region of immunoglobulin molecules without interacting at the antigen binding site. This property permits the formation of tertiary complexes consisting of Protein A, antibody and antigen. Protein A can be isolated from the bacterial cell wall or culture medium (from a protein A secreting strain).<sup>6</sup>

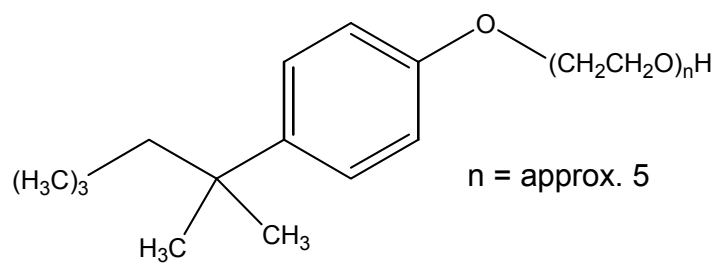
**Peroxidase:** An enzyme from horseradish. Peroxidase is a glycoprotein with a hemin prosthetic group and bound Ca<sup>++</sup>. The molecular weight of this protein is approximately 44,000.<sup>7</sup>

**Protein A Peroxidase:** Protein A coupled to peroxidase. This complex has a binding capacity of 2 – 5 mg of human IgG per mg of solid and a peroxidase activity of 100 – 200 units per mg of protein.<sup>8</sup>

**Tris Base:** Established as an excellent biochemical buffer, Tris has a pK<sub>a</sub> of 8.1 at 25°C. Unlike other buffer solutions Tris does not precipitate calcium salts, and also maintains the solubility of magnesium salts.<sup>9</sup>



**Triton x-100:** a widely used non-ionic surfactant for the recovery of membrane components under non-denaturing conditions.<sup>10</sup>



## **REFERENCES**

1. *Merck*, 13, 209.
2. Yarbrow, J.W. *Semin. Oncol.*, **1992**, 19, 1-10.
3. *Merck*, 13,4116.
4. Malarkannan, S., Mendoza, L. M., Shastri, N. *Methods Mol. Biol.*, **2001**, 156, 265-272.
5. Tas, J. and Westerneng, G. *J. Histochem. Cytochem.*, **1981**, 29, 929.
6. Goden, J.W. *J. Immunol. Methods*, **1978**, 20, 241-253.
7. Veitch, N.C. *Phytochem.*, **2004**, 65(3), 249–259.
8. Eliades, P., Karagouni, E., Stergiatou, I., Miras, K. *J. Immunol. Methods*, **1998**, 218(1-2), 123-32.
9. *Merck*, 13, 9842.
10. Collins, M. L. and Salton, M. R. *Biochim. Biophys. Acta.*, **1979**, 553, 40-53.